Assessing vegetation dynamics in response to climate variability and change across sub-Saharan Africa

by Claire Davis-Reddy

UNIVERSITEIT
iYUNIVESITHI
STELLENBOSCH
UNIVERSITY

Dissertation presented for the Degree of Doctor of Philosophy in the Faculty of Sciences, at Stellenbosch University

Supervisor: Prof. Guy Midgley

March 2018

Declaration

By submitting this thesis electronically, I declare that the entirety of the work contained therein is my own original work, that I am the authorship owner thereof (unless to the extent explicitly otherwise stated) and that I have not previously in its entirety or in part submitted it for obtaining any qualification.

Date: March 2018

Abstract

Understanding and predicting how anthropogenic climate change is likely to impact terrestrial ecosystems across sub-Saharan Africa is a key question for both ecology and for regional and global climate policy development. This predictive understanding hinges on a far better ability to detect, interpret, and attribute changes in vegetation cover and productivity, which is the basis for ecosystem response and resilience to anthropogenic climate change.

Monitoring and modelling of vegetation dynamics in the context of climate change requires long-term datasets of key ecosystem indicators such as vegetation productivity and phenology. The use of remotely sensed vegetation indices to detect vegetation change related to climate has become an important application of remotely sensed imagery. The third generation Normalized Difference Vegetation Index (NDVI3g) time series from the Global Inventory Modeling and Mapping Studies (GIMMS) has a 34-year long history (1982-2015) and provides unprecedented opportunity to examine vegetation dynamics in response to changes in temperature, rainfall, and increases in atmospheric carbon dioxide (CO_2).

This thesis makes use of the NDVI3g time-series to examine the influence of climate on vegetation productivity and phenology in order to (i) assess recent shifts in vegetation across sub-Saharan Africa (SSA) and (ii) facilitate improved simulations of vegetation by Dynamic Global Vegetation Models (DGVMs). The NDVI3g information was integrated with climate data and large-scale climate fluctuations and oscillations in sea surface temperature and atmospheric pressure to test hypotheses on the role of both climate variability and change on vegetation activity. Seasonal and long-term patterns of change were compared with projections of a dynamic global vegetation model, the "adaptive Dynamic Global Vegetation Model" (aDGVM) that was initially developed for application in sub-Saharan Africa.

In the first component of the thesis results show that the vegetation of SSA is driven by rainfall and associated fluctuations and oscillations in sea surface temperature (SST) and atmospheric pressure, with the El Niño-Southern Oscillation (ENSO) being the most dominant driver of variability in both vegetation productivity and phenology over eastern and southern Africa. Vegetation tends to show a stronger positive response to rainfall in the 3 months preceding vegetation growth suggesting that time-lag effects are significant when assessing the influence of climate.

In the second component, trend analyses provide evidence for a number of important spatial and temporal patterns of change in vegetation productivity and phenology over SSA, which are generally consistent with independently reported long-term trends. Significant added value was provided to previous studies through the use of productivity and phenology metrics, which facilitated an assessment of vegetation dynamics at both the seasonal and inter-annual scale.

A clear latitudinal pattern of change was detected where significant increases in both productivity and the length of the growing season were observed over the northern hemisphere tropics (0-10°N) and sub-tropics of southern hemisphere (20-35°S) and significant decreases observed over the southern hemisphere tropics (0-20°S). The greening trends account for approximately 50% of the observed changes over SSA. Over West Africa and parts of central Africa the greening trends are linked to increases in rainfall and possibly atmospheric CO_2 concentration as well as reforestation efforts in some countries. Over the south-western Cape, eastern coastline, and northeast extent of South Africa the greening trends are consistent with the observed patterns of bush encroachment and expansion of alien invasive species in these regions. The trends in many of these regions have been attributed at least partly to increased atmospheric CO_2. Over southern Africa, simulations of vegetation productivity derived from the adaptive DGVM indicate that vegetation should have been increasing across southern Africa over the last 30 years. This finding combined with the lack of evidence of substantial changes in rainfall over the region suggests the role of land-use in limiting the increase in vegetation as observed in the aDGVM simulations.

Lastly, the comparison between observed remotely sensed vegetation indices and historical simulated values of vegetation productivity from the aDGVM over SSA provided valuable insight into the utility of remotely sensed vegetation indices to assist in the validation, refinement and overall improvement of simulation of vegetation by DGVMs. While the model performs well over grassland and savanna regions of southern Africa it tends to underestimate grass productivity in East Africa and over the Sahel, overestimate tree cover in tropical humid forests of central and West Africa. The model also fails to capture the unique seasonal pattern of the Mediterranean-type vegetation of south-west cape of South Africa and the inter-annual pattern of variability in vegetation over SSA. These biases and limits of the model are likely to have implications for the performance of model in projecting future vegetation cover over these regions.

This research contributes to the understanding of landscape-scale vegetation response patterns that will provide an important benchmark against which future vegetation change can be assessed. Importantly, it highlights that testing the performance of dynamic vegetation models in the context of regional climate models is a research imperative.

Acknowledgements

I would like to firstly thank my supervisor, Prof. Guy Midgley for his contributions, guidance, and encouragement over the last three years. I am truly grateful for his willingness to let me pursue my research unbounded while providing invaluable suggestions along the way.

I would also like to thank my Research Group Leader at the CSIR, Dr. Francois Engelbreght and the rest of the team, especially Dr. Daleen Lötter, for their continued support most importantly taking over my responsibilities in the last four months. Without this support I would have not had enough dedicated time to focus on the write up of my thesis.

Dr. Simon Schieter from the Johann Wolfgang Goethe-Universität conducted the aDGVM model runs used in this research. I am grateful for the timely provision of the aDGVM outputs as well as valuable comments on draft versions of the research.

The regional climate simulations were performed on the computer clusters of the Centre for High Performance Computing (CHPC) of the Meraka Institute of the CSIR in Cape Town, South Africa. Access to the data was provided Jacobus Van Der Merwe of the CSIR.

The research conducted in this PhD was supported by the CSIR Young Researcher's Establishment fund, the Southern African Science Service Centre for Climate Change and Adaptive Land Use (SASSCAL) programme funded by the German Ministry of Education and Research (www.sasscal.org), and the Future Climate for Africa UMFULA project with financial support from the UK Natural Environment Research Council (NERC), grant ref NE/M02007X/1, and the UK Government's Department for International Development (DFID).

Finally, I would like to thank my husband, Marsh, for his continued love, patience and support and for constantly ensuring that I had well-balanced life while pursuing my PhD. He was always willing to listen to my ideas, concepts, and countless statistical and data challenges providing suggestions and a renewed sense of inspiration to keep me going. With him everything becomes possible.

Table of Contents

List of Figures

List of Tables

List of Abbreviations

AAO	Antarctic Oscillation
aDGVM	Adaptive Dynamic Global Vegetation Models
AMO	Atlantic Multidecadal Oscillation
AMP	Seasonal amplitude
ANN	Artificial Neural Network
AR5	Assessment Report Five
AVHRR	Advanced Very High Resolution Radiometer
LAI3g	Third generation of AVHRR GIMMS LAI
BFAST	Breaks for Additive Seasonal and Trend
BP	Breakpoint
Br	Browning
CABLE	CSIRO Atmospheric Biosphere Land Exchange
CCAM	Conformal-cubic atmospheric model
CGCMs	Coupled General Circulation Models
CHPC	Centre for High Performance Computing
CLD	Cloud cover
CMIP5	Coupled Model Intercomparison Project Phase 5
CO_2	Carbon dioxide
CRU	Climate Research Unit
CSIR	Council for Scientific and Industrial Research
CSIRO	The Commonwealth Scientific and Industrial Research Organisation
DGVM	Dynamic Global Vegetation Models
DJF	December-January-February
ENSO	El Niño Southern Oscillation
EOS	End of season
EVI	Enhanced Vegetation Index
FAPAR	Fraction of absorbed photosynthetically active radiation
GHCN	Global Historical Climatology Network

GIMMS	Global Inventory Modeling and Mapping Studies
GPCC	Global Precipitation Climatology Centre
GPCP	Global Precipitation Climatology Product
Gr	Greening
IOD	Indian Ocean Dipole
IPCC	Intergovernmental Panel on Climate Change
ITCZ	Inter-Tropical Convergence Zone
JJA	June-July-August
LAI	Leaf Area Index
LI	Large integral
LOS	Length of season
MAM	March-April-May
MAX	Maximum NDVI
MID	Timing of maximum NDVI
MODIS	Moderate Resolution Imaging Spectroradiometer
NAO	North Atlantic Oscillation
NASA	National Aeronautics and Space Administration
NDVI	Normalised Difference Vegetation Index
NDVI3g	Third generation of AVHRR GIMMS NDVI
NIR	Near Infrared
NOAA	National Oceanic and Atmospheric Administration
ONI	Oceanic Niño Index
PCA	Principal component analysis
PDO	Pacific Decadal Oscillation
PFTs	Plant functional types
PRE	Precipitation
RCM	Regional Climate Model
S1	Season 1
S2	Season 2

SAM	Southern Annual Mode
SARAH	Surface Solar Radiation Data Set - Heliosat
SD	Standard deviation
SG	Savitzky-Golay
SIS	Surface solar irradiance
SLA	Specific leaf area
SON	September-October-November
SOS	Start of season
SSA	Sub-Saharan Africa
SST	Sea surface temperature
TMP	Temperature
TS	Theil-Sen
UDEL	University of Delaware

Chapter 1:

1. Introduction

1.1 Climate change and terrestrial ecosystems

There is strong scientific evidence that atmospheric CO_2 and global mean annual temperatures have been steadily rising since 1880 (Stocker et al. 2013). Over Africa, drastic increases in land surface temperatures have been reported (Jones et al. 2012; Engelbrecht et al. 2015) and future projections indicate that temperatures are to continue to rise, at 1.5 to 2 times the global rate of temperature increase (Niang et al. 2014). Changes in rainfall patterns including increases in the frequency and intensity of drought events (Engelbrecht et al. 2013) as well the occurrence of El Niño events (Cai et al. 2014) are expected. These changes in temperature and rainfall combined with rising atmospheric CO_2 concentrations are likely to have profound implications for the terrestrial ecosystems of Africa (Scholes et al. 2004; Midgley & Bond 2015). These impacts are likely to be confounded by multiple existing stressors such as land-use change, livestock grazing, fuel wood harvesting and invasions by alien species (Midgley et al. 2003; van Wilgen et al. 2008).

Understanding and predicting how climate change is likely to alter ecosystem structure and function is a key question in ecology and there is a growing research impetus to detect early signs of climate change impacts and to identify vulnerable regions. The response of vegetation to climate change depends on the magnitude of change, the relationships between the variables (e.g. temperature, rainfall and CO_2) and the historical environmental conditions (e.g. land-use change).

In Africa, changes and shifts in the distribution and dynamics of terrestrial ecosystems, including deserts, grasslands and shrublands, savannas have already occurring (Field et al. 2014). Increases in woody vegetation in central, eastern and sub-Saharan Africa have been well documented (Bond & Midgley 2000; Wigley et al. 2009; Ward et al. 2012; Mitchard & Flintrop 2013; Stevens et al. 2016) and modelling studies focusing on vegetation responses to climate change project that the extent of woody vegetation is likely to continue to increase resulting in a variety of biome shifts (Scheiter & Higgins 2009; Higgins & Scheiter 2012). Evidence suggests that as critical CO_2 levels are crossed, these may trigger vegetation structural switches with important consequences for both biodiversity and carbon storage (Bond & Midgley 2000).

Uncertainty in how climate is likely to change coupled with uncertainty in the mechanisms driving the change is currently limiting the ability to project future ecosystem change (Midgley & Bond 2015). Evidence required to resolve divergences in model outputs is limited due to the lack of quantitative spatially explicit evidence the impact of climate on terrestrial ecosystems. In addition, the current understanding of the mechanism and extent of the influence of atmospheric CO_2 on ecosystem change is far from complete. Improved long-term monitoring at regional spatial scales of changes in vegetation structure and dynamics combined with improved models of vegetation function is required in order to provide accurate assessments of current vegetation states and functions as well as future projections of change (Hill et al. 2011). The necessity of such detailed information has increased not only to assist decision-making but also for improving climate models at regional and global scales.

1.2 Rationale

Monitoring and modelling vegetation dynamics in the context of climate variability and change requires long-term datasets of key ecosystem indicators such as vegetation productivity and phenology (Zhu et al. 2013). Satellite-based remote sensing remains the most effective means for monitoring vegetation dynamics at a variety of spatial and temporal scales (Justice et al. 1985; Hobbs 1990; Zhao et al. 2012; Wessels et al. 2012). The detection of vegetation changes through the creation of vegetation indices, such as the Normalised Difference Vegetation Index (NDVI), has become an important application of remotely sensed imagery (de Jong et al. 2011a).

NDVI provides a proxy for vegetation productivity and has been crucial in monitoring a variety of global land vegetation processes and fluctuations over time (e.g. Townshend & Justice 1986; Myneni et al. 1997; Nemani et al. 2003; Nagendra et al. 2013; Zhu et al. 2016). More specifically, NDVI has been used study vegetation–climate interactions (e.g. Herrmann et al. 2005; Martiny et al. 2006; Brown et al. 2010; Philippon et al. 2011; Anyamba & Tucker 2012; Wang et al. 2015; Gao et al. 2016), long-term vegetation trends (e.g. Anyamba & Tucker 2005; Wessels et al. 2007b; de Jong et al. 2011b; Fensholt et al. 2012; Fensholt et al. 2013; de Jong et al. 2013), vegetation phenology (e.g. Heumann et al. 2007; Wessels et al. 2010; de Jong et al. 2011b; Eklundh et al. 2012; Vrieling et al. 2013; Buitenwerf et al. 2015; Zhang et al. 2017b), and more recently to provide evidence of the impact of climate change on vegetation (e.g. Wu et al. 2015; Zhu et al. 2016).

Remote sensing techniques have undergone substantial progress over the past few decades and the increased availability of remotely sensed time series data has enabled researchers to address issues related to climate change (Southworth et al. 2017). The Advanced Very

High Resolution Radiometer (AVHRR) instruments on-board the National Oceanic and Atmospheric Administration (NOAA) satellite series have provided one of the longest time series of observations of global vegetation. The third generation Normalized Difference Vegetation Index (NDVI3g) time series from the Global Inventory Modeling and Mapping Studies (GIMMS) now has more than a 34-year long history (Pinzon & Tucker 2013). The NDVI3g provides unprecedented opportunity to examine long-term vegetation dynamics as well as changes and shifts in response to changes in climate (temperature and rainfall) and increases in atmospheric CO_2. Understanding climatic influences on vegetation productivity and phenology will facilitate a greater understanding of the response of ecosystems to climate change and will enables improved predictions of changes under different future climatic conditions.

Predictions of vegetation responses to projected future climate change tend to be based on process-based model approaches such as Dynamic Global Vegetation Models (Hartig et al. 2012a). Dynamic Global Vegetation Models (DGVMs) are designed to simulate the response of vegetation responses to long-term atmospheric changes in temperature, precipitation and atmospheric CO_2 concentrations (Cramer et al. 2001; Sitch et al. 2003; Sitch et al. 2008; Quillet et al. 2010). By monitoring growth, carbon allocation, photosynthesis, mortality and regeneration, DGVMs provide a bottom-up description of plant communities. Because dynamic models do not rely on assumptions of equilibrium between vegetation and the environment, they can effectively model the relationship between vegetation dynamics and changes in environmental and climatic conditions (Hartig et al. 2012b). The models support the primary importance of climate in determining the patterns vegetation productivity but more recently models have included aspects of disturbance such as fire and grazing (Thonicke et al. 2001; Scheiter et al. 2012).

The major disadvantage associated with DGVMs is that they are derived from experiments and observations that often lack the appropriate temporal and spatial resolution (Hartig et al. 2012b). There is considerable potential for the use of observations from remotely sensed data to assess historical simulations of vegetation from DGVMs. Simulations that are more likely to match historical and current conditions are likely to produce more reliable future projections (Moncrieff et al. 2014). There is also the potential for remote sensing products to be integrated into DGVMs to produce multi-scale vegetation modelling products.

1.3 Thesis aims and research approach

There are still substantial gaps and uncertainties in the future projections of terrestrial ecosystems as a result of climate change. In this context there is a strong need to expand and improve our understanding of the mechanisms and drivers of vegetation change.

Changes in climate impact vegetation in a manner that can be monitored using remotely sensed vegetation indices. This study aims to evaluate and assess the response of vegetation dynamics to climate variability and change. The ability to effectively evaluate vegetation change using remotely sensed time series data has the potential to assist in characterising the response of vegetation to climate forcing and could represent a basic reference for testing the performance of dynamic vegetation models in the context of regional climate models. This research extends upon previous studies by incorporating a range of methodological approaches and techniques in order to firstly link landscape level change to changes in climate, specifically temperature and rainfall, as well as increases in atmospheric CO_2 and secondly to provide potential linkages between remotely sensed observations and dynamic global vegetation models, which provide predictions of future vegetation states over Sub-Saharan Africa (SSA).

The focus region of this study is SSA, including Madagascar. Sub-Saharan Africa refers to the area of Africa south of the Sahara between 10-15°N and 35°S (Figure 1.1 & 1.2). The region is characterised by a wealth of biodiversity and a number of biologically and ecologically unique ecosystems. Ecosystems of SSA range from the semi-arid savanna of the Sahel to equatorial tropical forests of central and West Africa, tropical and subtropical grasslands and savannas over southern and East Africa, arid shrublands of the Kalahari Basin, temperate grasslands of South Africa, and the Mediterranean-type ecosystems of south-west Cape of South Africa (Figure 1.2).

Using the third generation 8 km Normalised Difference Vegetation Index (NDVI3g) derived from Advanced Very High Resolution Radiometer (AVHRR) as a proxy for vegetation growth this study address three key research questions, namely:

1. Is there evidence for abrupt local or regional shifts in vegetation productivity and phenology?
2. How has vegetation productivity and phenology responded to climate and atmospheric CO_2 change, and how does this compare with the current understanding of the drivers of ecosystem change?
3. Can improvements be made to the simulations of vegetation by Dynamic Global Vegetation Models (DGVMs) in order to increase the confidence in projections of future regional vegetation change?

Answering all these questions required that a range of methodological approaches and statistical techniques were explored and applied to remotely sensed vegetation index (Figure 1.3). The AVHRR NDVI3g dataset was utilised as it provides the longest continuous temporal record of terrestrial vegetation dynamics, compatible with climate metrics data.

The first component of the research involved the pre-processing of the NDVI3g data to remove residual noise from the time-series and to extract key growing season metrics including the start, end and length of the season over the region (**Chapter 3**). The methodology applied here attempts to successfully capture the full range of seasonal vegetation characteristics and dynamics experienced over SSA. Validation of the spatial patterns of phenology and productivity was conducted through a comparison with existing studies of vegetation dynamics over Africa.

The second component builds upon the techniques used in number of previous studies (e.g. Wessels et al. 2010; de Jong et al. 2013; Vrieling et al. 2013) to detect trends and abrupt shifts in the vegetation dynamics across the region (**Chapter 5**). By using range different trend detection methods, including the application of linear trend models and the spatial explicit detection of abrupt changes and trend shifts in the time-series, this study provides a more robust understanding of the trajectory of vegetation change over SSA. This component provides the necessary information to address the first research question.

The third component of the research quantifies the climate drivers of vegetation productivity over SSA in order to address the second research question. By investigating the role of climate, specifically temperature, rainfall and atmospheric CO_2, firstly on the inter-annual variability of vegetation and key phenology metrics (**Chapter 4**) and secondly the role in driving shifts and changes in vegetation (**Chapter 5**). Chapter 4 and 5 differ in the time-scale at which the role of climate is assessed. **Chapter 4** contributes to the body of work on understanding the role of climate in driving inter-annual variability in vegetation whereas **Chapter 5** provides evidence of longer-term shifts and changes in vegetation over the entire assessment period (1982-2015). This involved quantifying recent historical trends in climate (**Chapter 2**) across the region and determining the association between key climatic variables and the vegetation parameters derived from the remotely sensed data.

In order to effectively understand the role of climate in driving vegetation change the impacts of climate change need to be distinguished from those of other disturbances such as land-use change. The research presented here attempts to focus solely on the climatic drivers of vegetation change by excluding all anthroponegically-altered landscapes, such as agricultural and urban areas from the analysis. This assumes that observed trends in vegetation in these masked regions can be primarily attributed to mainly land cover and land use change such as the expansion of croplands or urban areas whereas as those trends experienced elsewhere are more likely to be indicative of the response to climate change.

The last component of the research evaluates vegetation outputs from a dynamic global vegetation model (DGVM) by comparing observed remotely sensed vegetation indices to

historical simulated values over Sub-Saharan Africa (**Chapter 6**). The motivation behind the inclusion of this chapter in this thesis is that the models' ability to simulate present-day vegetation dynamics strongly determines the confidence in future vegetation states projected by that model (Zhu et al. 2013). This chapter builds on the understanding of vegetation dynamics derived from previous chapters in order to assess the ability of a DGVM to simulate observed patterns and trends relative to the remotely sensed data and to determine where improvements can be made. The information presented here provides the necessary evidence to address the third research question. The modelling of future projected impacts of climate change on vegetation was beyond the scope of this thesis.

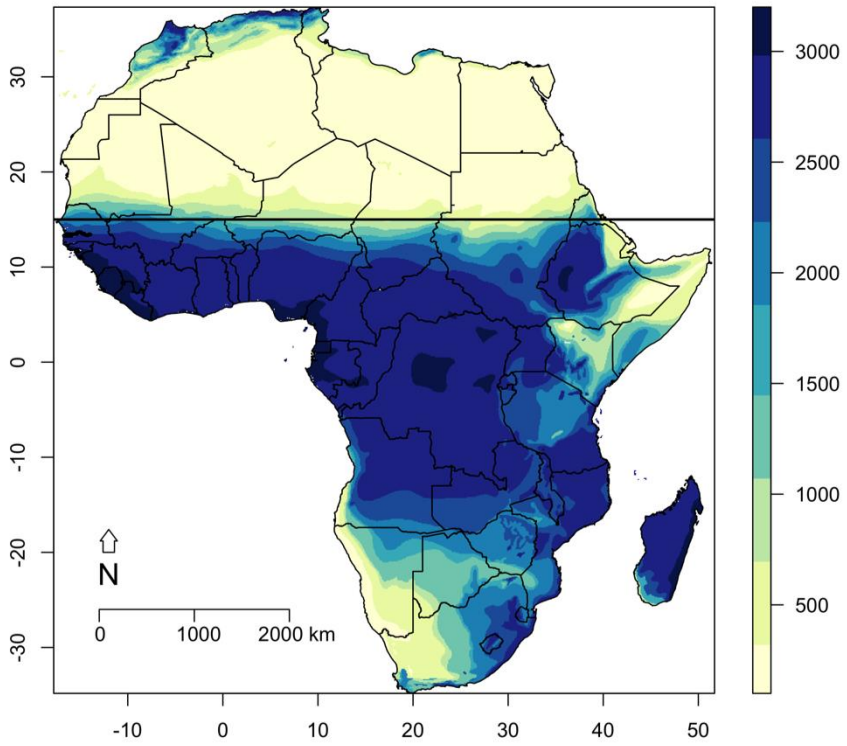

Figure 1.1: Mean annual rainfall expressed as millimetres (mm) (Source: FAO/Agrhymet Network and ESRI). The thick black line represents the northern extent of the study area at 15°N.

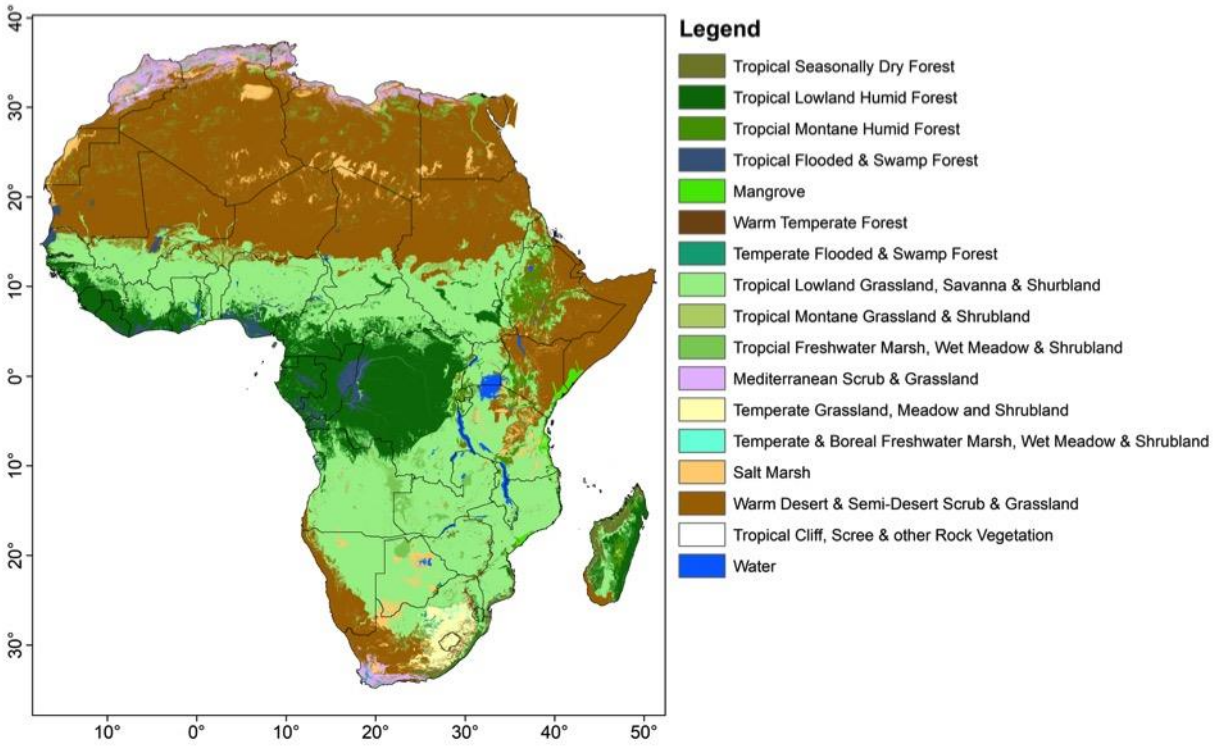

Figure 1.2: Primary terrestrial biomes of Africa as described by Sayre et al.(2013)

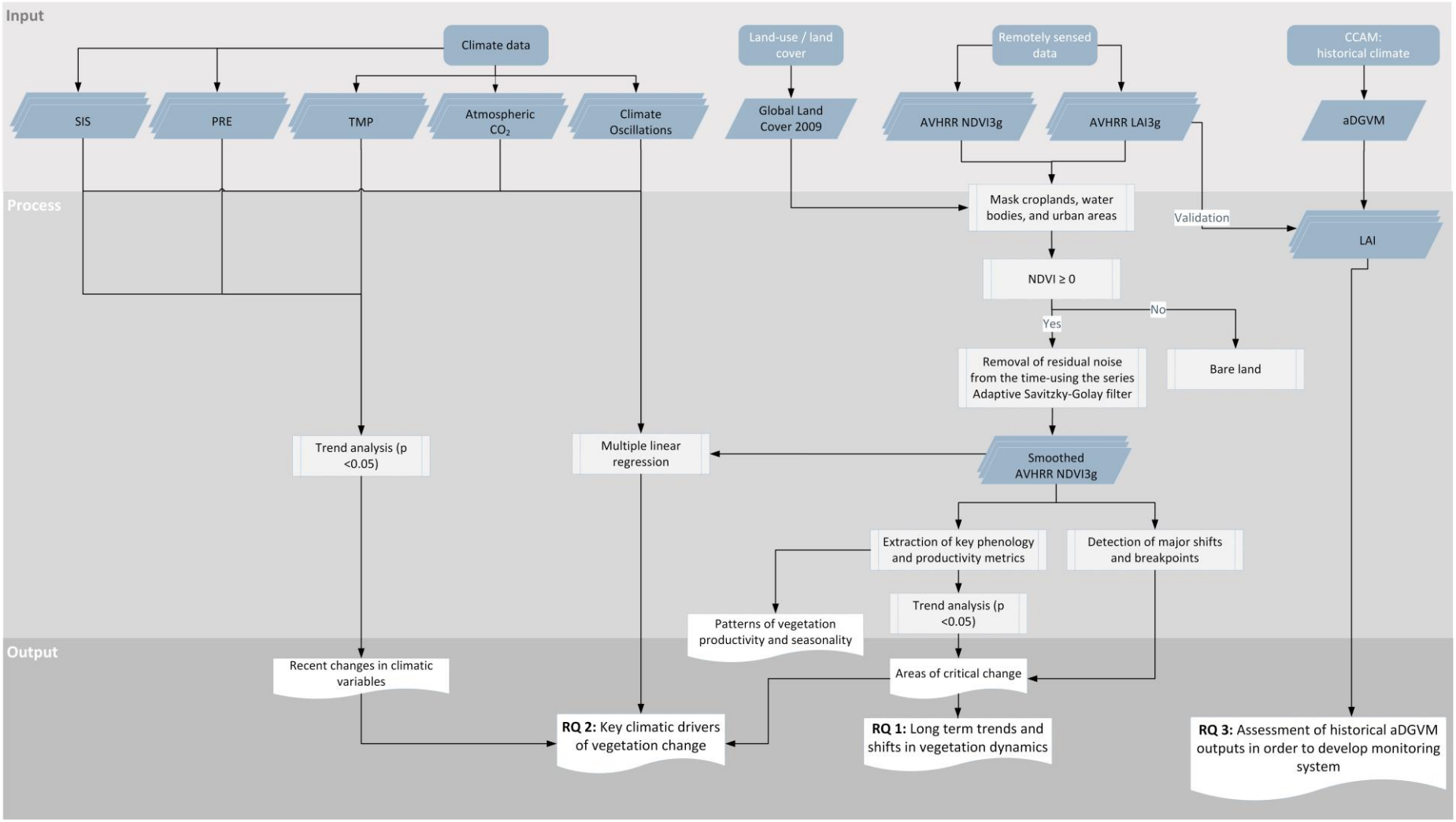

Figure 1.3: Conceptual framework of the study outlining the approach and methodology taken to address the three research questions.

1.4 Thesis structure

This introductory chapter (**Chapter 1**) serves to outline the problem statement and explain the overall aim and research questions of this thesis. The four chapters that comprise the body of this thesis (**Chapters 3 to 6**) are written as stand-alone research papers. **Chapter 2** was published, in part, in Davis-Reddy, C.L. and Vincent, K. 2017: Climate Risk and Vulnerability: A Handbook for Southern Africa (2nd Edition), Council for Scientific and Industrial Research, Pretoria, South Africa[1].

Since the AVHRR NDVI3g dataset is utilised in all four chapters (**Chapters 3 to 6**) a separate chapter was included (**Chapter 3**) which describes the characteristics and limitations of the remotely sensed vegetation index as well as the filtering algorithms applied to the time-series to extract productivity and phenology metrics. Supplementary information and figures including a detailed description of the climate of SSA are provided in the Appendices. The conclusion (**Chapter 7**) draws out the key findings from all the chapters and discusses what has been achieved, and how it contributes to improving our understanding of climate driven vegetation change over Sub-Saharan Africa.

[1] This Chapter was solely authored by myself and a peer-review process was followed for the book and evidence of comments and revisions to to the chapter can be provided.

Chapter 2:

2. Observed trends in recent historical climate of Sub-Saharan Africa

2.1 Introduction

2.1.1 Background

The body of work on historical climate trends has been steadily increasing during the last decade and significant progress has been made in projecting and understanding climate change for the African region. There is strong scientific evidence that increases in annual global temperatures and temperature extremes are attributable to human activities (New et al. 2006; Seneviratne et al. 2012; Stocker et al. 2013; Engelbrecht et al. 2015).

Global mean annual temperatures have increased by 0.85°C since 1880 and are projected to increase by 0.3 to 2.5°C by 2050, relative to the 1985-2005 climatological average (Stocker et al. 2013). The regional distribution of temperature increases is not uniform, however, and some regions have experienced greater change than others. For the African continent, the recent studies of Jones et al. (2012) and Engelbrecht et al. (2015) are indicative of drastic increases in surface temperature. Evidence also shows that the region has already experienced increased frequency of hot days and a decreased frequency of extremely cold days (New et al. 2006; Seneviratne et al. 2012).

Rainfall trends are variable but where records are of sufficient length there have been detectable increases in average rainfall intensity and the length of the dry season over parts of southern Africa (New et al. 2006; Tadross et al. 2009) as well as evidence that droughts have become more intense across some countries in SSA (Fauchereau et al. 2003; Shongwe et al. 2009; Zhao & Dai 2016).

Temperatures are expected to continue to rise over the continent during the 21st century under low mitigation futures (Niang et al. 2014). Temperatures are projected to rise rapidly, at 1.5 to 2 times the global rate of temperature increase (Engelbrecht et al. 2015). Moreover, the southern African region and Mediterranean North Africa are likely to become generally drier under enhanced anthropogenic forcing, whilst East and tropical Africa are likley to become wetter (Christensen et al. 2007; Engelbrecht et al. 2009; James & Washington 2013; Niang et al. 2014). More frequent occurrence of dry spells are also more likely over most of the interior of southern Africa (Christensen et al. 2007; Engelbrecht et al. 2009) and cut-off low related flood events are also projected to occur less frequently over South Africa (MacKellar et al. 2007; Engelbrecht et al. 2013) in response to a poleward displacement of the westerly wind regime. More uncertainty surrounds the projected climate futures of West

Africa and the Sahel, with some climate models projecting wetter conditions and equally credible models projecting drier conditions under climate change (Christensen et al. 2007; Niang et al. 2014).

2.1.2 Objectives and rationale

Changes in climate, based on available observational records, provide the first indication of the direction and magnitude of possible future changes. Observational records have already provided evidence of a changing global climate over the last century. In this chapter, recent trends in historical climate for sub-Saharan Africa are investigated in order to provide the necessary evidence for understanding observed changes in vegetation as described by remotely sensed vegetation indices (**Chapter 5**). Specifically, this chapter presents:

- A description of the climate of sub-Saharan Africa; and
- An analysis of observed trends in land-surface air temperature, incoming shortwave radiation, and rainfall across sub-Saharan Africa over the last 34 years (1982-2015).

2.2 Overview of the climate of sub-Saharan Africa

The climate of sub-Saharan Africa is highly diverse and driven by a range of distinct climate systems. The climate is determined by the position of the continent in relation to the major circulation patterns, the seasonal migration of the Inter-Tropical Convergence Zone (ITCZ), the topography, the existence of large lakes, and the surrounding oceans (Nicholson 2000). Temperatures are highest in the northern Sahara desert with cooler areas over high altitude plateaus and mountainous regions (Figure 2.1). Rainfall varies considerably across the continent (Figure 1.2) with the northern and southern extremes of the continent experiencing winter rainfall associated with the passage of mid-latitude cyclones. Over the Kalahari and Sahara deserts subsiding air pressure systems are dominant and inhibit rainfall for most parts of the year. Moderate to high rainfall is associated with the ITCZ over the equatorial and tropical areas of Africa with these regions experience rainfall through the year; i.e. no dry season (Figure 2.2). The near-equatorial regions experience two rainy seasons as a result of the shift in position of rainfall-bearing low pressure systems whereas poleward regions experience one distinct rainfall season.

Rainfall over Africa also exhibits a high degree of natural variability. In general, rainfall exhibits three significant time scales of variability: inter-decadal (15-28 years), quasi-decadal (8–13 years), and inter-annual (2–8 years). Variability is observed regionally, for example, as severe drought on yearly time-scales or as more prolonged over one or more decades (Hulme et al. 2001). The following section details the climate of each of the three key regions of Africa; West (11.4°S to 15°N; 20°W to 25°E), East Africa (11.3°S to 15°N; 25°E to 52°E), and southern Africa (35°S to 11.4°N; 10°W to 52°E) (Stocker et al. 2013); (refer to Appendix A Figure A.1 for geographical extents).

2.2.1 West Africa

The relief of West Africa ranges from coastal plain to a low undulating plateau region with an average elevation of between 200 and 400m asl. Elevation in the Fouta Djalon mountain chain reaches 1752 masl. West Africa is bordered on the west and south by the Atlantic Ocean and the Sahara Desert to the north (Hayward & Oguntoyinbo 1987; Jalloh et al. 2013). The climate ranges from humid tropical monsoon along the coast to semi-arid Sahel transect to desert in the north. Temperatures range from 26°C along the coast to 30°C in the Sahel and above 30°C on the border of the desert (Figure 2.1). Maximum temperatures in the central Sahara during summer can reach 58°C and minimum temperatures can reach a low of 4°C demonstrating a high diurnal temperature range of between 10 and 35°C. The savannas of West Africa are the most frequently and extensively burnt (Giglio et al. 2010; N'Datchoh et al. 2015).

The general rainfall pattern over West Africa is modified by warm waters of the tropical Atlantic Ocean, migration of ITZC, and topographical features and is subject to a high degree of spatial and seasonal variability (Jalloh et al. 2013). The West African monsoon is driven by seasonal shift in prevailing wind direction and affects the majority of the region. The majority of the region experiences a single rainy season that occurs during summer (April to September) when the ITCZ shifts northwards (Figure 2.2). The dry season occurs during winter (November to April) and is driven by the tropical northern high-pressure system, which results in dry and dusty north-easterly wind over the region. The wet season is driven by the moisture-laden equatorial air mass, which produces south-westerly winds. Some coastal regions including Ghana and Cote d'Ivoire receive two peaks in rainfall with one occurring in May and June and a second in September and October with relatively drier conditions between.

Rainfall generally decreases northward from the coast (Figure 1.2) with the coastlines of Guinea, Sierra Leone, Liberia, and Nigeria (humid zone) receiving the highest amount of rainfall per year of between 1,500 to 4,000mm. The sub-humid zone includes areas receive 900-1,500mm of rainfall whereas the further north dry sub-humid zone receives 550-900mm of rainfall. In the Sahel (semi-arid zone), rainfall ranges from 250-550mm occurring within a short raining season. The length of the growing period is between 60 and 90 days with an extended dry season of up to 10 months (Jalloh et al. 2013). The dry season can extend into years resulting in severe drought over the region. The Sahara (arid-zone) experiences less than 200mm per year between the months of July and September. Along the coast coastal areas the annual rainfall variability ranges from 10 to 20%, while in the Sahel it may exceed 40%.

2.2.2 East Africa

Eastern Africa has a broad diversity of terrain and climate with the two of the highest mountains in Africa, Mt. Kenya and Mt. Kilimanjaro, and one of the largest lakes, Lake Victoria. The climate of the region ranges from arid in the east to tropical monsoon conditions in the west. Arid regions occur in the Sahel region of central and southern Sudan as well as areas of Tanzania, Kenya and Ethiopia. The climate is driven by large-scale atmospheric patterns such as the migration of the ITZC and the presence of the warm Indian Ocean along the east coast. Average temperatures across the region are moderate except for the more arid northern regions of Kenya, Sudan and Eritrea which experience temperatures above 28°C (Figure 2.1). The highlands of Ethiopia and Eritrea as well as mountainous areas of Tanzania and Kenya experience cooler temperatures between 20-25°C.

The areas that receive the highest rainfall are those with the longest rain seasons. These include the areas in the northwest, high altitude regions surrounding Mt. Kenya and Mt. Kilimanjaro, and the areas in the northeast of Lake Malawi, northwest of Lake Victoria and Ethiopia (Figure 1.2). Mean annual rainfall in these regions ranges from 800 to 2000 mm. Rainfall in the regions to the northeast is on average less than 400 mm per annum. Northern Somalia is one of the driest areas of East Africa with an average annual rainfall of less than 150 mm. These areas are in the rain shadow created by the mountain ranges and Ethiopian highlands to the east.

The majority of East Africa experiences a bimodal seasonal distribution of rainfall with two rainy seasons; one from April to May and another lighter one from October to December (Figure 2.2). In some areas of Kenya there is a third maximum occurring in July / August (Nicholson 1996). The seasonal rainfall is driven by the double passage of the ITCZ, which migrates southwards during January and February and returns northwards in March, April and May. Inter-annual variations in rainfall are largely driven by variations in the sea surface temperature in the Indian Ocean and the El Niño Southern Oscillation (ENSO). The northern and southern extremes of East Africa experience one rainy season with the peak rainfall occurring during summer; northern regions in June to August and southern regions in December to February (Nicholson 1996).

2.2.3 Southern Africa

Southern Africa has a warm climate with the majority of the region experiencing an average annual temperature above 17°C (Figure 2.1). In summer the temperatures are highest over the desert regions of Namibia and Botswana and exceed 40℃ during the day. The diurnal temperature range in these regions is also large. Over the interior plateau regions and to the south-west cooler conditions are experienced due to the cloud cover associated with the summer rains. In winter the temperature regimes display a latitudinal gradient where

temperature decreases southward. The coldest temperatures are experienced over high altitude regions of South Africa, including Lesotho and Zimbabwe.

The majority of the region has two distinct seasons; a wet season in the summer half of the year from roughly November to March and a dry season during winter from April to October. Rainfall peaks between December and February when most of the region receives between 80% and 90% of its annual rainfall (Hobbs et al. 1998). The exception is the south-western Cape, which experiences rainfall in winter (Figure 2.2). Tropical cyclones are common along the Mozambican and South African coastlines, bringing significant rainfall and associated flooding to Mozambique, the northern parts of South Africa, western Madagascar, and Zimbabwe.

There is a high degree of spatial variation in rainfall across southern Africa due to the influence of the ocean currents and prevailing winds. The highest amount of rainfall occurs in the tropics towards the equator and in eastern Madagascar, which can receive up to 3100 mm per year (Figure 1.2). In the interior of southern Africa there is a strong east to west gradient where rainfall decreases westward with areas in the Kalahari receiving less than 100 mm per year. The warm Agulhas Current provides a source of additional moisture leading to higher rainfall in the eastern parts of the region whereas the cold Benguela Current results in lower rainfall in the western parts. Large areas of southern Africa are susceptible to dry conditions and experience frequent droughts (Masih et al. 2014), which have been linked to the ENSO phenomenon (Rouault & Richard 2005; Rojas et al. 2014; WFP 2016).

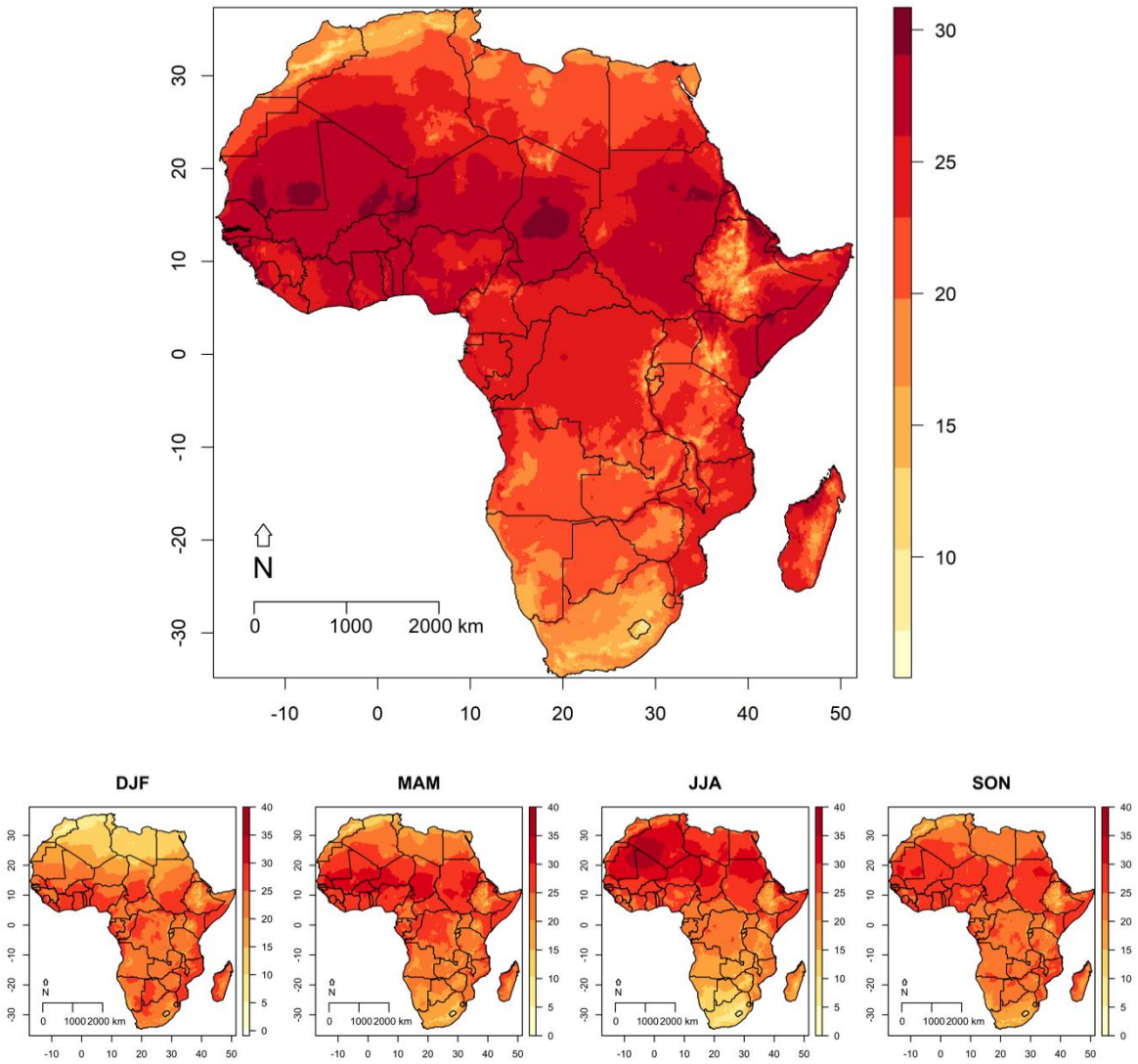

Figure 2.1: Average annual and seasonal temperatures (°C) over Africa (Source: Hijmans et al. 2005). Seasons are given as summer (December-January-February), autumn (March-April-May), winter (June-July-August), and spring (September-October-November).

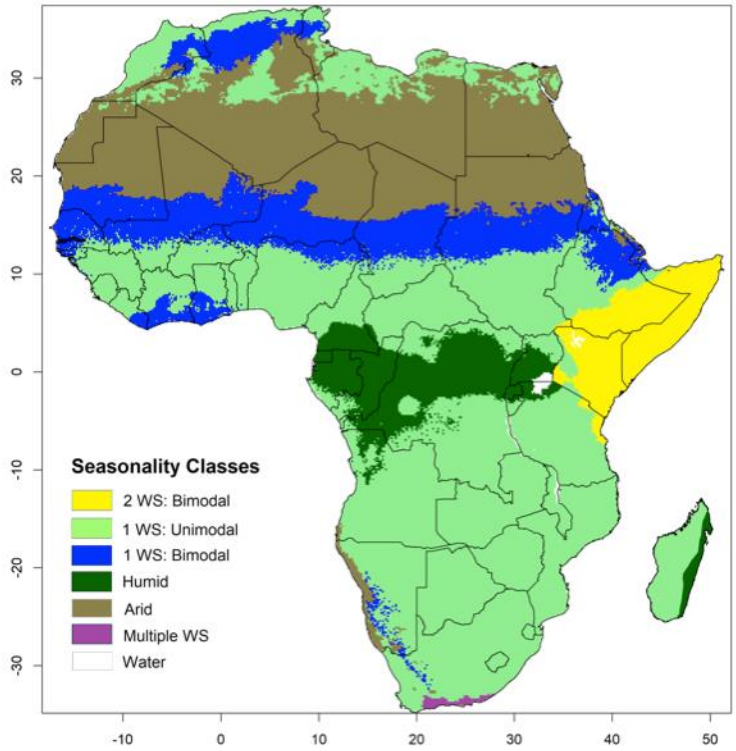

Figure 2.2: Rainfall seasonality map indicating regions with a single (unimodal), dual (bimodal), and multiple wet season regimes. Seasonality information was extracted from rainfall data-set using Savitzky-Golay (SG) filter in TIMESAT (Jönsson & Eklundh 2004) and is consistent with that presented by Herrman and Mohr (2011).

2.3 Methodology

2.3.1 Climate Data

The three climate parameters assessed in this study (refer to Table 2.1) were selected assumption that vegetation is limited by water availability, temperature and solar radiation. The gridded monthly CRU TS 4.00 (Climatic Research Unit Time Series version 4) dataset (Harris et al. 2013) was used to assess changes in temperature and rainfall over Africa. These two parameters are represented at a spatial resolution of 0.5°. Gridded climate datasets are developed by interpolating of over 4000 individual weather station records across the globe in order capture the local spatial and temporal variability of temperature and rainfall (New et al. 2002; Mitchell & Jones 2005; Hewitson & Crane 2006). The CRU data sets has been validated, well documented and homogenised and has been used previously to study trends in climate (Niang et al. 2014). Due to the lack of weather stations and/or sufficiently long enough records, gridded datasets may however, not as precise in some regions as others.

Trends in surface solar irradiance, also referred to as shortwave incoming solar radiation, was based on data from Monthly Surface Solar Radiation (W/m^2) Data Set - Heliosat (SARAH) derived from Meteosat satellite observations from 1983 to 2013 (Müller et al. 2015). Data for the years 2014 and 2015 were not available at the time of analysis.

Table 2.1: Climate parameters utilised in this study

Label	Climate parameter	Unit	Source
PRE	Rainfall	mm	CRU TS 4.00 (Harris et al. 2013)
TMP	Daily mean temperature	°C	CRU TS 4.00 (Harris et al. 2013)
SIS	Surface solar radiation	W/m^2	SARAH (Müller et al. 2015)

2.3.2 Detecting trends in historical climate

Data related challenges

Detecting regional climate trends is considerably more difficult than doing so for global climate (Stocker et al. 2013). Firstly, across Africa there is a lack of an accurate, long-term, well-maintained and dense spatial network of observational stations to detect regional climate signals. This is particularly evident in Africa where weather stations are sparsely distributed (Figure 2.3). Since each station represents only a single locality, the information collected may not adequately represent the surrounding region. Furthermore, the number of weather stations across southern Africa has decreased drastically since the 1980s (Schulze 2007) meaning that there are relatively few stations available that have sufficient data for analysis spanning several decades.

Secondly, many climate variables, in particular those related to rainfall, exhibit very high variance on time scales ranging from daily through to multi-decadal. This challenge is particularly relevant for Africa, a region that displays pronounced variability in rainfall (see section 2.3.2 on the influence of ENSO). This high temporal variability means that, while linear (or linear-like) trends can be calculated, the probability that the calculated trend is indicative of climate change is low. Interpreting the trend in climate requires an understanding of the extent to which the modes of variability are being altered by climate change (Hulme et al. 2001).

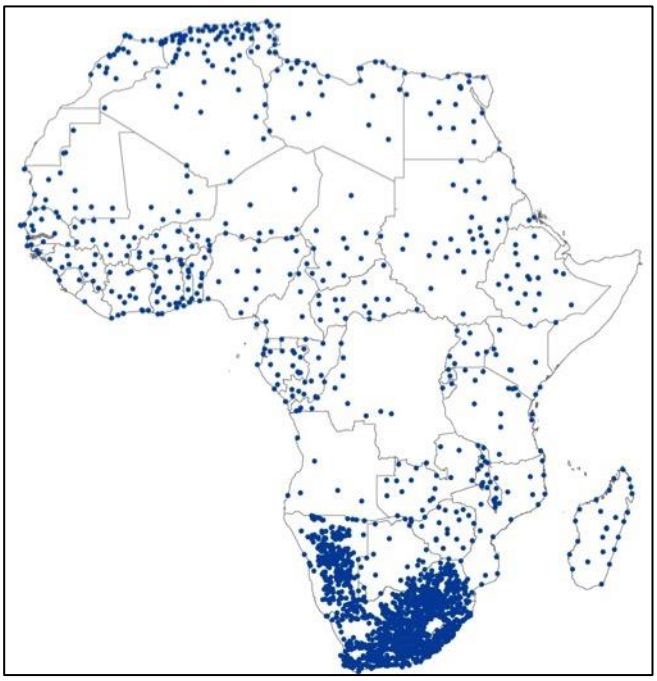

Figure 2.3: The location of NOAA's Global Historical Climate Network (GHCN) weather stations, as used by CRU, across Africa.

Trend Analysis

Despite the difficulties described above, the observational record for sub-Saharan Africa between 1982 and 2015 is examined for evidence of climate trends. The period 1982 to 2015 was chosen in order to match the AVHRR NDVI3g time-series.

Temporal trends in climate statistics were assessed using the Theil-Sen technique (Theil 1950) and the associated test for its statistical significance. The Theil-Sen slope is a linear (uniform) trend index that provides a spatially-explicit expression of the rate of change per year by calculating the slope between every pairwise combination and the median slope value. Negative (positive) slopes indicate areas that have experienced a decline (increase). Anomalies (observation in year *t* minus the long-term mean observation) were used in the calculation of trends.

The Theil-Sen index is a more robust than traditional linear trend analyses in that is is not sensitive to outliers in data and less sensitive to the exact shape of the trend. In addition, the uncertainty is not influenced by whether the data distribution follows a normal distribution. While interpreting the results, a p-value of 0.05 was considered as a threshold of significance.

2.4 Results and Discussion

2.4.1 Land surface air temperature

There is strong evidence that the average land surface temperature has increased have been increasing over the last century across Africa (Figure 2.4). Temperature increases are not spatially uniform across Africa with some regions have experienced greater change than others. The largest trends, of more than 3°C per century, are observed over the northern and eastern regions of Africa (Figure 2.5). The average rate of temperature change over Africa for the period 1900-2014 is 0.84°C per century which is consistent with detected increases in regional temperatures since 1900 (Niang et al. 2014; MacKellar et al. 2014; Osborn & Jones 2014; Engelbrecht et al. 2015).

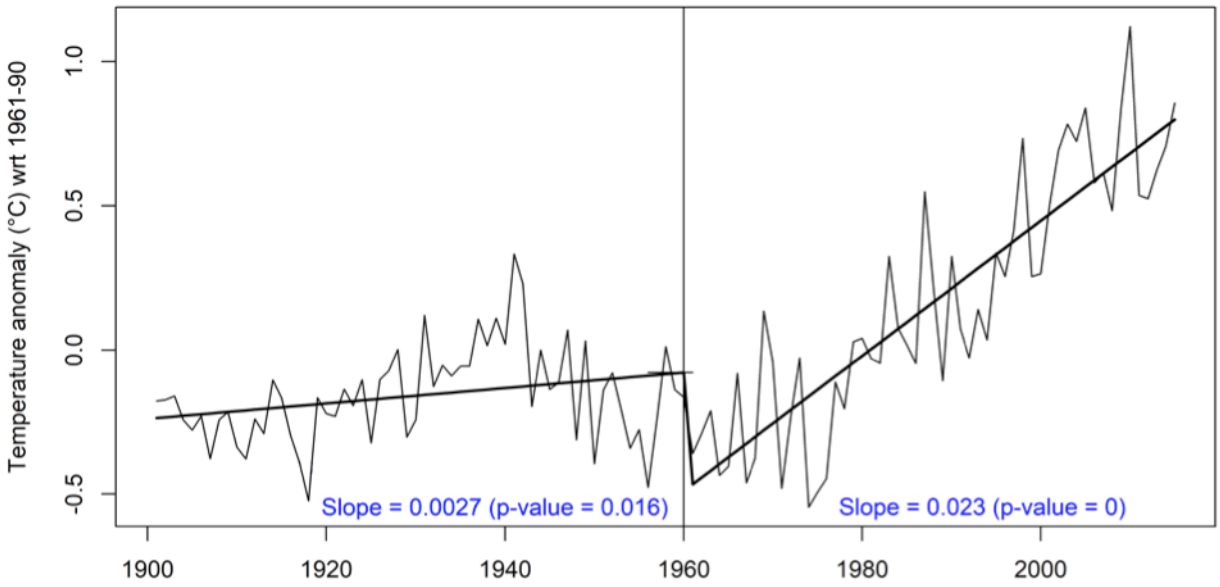

Figure 2.4: Mean annual temperature anomaly (°C) over Africa from 1901 to 2015 with respect to the long-term average climatology 1961-1990; based on the gridded CRU TS 4.00 dataset. The vertical line indicates the breakpoint at 1960. The rate of temperature increase post 1960 is 0.23°C per decade (p<0.0001).

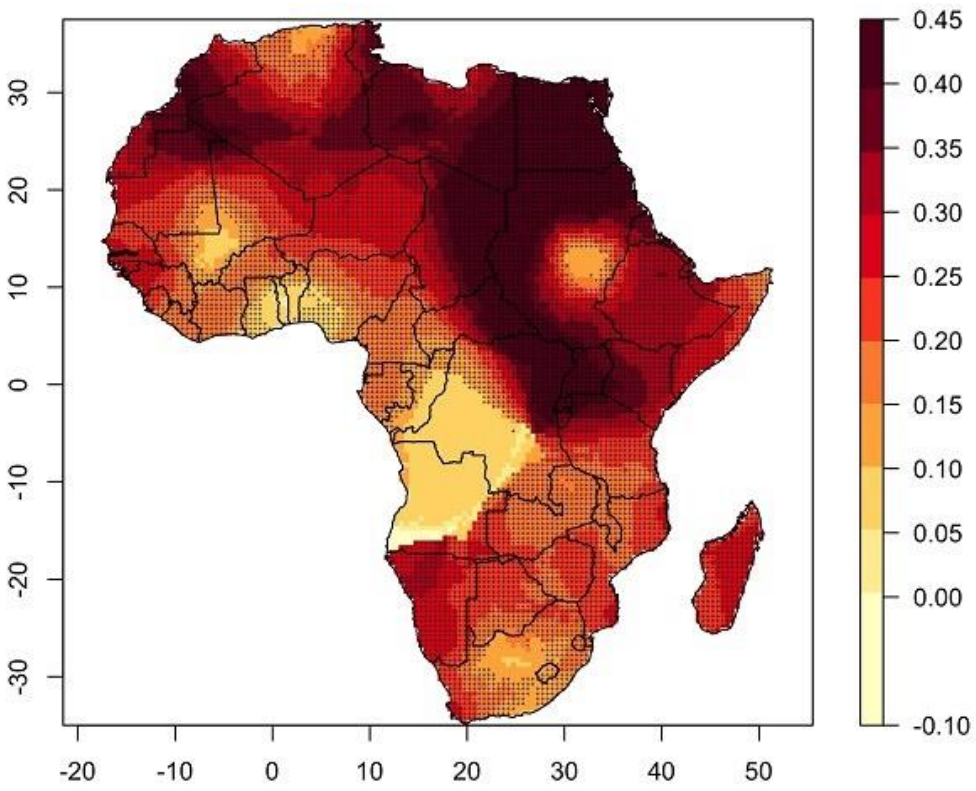

Figure 2.5: Observed trends in annual average near surface temperature (°C per decade) over Africa for the period 1982-2015 based on the CRU TS 4.00 dataset. Crosses indicate grid boxes where the trend is statistically significant. White areas indicate incomplete or missing data.

2.4.2 Incoming solar radiation

Increases in surface solar irradiance (SIS) derived from surface solar radiation dataset - Heliostat (SARAH) are observed over parts of East Africa and southern Africa while declines are observed over South Africa and West Africa (Figure 2.6). These patterns are consistent with Müller et al. (2015) and over South Africa with a recent study by Singh & Kruger (2017). SIS is affected by cloud cover and aerosol particles, including air pollution and dust where increasing aerosols and cloud optical depth results in a reduction of surface solar radiation (Qin et al. 2007; Stocker et al. 2013). Figure 2.7 indicates that over East Africa and parts of southern Africa cloud cover has decreased whereas over parts of West and central Africa cloud cover has increased. Over South Africa cloud cover has decreased so increasing atmospheric aerosol content could explain the reductions in solar irradiance (Singh & Kruger 2017).

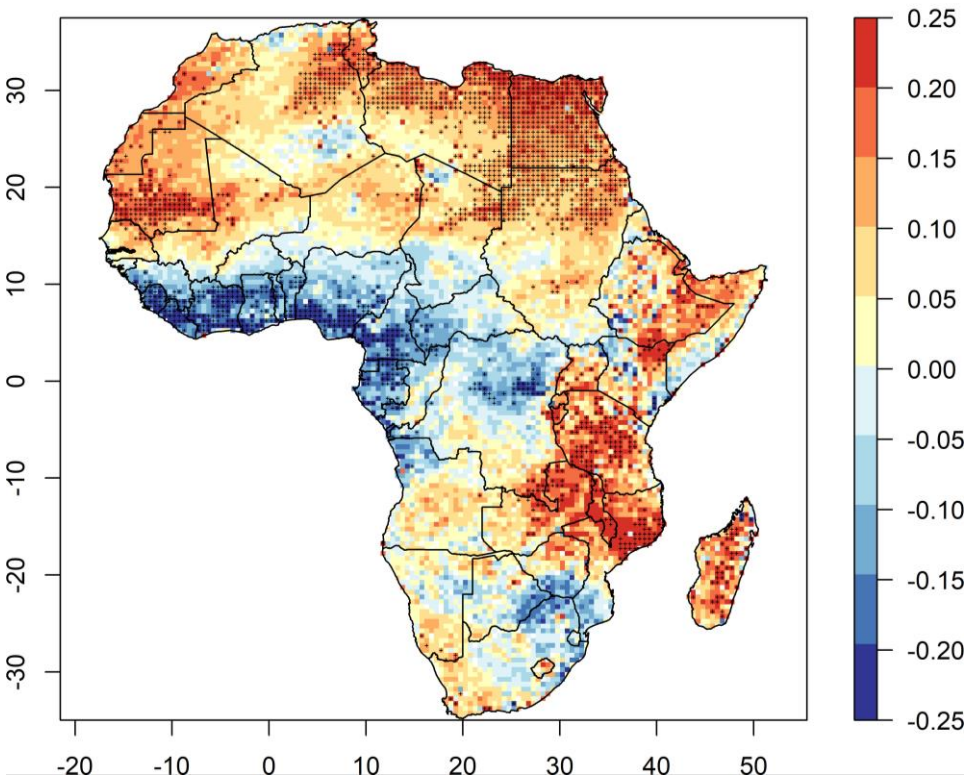

Figure 2.6: Observed trends in incoming solar radiation (SIS) (W/m^2 per year) over Africa over Africa for the period 1982-2013. Crosses indicate grid boxes where the trend is statistically significant.

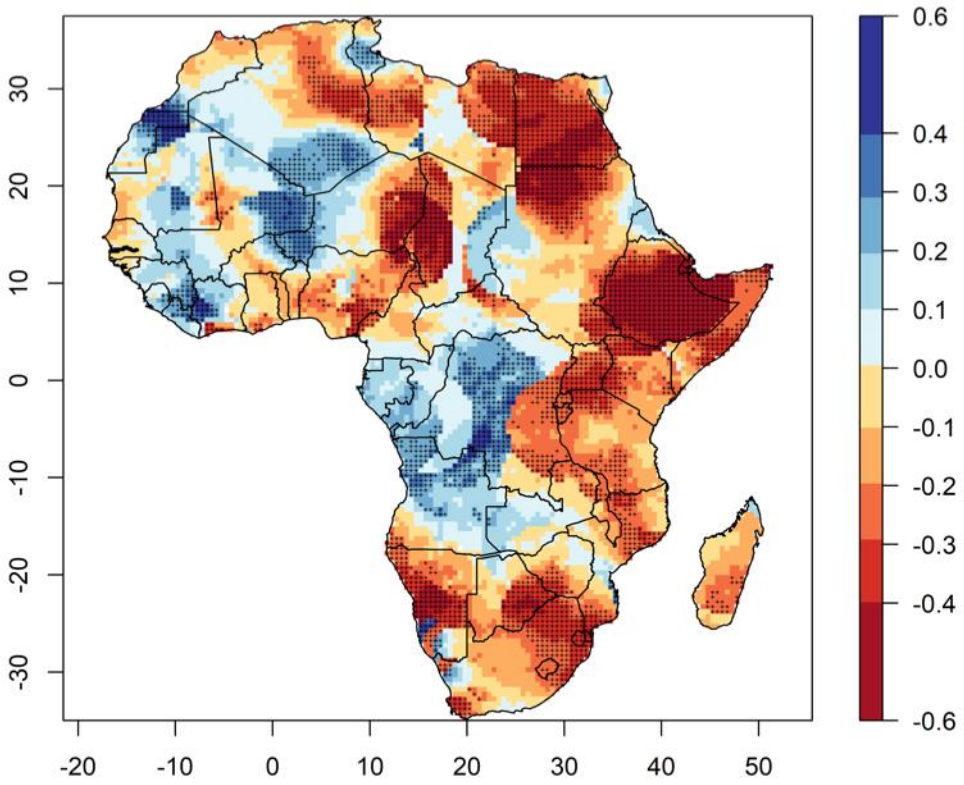

Figure 2.7: Observed trends in annual cloud cover (CLD) over Africa for the period 1982-2015 based on CRU TS 4.00 data. Crosses indicate grid boxes where the trend is statistically significant. White areas indicate no data.

2.4.3 Rainfall

The rainfall time series for West, East and southern Africa (Figure 2.8) is characterised by periods of above and below average rainfall demonstrating a strong pattern of inter-annual variability. There is little evidence of a substantial overall wetting or drying trend over the 3 sub-regions. The alternating patterns of above and below normal rainfall periods illustrate the rainfall wet and dry cycles prevalent in each of the regions. The multi-decal variability in rainfall over Africa is explored further in Figure 2.9. The decade 1960-1969 was characterised by above normal rainfall over most of Africa, except for parts of southern Africa. Later in the 1970s this rainfall anomaly pattern was reversed with parts of southern Africa experiencing above normal rainfall while the majority of the remaining areas experienced a deficient in rainfall. This drying trend intensified over the Sahel in the 1980s resulting in widespread drought (Lamb 1980; Nicholson 2000). Over the 1990s and 2000s rainfall has slowly started to recover with positive rainfall anomalies observed over larger parts of the region. Southern Africa was considerably drier in the 1990s compared to the other decades and is likely a result of the impact of the 1991/1992 drought. The 2000s were wetter for most of the region except for the countries along the south-western coast of Africa.

Spatially, there is some evidence to suggest changes in the patterns of rainfall over Africa based on trends in CRU TS 4.00 between 1982 and 2015 (Figure 2.10):

- Over the eastern and western Sahel, increases in rainfall are observed in the CRU TS 4.00 time-series, which is likely indicative of the recovery of rainfall from extensive droughts during the 1970's and 1980's (Nicholson 2000; Lebel & Ali 2009; Niang et al. 2014).
- Over East Africa, decreases are observed over Tanzania and parts of Kenya whereas increases are observed over South Sudan, Ethiopia, Uganda, and Rwanda. While rainfall in this region shows a high degree of temporal variability, a number of studies have, however, indicated that over the last 3 decades rainfall in the spring (long rains) has decreased (Lyon & DeWitt 2012; Liebmann et al. 2014; Rowell et al. 2015).
- Over southern Africa, decreases in annual rainfall are observed over south-west parts of South Africa, southern Botswana, northern Madagascar, Republic of Congo, parts of DRC, and northern Mozambique based on the CRU TS. 4.00 time-series. While some studies in the region have indicated that rainfall has decreased in some areas (McSweeney et al. 2010; Harrison et al. 2015) and that inter-annual variability in rainfall has increased (Hulme et al. 2001; Fauchereau et al. 2003; New et al. 2006), clear spatial patterns of change are lacking. Over South Africa, positive trends in annual rainfall totals over the southern interior of the country and a drying trend in

the north and north-east were observed over the period 1921 to 2015 (MacKellar et al. 2014; Engelbrecht et al. 2017 in press).

These trends, are however different when assessing CRU TS 4.00 rainfall data over a longer period, for example 1961 to 2015 (Appendix A Figure A.2). Most noticeably, a stronger drying trend is observed over most of SSA relative to 1982-2015 trend map. Furthermore, trends are not consistent across different observed precipitation datasets (refer to Appendix A Figure A.3) and any signals of systematic change are weak. Increases in rainfall are observed over parts of southern Africa, East Africa and the Sahel in the GPCP v2.2 and GPCC v7 datasets whereas the GHCN v3.3 and UDEL datasets demonstrate a general drying trend over SSA.

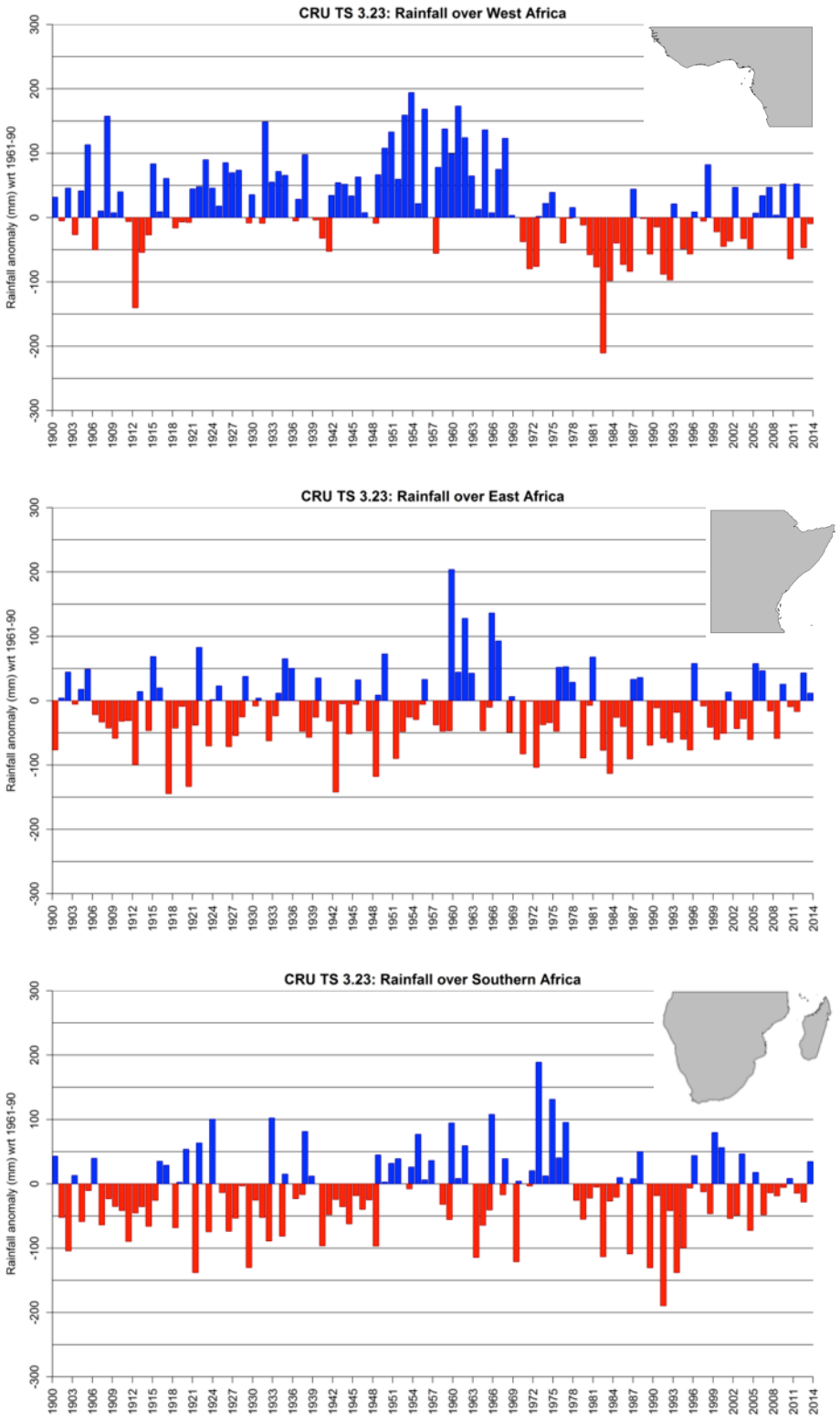

Figure 2.8: Mean annual rainfall anomaly (mm) over (a) West Africa, (b) East Africa, and (c) southern Africa from 1901 to 2014 with respect to the long-term average climatology 1961-1990; based on the gridded on CRU TS 4.00 dataset. Red represents positive anomaly and blue a negative anomaly in temperature.

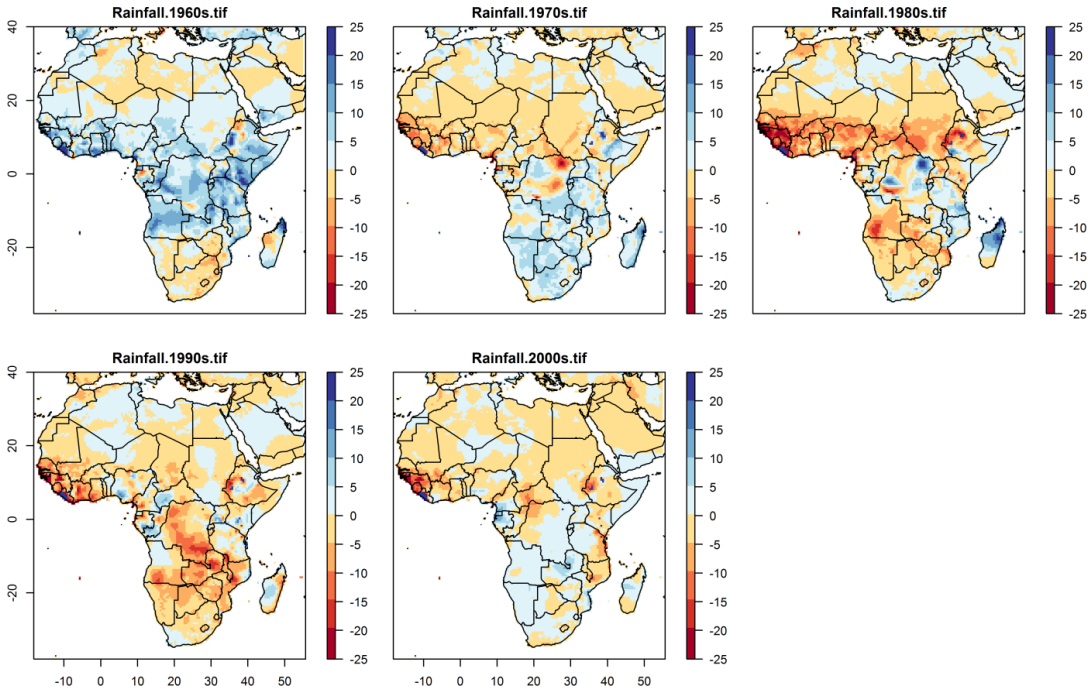

Figure 2.9: Decadal anomalies in rainfall 2014 with respect to the long-term average climatology 1961-1990; based on CRU TS 4.00 data.

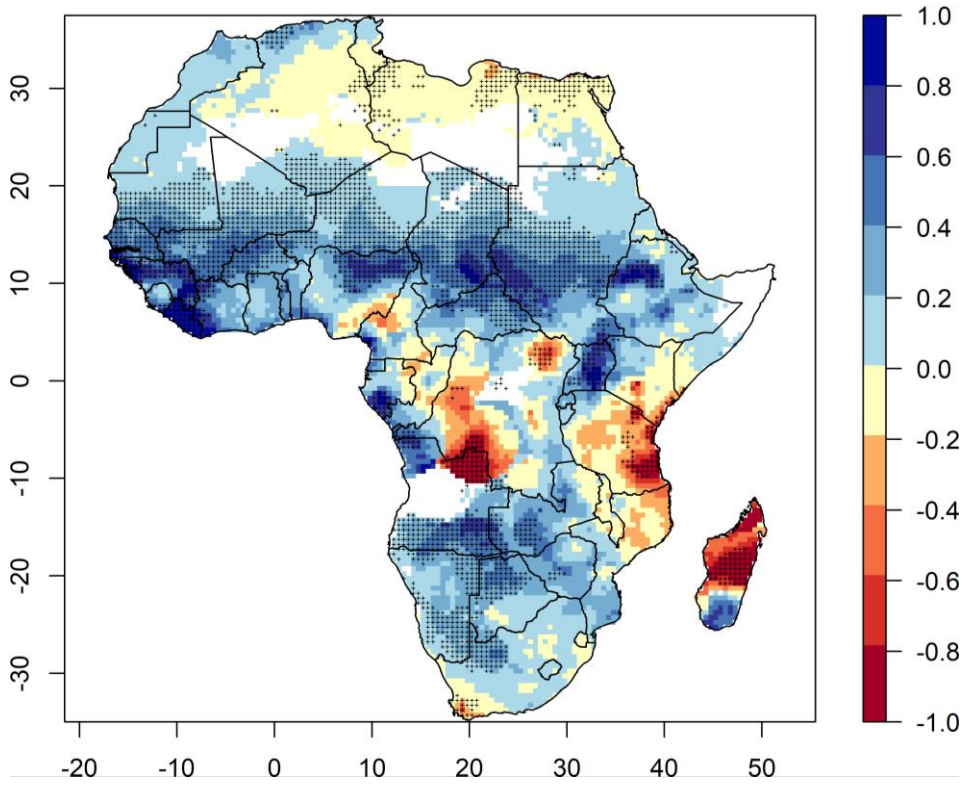

Figure 2.10: Observed trends in annual rainfall (mm per year) over Africa for the period 1982-2015 based on CRU TS 4.00 data. Crosses indicate grid boxes where the trend is statistically significant. White areas indicate no data.

2.5 Conclusion

This chapter presents observed trends in historical climate for sub-Saharan Africa in order to continue the understanding of climate change over the continent and to provide the necessary evidence to support the interpretation of recent changes in vegetation productivity and phenology presented in a subsequent chapter in this thesis (Chapter 4 and 5).

Observational records show that temperatures over Africa have been increasing over the last century at a rate of 2°C per century, which is more than twice the global rate of temperature increase. Increases in surface solar irradiance (SIS) are observed over parts of East Africa and southern Africa while declines are observed over South Africa and West Africa.

The rainfall time series is characterised by strong inter-annual and inter-decadal variability and there is little evidence for any signals of systematic change. Trends in rainfall need to be treated cautiously as most of the continent lacks sufficient observational data to draw robust conclusions on the trends in rainfall (Niang et al. 2014). Furthermore, rainfall across Africa varies considerably at the inter-annual and inter-decadal scale, which makes anthropogenic changes in rainfall harder to detect.

Continued monitoring and increased observational network across the continent will assist in the detection and attribution of changes in climate. While the information presented here is sufficient to assist in interpreting trends in vegetation dynamics over the last 34 years, further research is required to evaluate the trends in rainfall in the context of daily national and local weather station observations.

Chapter 3:

3. Spatial patterns of vegetation productivity and phenology over sub-Saharan Africa derived from the third generation GIMMS AVHRR NDVI product

3.1 Introduction

3.1.1 Background

The time-series of Normalized Difference Vegetation Index (NDVI) derived from the Advanced Very High Resolution Radiometer (AVHRR), can be used to provide spatially explicit information on seasonal vegetation dynamics (Justice et al. 1985; Reed 2006). More specifically, phenology derived from NDVI allows for the modelling of vegetation patterns related to climate variability and provides a better understanding of the drivers of changes as changes and shifts in seasonal cycles in response to climate change (Zhang et al. 2001; De Beurs & Henebry 2005; Klopper et al. 2006). In previous studies using AVHRR NDVI, phenology metrics were able to correctly capture the seasonality, productivity and inter-annual variability of vegetation dynamics across Africa (Heumann et al. 2007; Wessels et al. 2011).

NDVI is an indicator that uses the reflected radiation in the near-infrared and visible wavelengths to quantify the density of vegetation cover (Tucker et al. 1991). It is expressed as:

$$NDVI = \frac{(\text{Near Infrared} - \text{Red})}{(\text{Near Infrared} + \text{Red})}$$

NDVI values range between -1 and 1 with higher values indicating higher photosynthetic activity (Sellers 1985). Negative values represent the presence of water whereas values of less than 0.1 tend to represent bare soil or exposed rock surfaces (Zhang et al. 2017a). The relationship between NDVI and vegetation productivity and biomass is well established (Bellone et al. 2009). A number of studies have demonstrated the association between NDVI and field based observations of leaf area index (LAI) and aboveground vegetation cover and biomass (e.g. Prince 1991; Fensholt et al. 2004; Tucker et al. 2005; Anyamba & Tucker 2005).

By fitting mathematical functions to the NDVI time-series phenology metrics, such as the start and end of the growing season can be quantitatively determined (Zhang et al. 2003; Jönsson & Eklundh 2004; De Beurs & Henebry 2005; Reed 2006; Wessels et al. 2010; de

Jong et al. 2011b; Eklundh et al. 2012; Vrieling et al. 2013). The time-series analysis program, TIMESAT for example, was specifically developed for the investigation and extraction of various phenology parameters from remotely sensed time-series data (Jönsson & Eklundh 2004). TIMESAT has been used in a number of studies assessing vegetation phenology based on (e.g. Heumann et al. 2007; Wessels et al. 2010; Tan et al. 2011; Davis et al. 2017; Cho et al. 2017).

3.1.2 Objective and rationale

In this chapter, the AVHRR NDVI3g times-series is used to characterise baseline phenological patterns over sub-Saharan Africa. The high temporal frequency of the data (16-day intervals) is sufficient for phenological studies. The first section of the chapter provides a description of the NDVI3g dataset including the limitations of the AVHRR instruments and the methods of pre-processing used to circumvent some of these issues. The second section then describes the methodology used to extract seasonal parameters from the AVHRR NDVI3g time-series using TIMESAT version 3.2 (Lund University & Malmo University, Lund & Malmo, SE) (Eklundh & Jönsson 2012). The metrics derived from this process are used in Chapter 4 and 5 to assess the relationship between vegetation and spatial and temporal patterns of climate variability and to detected changes in vegetation across the entire SSA region in the context of climate change.

3.2 Methodology

3.2.1 Description of AVHRR NDVI3g product

The 8 km resolution AVHRR NDVI dataset constructed by the Global Inventory Modelling and Mapping Studies (GIMMS) project is now in its third generation (referred to as NDVI3g) and spans the period from July 1981 to December 2015. The time-series contains two maximum-value NDVI composites per month. The data was produced by NASA Global Inventory Modelling and Mapping Studies (GIMMS) and downloaded from https://ecocast.arc.nasa.gov/data/pub/gimms/ (version 2). Although the data record spans several different satellite AVHRR sensors (refer to Table 3.1), considerable efforts have been made to produce a consistent time-series (Fensholt et al. 2006; Pinzon & Tucker 2013). Data from NOAA-9 was used from September 1994 until January 1995 when NOAA-11 malfunctioned and its replacement NOAA-13 failed shortly after launch (Pinzon & Tucker 2013). The estimated overall uncertainty measurement of the dataset is ± 0.005 NDVI units throughout the time-series (Pinzon & Tucker 2013).

As with the original NDVI GIMMS dataset the third generation takes into account the effects of calibration loss, orbit drift, and volcanic eruption (Tucker et al. 2005). Furthermore, this new dataset aims to improve calibration and the cloud masking (Pinzon & Tucker 2013). To

demonstrate the dataset, the long term average and variance of NDVI over Africa is shown in Figure 3.1. The relationship between annual rainfall totals (CRU TS 4.00) and NDVI3g is shown graphically (Figure 3.1C) based on values averaged over of the SSA region (R^2=0.8).

There are however certain drawbacks of NDVI that can limit the identification and attribution of changes in vegetation cover:

- Over arid regions, seasonal variations atmospheric aerosol content, such as dust, and background soil colour are like to result in substantial variations in NDVI that are not accompanied by actual observed changes in vegetation (Huete & Tucker 1991; Pinzon & Tucker 2014a).
- Since NDVI is based on the red and Near Infrared (NIR) portion of the electromagnetic spectrum it tends to saturate in densely vegetated areas such as the tropical forests of Africa (Mutanga & Skidmore 2004). This is demonstrated by the asymptotic relationship observed between NDVI and rainfall in Figure 3.1.
- Trends derived from NDVI in the tropical regions are likely to be affected by the decline in NDVI in mid-1991 due to the Pinatubo eruption and subsequent cooling (Pinzon & Tucker 2013).

To attempt to overcome these constraints the data from these regions and periods are treated with caution and a variety of different trend assessment methods including breakpoint detection are utilised in Chapter 5 in order to present a robust assessment of changes in vegetation over Sub-Saharan Africa. In order to assess the suitability of the AVHRR NDVI3g it was compared it the MODIS Enhanced Vegetation Index (EVI) for overlapping years between 2001 and 2013 (Figure 3.2).

The MODIS EVI has often been used as an alternative to NDVI. The EVI index is more effective than NDVI in capturing a wide range of canopy densities and is less sensitive to atmospheric and soil effects (Huete et al. 2002; Zhang et al. 2005; Martiny et al. 2006). The MODIS EVI dataset (500 m resolution) was resampled to match the 8 km grid size of the NDVI3g dataset and a pixel-wise liner regression run.

A high correlation between AVHRR NDVI3g and MODIS EVI (R^2=0.96) is observed over sub-Saharan Africa indicating a good correspondence between the two products (Figure 3.2). Low R-values are associated with humid tropical forests of West Africa and eastern Madagascar, which experience a high percentage of cloudy days per year (refer to Appendix B Figure B.1). Clouds and poor atmospheric conditions tend to lower NDVI values (Chen et al. 2004) and result in sudden drops in NDVI time-series, which should be regarded as noise and should be removed from the time-series through smoothing techniques (Pettorelli et al. 2005).

Table 3.1: List of National Oceanic and Atmospheric Administration (NOAA) polar orbiting environmental satellites change times used for the GIMMS dataset (Pinzon & Tucker 2013).

AVHRR Instrument	Start Date	End Date
NOAA-7	July 1, 1981	February 8, 1985
NOAA-9	February 11, 1985	November 7, 1988
NOAA-11	November 11, 1988	September 19, 1994
NOAA-9 (descending)	September 20, 1994	January 18, 1995
NOAA-14	January 19, 1995	October 31, 2000
NOAA-16	November 1, 2000	December 31, 2003
NOAA-17	January 1, 2004	January 2009
NOAA-18	December 20, 2005	Continuing
NOAA-19	February 6, 2009	Continuing

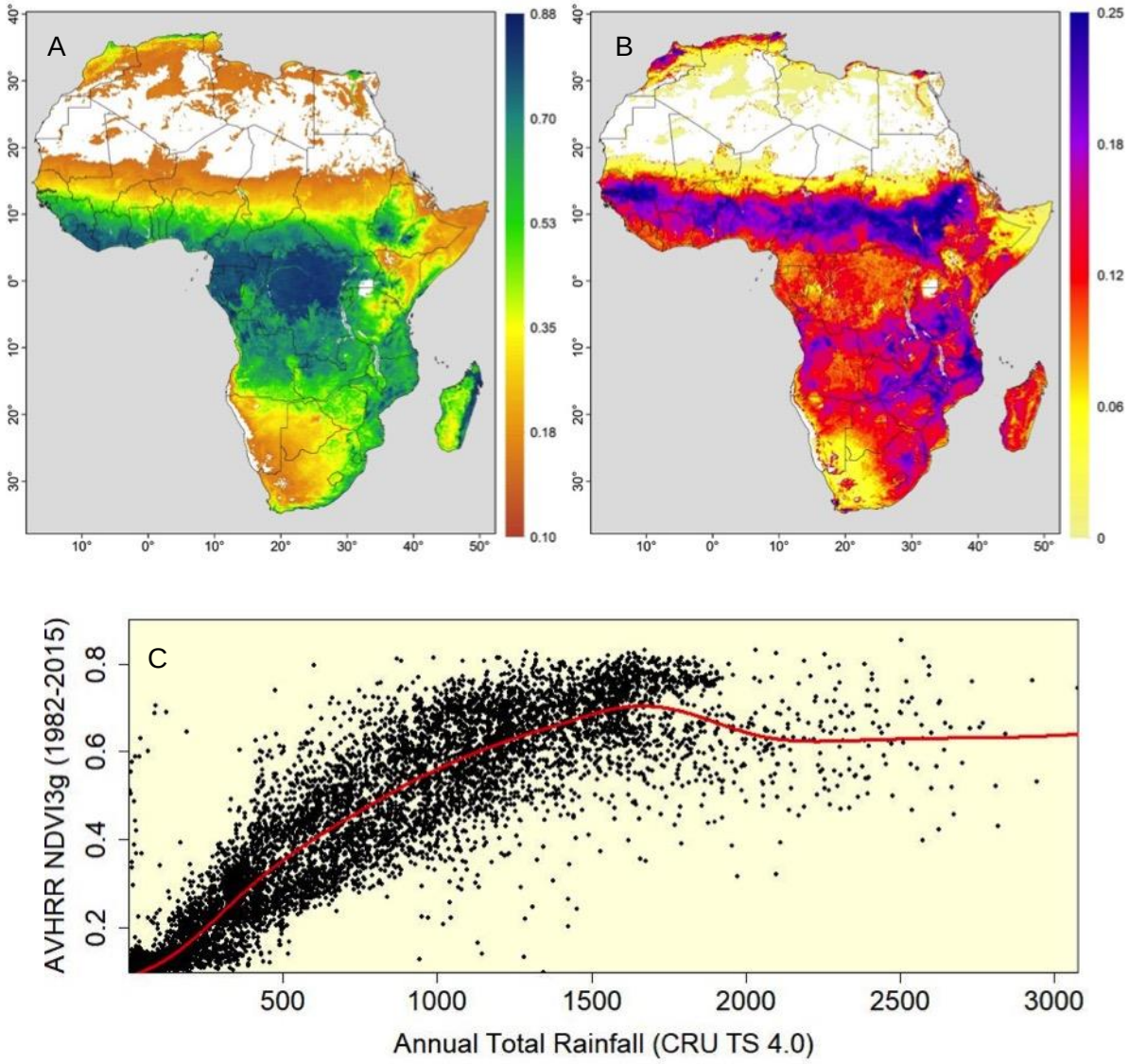

Figure 3.1: (A) Long-term median and (B) standard deviation of annual NDVI derived from AVHRR NDVI3g for the period 1982-2015. White indicates bare soil (NDVI < 0.1) and water bodies. (C) Scatterplot of mean annual rainfall and NDVI3g for 1982-2015 based on annual values averaged over Africa. The red line represents the fitted function.

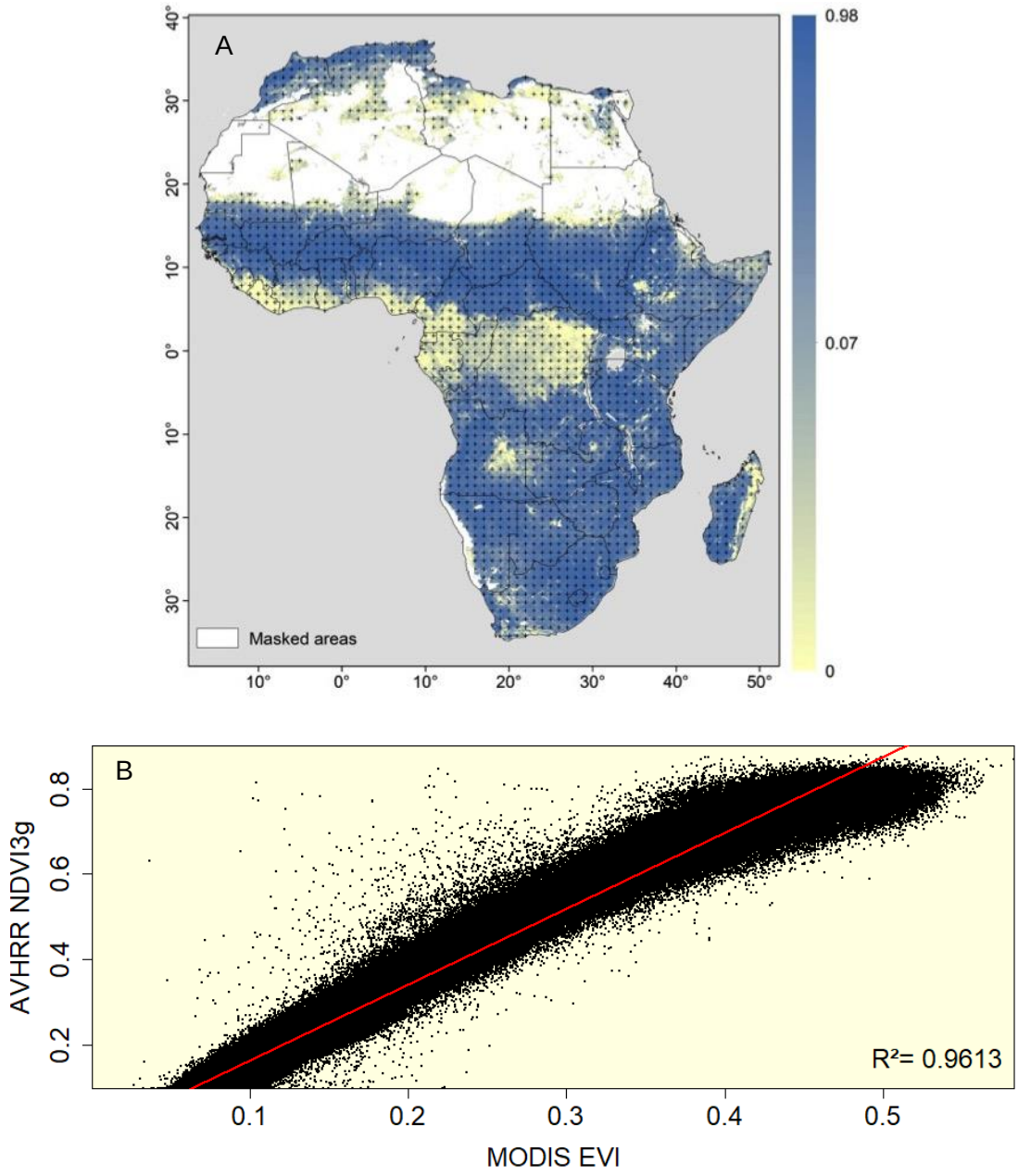

Figure 3.2: (A) Map of Pearson correlation coefficient (R-values) for monthly AVHRR NDVI3g and MODIS EVI for the period 2001 to 2013. The blue (red) colours indicate a positive (negative) correlation. Statistically significant pixels ($p < 0.05$) are hatched. White indicates bare soil (NDVI < 0.1) and water bodies. (B) Scatterplot of average AVHRR NDVI3g and MODIS EVI over Africa. The red line represents the linear regression.

3.2.2 Pre-processing of AVHRR NDVI3g

The time-series program, TIMESAT version 3.2 (Lund University & Malmo University, Lund & Malmo, SE) (Jönsson & Eklundh 2004; Eklundh & Jönsson 2012) was used in this study to (i) remove any residual contaminated pixels and (ii) extract growing seasons metrics from the time-series data (Figure 3.3). The TIMESAT application was selected in this study as it a computationally simple but robust method for extracting key phenology metrics (Wessels et al. 2010).

Before the application of the filter, NDVI values below 0.1 were masked from the dataset to remove the influence of background soil brightness in arid regions of SSA. Areas defined as croplands (irrigated, mosaic and rain-fed), water, artificial surfaces and associated urban areas (urban areas > 50%) in the GlobCover 2009 Version 2.3 (Bontemps et al. 2011) were masked out. These areas occupy 27.7% of the land-area of Africa with the bare areas making up 17.5% of that total (refer to Appendix B Figure B.2). While acknowledging that GlobCover 2009 land-cover database does not extend to 2015 to match the AVHRR NDVI3g time-series it provides the only available input on the extend of anthropogenically altered land surfaces over Africa. Although the NDVI signal in tropical evergreen forest is likely to saturate (de Jong et al. 2012; Mutanga & Skidmore 2004), these regions were not omitted from the analysis because abrupt changes and shifts in productivity may still be detectable.

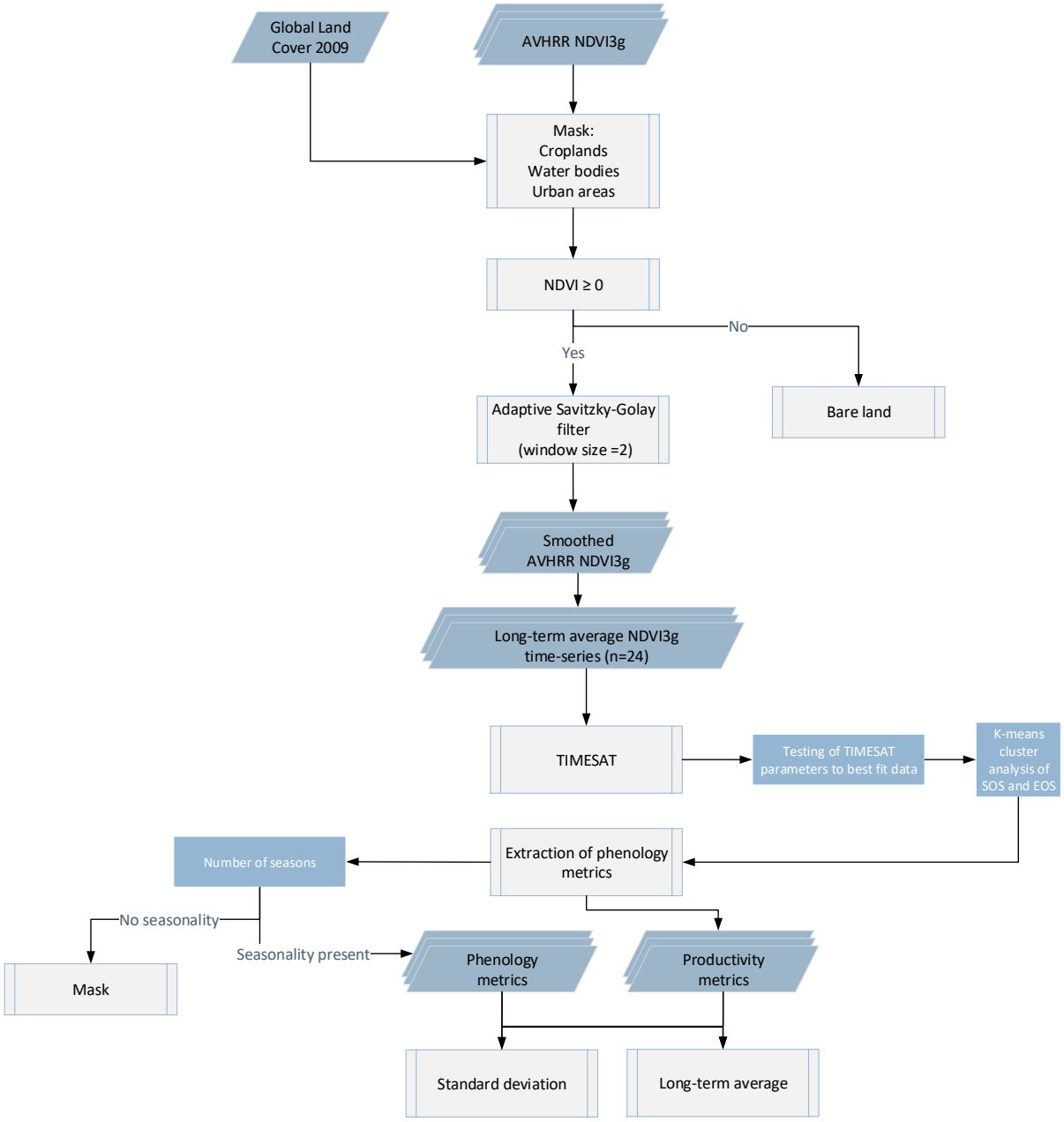

Figure 3.3: Flow diagram of the method used to prepare the AVHRR NDVI3g time-series

Adaptive Savitzky-Golay filter

In order to ensure that the dataset does not contain any residual noise the AVHRR NDVI3g time-series was smoothed using an adaptive Savitzky-Golay filter (Jönsson & Eklundh 2004). The filter was applied to the AVHRR NDVI3g time-series using TIMESAT version 3.2 (Eklundh & Jönsson 2012). This method was specifically developed by Chen et al. (2004) to smooth NDVI time series so that abnormally high and low values can be removed. The adaptive SG filter has been shown in previous studies to effectively distinguish noise from cloud and atmospheric contaminants (Wessels et al. 2010). The method iteratively applies

the Savitzky-Golay filter (Savitzky & Golay 1964) in order to fit the curve to the upper envelope of NDVI observations (Eklundh & Jönsson 2012).

In this study the window size (i.e. the number of successive observations) of the SG filter was set at 2 for 16-day composite data (i.e. 24-days). The second order polynomials were used in order to preserve the variations in NDVI while smoothing the time-series. The difference between the filtered and original time-series from 1982 to 2015 are summarised graphically in Appendix B Figure B.3 for West Africa, East Africa and southern Africa regions.

3.2.3 Extraction of vegetation phenology from the AVHRR NDVI3g time-series

Besides, eliminating the influence of clouds, the adaptive Savitzky-Golay filter provides smoothed NDVI curves that can be used for the determination of phenological parameters including start, end and length of the growing season. Furthermore, it allows for the calculation of NDVI values integrated during the growing season, which are frequently used as a proxy of vegetation growth during the primary growing season as it removes background noise from the data.

To overcome the challenge of capturing the dynamics multiple vegetation seasons across Africa, a test run was conducted on an average annual AVHRR NDVI3g (n=24) that was repeated three-times. The phenology metrics were computed from the fitted model function based on the central period of the dataset to prevent border effects at the beginning and end of the year. The start (end) of the growing season was set as the date at which the left (right) minima increased (decreased) to 50% (Figure 3.4). By using a dynamic threshold based method, the growing season is variable in timing and length. A 50% threshold was chosen as the optimal value based on the visual analysis of the fitted time-series curves for a number of individually sampled pixels taken from across SSA. After a number of tests, the number of envelope iterations was set as one and the seasonality parameter at 0.2 in order to capture dual seasonality in the dataset.

The test output from TIMESAT was then clustered into unique categories based on the start and end date of the growing season as well as the number of growing season using a k-means cluster analysis (refer to Appendix B Figure B.4 for the geographical extent of each cluster). Three primary geographical patterns emerged which matched the general patterns and seasonality of rainfall over SSA. Firstly, over the Horn of Africa the first growing season was observed between February and July and the second between September and December. Secondly, across the regions of south-western extent of SSA and the Sahel a primary vegetation season between April and November was observed. The remaining

southern African region experiences one vegetation season between November and May (Appendix B Figure B.4 provides the average annual phenology cycles for each cluster).

Using the full 34-year AVHRR NDVI3g time-series, a number metrics were extracted (Table 3.2) separately for each of these three unique regions using settings matching the seasonal characteristics. In areas that experienced two vegetation seasons the seasonality parameter at 0.2 (Cluster 1) whereas regions that experienced only one season the parameter was set at 1 (Cluster 2 & 3). For the regions over the southern hemisphere (Cluster 3) the year was defined as August to July compared to January to December (Cluster 1 & 2). This ensured that areas characterised by high (low) vegetation productivity, dual seasonality, as well as summer (winter) growth seasons are correctly identified. The outputs from each cluster were then mosaicked to create a time-series of each metric, which could be used to test for changes and shifts in seasonality over the region (refer to Chapter 4). The start and end of the season outputs are given as dates of the calendar year.

Since phenology can only be obtained for areas where NDVI signal follows a discernable seasonal pattern (Vrieling et al. 2013; Verger et al. 2016), the areas that did not exhibit seasonality were masked from the analysis. In this thesis 'phenology metrics' refer to the start, end, length, peak, and seasonal amplitude of the growing season while productivity metrics' refer to the large integral and maximum NDVI (Jönsson & Eklundh 2004). The large integral (LI) provides an important estimate of vegetation productivity over the growing season (Jönsson & Eklundh 2004; Eklundh & Jönsson 2012). The large integral and maximum the outputs for seasons 1 and 2 were incorporated into one image for each time-step in order to provide an estimate of the total productivity over SSA as well as to be able to include an estimate of productivity for areas that experience continuous growth throughout the entire year (e.g. tropical evergreen forests).

The long-term mean and the inter-annual variability, expressed as standard deviations (SD), were calculated for each of the metrics. For the 34-year period 33 full growing seasons were identified in regions experiencing a single growing season whereas 66 growing seasons were identified in regions experiencing dual seasonality.

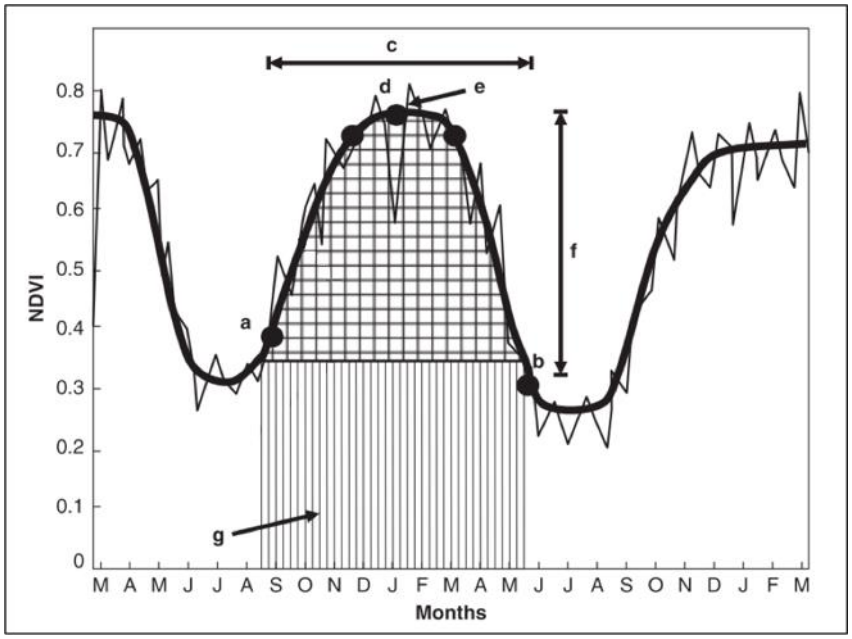

Figure 3.4: Phenology metrics, as defined in TIMESAT, extracted from the fitted functions using the adaptive Savitzky-Golay filter (after Jönsson & Eklundh 2004) where (a) start of season, (b) end of season, (c) length of season, (d) mid position of season, (e) maximum NDVI, (f) seasonal amplitude, and (g) large seasonal integral.

Table 3.2: Definitions of the metrics shown in Figure 3.4 (after Jönsson and Eklundh, 2004)

Metric		Description
Start of growing season	SOS	Increase to 50% of seasonal amplitude as measured from the left minima of curve
End of growing season	EOS	Decrease to 50% of seasonal amplitude as measured from the right minima of curve
Length of growing season	LOS	Length of time from start to end of season
Mid position of season	MID	Mean position/date of the seasonal peak
Seasonal amplitude	AMP	Difference between the maximum and minima of the curve
Maximum NDVI	MAX	Largest data value for the fitted function during the season
Large integral	LI	Estimate of total vegetation production

3.3 Results and Discussion

3.3.1 Number of growing seasons and NDVI3g amplitude

Two growing seasons were identified over the Horn of Africa (Figure 3.5a), which experiences a bimodal rainfall regime (refer to Appendix A Figure A.2). Bimodal vegetation patterns over this region have been demonstrated by a number of studies (Davenport & Nicholson 1993; Anyamba et al. 2002; Vrieling et al. 2013; Clements et al. 2014). Dual seasons are also detected over the northern extent of the Sahel and over south-western of South Africa and Namibia. Over South Africa these bimodal regions could be indicative of the transition zone between summer and winter rainfall regimes. The bimodal areas of Namibia and Sahel are located along the boundaries of arid desert regions which areas are constrained by water availability. These pixels would also be indicative of be artefacts in the dataset. Seasonality is absent from parts of the Congo Basin, West Africa, and eastern region of Angola. The vegetation over central Africa is characterised by dense evergreen tropical forests with high average NDVI values greater than 0.75 (refer to Figure 3.1). These areas were excluded from the analysis of start, end and length of the season.

The amplitude, of NDVI3g (Figure 3.5b) follows the general pattern of the distribution of biomes over Africa with the highest amplitudes around 0-10° latitude and parts of southern Africa. The vegetation cycle in these regions follows a distinct seasonal cycle of growth. The lowest amplitudes are observed over semi-arid regions of Sahel, East Africa and southern Africa where NDVI3g values are generally lowest. Over central Africa the amplitudes are fairly low due to the abundance of rainfall throughout the year.

3.3.2 Spatial patterns of long-term phenology

The spatial pattern of the derived phenology over Africa (Figure 3.6 to 2.9) reflects the distributions of climatic drivers, length of rainfall season (refer to Appendix B Figure B.5) and biomes. The pattern of maximum and large integral (LI) metrics derived from the AVHRR NDVI3g reflects the characteristics of rainfall where higher (lower) vegetation productivity is observed over higher (lower) rainfall regions (Figure 3.6). The highest variability in maximum NDVI and LI is observed over south-eastern coastline of South Africa, which experiences both summer and winter rainfall, and tropical forest regions of central Africa, Mozambique and Madagascar.

Figure 3.7 shows the average start, peak and end of the vegetation season over Africa for uni-modal regions in the first panel and for second season over bimodal regions. The first and second season refer the first and second SOS dates of calendar year. Over the Sahel the season starts in July and then shifts earlier to March-April southwards over 0-10° latitude. The vegetation season peaks in August-September over most of this region with the EOS

occurring in September over the Sahel and November-December over the 0-10° latitude. Consequently, the season is considerably shorter over the Sahel (Figure 3.9). The length of the season over the Sahel demonstrated a high inter-annual variability most likely a result of this region being water constrained. These patterns are in agreement with climatic patterns of SSA and the movement of the ITZC northwards during the boreal summer. Despite different NDVI time-series and phenology extraction methods, these patterns are consistent with those found by Heumann et al (2007). The pixels in the second season over Sahel appear to be artefacts in the data and are likely to not be representative of actual vegetation in the region.

Over the majority of East Africa two vegetation seasons are observed with the first starting in April, peaking in May and ending in June and the second starting in September-October, peaking in November and ending in December. The length of the season over these bimodal zones tend to be fairly short (2-4 months) as they occur in semi-arid climate with low NDVI values of less than 3.5 (Figure 3.1). The second season is slightly longer relative to the first occurring over four months compared to the first. The March to May rainfall season in East Africa tends to be longer than the October to November rains and are often referred to as the “long rains” and “short rains” respectively (Herrmann & Mohr 2011; Vrieling et al. 2013). The response of vegetation in the second vegetation season as observed here could be a result of a lag in response to rainfall in the first season. Furthermore, the second season tends to be more variable in SOS, EOS and LOS than the first. Climatology studies over East Africa have found that the majority of the variability in rainfall is associated with the second rainfall season (short rains) (Liebmann et al. 2014; Nicholson 2015) and this could account for the variability in vegetation phenology observed in the second season (Figure 3.8).

A clear gradient is observed over southern Africa with the majority of the region experiencing SOS in October-November, peak in January-February, and EOS in May-June. The average LOS over this region is between 4 and 8 months with regions closer to the equator experiencing longer seasons than those closer to the Kalahari Basin. This pattern follows that of the rainfall season with longer periods of rainfall experienced over central Africa (Appendix B Figure B.5). Over the boundary region where between summer and winter rainfall a later SOS is observed in January-March, peak in March-April and EOS in May-June. This region experiences a shorter vegetation season relative to other parts of southern Africa as well as higher variability in the both the SOS and EOS dates of up to 4 months. Other regions of Southern Africa demonstrating a high inter-annual variability in the LOS include areas of Mozambique and areas located on the boundary of the Congo Basin where no SOS/EOS was detected in the time-series. Over the south-west Cape of South Africa a different pattern is observed that matches the Mediterranean-type climate where rainfall occurs in winter as a result of the passage of mid-latitude cycles. The season lasts about 4 to

5 months with the SOS occurring in May-June, peak in August, and EOS in October-November. These patterns are consistent other studies for southern Africa (Wessels et al. 2010; Cho et al. 2017; Davis et al. 2017).

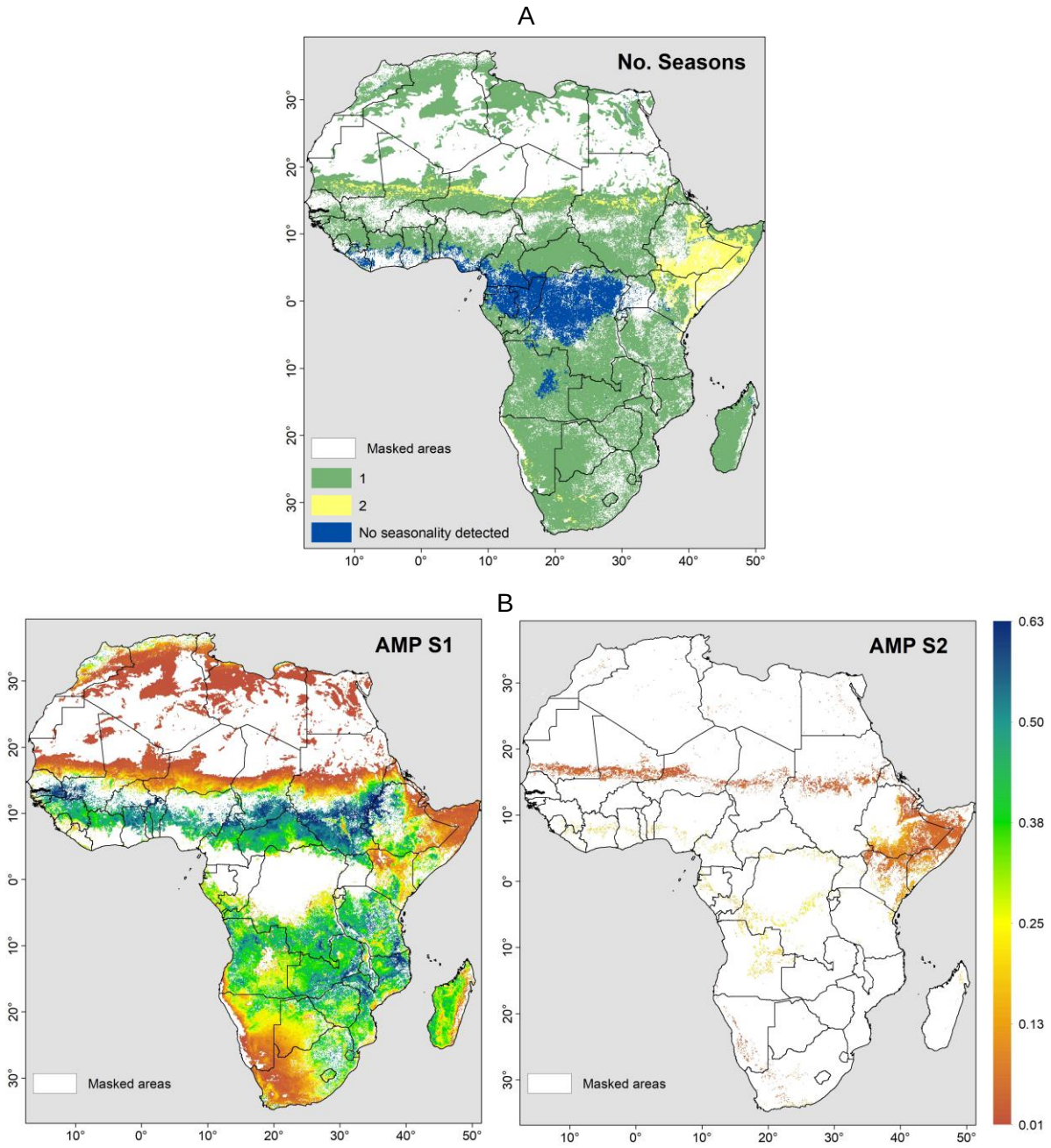

Figure 3.5: (A) The number of growing seasons detected, and (B) the seasonal amplitude of AVHRR NDVI3g for the first and second growing seasons. White regions indicate masked areas including bare soil (NDVI < 0.1), water bodies, and anthropogenic land uses.

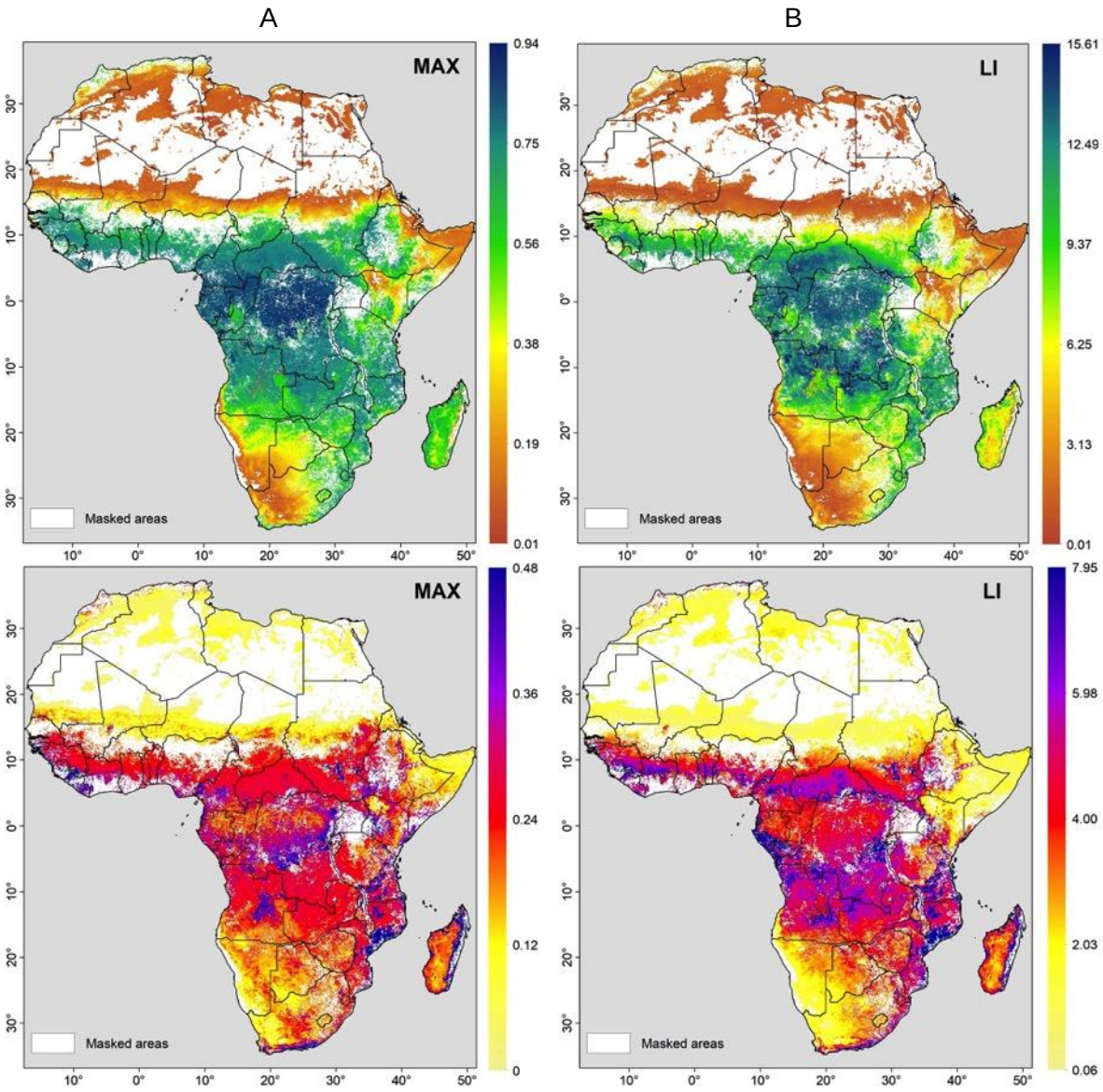

Figure 3.6: Average (top) and inter-annual variability (bottom), expressed as standard deviation in (A) maximum NDVI and (B) large integral derived AVHRR NDVI3g time series from 1982-2015. White regions indicate areas masked from the analysis.

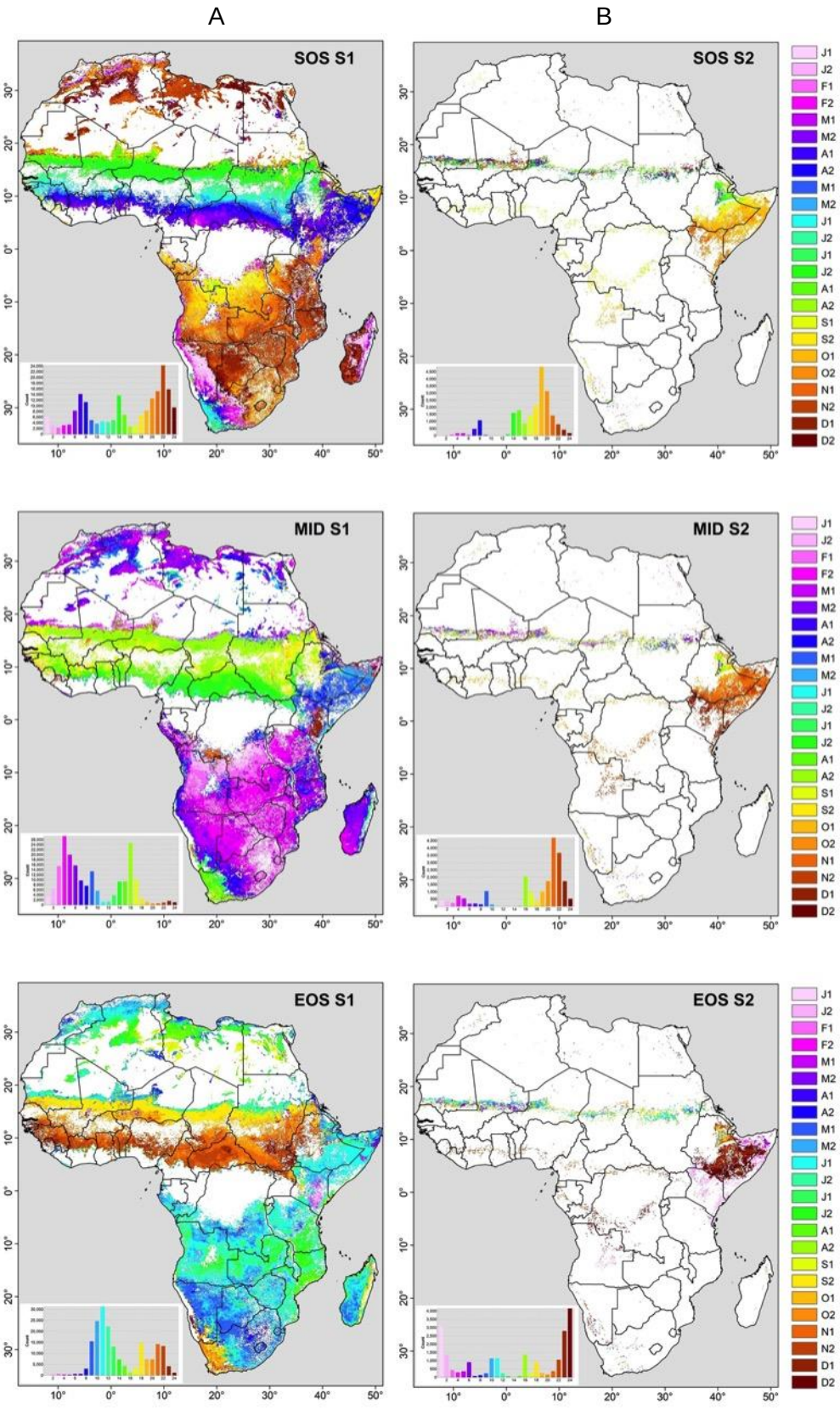

Figure 3.7: (A) average start date (SOS) of the growing season, its peak, and its end date and (B) average start, peak and end of the second season. The bi-weekly (16 day) periods are named by the first letter of the month (J,F,…D) followed by the number (1–2). Areas masked from the analysis and those with no seasonality are shown in white. The histograms inset into the figure denotes the number of pixels in each of the 16-day categories (n=24).

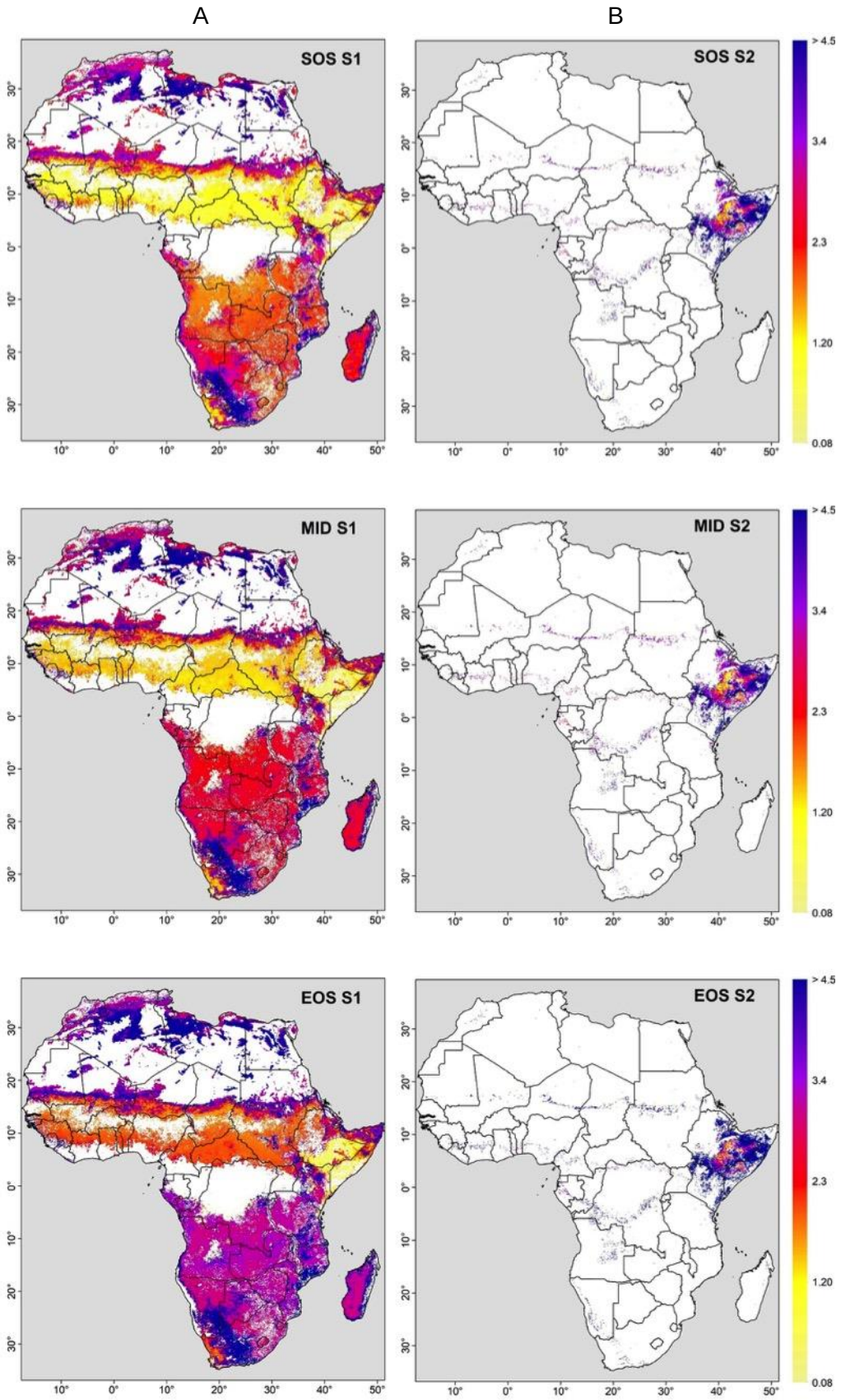

Figure 3.8: Same as Figure 3.7 but for inter-annual variability, expressed as standard deviation (in months) in start date (SOS) of the growing season, its peak, and its end date.

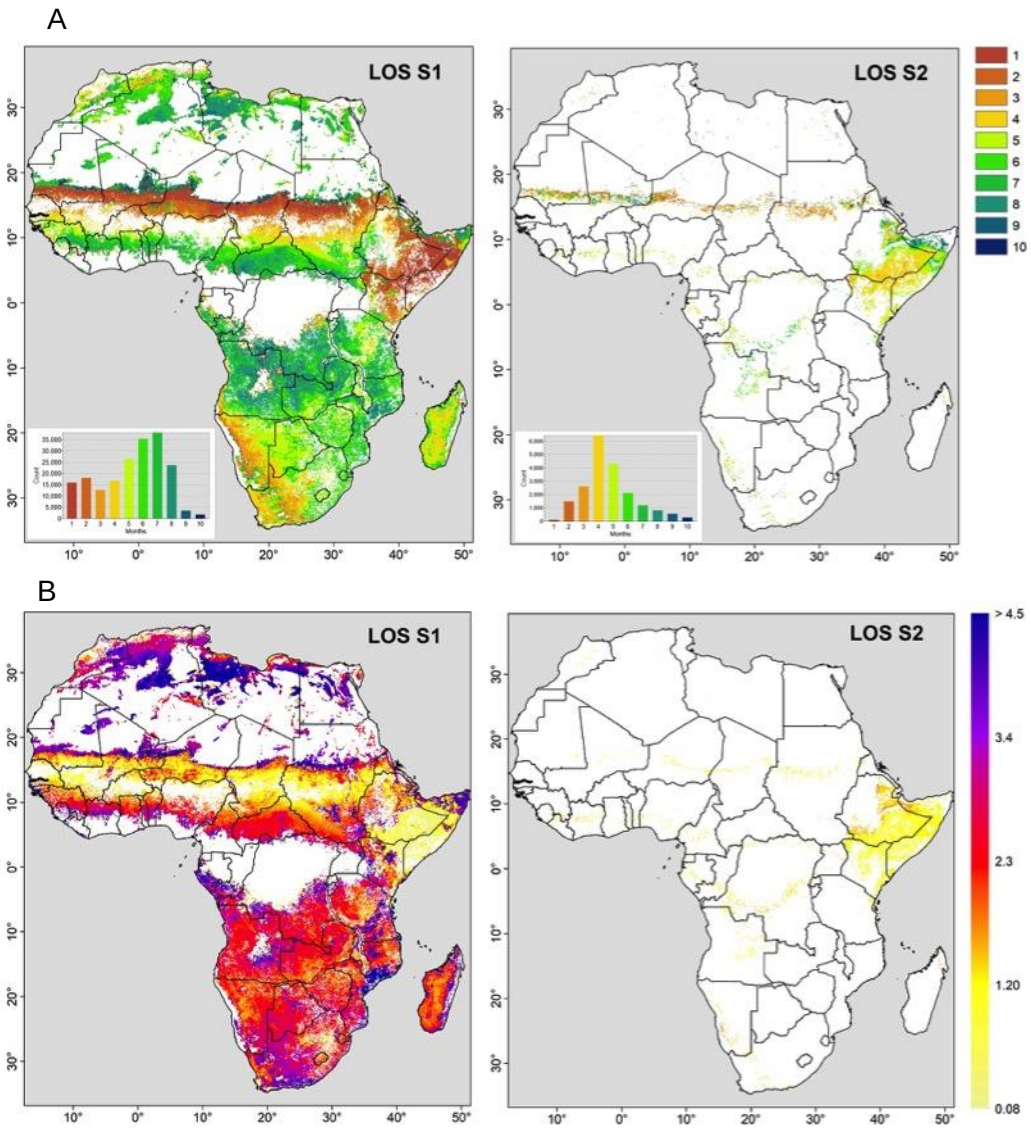

Figure 3.9: (A) Average length of the growing season (in months) for the first and second season of the year. The histograms inset into the figure denotes the number of pixels with a growing season length of between 1 and 10 months for each season. (B) Inter-annual variability, expressed as the standard deviation (in months) of growing season length.

3.4 Conclusion

Remotely sensed vegetation indices are a valuable tool for evaluating the rates of change and shifts or responses in vegetation to climate variability and change across SSA. Despite a relatively coarse spatial resolution, the AVHRR NDVI3g time-series is the one of the most popular indices due to its exceptional temporal record of terrestrial vegetation dynamics. The application of the adaptive Savitzky-Golay filter attempted to reduce the noise in the time-series particularly the observations associated with interference of clouds in the humid tropics. The adaptive Savitzky-Golay filter was further utilised to determine the phenological parameters of vegetation over SSA. This provided a comprehensive assessment of the spatial patterns phenology and productivity within the growing seasons. The patterns of seasonality described here are consistent with other studies over the region (e.g. Vrieling et al. 2013; Verger et al. 2016). Results from this Chapter demonstrated that the average length

of the season ranged from 9 months in sub-tropical humid climates to less than two months in semi-arid regions. The majority of the region experiences one primary vegetation season with the exception being areas across the Horn of Africa which experiences two vegetation seasons, which align with the timing of the long and short rains experienced in this region.

Characterising vegetation phenology and productivity over SSA is essential in the context of the larger thesis as it provides spatially explicit information on vegetation required to understand changes over the last 34 years. The phenology and productivity metrics presented here are used in this thesis to assess (i) fluctuations and shifts in vegetation activity across SSA (Chapter 5), and (ii) the role of climate in driving the observed shifts in vegetation (Chapter 4 & 5).

Chapter 4:

4. Inter-annual variations in vegetation dynamics over Sub-Saharan Africa in response to climate variability

4.1 Introduction

4.1.1 Background

As described in the previous Chapter, the climate of Africa is highly diverse and driven by a range of distinct climate systems. The natural variability in the climate of SSA, particularly rainfall, is driven by variations in sea surface temperatures and atmospheric circulation patterns. These include the El Niño-Southern Oscillation (ENSO), North Atlantic Oscillation (NAO), Antarctic Oscillation (AAO)[2], Atlantic Multidecadal Oscillation (AMO), and Pacific Decadal Oscillation (PDO). The best known of these, ENSO, is a recurring natural climate phenomenon that is characterised by fluctuations in sea-surface temperatures across the equatorial Pacific (Schreck & Semazzi 2004). Over the summer rainfall region of southern Africa warm (cool) ENSO events generally result in dry (wet) conditions (Lindesay 1988; Reason et al. 2000). The PDO tends to amplify the drought conditions in southern Africa during El Niño (Wang et al. 2014b). East Africa, however experiences above-normal rainfall during the short rain season of October through to December during warm ENSO events. Cold ENSO events bring a drier than average season during this short rain season (Ropelewski & Halpert 1987; Nicholson 1996; Indeje et al. 2000; Schreck & Semazzi 2004; Nicholson 2015). Over West Africa, there is evidence to suggest that ENSO events results in reduced monsoon flow and dryer than normal conditions of over the region but is not the dominant factor controlling rainfall (Camberlin et al. 2001; Joly & Voldoire 2009). A number of regional and global sea surface temperature (SST) anomaly patterns influence rainfall over the West Africa, including the Sahel (Nicholson 2000; Buontempo et al. 2010). At decadal time scales, warming over the North Atlantic (positive Atlantic Multidecadal Oscillation; AMO) leads to an increase in West African monsoon (WAM) rainfall (Rodríguez-Fonseca et al. 2015).

Variability in climate plays an important role in the growth of vegetation across the terrestrial ecosystems of sub-Saharan Africa (Zeng & Neelin 2000; Ugbaje et al. 2017). Understanding the response of vegetation to both mean climate states and climate variability provides the central basis to developing a comprehensive analysis of the impacts of climate change on

[2] AAO is also known as the Southern Annual Mode (SAM).

vegetation. The Normalised Vegetation Index is a sensitive indicator of seasonal and inter-annual climate patterns (Anyamba & Eastman 1996) and has been commonly used to assess the response patterns of vegetation to climate variability and change. Relationships with climate including large-scale oscillations and rising CO_2 have been documented by various modelling and correlation studies (e.g. Churkina & Running 1998; Nemani et al. 2003; Fensholt et al. 2012; Zhu et al. 2016). In general, vegetation growth is limited primarily by rainfall, temperature and solar radiation with the dominant factors being radiation over humid tropics, rainfall in semi-arid and arid regions, and temperature at high northern latitudes (Nemani et al. 2003). Wu et al. (2015) and Jong et al. (2003) demonstrated that climate explained 64% and 54% of the global variation in vegetation respectively. Over Africa, variability in NDVI is closely correlated with rainfall and temperature (e.g. Richard & Poccard 1998; Chamaille- Jammes et al. 2006; Rishmawi et al. 2016) but the responses to tend to vary spatially and at different time-lags.

4.1.2 Objectives and rationale

This study provides an analysis of the temporal and spatial response of vegetation productivity and phenology to climate across sub-Saharan Africa over the last three decades using the 8 km resolution AVHRR NDVI3g (third generation) product. The AVHRR NDVI3g time-series provides a sufficiently long enough time span to analyse such spatiotemporal relationships. This chapter focuses on 2 key aspects:

- Exploration of climatic controls on vegetation growth including the role of large scale climate oscillations and atmospheric CO_2; and
- Time-lag effects of the vegetation response to climate.

Climate parameters were selected under the assumption that vegetation is limited by water availability, temperature and solar radiation (de Jong et al. 2013) as well as atmospheric CO_2. Changes in any of these parameters may induce changes in vegetation productivity and phenology and in the NDVI proxy used in this study. While acknowledging that other environmental factors such as soil nutrients, Nitrogen deposition, and land use type and management have important effects on vegetation they are not included in this study.

4.2 Methodology

4.2.1 AVHRR NDVI3g data

De-seasoned time-series

Anomalies are the most commonly used form of de-seasonsing and are a measure of the deviation from the long-term mean. Using the smoothed AVHRR NDVI3g dataset, as

described in Chapter 2, monthly anomalies were calculated as a measure of the deviation from the long-term mean:

$$NDVI_{\sigma} = NDVI_{\alpha} - NDVI_{\mu}$$

Where $NDVI_{\sigma}$ are the respective monthly anomalies, $NDVI_{\alpha}$ are monthly values in month t year t, and $NDVI_{\mu}$ are long-term mean observation, respectively.

Growing season metrics

Phenological parameters extracted from the smoothed AVHRR NDVI3g time-series using TIMESAT version 3.2 (Eklundh & Jönsson 2012) include the start (SOS), end (EOS), length (LOS), mid position (MID), and seasonal amplitude (AMP) of the growing season (refer to Chapter 3 Section 3.2.3 for details on the method). Metrics integrating NDVI values over the growing season include the large integral (LI) and maximum NDVI (MAX). These metrics are often used as proxy measurements for seasonal vegetation productivity as they remove residual noise from the data, which may not be reflective of vegetation greenness during the primary growing season (Jönsson & Eklundh 2004; Eklundh & Jönsson 2012). Areas with no discernable seasonal patterns, such as the humid tropical forests of Africa, are masked from the phenology metrics but included in the productivity metrics in order to provide an estimate of productivity throughout the entire year (i.e. length of season was set as 12).

The productivity and phenology metrics are provided at a seasonal time-scale with one raster image given per growing season. For the 34-year period 33 full growing seasons were identified in regions experiencing a single growing season whereas 66 growing seasons were identified in regions experiencing dual seasonality (refer to Chapter 3 Figure 3.5).

4.2.2 Climate Data

Gridded monthly datasets of temperature and rainfall from A high-resolution (0.5°x0.5°) gridded monthly climate datasets provided by the Climatic Research Unit of the University of East Anglia (CRU TS 4.00) for the period 1982 to 2015 were used in this study (Harris et al. 2013).

Monthly incoming shortwave surface solar radiation (SIS) data was obtained from Monthly Surface Solar Radiation (W/m^2) Data Set - Heliosat (SARAH) derived from Meteosat satellite observations from 1983 to 2013 (Müller et al. 2015). Data for the years 2014 and 2015 were not available at the time of analysis.

Monthly average atmospheric CO_2 data for 1982-2015 was obtained from NOAA Earth System Research Laboratory (https://www.esrl.noaa.gov/gmd/ccgg/trends/data.html). Where data was missing interpolated values were used. Values represent the monthly mean CO_2 mole fraction, expressed as parts per million (ppm), determined from daily averages.

Monthly data for five oscillations were used in this study; ENSO, North Atlantic Oscillation (NAO) (Jones et al. 1997; Hurrell 2002), Antarctic Oscillation (AAO) (Gong & Wang 1999), Atlantic Multidecadal Oscillation (AMO) (Enfield et al. 2001), and Pacific Decadal Oscillation (PDO) (Mantua et al. 1997; Zhang et al. 1997). The Oceanic Niño Index (ONI) defined as the 3 month running mean of ERSST.v3 sea surface temperature (SST) anomalies in the Niño 3.4 region (5°N-5°S, 120°-170°W) was used as an index of the ENSO phenomenon. The NAO and AAO are patterns of variability in atmospheric pressure whereas the ENSO, PDO and AMO are patterns in sea surface temperature. The data was obtained from NOAA Earth System Research Laboratory (http://www.esrl.noaa.gov/psd/data/climateindices/list/).

4.2.3 Regression analysis

Considering possible time-lag effects, both monthly NDVI anomalies and annual phenological and productivity metrics were used to evaluate the statistical relationship between vegetation across SSA and various climatic factors including large scale sea surface and atmospheric pressure oscillations and increases in atmospheric CO_2 (Figure 4.1). Both time-series are used in this chapter in order to provide a comprehensive assessment of the response of vegetation to climate driving vegetation at the monthly and seasonal time-scales.

In order to limit the assessment to climatic drivers, anthropogenically-altered land surfaces, as defined by GlobCover 2009 Version 2.3 (Bontemps et al. 2011), water bodies and bare soil (NDVI < 0.1) were masked from the analysis and result outputs (refer to Appendix B Figure B.2).

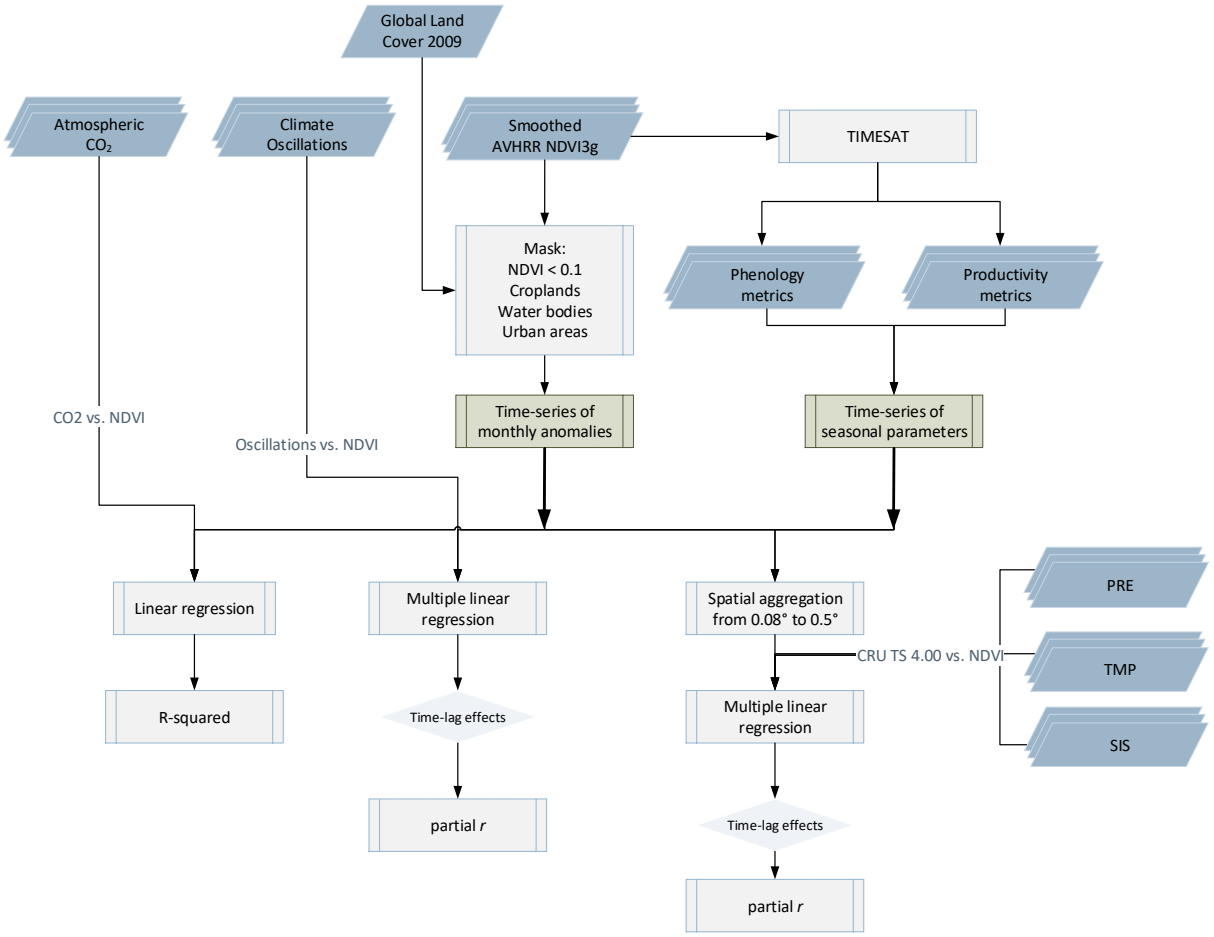

Figure 4.1: Flow diagram illustrating the methodological approach taken in this study to determine the relationship between AVHRR NDVI3g and (i) climate parameters, (ii) large-scale sea surface temperature and air pressure oscillations, and (iii) atmospheric CO_2

Response of vegetation to climate

A multiple linear regression analysis between the 34-year time-series of (i) monthly NDVI3g anomalies, (ii) metrics of growing season productivity (MAX and LI), and (ii) seasonality parameters (AMP, SOS, MID, EOS, and LOS) and each of the 3 climatic factors was performed to determine the response of vegetation to climate. This technique has been shown by a number of studies to be useful in quantifying correlations of a multitude of signals in both climate and NDVI (e.g. Wang et al. 2003; Martiny et al. 2005; Zhang et al. 2005; Wu et al. 2015).

Since, the native spatial resolution of the CRU TS 4.00 climate data is 0.5°, the AVHRR NDVI3g data (0.08° resolution) and surface solar radiation data (0.05° resolution) were resampled to 0.5° using bilinear interpolation. Climate variables were used as the independent variables, whereas the NDVI3g anomalies and seasonal metrics, which represent variability in vegetation activities, were used as the dependent variables.

The partial correlation coefficients (partial *r*) indicate the strength of the relationship between two variables when the effects of one or more related variables are removed (Eastman

2009). For example, the partial correlation coefficient of NDVI and temperature uses the other four climatic factors as control variables. Partial *r* values, as with correlation coefficients, range from -1 to 1. The R^2 value, referred to as the determination coefficient of the regression of NDVI3g with the 3 climatic factors provides an overall indication of the strength of the relationship between NDVI and climate and of the spatial differences across the region.

The dependency of vegetation on climate was evaluated at different time-lag scales. Previous studies have found that vegetation responds to climate in the preceding months (e.g. Richard & Poccard 1998; Wang et al. 2003; Herrmann et al. 2005; Wu et al. 2015). For the NDVI3g anomaly time series, time lags for zero and 3 months were considered. A lag of zero implies that NDVI3g and climate variables are being compared at corresponding months whereas a negative lag of 3 months shifts the climate variable by 3 months earlier. Since the productivity and phenology metrics are provided at a seasonal scale (1 or 2 growing seasons per calendar year), time lags for zero and 1 year were considered. Partial correlation coefficients for the first growing season are presented in this chapter while those for the second season are provided in Appendix C.

Response of vegetation to CO_2

The relationship between the NDVI3g and atmospheric CO_2 was calculated using a pixel-wise linear regression (r^2 value) of the monthly anomaly time-series from 1982 to 2015. To determine the response of the productivity and phenology metrics to CO_2, monthly CO_2 values were aggregated annually and a pixel-wise regression run and the different combinations. This analysis and resultant r^2 values provide an indication of the strength of each the relationship.

Response of vegetation to large-scale climate oscillations

Partial correlation analysis was used to investigate the relationship between NDVI3g anomalies and SST oscillations (ENSO, PDO and AMO) and atmospheric pressure oscillations (NAO and AAO) over sub-Saharan Africa. There are known correlations of these sea surface temperature and atmospheric pressure oscillations with rainfall (e.g. Lindesay & Vogel 1990; Nicholson 2000; Schreck & Semazzi 2004; Rodríguez- Fonseca et al. 2011; Mohino et al. 2011) but limited studies, to date have investigates the role of these oscillations on fluctuations in NDVI. Time-series of the five oscillations investigated (refer to Appendix C Figure C.1) demonstrate the inter-annual and inter-decadal variability of sea surface temperatures and air pressure:

- The El Niño-Southern Oscillation, shown by the Oceanic Niño Index (ONI), cycle is characterised by fairly regular alternating periods of warming and cooling. El Niño refers to the warm phase of the cycle where above-average sea-surface

temperatures develop across the east-central tropical Pacific Ocean and below-average SST occur across the western Pacific ocean due to a change in wind patterns. The opposite state is called La Niña; the cold phase of the ENSO cycle (Nicholson 1996).

- The Antarctic Oscillation (AAO) is a low frequency mode of atmospheric variability south of 20°S which is defined by air pressure anomalies between the Antarctic and southern hemisphere mid-latitudes (Gong & Wang 1999).
- The Pacific Decadal Oscillation (PDO) is an inter-annual to inter-decadal oscillatory pattern of sea surface temperatures of the Northern Pacific (poleward of 20°N) where the positive phase is associated with a warmer tropical central Pacific and a colder extra-tropical northwest Pacific (Mantua et al. 1997; Zhang et al. 1997).
- The North Atlantic Oscillation (NAO) is a high frequency mode that is present throughout the year in the Northern Hemisphere and is characterised by fluctuations in atmospheric pressure over the polar-regions (Jones et al. 1997; Hurrell 2002).
- The Atlantic Multi-Decadal Oscillation (AMO) is a low frequency mode with cool (warm) phases lasting for 20-40 years at a time. It is characterised by long-duration variations in the sea surface temperature of the North Atlantic Ocean (Enfield et al. 2001).

The relationship was evaluated at different lag periods where a lag of zero would translate into simultaneous changes in NDVI3g whereas a lag of positive (negative) 3 would translate into 3 months after (before) the peak anomaly. Since there are known correlations between sea surface temperatures (SSTs) in parts of the oceans with rainfall (Reason et al. 2000; e.g. Linderholm et al. 2011; Siam et al. 2014; Zhou et al. 2015), the relationship between rainfall and large-scale climate oscillations was also evaluated.

To assess the relationship between 5 large-scale climate oscillations and each of the productivity and phenology metrics, the time-series of the SST and air pressure oscillations were first aggregated annually and then the multiple linear regressions applied to the different combinations (e.g. SOS versus the 5 climate oscillations). No lags were considered for the productivity and phenology metrics.

4.3 Results

4.3.1 Spatial patterns of inter-annual NDVI variation

The annual NDVI anomalies for the years 1982 to 2015 (Figure 4.2) demonstrate considerable inter-annual variability in NDVI over sub-Saharan Africa. Over the northern hemisphere tropics (0-20°N) negative anomalies were prevalent during the 1980s and in the early 1990s most noticeably during 1984. The region experienced below-normal rainfall during the 1980's (Figure 4.3) with the most severe drought conditions from 1983 to 1985

(Lamb 1980; Nicholson 2000). During the late 1990s and 2000s rainfall over West Africa started to slowly recover with positive NDVI anomalies observed over larger parts of the region.

The pattern of below normal NDVI observed between 1982 and 1984 is reflective at the continental scale with negative NDVI anomalies also observed over East and southern Africa. Positive anomalies in NDVI over East Africa persisted for the 1997/1998 years corresponding to above normal rainfall and warm ENSO event in 1997 (Anyamba & Eastman 1996). Negative anomalies are observed in 1984, 2005, and 2009 and correspond below normal rainfall. Over Southern Africa, negative anomalies in 1992/1993 and 2015, tend to coincide with warm ENSO phase and low rainfall events over the region. Positive NDVI anomalies are observed in 1997, 2006, and 2011.

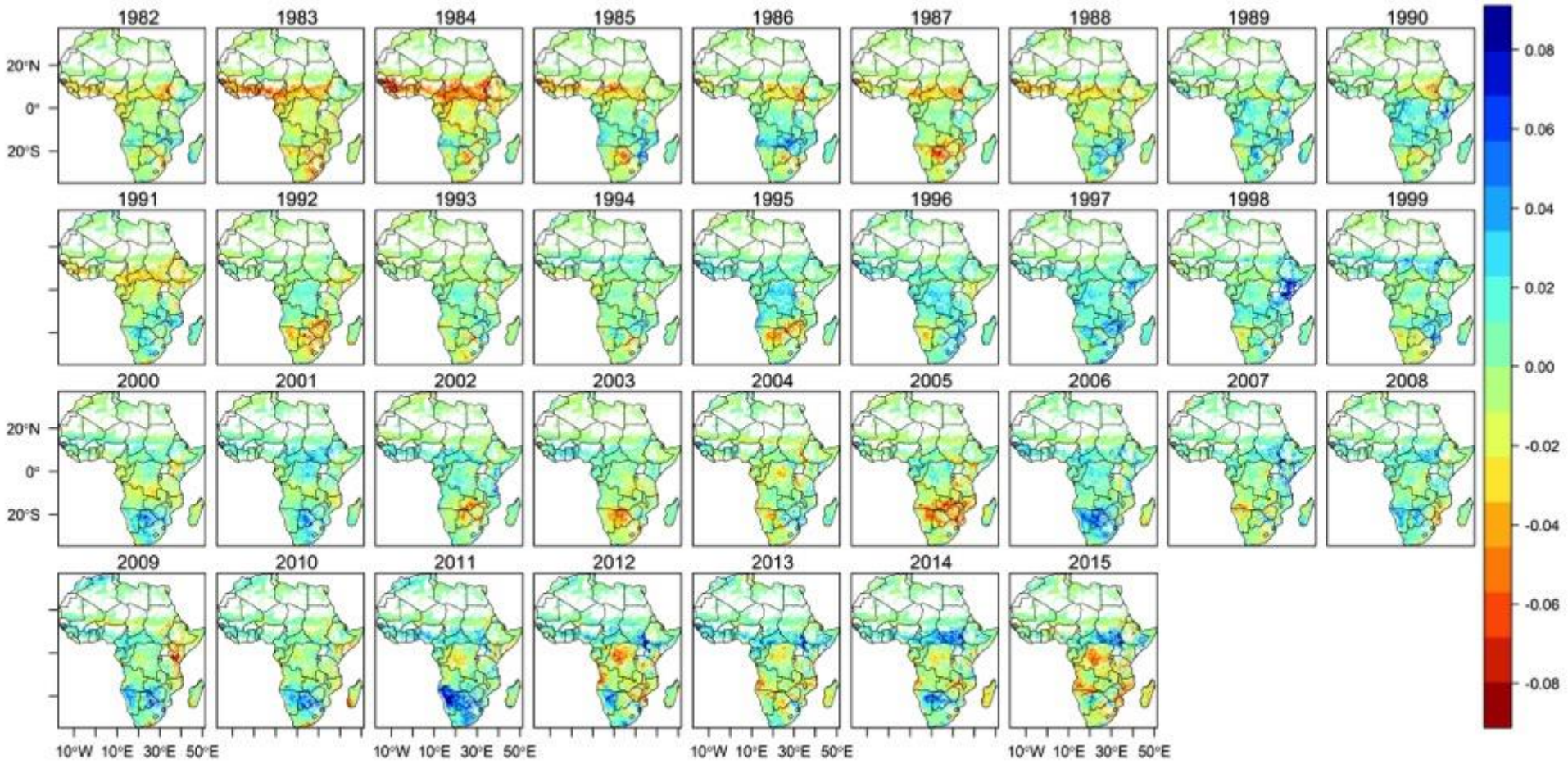

Figure 4.2: Average annual anomalies derived from AVHRR NDVI3g for the years 1982 to 2015 expressed as departures from the long-term mean. White regions indicate masked areas including bare soil (NDVI < 0.1), water bodies, and anthropogenic land uses.

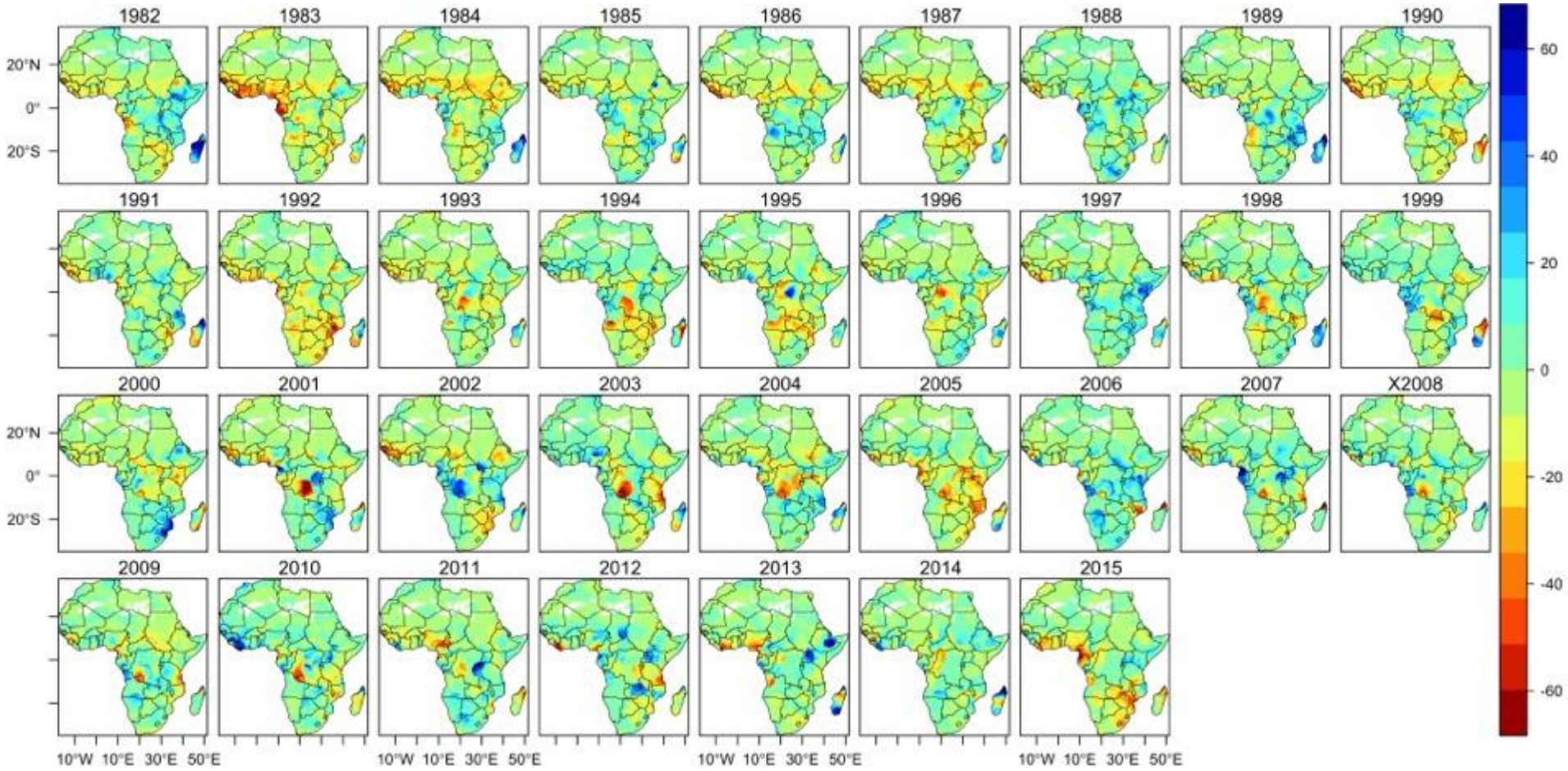

Figure 4.3: Average annual rainfall anomalies for 1982 to 2015 with respect to the long-term average climatology 1961-1990 derived from CRU TS 4.00 data. White areas indicate incomplete or missing data.

4.3.2 Response of vegetation to climate factors

Overall, the variation in the three climate factors accounts for up to 70% of the vegetation growth over the semi-arid regions of SSA with the maximum NDVI3g (MAX), large seasonal integral (LI), and seasonal amplitude showing the strongest response to climate conditions in the previous year (Figure 4.4). Weaker relationships are observed between NDVI3g anomalies and climate metrics with climate accounting for between 40 and 50% of the vegetation growth (Appendix C Figure C.2). Strong associations with climate, up to 70%, are also observed for the phenology metrics (Appendix C Figure C.2). Over parts of central and southern Africa, a weak relationship between climate and vegetation within the primary growing is observed (Figure 4.4).

Both productivity and phenology metrics are strongly correlated to rainfall over the Sahel, East Africa and parts of southern Africa (Figure 4.5, 3.6 and Appendix C Figure C.4). Time lag effects are evident over South Africa, Namibia, Zimbabwe, and Botswana with MAX, LI, AMP and LOS showing a positive response to rainfall in the previous season (time lag = -1). A negative relationship with the start (SOS) and peak (MID) of the season is observed of semi-arid regions suggesting that an increase in rainfall (time lag = 0) results in an earlier start and peak date of the season. Over southern Africa, the end of the season responds most strongly to rainfall in the previous season (time lag = -1) whereas over the Sahel and East African regions vegetation responds to rainfall in the same season (time lag = 0). Over other parts of Southern Africa and Madagascar (time lag = 0) a weak and in some cases negative correlation between productivity metrics and rainfall is observed.

In terms of the response to temperature, areas of Southern Africa and the Sahel demonstrate positive correlations (time lag = 0) with MAX NDVI3g (Figure 4.5). Similar patterns are observed for AMP and LI with the relationship being weaker for LI relative to MAX (Appendix C Figure C.4 and C.6). Negative correlations are observed over Namaqualand (time lag = 0) and over parts of South Africa, Mozambique and the Sahel with temperature in the previous season. Key differences are observed with NDVI3g anomalies where negative correlations are observed over southern Africa and the Sahel (Appendix C Figure C.5). Positive correlations between NDVI3g and temperature are observed in the preceding 3 months over areas of Central African Republic, Cameroon, and Uganda.

The response of NDVI3g to solar radiation demonstrates a fairly weak positive relationship with MAX NDVI3g and LI over central Africa, Madagascar and parts of South Africa (time lag = 0) with stronger relationship observed along the eastern coastline of South Africa extending into Mozambique (Figure 4.5 and Appendix C Figure C.4). Negative correlations with SIS in the previous year (time lag = -1) are observed over isolated areas of SSA including western South Africa, Zambia, Somalia, and Central African Republic. In addition, there is a negative relationship between seasonal amplitude (AMP) and solar radiation over most of central

Africa at time lag zero and over parts of Sahel and East Africa in the previous year (Appendix C Figure C.6). The response of other phenology metrics to SIS is not spatially consistent with a number of differing responses across SSA.

In terms of the role of atmospheric CO_2, strong correlations are observed between MAX NDVI3g over 0-10°N latitudinal band and particularly over Cameroon, Central African Republic and southern Sudan (Figure 4.7). This pattern is consistent with that of NDVI3g anomalies and large seasonal integral (LI) (Appendix C Figure C.9). NDVI3g in parts of southern Africa, western Madagascar and northern extent of the Sahel also demonstrate strong responses to CO_2. Since the atmospheric CO_2 has been steadily increasing over the last 34 years, the correlation could be indicative of positive trends in the NDVI time-series.

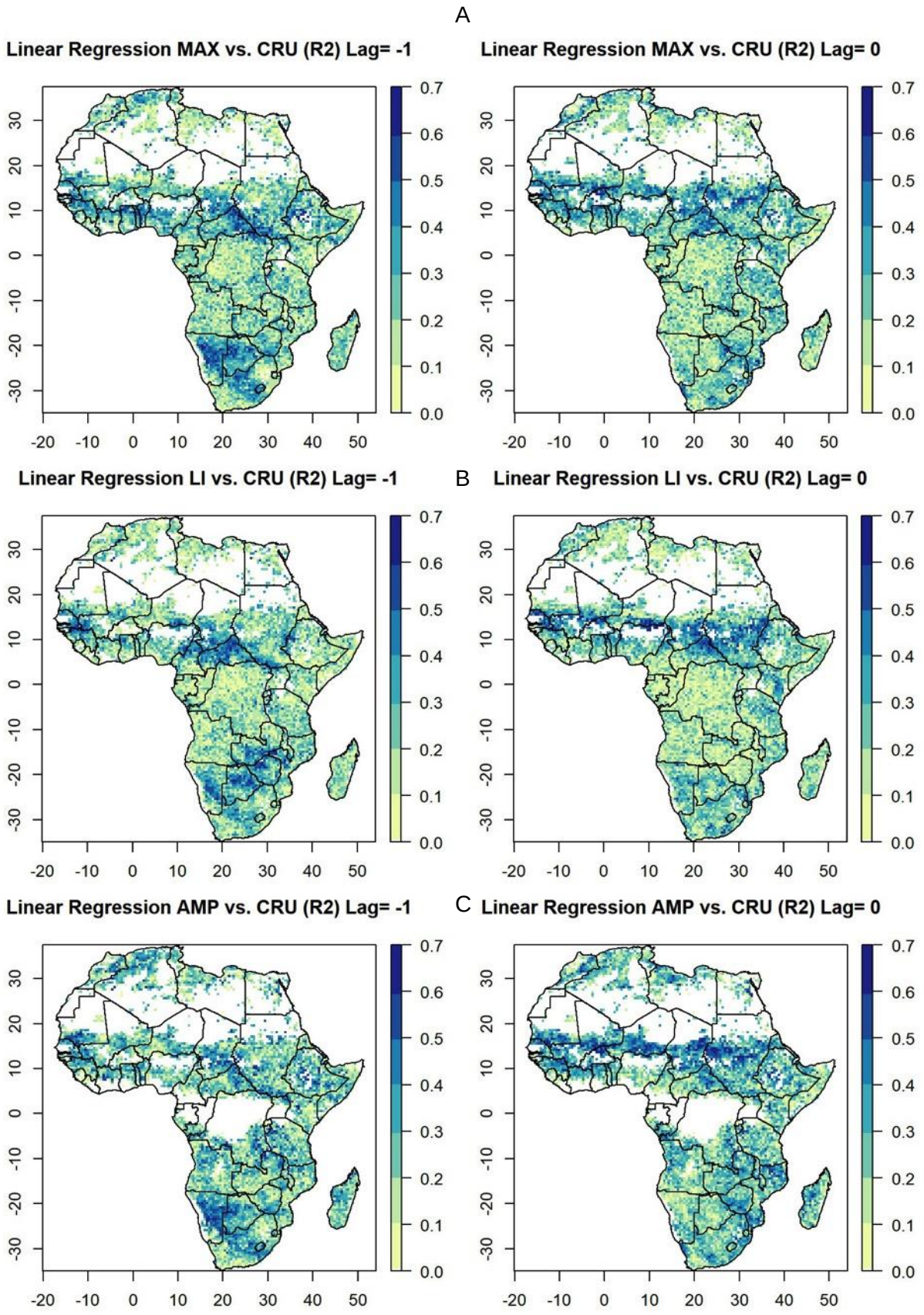

Figure 4.4: Spatial distribution of the determination coefficient (R2) of the multiple linear regression between (A) maximum (MAX) NDVI3g, (B) large seasonal integral (LI), and (C) seasonal amplitude (AMP) for the first growing season and climatic factors for the period 1982–2015 with considering time-lag effects. Two images are given per climate metric representing 1 year before the peak event (lag = -1), and peak occurrence (lag = 0). White regions indicate areas masked from the analysis.

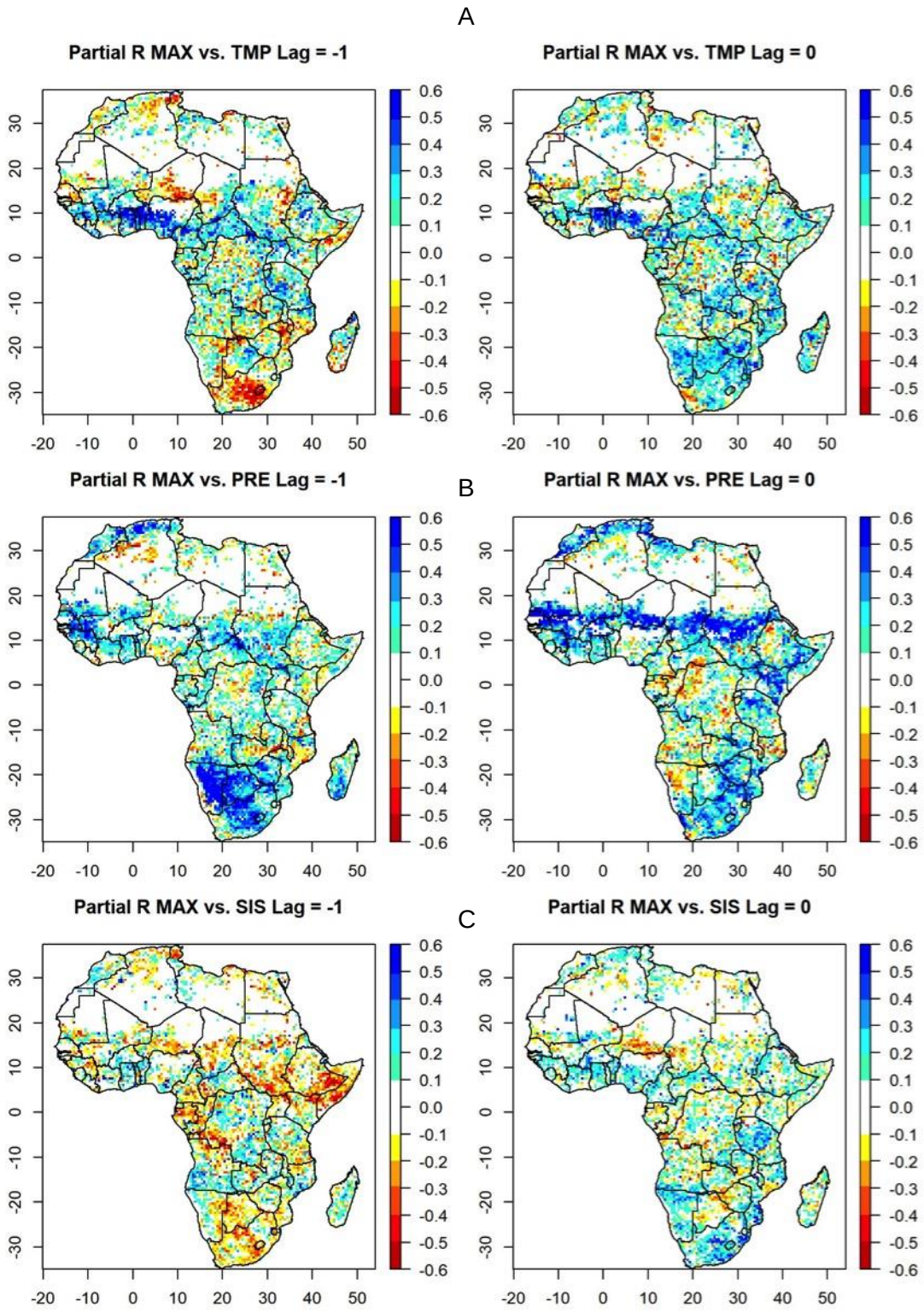

Figure 4.5: The responses of Maximum (MAX) NDVI3g for the first growing season to CRU temperature (TMP), precipitation (PRE), and solar radiation (SIS) considering time-lag effects. (A) Spatial distribution of the partial correlation coefficient between MAX and temperature (TMP) after controlling for precipitation (PRE) and solar radiation (SIS), (B) spatial distribution of the partial correlation coefficient between MAX and precipitation (PRE) after controlling for temperature (TMP) and solar radiation (SIS), (C) spatial distribution of the partial correlation coefficient between MAX and solar radiation (SIS) after controlling for temperature (TMP) and precipitation (PRE). Two images are given per climate metric representing 1 year before the peak event (lag = -1), and peak occurrence (lag = 0). The blue (red) colours indicate a positive (negative) correlation. White regions indicated pixels masked from the analysis.

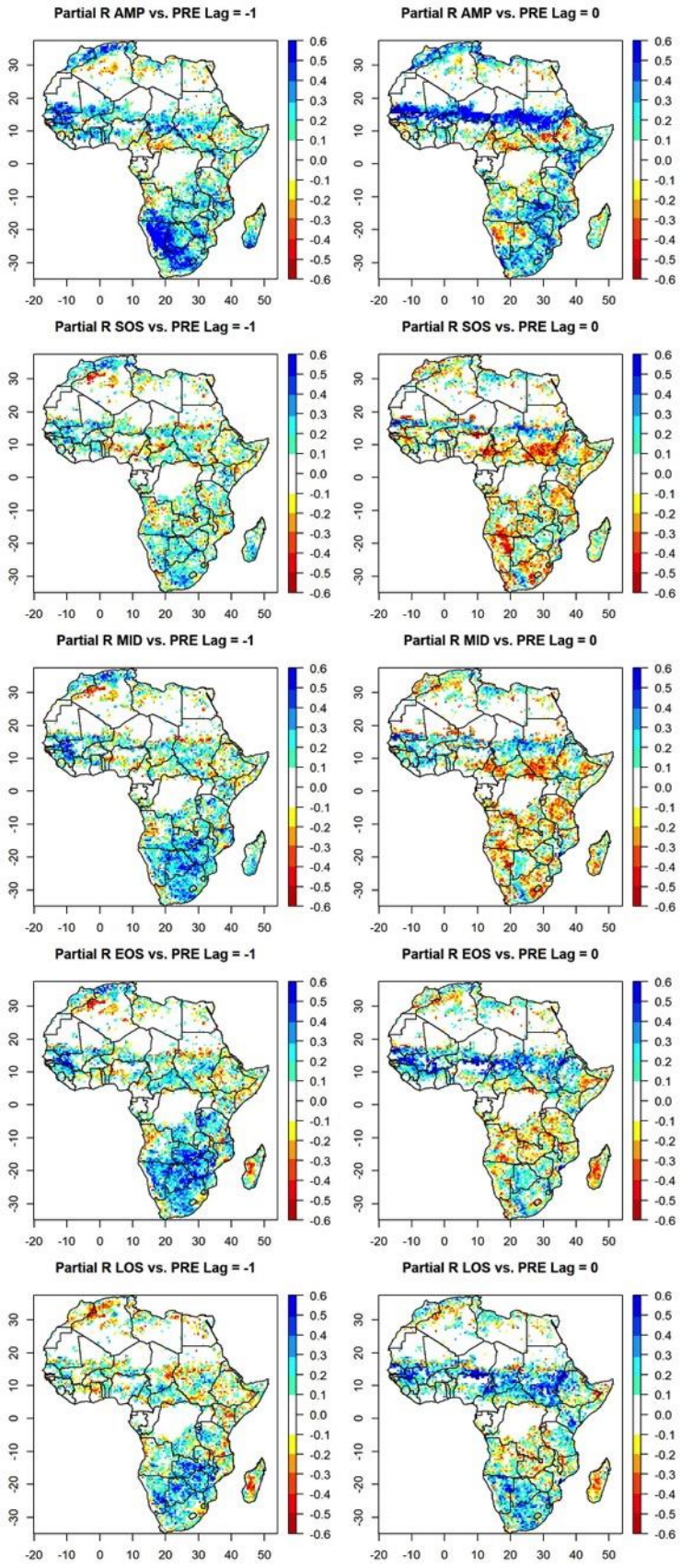

Figure 4.6: Spatial distribution of the partial correlation coefficients between phenology metrics (AMP, SOS, MID, EOS, and LOS) for the first growing season and precipitation (PRE) after controlling for temperature (TMP) and solar radiation (SIS). Two images are given per climate metric representing 1 year before the peak event (lag = -1), and peak occurrence (lag = 0). The blue (red) colours indicate a positive (negative) correlation. White regions indicated pixels masked from the analysis.

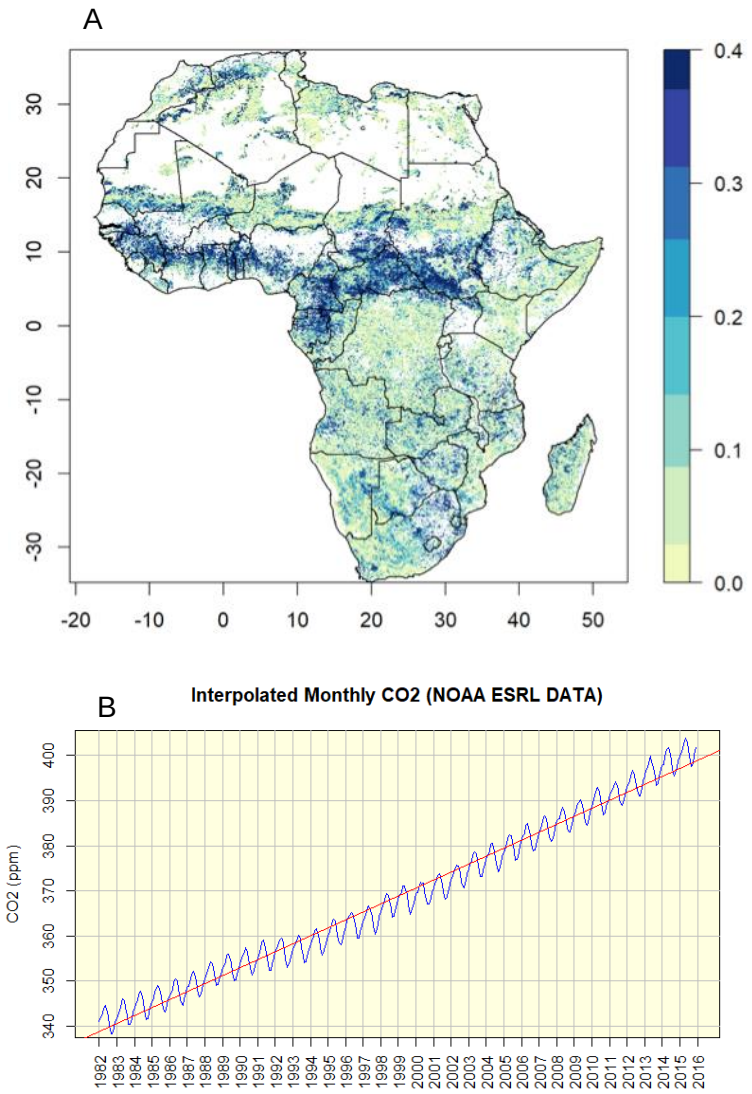

Figure 4.7: (A) Spatial distribution of the determination coefficient (R2) of the linear regression model between global monthly mean CO_2 values (ppm) and maximum (MAX) NDVI3g for the first growing season over Africa for the 1982-2015 period. White indicates masked areas with NDVI values < 0.1. The blue (red) colours indicate a positive (negative) correlation. (B) Time-series of monthly mean CO_2 values (ppm) from 1982-2013 with the red line indicating the linear trend.

4.3.3 Response of vegetation growth to large scale climate oscillations

The five large-scale climate oscillations are shown to affect NDVI3g across Africa to different degrees (Figure 4.8). In general, similar patterns are observed for rainfall (Figure 4.9). The partial correlation coefficients demonstrate that during the El Niño phase, lower vegetation productivity is observed over southern Africa compared to higher productivity over east Africa. The strongest relationship is observed over Southern Africa, particularly Zimbabwe and southern Mozambique, three months after the peak event (lag = +3), i.e. in March. For East Africa the relationship is strongest at the peak of the oscillation event (lag = 0), i.e. December. This suggests that vegetation in East (southern) Africa is responding to higher (lower) rainfall amounts associated with El Niño phase. This pattern is also observed for the partial coefficients between phenology and productivity metrics and Oceanic Niño Index (ONI) (Appendix C Figure C.10 and C.11). During the El Niño phase, a strong negative relationship is observed for MAX, LI and AMP metrics over southern Africa. Furthermore, a later start, earlier end and consequently a shorter length of the season are observed during the El Niño phase indicating restricted vegetation growth. The productivity and phenology metrics for the second growing season over East Africa show a positive relationship with the El Niño phase with higher vegetation productivity (MAX and LI) and a longer length of the season observed (Appendix C Figure C.11).

Over southern Africa, there is a positive association with the Antarctic Oscillation (AAO) and enhanced rainfall and NDVI3g over southern Africa. There is some disagreement with phenology and productivity metrics over this region with negative correlations observed. The link between the AAO and NDVI3g over the southwest Cape of South Africa is weaker than that observed with rainfall. The results for the productivity and phenology metrics are less consistent over this region with negative correlations observed between MAX and AAO whereas positive correlations, particularly over Namaqualand, are observed between LI and AAO Appendix C Figure C.12). The positive phase of AAO tends to be associated with earlier SOS and EOS across this region.

Over the 0-20°N latitudinal band there is negative relationship between both NDVI3g and rainfall and the Pacific Decadal Oscillations (PDO). This pattern is particularly evident over the Sahel when considering vegetation productivity confined to the primary growing season, as indicated by MAX and LI (Appendix C Figure C.13). The length of the season over the Sahel tends to also be shorter with an earlier start and end of season observed. Over southern Africa the relationship between PDO and NDVI3g is stronger than that of rainfall and PDO particularly over western region of South Africa extending into Angola and Botswana with the positive PDO phase resulting in reductions in vegetation growth. Positive correlations are observed between the productivity and phenology metrics as well as rainfall to PDO in some areas of southern Africa.

The relationship between the North Atlantic Oscillation (NAO) and NDVI3g as well as productivity and phenology metrics is fairly weak compared to the clear negative correlation with rainfall over the Sahel region (time lag = 0). Over southern Africa, a negative relationship between NAO and MAX, LI and LOS is observed Appendix C Figure C.14) suggesting the positive phase of the NAO limits vegetation growth over this region.

The spatial pattern of the response of rainfall and NDVI3g to the Atlantic Multidecadal Oscillation (AMO) demonstrates that a positive AMO leads to an increase in rainfall over West Africa. The pattern of NDVI3g response as well as the response of productivity and phenology metrics (Appendix C Figure C.15) to the AMO demonstrates strong positive correlations over the 0-10°N latitudinal band and parts of southern Africa including South Africa, Angola and Botswana. For the NDVI3g time-series, strong negative correlations are observed over central southern Africa. There is very little difference between the correlations at the three different time lags.

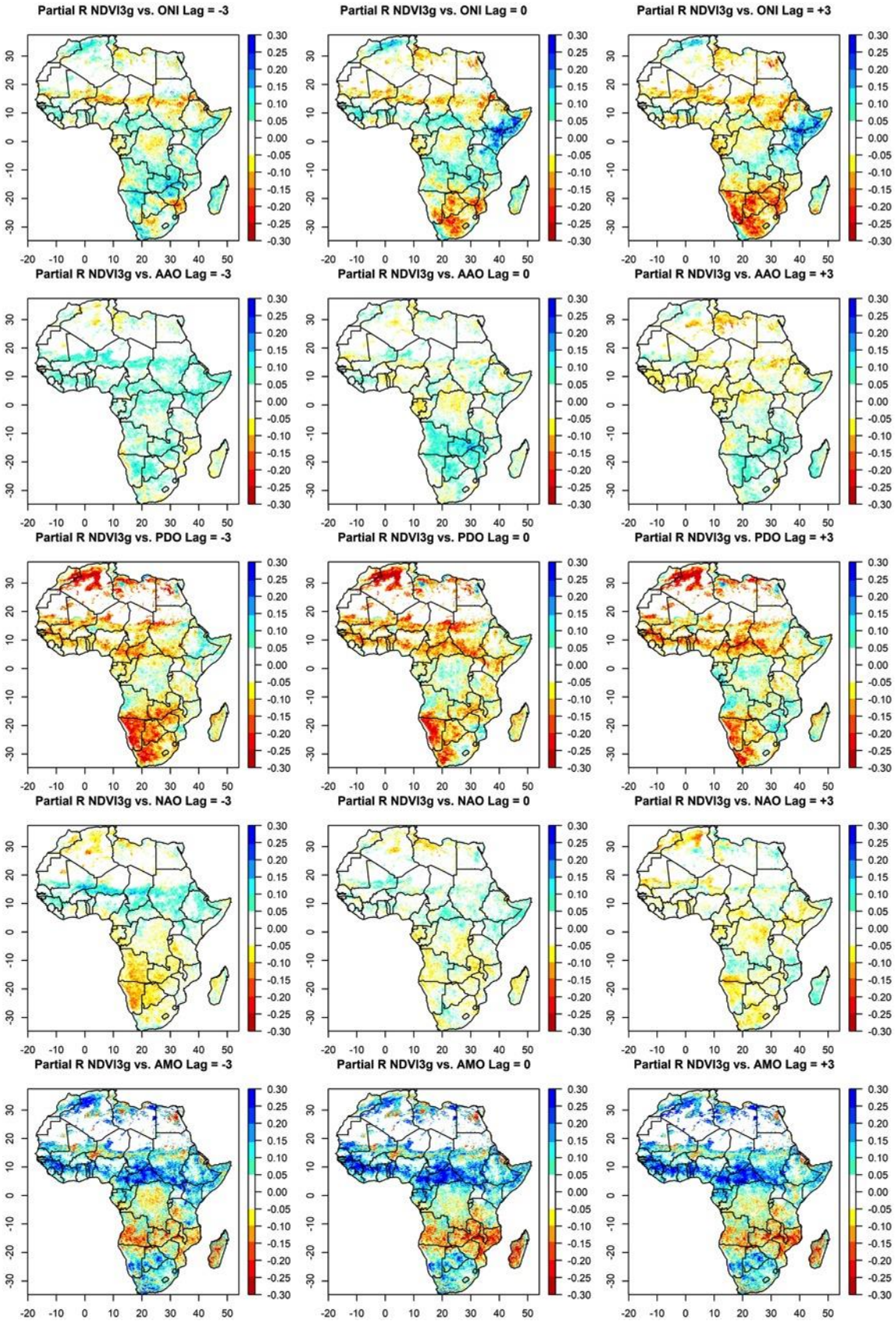

Figure 4.8: Partial correlation coefficients (r-value) between AVHRR NDVI3g and 2 atmospheric pressure oscillations (NAO and AAO) and 3 sea surface temperature oscillations (ONI, AMO, and PDO) based on monthly anomalies for the period 1982-2015. Three images are given per oscillations and represent 3 months before the peak event (lag = -3), peak occurrence (lag = 0), and 3 months after the peak event (lag = +3). The blue (red) colours indicate a positive (negative) correlation. White regions indicated pixels masked from the analysis.

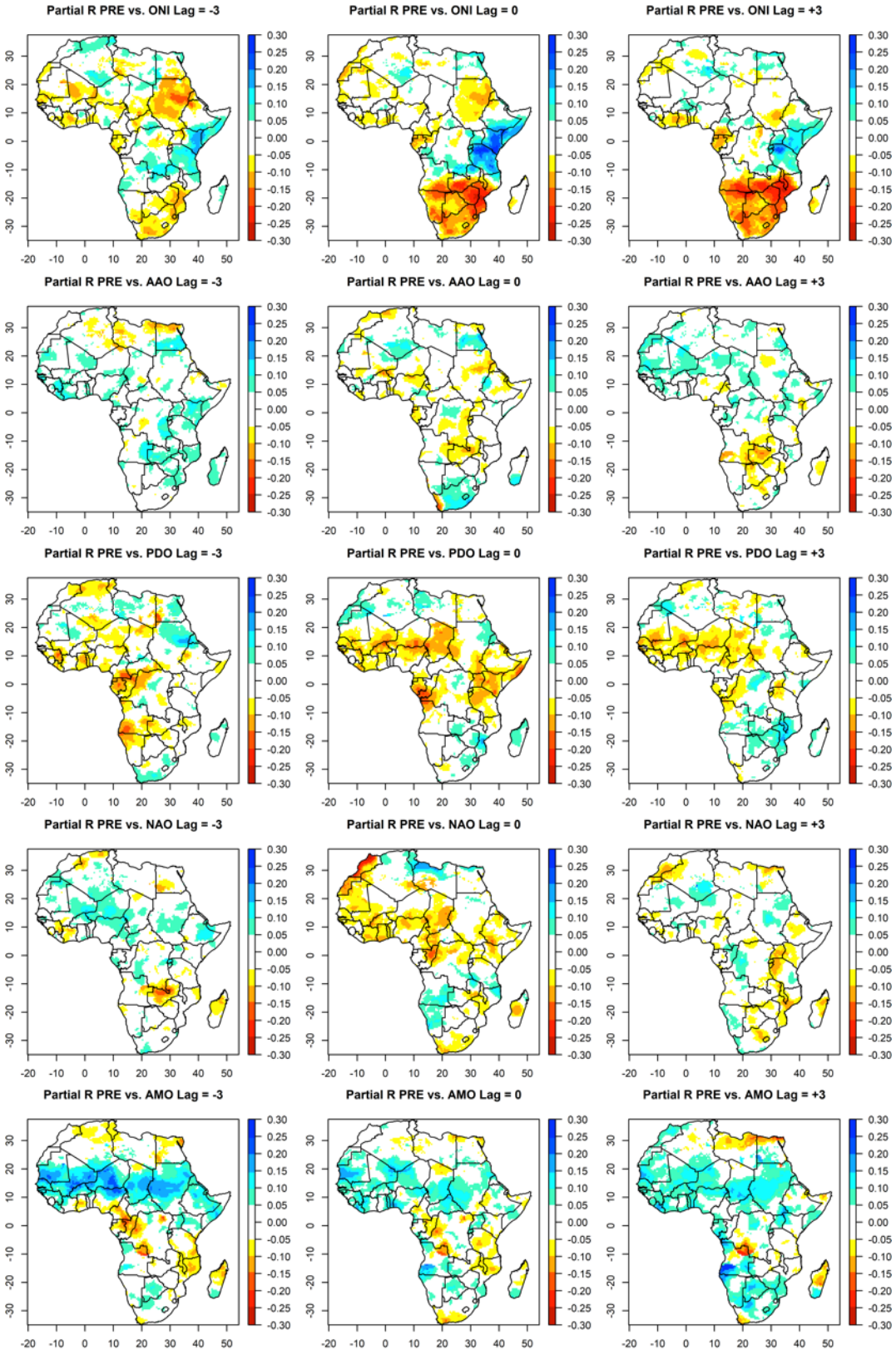

Figure 4.9: Same as Fig. 4.8 but for CRU TS 4.00

4.4 Discussion

Using the third generation AVHRR NDVI3g time-series for 1982 to 2015 this chapter has demonstrated associations between vegetation and key climate variables and has accounted for the temporal lags between climate predictors and vegetation response. This assessment is unique in that it combined the response of both productivity and phenology metrics to climate. Previous studies have tended to focus on either productivity (e.g. Mohamed et al. 2004; Jong et al. 2013; Wu et al. 2015) or phenology (e.g. Zhang et al. 2005; Woodward et al. 2008; Brown et al. 2010; Vrieling et al. 2011).

4.4.1 Major climatic drivers of vegetation growth

The strength of the correlation between NDVI and rainfall and temperature parameters is similar to that reported by other studies using previous versions of the CRU dataset and AVHRR NDVI time-series (Nemani et al. 2003; Jong et al. 2013; Wu et al. 2015). Considering vegetation productivity confined to the growing season, as described by maximum NDVI3g (MAX) and large seasonal integral (LI), enhanced the strength of this relationship.

The results indicate that the vegetation is primarily affected by rainfall over semi-arid regions of SSA, which include southern Africa, the Sahel, and East Africa regions. These areas are characterised by low annual rainfall totals and water availability is the primary constraint for vegetation growth (Fensholt et al. 2012). Furthermore, vegetation tends to show a stronger positive response to rainfall in the previous season suggesting that time-lag effects are of significant value when assessing climate variations in vegetation growth.

While noting some differences between productivity metrics used, higher temperatures tend to increase vegetation productivity over areas of Southern Africa and the Sahel. While some studies have found similar patterns others have found that in warmer semi-arid regions increased temperatures reduce photosynthesis efficiency and overall vegetation productivity (Midgley et al. 2004). The negative correlation between vegetation productivity and temperature over Namaqualand observed here is replicated in the study by Wu and co-workers (2015) and could be attributed to the fact that vegetation growth occurs primarily during the austral winter when temperatures tend to be lower relative to the rest of the year. In general, the patterns of response to SIS are not consistent with previous studies (e.g. Wu et al. 2015) and this could be attributed to the use of difference datasets. For tropical humid forests of central Africa, studies have shown that vegetation over these regions is limited by solar radiation as a result of increased cloud cover during the wet season (Nemani et al. 2003; Wu et al. 2015).

It is important to note however, that the predictive power of the statistical methods applied here may be limited by the lack of weather stations records in parts of southern and central

Africa (Creese & Pokam 2016) and the spatial interpolation of available climate records CRU TS. 4.00. A denser network of climate observations would increase the predictive power and relationships observed between climate and NDVI and possibly reduce the inconsistencies observed between productivity metrics. Although the value in CRU datasets resides in its high temporal resolution matching that of the NDVI time-series, alternative satellite derived measurements of rainfall could be useful in addressing this challenge.

The role of CO_2 in driving variability in NDVI time-series cannot be fully established in this study as both similar patterns of change in both time-series and do not necessarily provide evidence of major driving forces of vegetation variability, i.e. correlation does not imply causation. The statistical models applied here cannot account or resolve this influence at the large spatial scale applied here.

4.4.2 Drivers of inter-annual variability

Substantial variation in NDVI is observed between 1982 and 2015 over sub-Saharan Africa with patterns of below normal, normal and above normal vegetation activity being observed. This inter-annual variability in NDVI over SSA is largely driven by rainfall and associated large-scale climate fluctuations and oscillations in SST and atmospheric pressure. Overall, stronger correlations are observed over semi-arid regions of Southern Africa, East Africa and the Sahel confirming that vegetation productivity in these regions is strongly related to rainfall (Nemani et al. 2003; Fensholt et al. 2012). The consideration of time-lag effects revealed important patterns of the response of vegetation to particularly rainfall in the 3 months preceding vegetation growth.

On inter-annual timescales, there is considerable evidence that basic modes of variability, including sea surface temperature and air pressure oscillations that occur on both short- and long-time scales drive fluctuations in both NDVI and rainfall over the continent. The most dominant mode of climate variability over eastern and southern Africa is the El Niño-Southern Oscillation (ENSO). NDVI anomalies as well as vegetation productivity and phenology over both these regions correspond with identified ENSO-precipitation teleconnection patterns (Ropelewski & Halpert 1987; Anyamba & Eastman 1996; Anyamba et al. 2002; Schreck & Semazzi 2004; Nicholson 2015) where negative (positive) anomalies in NDVI are associated with warm phase of ENSO over southern (East) Africa. Over southern Africa NDVI correlates with ENSO three months after the peak event (i.e. in March) whereas over East Africa the strongest correlations are observed at peak event in December which coincides with the end of the second growing season over this region (refer to Chapter 3). Furthermore, the results have demonstrated that during the El Niño phase / warm phase of ENSO the length of the season and vegetation growth within the season are restricted over southern Africa but enhanced over East Africa, particularly in the second growing season. This suggests that during the El Niño phase vegetation growth over East Africa may

extend beyond the average end of the season (i.e. January or February). This is supported by a number of other studies in the region, which have shown that the above normal rainfall during El Niño results in an extended growing season (e.g. Anyamba et al. 2001; Anyamba et al. 2002). Some studies have also highlighted the role of the Indian Ocean Dipole (IOD) as a control on the multi-decadal variability over East Africa where cool SSTs in the Indian Ocean are associated with enhanced rainfall over East Africa during October-November (Tierney et al. 2013; Degefu et al. 2017). This study did not consider the IOD but it may be useful to include in further studies.

Other drivers of inter-annual variability over southern Africa include the Antarctic Oscillation (AAO), the Pacific Decadal Oscillation (PDO), and the North Atlantic Oscillation (NAO). The correlation coefficients demonstrate that NDVI responds to the positive phase of the AAO, which has been found to result in enhanced rainfall over central southern Africa (Pohl et al. 2010). Over the southwest Cape of South Africa there is evidence to suggest that during the positive phase of AAO rainfall is reduced as a result of the contraction of westerly winds towards Antarctica (Reason & Rouault 2005; Gillett et al. 2006). This response is however not reflected in the correlations coefficients with NDVI values as well as productivity and phenology metrics with very weak associations demonstrated in the results. This suggests that while AAO is important driver of variability in rainfall it is not as important predictor of vegetation variability as compared to ENSO.

The positive phase of both the PDO and NAO are associated with decreased rainfall over southern Africa (McHugh & Rogers 2001; Reason & Rouault 2002; Ambrosino et al. 2011; Wang et al. 2014b) and evidence presented here suggests that vegetation growth is constrained as a result. Brown et al. (2010) found similar associations with strong correlations between start of the season and NAO over southern Africa reported.

Over West Africa, the strong correlation between rainfall and the AMO has been well documented. During an AMO warm phase summer rainfall (April-September) associated with the West African Monsoon is enhanced (Rodríguez-Fonseca et al. 2011). The response of vegetation to the AMO presented here may not be directly linked to the role the West African Monsoon. This is as the time-series of AMO (refer to Appendix C Figure C.1) shows that after 1997 the AMO entered a positive phase and the strong positive correlations with NDVI3g across SSA could be evidence of the both time-series demonstrating similar temporal patterns.

Over the Sahel, this study provides evidence to suggest that the Pacific Decadal Oscillation (PDO) and the North Atlantic Oscillation (NAO) are the dominant drivers of inter-annual variability. A number of studies have demonstrated that a link between the warm phase of the PDO and lower rainfall over the Sahel and parts of West Africa (e.g. Rodríguez- Fonseca et al. 2011; Huber & Fensholt 2011; Diatta & Fink 2014). Brown et al. (2010), for example,

found strong correlations between PDO and the growing season over West Africa. The NAO has been linked to changes in dust intensity over the Sahel and there is evidence that it has an influence of rainfall variability in this region (Moulin et al. 1997; Moulin & Chiapello 2004). The results from this study demonstrate that the NAO influences rainfall more directly compared with the response of NDVI3g, which tended to be weak. Studies linking vegetation and the NAO have been contradictory with some showing strong negative correlations (Oba et al. 2001) and others finding no consistent relationships (Wang 2003).

4.5 Conclusion

By modelling the response of AVHRR NDVI3g to various climatic factors this study demonstrated that (i) variations in climate affect vegetation growth and seasonality across SSA and (ii) in some cases these patterns of response illustrate important time-lag effects. An improved understanding of the response of vegetation to climate variability will provide crucial knowledge for interpretation of long-term trends and projections of future changes.

The spatial and temporal relationships presented here are sufficiently consistent with those shown in previous studies and demonstrated that vegetation response to climate varies considerably across SSA and at different time-lags. The multiple regression analysis between vegetation and climate correlation and successively provided a quantitative insight into the response of vegetation to key climatic parameters. This study adds value by firstly, using the latest time-series of NDVI3g available that spans the period 1982 to 2015, secondly assessing both the response of vegetation productivity and phenology to climate variations, and lastly by integrating the response of vegetation to climate parameters, atmospheric CO_2, and large-scale climate oscillations into a comprehensive assessment for SSA. The information presented here provides value for the interpretation of changes and trends vegetation productivity and phenology presented in the subsequent chapter in this thesis (Chapter 5).

Chapter 5:

5. Long-term trends and abrupt shifts in vegetation activity over Sub-Saharan Africa using the GIMMS AVHRR NDVI3g dataset from 1982 to 2015

5.1 Introduction

5.1.1 Background

Considerable attention has been directed towards understanding how climate change is likely to alter the structure and function of terrestrial ecosystems across the globe (Zhang et al. 2013) and there is a growing research impetus to detect early signs of change and to identify vulnerable regions. A number of studies have provided evidence to suggest that terrestrial ecosystems are sensitive to climate change. The patterns of detected changes to date suggest an increase in vegetation activity over the last 25 to 30 years in many parts of the world (Fensholt et al. 2012; Zhu et al. 2016) including greening over the Sahel (Eklundh & Olsson 2003; Herrmann et al. 2005; Anyamba & Tucker 2005; Dardel et al. 2014a; Brandt et al. 2015) and increases in woody vegetation across southern Africa (Buitenwerf et al. 2012; Mitchard & Flintrop 2013; Stevens et al. 2016; Devine et al. 2017). Future changes in rainfall and continued increases in temperature and atmospheric CO_2 are likely to drive important changes in the distribution, condition, composition, and functioning of terrestrial ecosystems of sub-Saharan Africa as well as alterations in plant phenology (Gonzalez 2010; Field et al. 2014).

Since vegetation productivity is strongly linked to climate factors studies often utilise remotely sensed vegetation indices to assess and monitor changes in terrestrial ecosystems (Fensholt et al. 2012; Zhu et al. 2016). The Normalised Difference Vegetation Index (NDVI) derived from the Advanced Very High Resolution Radiometer (AVHRR) sensor is one of the most commonly used proxies of terrestrial vegetation productivity. It has been by numerous studies to detect and monitor long-term vegetation change over large geographical areas (Pinzon & Tucker 2013). Despite a relatively coarse spatial resolution, the AVHRR NDVI3g time-series is the longest continuous temporal record of terrestrial vegetation dynamics and as such represents unprecedented opportunity to understand the responses of vegetation to climate change (Wang et al. 2014a). The low uncertainty measurement of the dataset (± 0.005) as reported by Pinzon and Tucker (2014) has provided the foundation for the use of NDVI3g in the detection of seasonal and inter-annual changes in vegetation.

The presence of trends in such records has been demonstrated by a number of studies and a range of methods has emerged to analyse vegetation indices across a range of spatial scales. These include:

- Statistical approaches such as principal component analysis (PCA) that decompose the NDVI image time series into various spatial and temporal components (e.g. Ivits et al. 2014);
- Statistical-frequency techniques such as Fourier analysis which can detect temporal variability patterns by breaking NDVI into phase and amplitude components (e.g. Azzali & Menenti 2000; Eastman et al. 2009);
- Time series analysis which comprise methods that attempt to understand underlying forces structuring the data, identifying patterns and trends, detecting changes (e.g. Van Den Bergh et al. 2012);
- Temporal trend persistence probability (Lanfredi et al. 2004); and
- Decomposition of time series into trend, seasonal and noise components (e.g. Verbesselt et al. 2010a; de Jong et al. 2012).

These analytical approaches differ in mathematical complexity, processing and analysis intensity, classification technique, and interpretability. The selection of a single technique is not a straightforward task and often different trend assessments, based on similar vegetation index data, produce conflicting results in terms of which areas are experiencing greening or browning trends (Wessels et al. 2012). The limited observational data to support or evaluate the trends observed from different techniques often results in fierce debates within the literature and remote-sensing community. Ultimately the choice of method and subsequent findings has important implications for management decisions.

5.1.2 Objectives and rationale

Monitoring of terrestrial landscapes using remotely sensed vegetation indices over long periods of time is required to improve the understanding of the processes and drivers related to change. This chapter builds of the analysis conducted in previous studies and uses a range of trend detection techniques and models in order to provide robust assessment of the trajectory of vegetation change over sub-Saharan Africa between 1982 and 2015. The high temporal resolution AVHRR NDVI3g provides the necessary baselines to assess how recent changes in climate are impacting the vegetation productivity. Since changes in NDVI may be related to climatic as well as non-climatic factors (Fensholt et al. 2012) such as land-use an important component of this chapter is to attempt to attribute the change to climate.

The purpose of this chapter is to:

- Detect long-term trends and abrupt local or regional shifts in vegetation productivity and phenology;
- Investigate the role of climate in driving the observed changes in vegetation activity;
- Evaluate the use of AVHRR NDVI3g for the assessment of long-term trends at a continental scale; and
- Evaluate the performance of the different methods for detecting changes in vegetation productivity.

By evaluating the performance of different trend detection approaches this study will enable a critical appraisal of combined trend detection methods and a more robust understanding of the trajectory of vegetation change over Sub-Saharan Africa. The methods chosen differ on the temporal resolution of NDVI time series, how seasonality of accounted for, and how the trend is estimated.

5.2 Methodology

The 8 km resolution AVHRR NDVI3g (third generation) covering the period 1982 to 2015 (refer to Chapter 3 for details on pre-processing method applied) was used to assess the spatial and temporal trends in both vegetation productivity and phenology over SSA through (i) the application of linear trend models and (ii) the detection of abrupt changes and trend shifts in the time-series (Figure 5.1). Productivity and phenology parameters extracted from the smoothed AVHRR NDVI3g time-series using TIMESAT version 3.2(Eklundh & Jönsson 2012) include the large integral (LI), maximum NDVI (MAX), start (SOS), end (EOS), length (LOS), mid position (MID), seasonal amplitude (AMP) of the growing season (refer to Chapter 3 Section 3.2.3 for details on the method). In order to assess the role of climate change driving shifts in vegetation, areas of critical change in NDVI3g were attributed to significant variations in key climate parameters, including temperature, rainfall, and surface solar radiation.

Anthropogenically-altered land surfaces, as defined by GlobCover 2009 Version 2.3 (Bontemps et al. 2011), water bodies and bare soil (NDVI < 0.1) were masked from the analysis and result outputs (refer to Appendix B Figure B.2). These areas occupy 27.7% of the land-area of Africa with the bare areas making up 17.5% of that total.

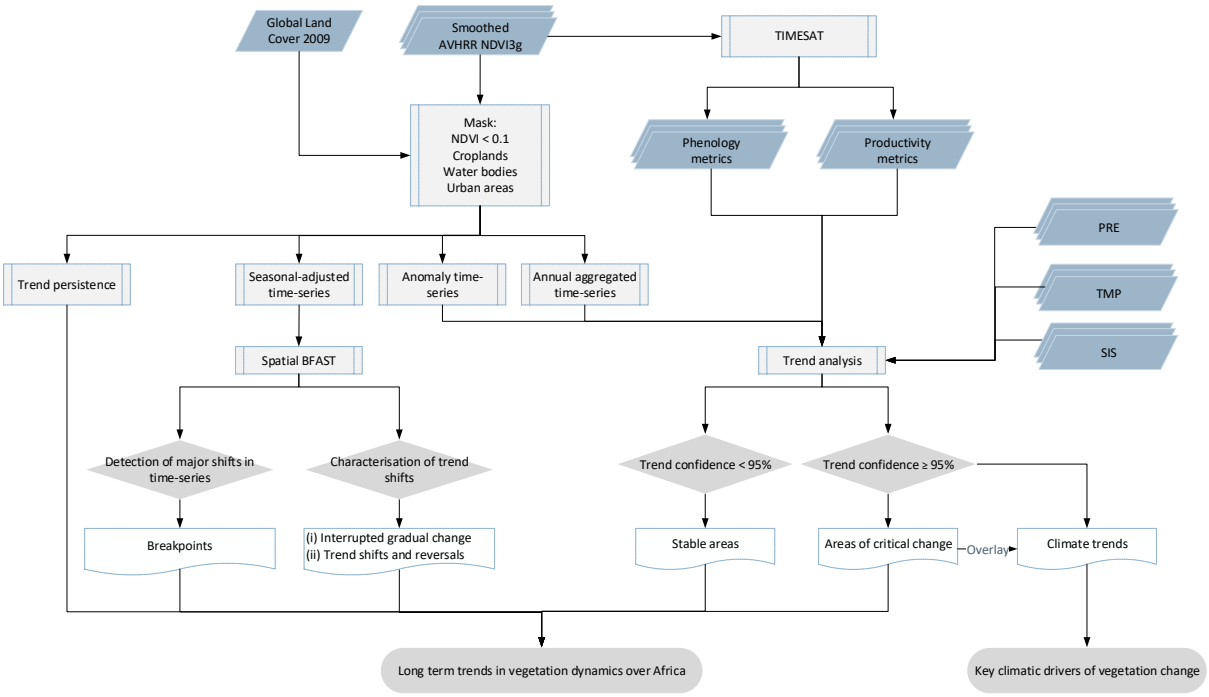

Figure 5.1: Flow diagram illustrating the methodological approach taken in this study to detect trends in AVHRR NDVI3g (1982-2013) over Sub-Saharan Africa.

5.2.1 Detecting long-term trends

Trends were investigated using a range of previously published techniques including (1) linear and non-parametric models, (2) methods which assess how greening or browning trends have persisted over time and (3) techniques which decompose the time-series into gradual trends and abrupt changes at breakpoints. The first set of techniques considers monotonic trends which assume that trends preserve their increasing or decreasing order throughout the time-series whereas the second set of technique does not assume monotonic trends (e.g. trend persistence and BFAST methods).

Non-parametric trend detection models

Temporal trends were assessed using the Theil-Sen technique (Theil 1950; Sen 1968) and the associated test for its statistical significance. The Theil-Sen slope is a linear (uniform) trend index that provides a spatially explicit expression of the rate of change per year by calculating the slope between every pairwise combination and the median slope value. Negative (positive) slopes indicate areas that have experienced a decline (increase).

Trends in (i) annual NDVI3g anomalies (observation in year *t* minus the long-term mean observation), (ii) annual aggregated NDVI3g values, and (iii) productivity metrics (MAX and LI) derived from TIMESAT version 3.2 (Eklundh & Jönsson 2012) were assessed using Theil-Sen trend estimator.

For the analysis of temporal trends in phenology metrics (AMP, SOS, MID, EOS, and LOS) the non-parametric Mann-Kendall (Tau) statistic (Kendall 1938; Hirsch et al. 1993) was applied. The Mann-Kendall statistic is a non-linear trend indicator that does not make assumptions about the distribution of the data or the linearity of any trends (Hollander & Wolfe 1973). It measures the degree to which a trend is consistently increasing or decreasing where a value of +1 indicates a trend that consistently increases and never decreases and the opposite is true of a value of -1. A value of 0 indicates no consistent trend.

Both of the adopted trend indices (Tau and Theil-Sen slope) are more robust than traditional linear trend analyses in that they are not sensitive to outliers in data and less sensitive to the exact shape of the trend. In addition, the uncertainty is not influenced by whether the data distribution follows a normal distribution (Yue et al. 2002).

While interpreting the results, a p-value of 0.05 was considered as a threshold of significance. It is hypothesised that a statistically significant slope indicates areas that have experienced a critical change in vegetation dynamics (Anyamba & Tucker 2005; Wessels et al. 2007b).

Trend persistence

The trend persistence procedure developed by Lanfredi et al. (2004) estimates the persistence of vegetation cover by determining the tendencies of NDVI to increase or decrease. Persistence is related to the concept of resilience in that it measures the ability of vegetation to recover from disturbances. Firstly, a reference image was created by calculating the linear NDVI trend over the reference period 1982 to 1991. Pixels for which the trend is positive are assigned a value of +1 and for negative trends a value of -1 is assigned. At one-year time steps, NDVI values are progressively added and a new trend evaluated. If the addition of a trend resulted in a zero slope value then it can be assumed that the vegetation is equivalent to the reference period. The persistence images are then summed resulting in an image where the pixels represent the number of years during which the negative or positive trend persisted (Lanfredi et al. 2004). This technique identifies changes in NDVI trends as opposed to changes in absolute NDVI values. It is advantageous as it limits the influence of the time period of assessment on the detection of linear trends (Wessels et al. 2012).

Detecting breakpoints and trend shifts using Breaks for Additive Seasonal and Trend (BFAST)

Breaks for Additive Seasonal and Trend (BFAST) is an additive decomposition model that iteratively fits a piecewise linear trend to a time series (Verbesselt et al. 2010a; Verbesselt et

al. 2010b; DeVries et al. 2015). This technique does not assume monotonic trends throughout the time-series but instead decomposes the time-series into gradual trends and abrupt changes at breakpoints.

A seasonally adjusted time-series of AVHRR NDVI3g was first calculated by fitting a seasonal cycle to the original dataset by decomposing the time-series into three components (trend, seasonal, and remainder) using the harmonic model (Verbesselt et al. 2010b) and then removing the seasonal component from the time-series. The BFAST model was then applied run spatially this seasonally adjusted time-series.

Various settings were tested on the sampled datasets prior to the analysis in order to determine if trend breaks occurred within the time-series. The number of breaks was set at one and the maximum number of iterations was one. While the time-series may contain more changes and shifts, a p-value of 0.05 was used in order to search for significant structural change in the time series.

5.2.2 Attribution of trends in vegetation to climate change

In order characterise the role of climate change on variation in vegetation over SSA, the observational record for SSA was examined for evidence of climate trends over the period 1982 to 2015. The analysis of temperature and rainfall trends is based on high-resolution (0.5°x0.5°) gridded climate products from CRU TS 4.00 (Harris et al. 2014b) and described in Chapter 4 Section 4.2.2. Trends in surface solar radiation (SIS) was based on Monthly Surface Solar Radiation (W/m^2) Data Set - Heliosat (SARAH) derived from Meteosat satellite observations from 1983 to 2013 (Müller et al. 2015).

Temporal trends in climate statistics were assessed using the Theil-Sen technique (refer to Section 4.2.1), after the removal of the seasonal cycle, and the associated test for its statistical significance. A detailed review and evaluation of recent historical in climate trends over SSA can be found in Chapter 2. Following the methodology applied by Wu et al. (2015), the resultant trend maps (Figure 5.2) were compared to trends in productivity and phenology metrics in areas with significant change ($p < 0.05$). Since AVHRR NDVI3g has a native spatial resolution of 0.08° the productivity and phenology trend maps as well as trends in SIS were spatially aggregated to 0.5°.

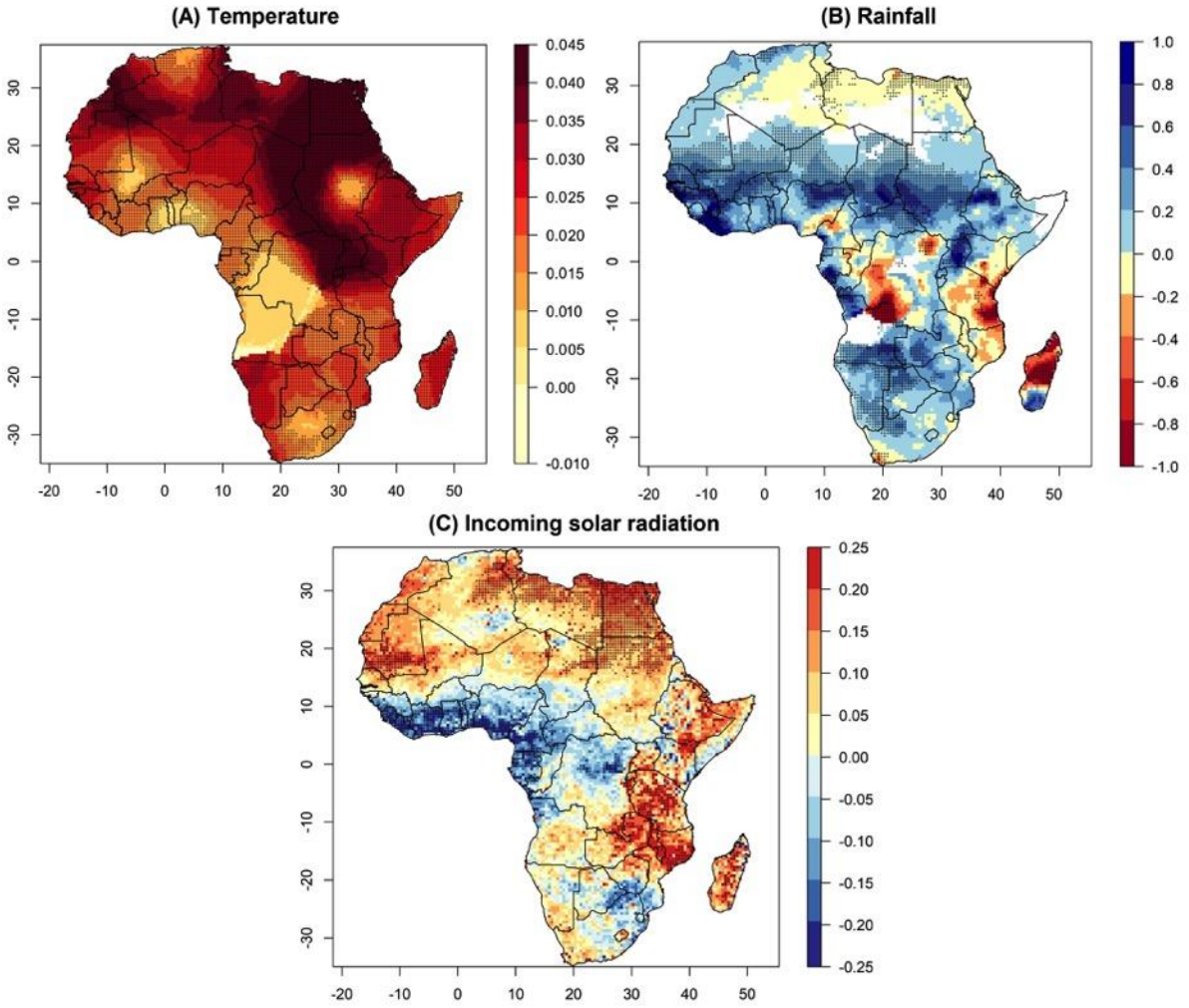

Figure 5.2: Temporal changes (1982–2015) in (A) land surface temperature (TMP) (°C per year), (B) mean annual rainfall (PRE) (mm per year), and (C) incoming solar radiation (SIS) (W/m^2 per year) over Africa. Statistically significant ($p < 0.05$) trends are indicated by a '+' sign. White areas indicate incomplete or missing data.

5.3 Results

5.3.1 Geographical pattern of long-term trends in vegetation over SSA

For the period 1982-2015, there is a clear latitudinal pattern of change in vegetation productivity over SSA, as described by the maximum NDVI3g and growing season integral (Figure 5.3 & 5.4). An increasing trend ($p < 0.05$) is observed over the northern hemisphere tropics (0-10°N) particularly over West Africa extending to central Africa as well as over the southern hemisphere sub-tropics (20-35°S) while declining trends are observed over the southern hemisphere tropics (0-20°S). This spatial pattern of change is fairly consistent between the different trend detection techniques used in this study (Appendix D Figure D.1-3). In these regions identified as experiencing significant changes in productivity there is also evidence of changes in seasonality as expressed by the trends in phenology metrics (Figure 5.5). Over the northern hemisphere tropics (0-10°N) a shift to an earlier start, later end and a

resultant increase in the length of the growing season (LOS), particularly over Central African Republic, was observed. Over Tanzania, northern Mozambique, and Gabon a decline in the LI is associated with a decrease in the start of the season (SOS) as well as the LOS. Increases in the LOS are observed over parts of southern Africa and the Sahel region.

Over the majority of the Sahel, increases in vegetation productivity are observed. Evidence of declines is observed of the southern extent of the Sahel predominantly in the anomaly and seasonally adjusted time-series as well as the trend persistence maps (Appendix D Figure D.1-D.3). The trend persistence maps however demonstrate that these declining trends have not persisted for more than 8 years compared to the increasing trends which have persisted for up 24 years. Over the southern extent of the Sahel in Niger there is evidence for an increase in length of season (Figure 5.5) of about 17 days. This can be attributed the decline in SOS and increase in EOS suggesting an earlier start and a later end of the growing season. Increases in seasonal amplitude are observed over the entire eastern and western Sahel.

A pattern of significantly increasing ($p < 0.05$) LI and MAX NDVI3g are observed over the majority of West and central Africa south of the Sahel (0-10°N). Based on the trend persistence method the positive trend over West and Central Africa has persisted for up to 22 since (i.e. from 1991 to 2013). There is also evidence that that seasonality has also shifted over these regions (Figure 5.5). The end of the season has shifted by between 4 and 17 days to a later date in the year (decreasing trend) over entire 0-10°N latitudinal band. Statistically significant changes in that start and length of the season are observed over Central African Republic. The start date of the season has shifted earlier by up to 20 days while the length of the season has increased.

Over West Africa, a noticeable difference between the direction of trends in LI and MAX is observed over the coastal regions Gabon and the Republic of Congo where decreases in LI are shown. Furthermore, the extent of the areas experiencing positive trends over northern DRC, Equatorial Guinea, Cameroon, and northern extent of Gabon is greater relative to the trends in LI.

Over East Africa, increases in both the LI and MAX NDVI3g are observed over South Sudan extending into northern Uganda as well as along the border between South Sudan and Ethiopia (Figure 5.4) while only increases in MAX are evident over parts of Ethiopia and Somalia. Negative trends are observed over central Kenya, parts of Somalia, and north-eastern border between Ethiopia and Eritrea. There is very little evidence for changes in the seasonality of the first and second growing seasons over East Africa. Slight increases in

seasonal amplitude are observed in both seasons except for over the north-eastern border between Ethiopia and Eritrea where declines in AMP are evident.

Over southern Africa, the most noticeable declines in vegetation productivity observed are observed in the large integral (Figure 5.4) over western Angola, parts of Zambia, south-west coastal region of Madagascar, northern Mozambique, Tanzania. Increases in vegetation productivity across southern Africa are observed over parts of South Africa, Namibia, Botswana and Zimbabwe. These trends are more widespread in MAX, NDVI3g anomalies, seasonally adjusted time-series of NDVI, and trend persistence maps relative to the LI particularly over north-eastern and south-western cape region of South Africa.

Differences in the trends in MAX and LI are observed over northern Mozambique and Tanzania suggesting that while peak productivity may be increasing in these regions total growth in the season has declined. This is supported by the trend in seasonal amplitude (AMP), which has increased significantly and as well as the LOS which has decreased significantly over northern Mozambique and Tanzania (Figure 5.5) by up to 34 days. There is also evidence that the SOS has increased suggesting a trend towards a later start date and a decline in EOS suggesting an earlier end date of the season over parts of Mozambique and Tanzania. Other changes in phenology metrics over other countries of southern Africa are less spatially consistent with isolated regions showing changes in SOS, MID and LOS. Over northern Namibia and central South Africa, for example, increases in LI and LOS are clear (Figure 5.4 & 4.5).

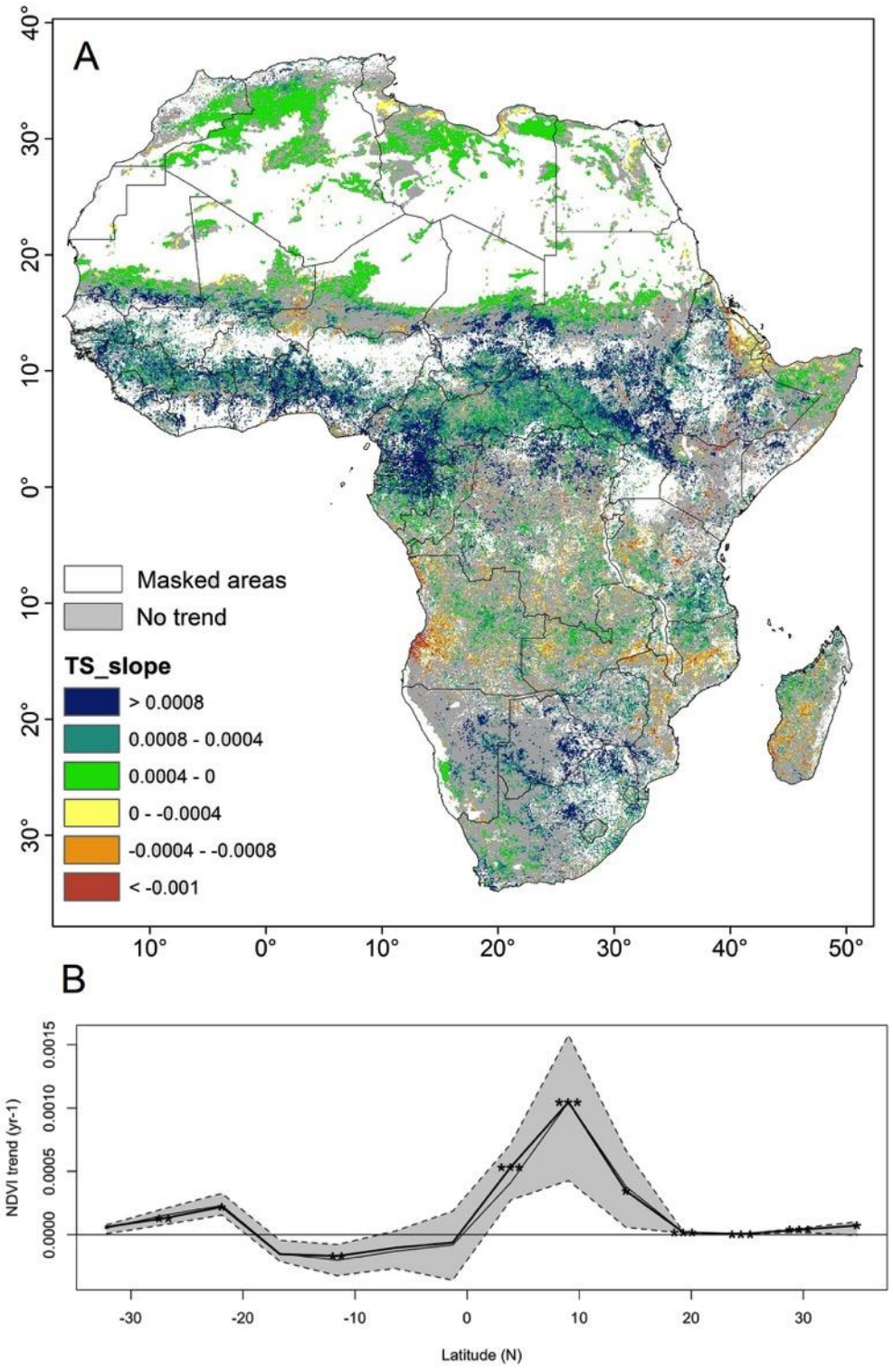

Figure 5.3: (A) Theil-Sen trend in maximum (MAX) NDVI3g for the period 1982-2015. Trends are displayed for statistically significant pixels (p < 0.05). White indicates pixels that were masked from the analysis and grey the pixels were no statistically significant trend was detected. (B) Latitudinal gradient of the Theil-Sen trend. The bold line with significance flags (*) is the estimated trend slope. The grey-coloured area and the thin line are the 95% confidence interval and the median represented by the light grey line. NDVI values below 0.1 and urban areas were masked from the analysis.

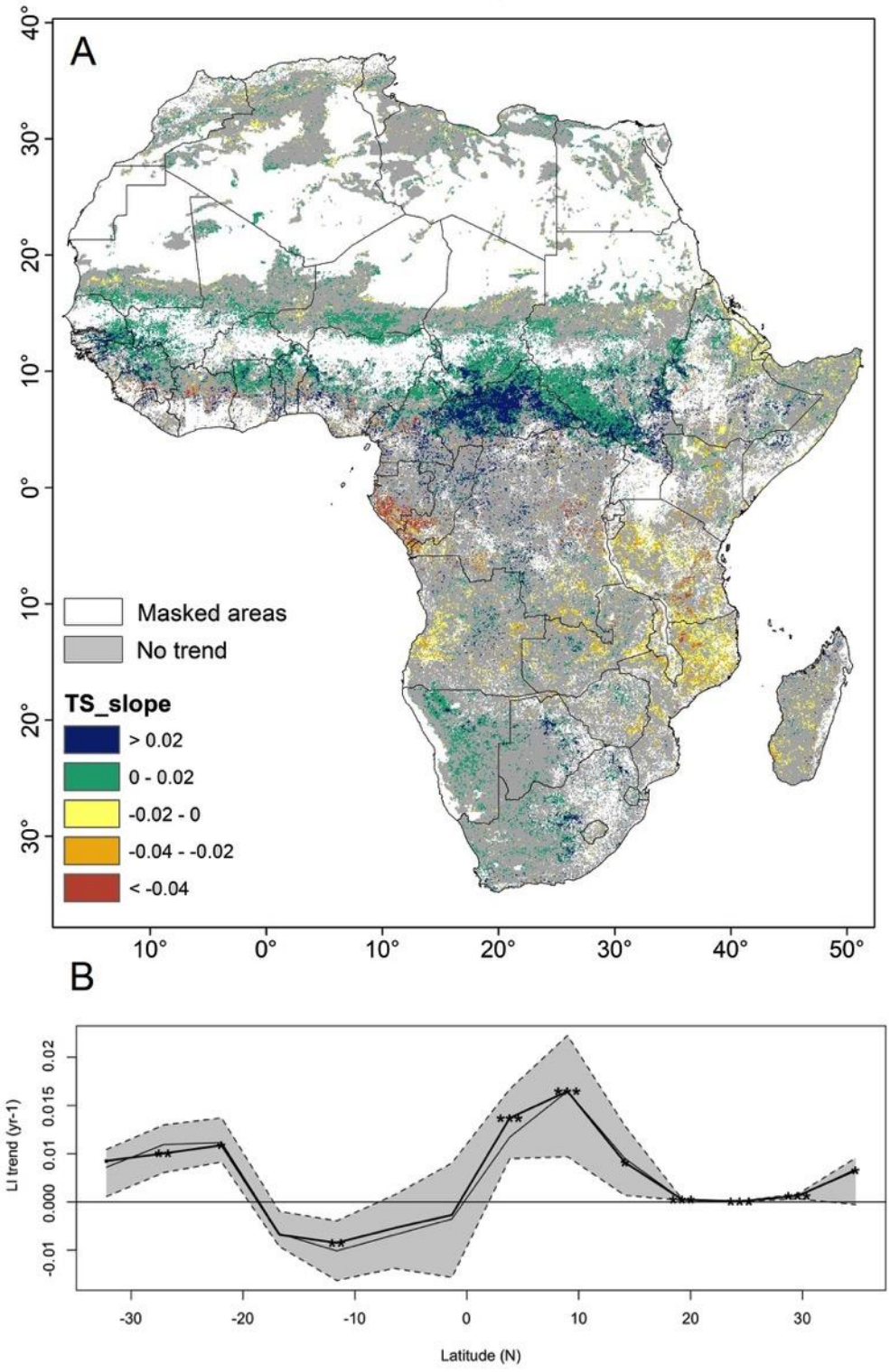

Figure 5.4: Same as Fig. 5.2 but for the large seasonal integral (LI)

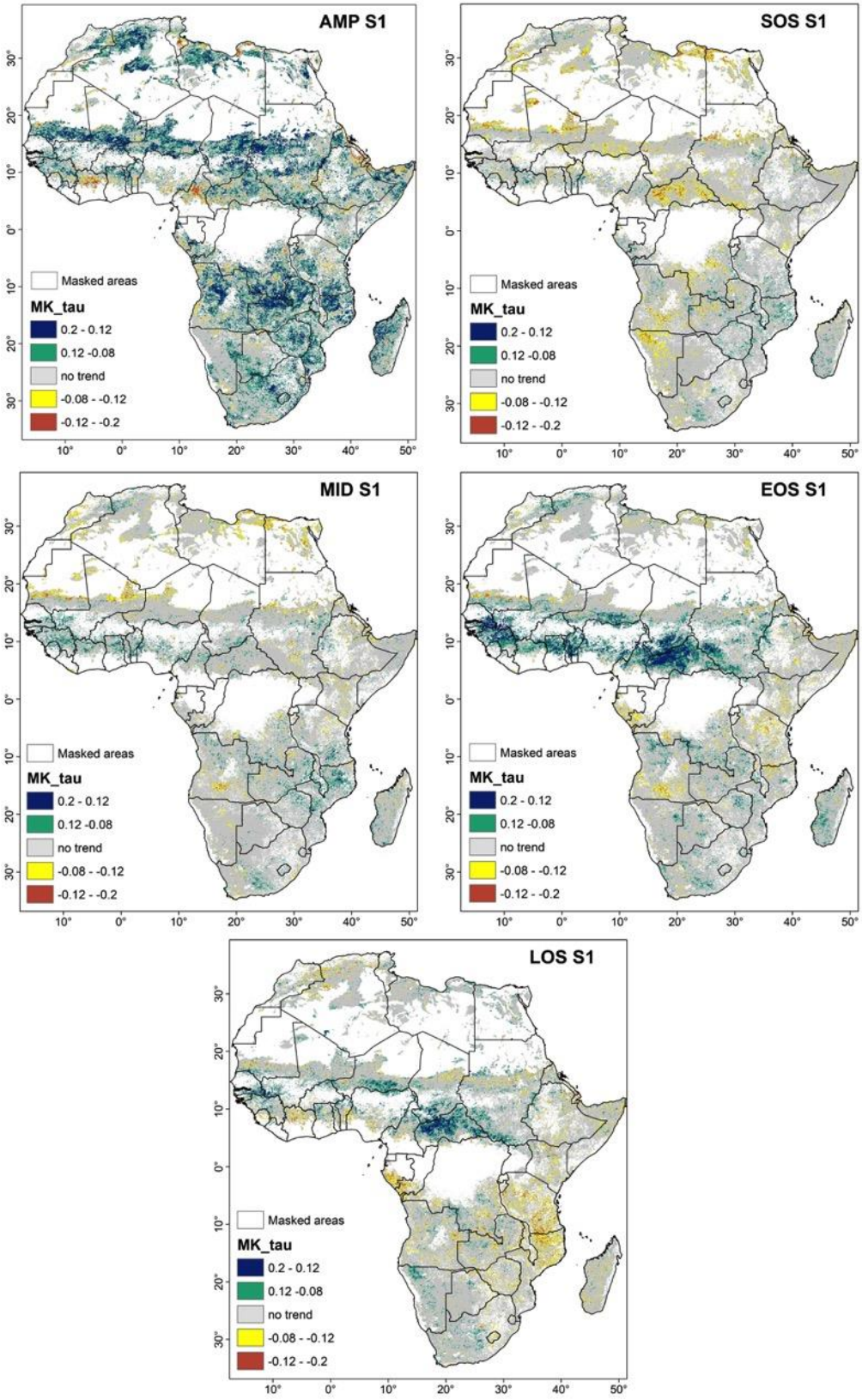

Figure 5.5: Trends in start date (SOS) of the first growing season, its peak (MID), its end date (EOS) and the length (LOS) derived from the AVHRR NDVI3g time series for 1982 to 2015 over Africa using the Mann Kendall trend test. White indicates pixels that were masked from the analysis and grey represent pixels were no trend ($p < 0.05$) was detected.

5.3.2 Spatial pattern of climate driven trends in vegetation

Figure 5.6 shows the comparison between climatic factors (temperature, rainfall and solar irradiance) and maximum NDVI3g in the areas with significant change. The MAX metric was chosen for this assessment as it comprised the highest number of pixels showing significant variation and which covered similar geographical locations as the changes in LI and phenology metrics ($p < 0.05$). Over SSA, regions demonstrating significant variations in MAX NDVI3g correspond to either one or multiple climatic factors. Variations in temperature accounted for 37% of the majority of the variation in MAX NDVI3g while precipitation and solar irradiance each accounted for 2%. The pixels showing significant variations in both temperature and solar irradiance accounted for 28% and those with significant variations in temperature and rainfall for 20%.

Over the Sahel, variations in temperature, rainfall and solar irradiance in some places account for increases in MAX NDVI3g observed previously. Over tropical humid forests of West Africa as well as over most of East and Southern Africa, temperature and solar irradiance account for the majority of trends in MAX NDVI3g observed. Over Angola and parts of central South Africa variations in rainfall correspond to variations in MAX NDVI3g. These spatial patterns are the same for the other productivity and phenology metrics (refer to Appendix D Figure D.5 for comparison with all pixels across SSA).

5.3.3 Spatial and temporal distribution of trend breaks

The Breaks for Additive Seasonal and Trend (BFAST) spatial analysis demonstrates that trends in NDVI3g over SSA are characterised by a break at a certain point in the time-series, which show distinct regional patterns (Figure 5.7A). Over the majority of the region breakpoints are concentrated towards the end of the time-series (2008-2010), (Figure 5.7B). This suggests that the vegetation in these regions was relatively stable in the early periods of the NDVI3g time-series.

Early shifts (1987-1989) are less geographical confined are spread over parts of East and West Africa, central Botswana, along the eastern coastline of South Africa, and central Madagascar. Since these shifts occur at the beginning of the time-series the breakpoint may not be an indicator of structural change but rather an indicator of short-lived changes, such as the recovery from short-term disturbances. This requires careful interpretation in terms of understanding long-term trends in vegetation. Later shifts (1998-2002) were concentrated over central Africa and parts of West Africa, as well as over the southern extent of the Sahel.

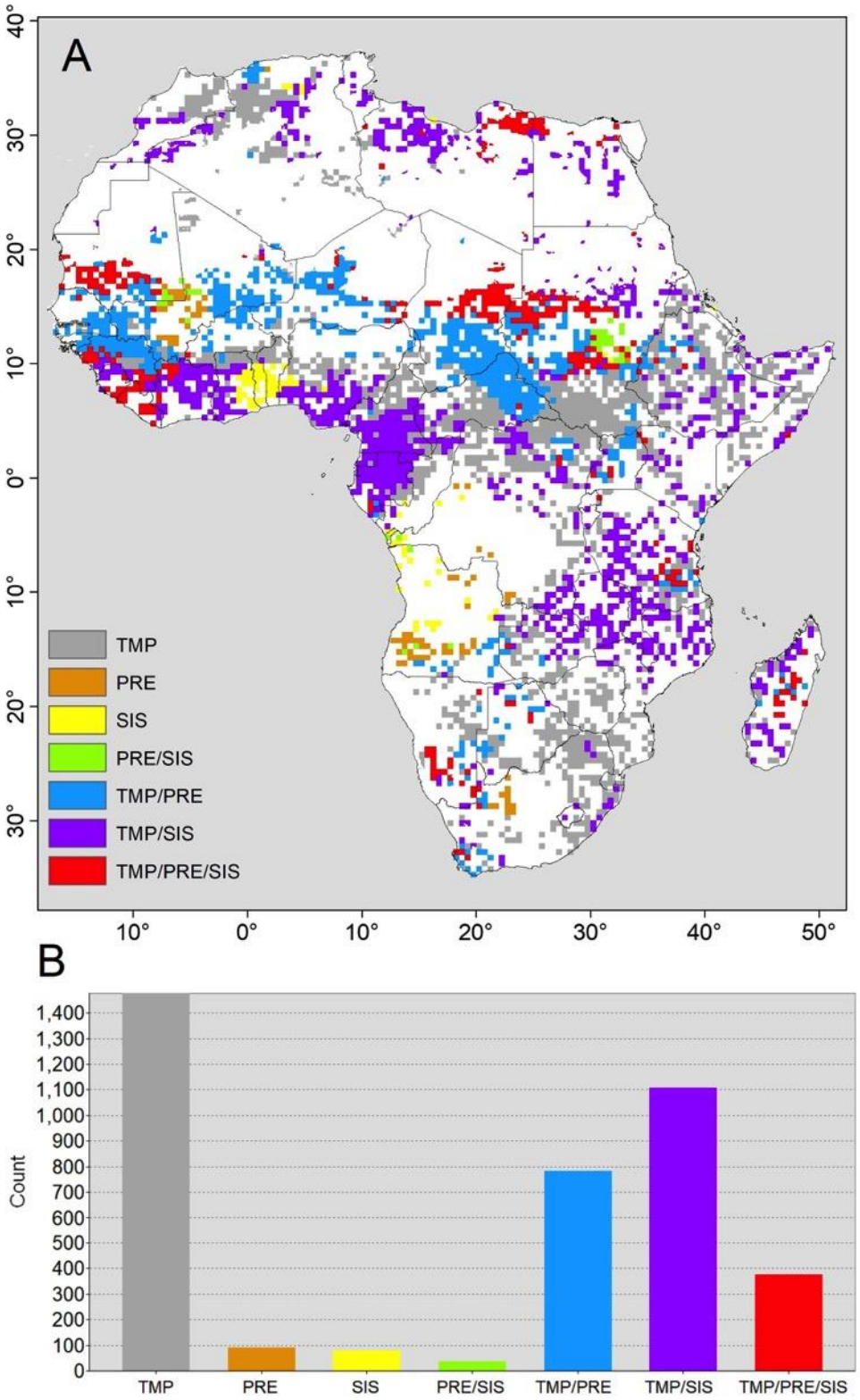

Figure 5.6: Comparison between trends in climatic factors and maximum NDVI3g (MAX) in the areas with significant variation ($p < 0.05$) over Africa for the period 1982-2015. TMP refers to temperature, PRE to rainfall, and SIS to incoming solar radiation.

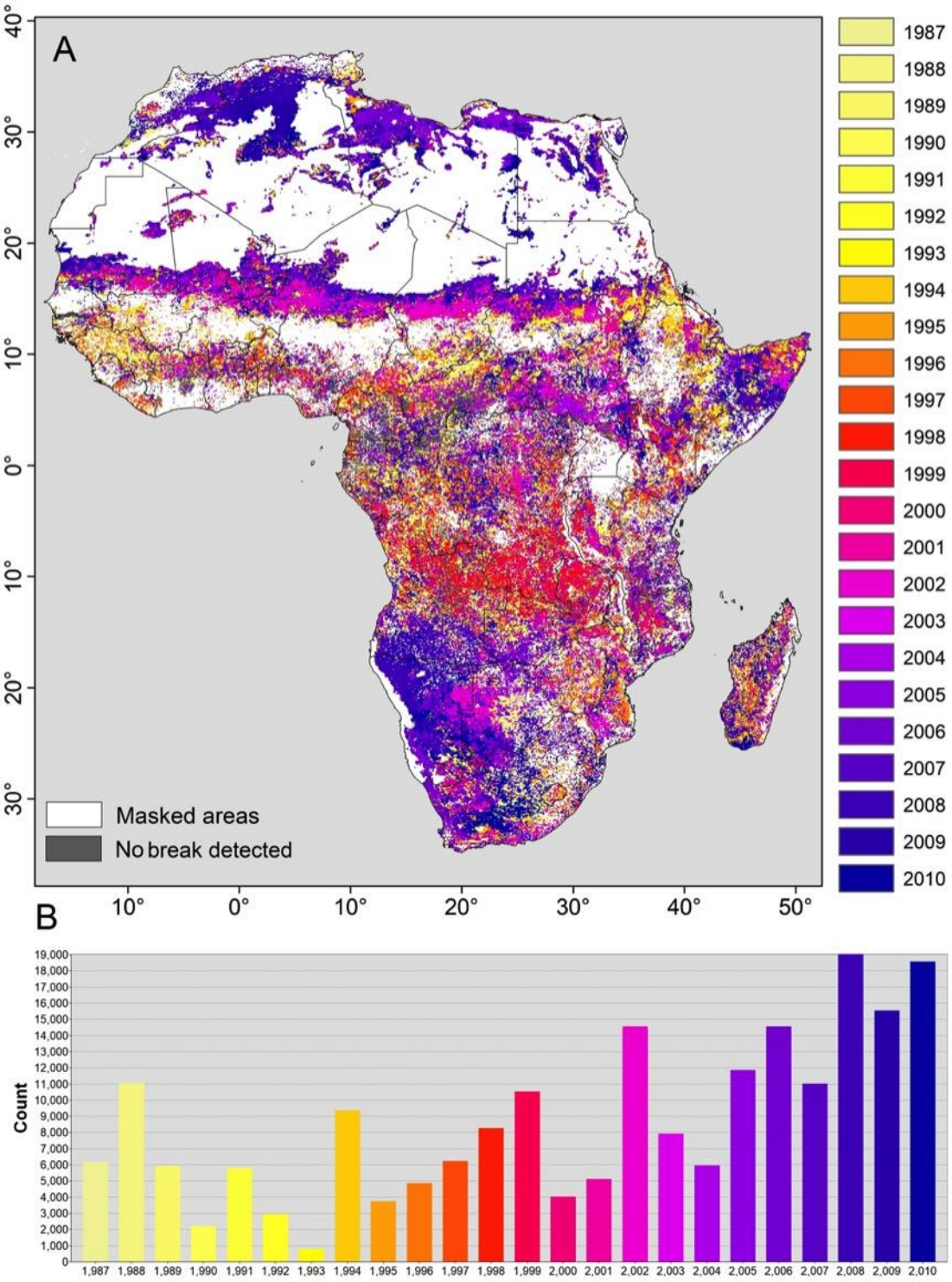

Figure 5.7: (A) Spatial distribution of the timing of shifts in AVHRR NDVI3g time-series. The detected breakpoints were binned into 1-year classes. White areas indicate areas that were masked from the analysis and grey areas represent pixels were no break was detected in the NDVI3g time-series. (B) Histogram of the number of grid cells experiencing a breakpoint in a particular year.

5.3.4 Geographical pattern of trend types

Building on from the previous results this section aims to add value to the interpretation of changes in NDVI3g by investigating shifts in trends over the time-series. The spatial trend patterns for two trend segments are shown in Figure 5.8 (the length of the trend segments are provided in Appendix D Figure D.6). The first (second) trend segment represents the trend before (after) the detected breakpoint (Figure 5.7). Following de Jong et al. (2012 & 2013), these trends can be separated into two general categories: (i) interrupted gradual change or (ii) shifts and reversals in trend direction. In the first trend segment greening trends are observed over most of SSA (Figure 5.8A), which is consistent with the findings of the linear trend analysis presented in Section 4.3.1. The majority of southern Africa has however experienced a setback with browning trends observed in the second trend segment (Figure 5.8B) demonstrating the presence of a number of more complex changes in the NDVI3g time-series. Increases in the magnitude of greening trends are observed over 0-10°N latitudinal band, particularly over East Africa, central Botswana, eastern coastline of South Africa (Figure 5.8B). The length of the segment tends to be shorter than the first except for central Botswana and areas over West Africa, which experienced an earlier breakpoint in the NDVI time-series (Appendix D Figure D.6). The geographical distributions of the two primary trend types are discussed in the following sections.

Interrupted gradual change

Gradual greening trends (Gr/Gr) in NDVI3g, similar to those observed in the linear trends, are observed over parts of the Sahel, West and East Africa across the 0-10°N latitudinal band, central Botswana, north-east South Africa extending northwards into Mozambique and Zimbabwe as well as over the south west Cape of South Africa (Figure 5.9A). The monotonic greening accounts 24% of the area of SSA, the second largest after the pixels experiencing greening only in first trend segment. A breakpoint in the monotonic greening trend is detected in 2002 but the magnitude of both trend segments remains similar (Figure 5. 10A).

Browning observed in both trend segments (Br/Br) is observed over most Madagascar, parts of Mozambique, northern Namibia extending into Angola and northern Botswana, and over the northern extent of Namaqualand, South Africa. This pattern of change accounts for 11% of the variation in NDVI3g and is consistent with the decline in NDVI3g observed in the linear trends presented previously suggesting that overall productivity has declined over the region (Figure 5.9B). The negative trend in NDVI3g amplifies post 2010 suggesting a recent strengthening of browning (Figure 5.10B).

Trend shifts and reversals

In a number of regions of SSA, trend segments demonstrate that shifts in trends in NDVI3g are more common than either consistent browning or greening and that periods of stability with no significant change in NDVI3g may be present in the time-series.

The reversal of browning trends (Br/Gr) is less spatially consistent relative to the other trend types with only a small number of isolated pixels (3%) over northern extent of Central African Republic and southern Madagascar showing this trend type over SSA (Figure 5.9C and Figure 5. 10C). This trend type is characterised by an initial brief decline in NDVI3g followed by an increase for the remaining time-series.

The reversal of greening trends (Gr/Br) accounts for 20% of the variation in NDVI3g. Over the central Congo lowland forests and parts of central South Africa, Namibia and Botswana trend segments demonstrate an initial increase in NDVI3g ($p < 0.05$) between 1982 and 2010 followed by a steep decline for the remaining 5 years of the time-series (Figure 5.9D and Figure 5. 10D). The breakpoint observed here is the same as the monotonic browning trends described previously (Figure 5. 10B). Since monotonic trend assessment techniques assess change over the entire period the recent decline may not be sufficient to change the overall direction of the trend. It is likely that if this trend persists into the future linear trend assessment techniques may detect a change in trend direction over this region.

A shift from a significant greening trend to a period of stable NDVI3g (Gr/No) post 1999 is evident over most of central Africa and parts of the Sahel with isolated pixels over rest of SSA (Figure 5.9E and Figure 5. 10E). This trend category accounts for 25% of the variation in NDVI3g and when combined with the monotonic greening trends (Gr/Gr) it shows that greening accounts for nearly half of the observed changes in vegetation over SSA.

Shifts from stable NDVI3g to browning trends (No/Br) post 1994 is observed over most of southern Africa and parts of the Sahel and East Africa (Figure 5.9F and Figure 5. 10F). This trend category covers 18% of SSA and is consistent with linear trends results presented previously suggesting that the decline in vegetation productivity over southern Africa has occurred consistently over the last 20 years.

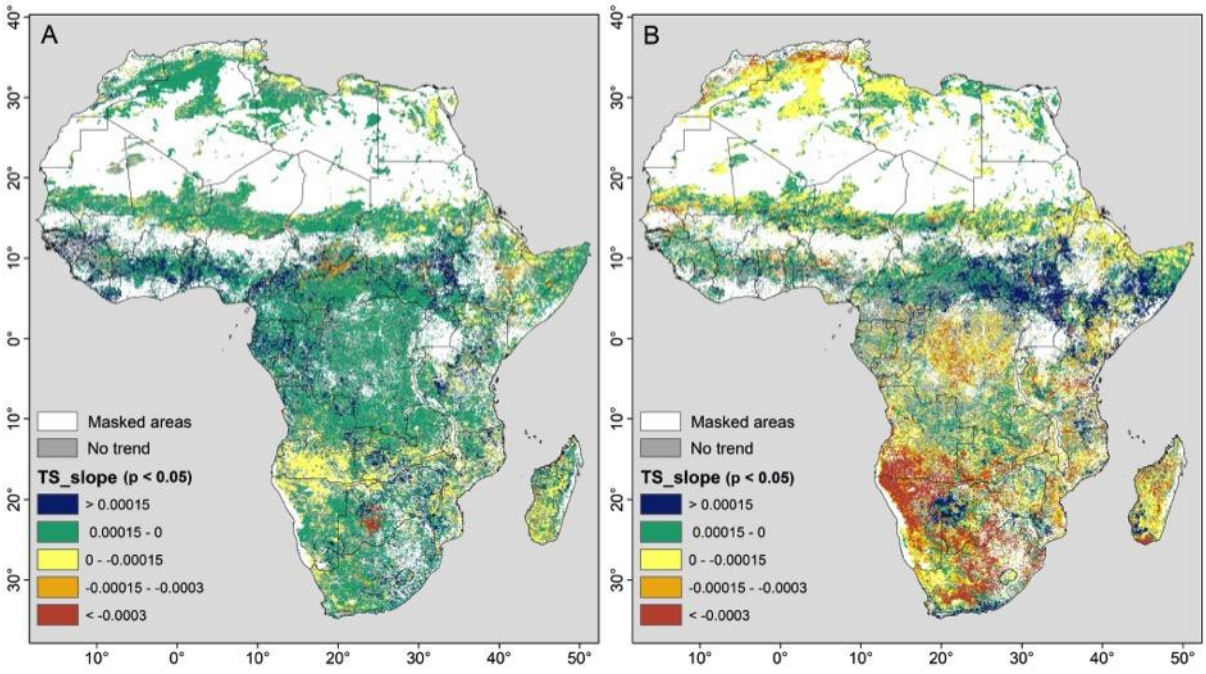

Figure 5.8: Magnitude of NDVI3g Theil-Sen trend for (A) first segment and (B) second segment using the BFAST spatial model. Statistically significant ($p < 0.05$) trends are displayed. White indicates pixels that were masked from the analysis and grey represent pixels were no trend ($p < 0.05$) was detected.

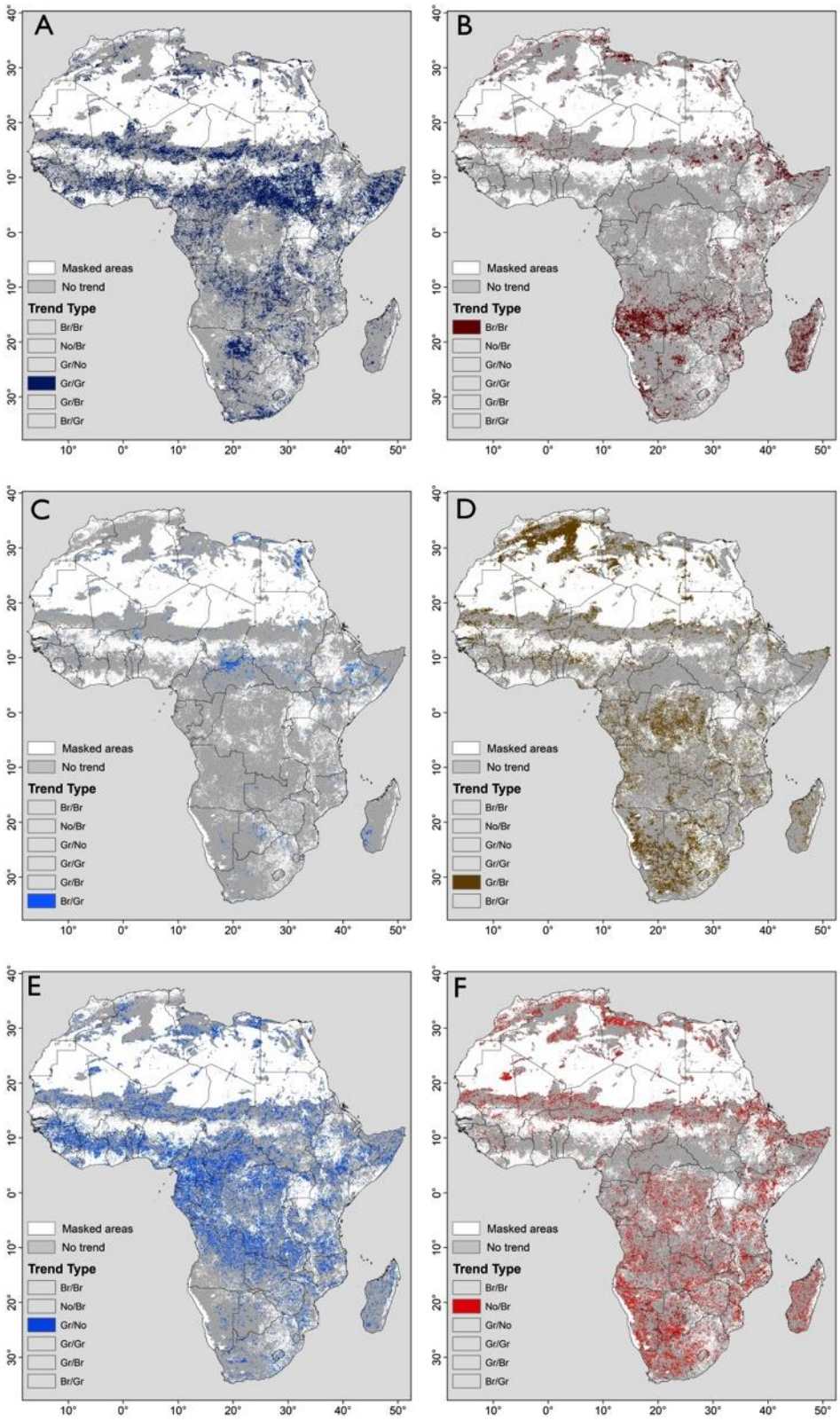

Figure 5.9: Spatial distribution of types of vegetation changes as defined as (A) monotonic greening (Gr/Gr), (B) monotonic browning (Br/Br), (C) browning to greening (Br/Gr), (D) greening to browning (Gr/Br), (E) greening in the first trend segment (Gr/No), and (F) browning in the second trend segment (No/Br). White indicates pixels that were masked from the analysis.

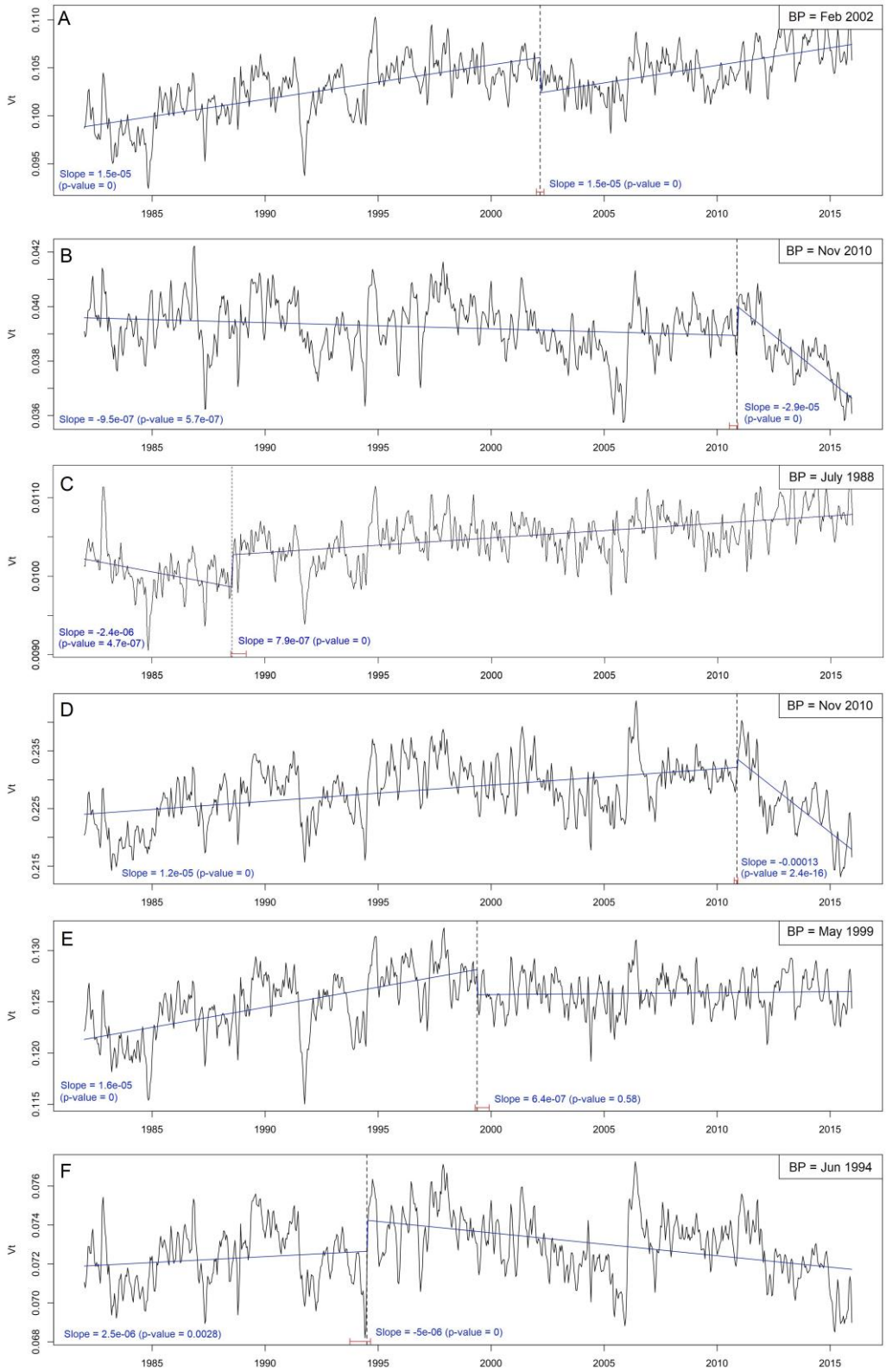

Figure 5.10: Detected gradual trends (blue) of different trend types (A to F as defined in Fig. 4.9) extracted from the AVHRR NDVI3g time series between 1982 and 2015. The data series (Vt) represents NDVI values that have been averaged across the trend class regions. The time of the change (---) together with its confidence intervals are also shown (|-|).

5.4 Discussion

In this chapter, the analysis of the 34-year AVHRR NDVI3g time-series using a variety of approaches provides a useful indication of the spatial and temporal changes in terrestrial vegetation over sub-Saharan Africa. This study extends the findings of previous studies. Firstly, both seasonal and inter-annual trends in vegetation were assessed in order to provide a comprehensive assessment of change over SSA. Secondly, long-term trends in vegetation were assessed in association with changes in climatic drivers in order to infer possible causes for observed greening or browning. Thirdly, this study utilised both linear models and techniques that decompose the time-series into gradual trends and abrupt changes at breakpoints in order to understand more complex temporal changes and shifts in NDVI3g.

5.4.1 Evidence for changes in vegetation productivity

Temporal changes in vegetation productivity over SSA consist of either gradual (monotonic) change throughout the time-series or segments of continuous change separated by short periods of abrupt changes and shifts in productivity. The linear trends in maximum (MAX) NDVI3g and large integral (LI) provided evidence for latitudinal changes in productivity with significant increases observed over the northern hemisphere tropics (0-10°N) and sub-tropics of southern hemisphere (20-35°S) and significant decreases observed over the southern hemisphere tropics (0-20°S). The results from piecewise linear trends technique (BFAST) demonstrated that greening over 0-10°N latitudinal band, East Africa, central Botswana, and parts of South Africa accounts for nearly half of the observed changes in vegetation productivity over SSA and that the majority of southern Africa has experienced a recent setback in vegetation productivity with browning trends prevailing post 2010. Similar spatial patterns and overall greening trends have been observed by other studies utilising the AVHRR NDVI time-series over similar assessment periods (e.g. de Jong et al. 2012; Mao et al. 2013; Vrieling et al. 2013; de Jong et al. 2013; Ivits et al. 2014; Hoscilo et al. 2015; Liu et al. 2015; e.g. Zhu et al. 2016).

5.4.2 Evidence for shifts in vegetation seasonality

The linear trends in phenology metrics provided evidence to suggest that the areas that have experienced significant changes in productivity tend to be associated with changes in seasonality. Longer seasons are observed over northern hemisphere tropics (0-10°N) and parts of southern Africa and the Sahel while shorter seasons are observed over the southern hemisphere tropics (0-20°S) particularly over Tanzania and northern Mozambique. Utilising an earlier version of the AVHRR NDVI dataset, Vrieling et al. (2013) reported similar patterns of change in the length of the growing season (LOS) with more pixels over 0-10°N latitudinal band demonstrating significant change ($p < 0.05$). Negative trends in the LOS over the Sahel

identified by previous studies were not found here (Heumann et al. 2007; Vrieling et al. 2013).

Changes in the temporal behaviour of NDVI and directional shifts in vegetation seasonality over long observational periods may indicate shifts in vegetation dynamics that are a result of changes in climate that either limit or promote the growth of vegetation (Reed 2006; Richardson et al. 2013; de Jong et al. 2013; Fitchett et al. 2015). This study provides evidence to suggest that recent changes in temperature, solar irradiance, and rainfall are associated with regions across SSA experiencing changes in length of the season as well as productivity within that primary growing season. This finding could provide an indication of the impacts of climate change over the region. Continued monitoring of vegetation seasonality across these regions is required in order to determine shifts in seasonality persist with future increases in temperature and changes in rainfall patterns. The use of climate change scenarios and DGVMs with detailed phenology characteristics, such as green-up date, will be particularly useful to further interrogate the link between changes in vegetation seasonality and climate.

5.4.3 Drivers of regional differences in vegetation change

Over the Sahel a fairly consistent greening trend is evident, which is consistent with previous assessments of NDVI3g and ground-based observations (Olsson et al. 2005; Dardel et al. 2014b; Brandt et al. 2015). While some studies across the Sahel have observed net decreases in woody vegetation in due to changing land-use and expansion of agriculture (Vincke et al. 2010; Gonzalez et al. 2012; Herrmann & Tappan 2013), the general greening of the Sahel is a well-documented phenomenon. Over the 1982 to 2015 period a significant increase in rainfall was observed (Figure 5.2) suggesting that the greening trend can be interpreted as a recovery from drought conditions that affected the region in the early to mid-1980s (Nemani et al. 2003; Heumann et al. 2007; Fensholt & Rasmussen 2011; Masih et al. 2014). More recently, the increasing trends could be also be linked to the implementation of a large-scale tree-planting project, known as the Great Green Wall (GGW), in the countries in the Sahel (Berrahmouni et al. 2014). The project was launched in 2005 in response to desertification, degraded soils, food insecurity, and climate change in the Sahel (Diallo et al. 2017).

In areas of West and central Africa (0-10°N) that showed an increase in vegetation productivity, studies have detected a rapid encroachment of savannas by forests in West Africa most noticeably in Ivory Coast (FAO 2015), Gabon (Delègue et al. 2001; FAO 2015), and Cameroon (Mitchard et al. 2009). While similar increases in vegetation productivity and length of season over Central African Republic are shown in some large-scale assessments of vegetation change (e.g. de Jong et al. 2012; Vrieling et al. 2013; Zhu et al. 2016) they have not been documented in local scale studies. A study by Aleman (2017) reported that

the vegetation gradient over the Central African Republic shows a clear shift from tropical forest to open grasslands but limited observational evidence was given to support this.

The expansion of the forest biome into surrounding savanna regions of West and Central Africa is understood in the literature to be driven by increases in rainfall combined with increases in atmospheric CO_2 concentration, reductions in factors that suppress woody vegetation growth including fire and grazing and the promotion of reforestation projects in some countries (Lewis et al. 2009; Mitchard & Flintrop 2013; Niang et al. 2014; Midgley & Bond 2015). In this study increases in productivity over this region were linked to increases in both temperature and rainfall over most of the 0-10°N latitudinal signalling the potential role of recent climate change on vegetation in these regions. Projections of future vegetation change as described by DGVMs demonstrate that above-ground woody vegetation cover over the tropical forests of Africa is likely to continue to increase (Higgins & Scheiter 2012; Moncrieff et al. 2014).

Similarly, over of parts of South Africa the gradual greening trend observed in this study could provide an indication of the expansion of woody vegetation into the savanna ecosystems. Over north-eastern extent of South Africa there was little evidence of substantial changes in rainfall suggesting the role of another driver. Increases in CO_2 have been shown to improve tree growth through the CO_2 fertilisation effect in a number of local case studies and is commonly argued as the most likely driver of changes in the balance between grasses and woody plants (Buitenwerf et al. 2012; O'Connor et al. 2014; Midgley & Bond 2015; Stevens et al. 2015; Stevens et al. 2016). Increase in vegetation over eastern coastline over South Africa could also be an indication of forest thickening due to increases in CO_2. Future scenarios expect that woody vegetation will continue to encroach these areas due to increases in rainfall and rising CO_2 (Driver et al. 2012).

Over the south-western Cape region of South Africa, a reduction in rainfall was observed between 1982 and 2015 suggesting that increases in vegetation productivity are more likely to be driven by invasive species possibly also in combination with increases in atmospheric CO_2. Studies across the region, particularly in the Fynbos Biome, have found that the landscape been transformed by the invasion of woody alien species (Rouget et al. 2003; van Wilgen 2009). An increase in forest patches and woody shrubs have been documented and are estimated to have invaded 21% of the biome (Richardson & Van Wilgen 2004; Le Maitre et al. 2016).

Over the remaining parts of southern Africa, the decline in vegetation productivity observed is similar to that found by de Jong et al. (2013). Harris et al. (2014a) found slightly different trend patterns with positive trends in vegetation being observed over southern Africa. This difference could be a result of the use of a shorter time-series of AVHRR NDVI from 1982 to 2006 by Harris et al. (2014a). While temperatures have increased over the region there is

little evidence of substantial changes or reductions in rainfall. The browning trends could thus be indicative of persistent land-use change (such as agricultural expansion). The consistent decline in vegetation productivity over southern Africa has been documented in a number of other remote sensing studies covering the DRC, Zambia and Angola. These studies have attributed the browning to deforestation of Miombo woodlands and tropical forests and land-use change as a result of growing populations (e.g. Bodart et al. 2013; FAO 2015; Hoscilo et al. 2015).

By using the GlobCover data to mask anthropogenically altered landscapes this study aimed to reduce the influence of land-use change on the trends in NDVI3g observed. Since the dataset only provides information up to 2009 more recent declines in vegetation over southern Africa post-2010 need to be investigated further in the context of more up to date understanding of local land use patterns. In addition continued assessment of AVHRR NDVI3g data will be required to confirm if the trend persists.

Over East Africa the direction and magnitude of trends were highly variable with gradual increases observed over Somalia, South Sudan, and northern Uganda and browning over parts of Kenya, northern Ethiopia, and Eritrea. While Vrieling et al. (2013) reported some changes in second vegetation season in East Africa, no substantial shifts in seasonality were observed in the study presented here.

A number of remote sensing studies presented evidence for declines in vegetation productivity over northern and eastern Ethiopia, along the Somali coast and in and central Kenya (De Jong et al. 2011; e.g. Pricope et al. 2013; Vrieling et al. 2013; Kim et al. 2013; Landmann & Dubovyk 2014). The declines in vegetation observed at certain intervals over East Africa have been attributed in previous studies to changes in land-use and non-climatic land degradation (Hoscilo et al. 2015). In this study, the greening over Uganda is associated with increases in rainfall between 1982 and 2015 suggesting the role of climate in driving the shifts in vegetation productivity. This effect is however limited only to northern Uganda region. A study in the Karamoja region of northern Uganda found that between 1986 and 2013 bushlands had expanded into surrounding grasslands and that alien species, such as *Prosopis* spp, had increased (Egeru et al. 2014). In the southern extent of Uganda agricultural expansion and land-use change would be limiting the expansion of woody species (Mwavu & Witkowski 2008). The more complex pattern of trends observed over East Africa could imply that changes in vegetation are context and location specific, which suggests that datasets with higher spatial resolution such as MODIS EVI may be more suitable.

5.4.4 Evaluation of the trend detection methods used in this study

Overall, the different trend techniques applied to the AVHRR NDVI3g time-series demonstrated similar spatial patterns of change in vegetation productivity over SSA. While these results were not validated using ground observations, the replication of results across methods provides some confidence in the trends in vegetation over the last 34 years. In addition, the analysis presented here demonstrated that the use of a range of different approaches is required to obtain a complete understanding of the spatial and temporal variability of vegetation productivity and seasonality.

Since the linear trend analyses are based on a limited time-series it is often difficult to detect vegetation change occurring within the first or last two years of the time series (Wessels et al. 2007a). This implies that the period of assessment also has a large influence on the detection of linear trends where the addition of years to the time-series could change the trend direction. The piecewise linear trends technique (BFAST) added considerable value in this study by demonstrating that trends in vegetation are often more complex with abrupt changes and shifts in vegetation productivity occurring in the NDVI3g time-series. The detection of breakpoints and trends in multiple shorter segments allowed for an improved understanding of temporal changes in NDVI3g as well as the potential drivers of these shifts in vegetation.

A challenge still remains in attempting to understand change is to distinguish between statistically significant changes and changes that are practically significant at the local scale (Forkel et al. 2013). Field-based validation of shifts in vegetation over a 34-year period across SSA remains unfeasible. A common approach, similar to that taken in this paper, is to use regional or global related publications to validate trend analyses but these are often insufficient since many of these studies utilise the same NDVI data and similar trend detection approaches. Future research is required to conduct smaller scale assessments over the regions, such as Central African Republic, which demonstrate substantial shifts in vegetation productivity and seasonality in order to assist in the interpretation of finer scale changes in vegetation dynamics and associated climatic drivers. The MODIS EVI time-series could also be used as a comparative time series to further understanding changes in both vegetation productivity and seasonality over SSA.

5.5 Conclusion

The purpose of this chapter was to assess changes in vegetation productivity and seasonality over Africa using the longest continuous temporal record available and a range of range previously published trend detection techniques. The research extends the results identified by previous studies and presents an important synthesis of changes in vegetation productivity over Africa over the last 32 years.

Evidence for a number of important spatial and temporal patterns of change in vegetation productivity over SSA is presented, which are generally consistent with independently reported long-term trends. Insights from the analysis include:

- Spatial patterns of trends provide evidence for latitudinal changes in productivity with significant increases in the northern hemisphere tropics and sub-tropics of both the southern hemisphere and significant decreases over the southern hemisphere tropics.
- Greening accounts for nearly half of the observed changes in vegetation productivity over SSA.
- In areas that have experienced significant increases in productivity tend to be associated with increases in the length of the season as a result of an earlier start and later end date of the season. This finding could potentially provide a first indication of the impact of recent climate change over these regions.
- Over the Sahel a consistent greening trend provides evidence for the recovery of vegetation from drought conditions that affected the region in the early to mid-1980s.
- While acknowledging that NDVI tends to saturate in densely vegetated areas, patterns of increasing productivity and length of season were observed over the parts of West and central Africa suggesting that forests are expanding into the surrounding savanna regions. This expansion is interpreted as a response to increases in rainfall combined with increases in atmospheric CO_2 concentration as well as reforestation efforts in some countries.
- Patterns of gradually increasing productivity were detected over the south western Cape, eastern coastline, and north-east extent of South Africa which are consistent with the observed patterns of bush encroachment and expansion of alien invasive species in these regions.
- Declines in vegetation productivity were observed over the majority of southern Africa most likely due to land-use changes and reduction in woody vegetation as a result of non-climatic factors including the clearing for agriculture and population expansions.
- Differing patterns of greening and browning were observed over East Africa suggesting the role of local-scale factors driving vegetation change.

While it is possible, to some extent, to attribute an underlying process or driver of change to a particular type of trend in this study, simulations of DGVM will assist in understand the influence of changing rainfall patterns and increases in atmospheric CO_2 in the context of rapidly changing land-use patterns in the region. Further analysis is needed to understand and identify the climatic mechanisms behind the observed trends in the content of local scale land-use change.

Chapter 6:

6. Simulating historical vegetation of Africa using aDGVM: an evaluation using time-series of satellite vegetation indices

6.1. Introduction

6.1.1. Background

Climate change is likely to drive substantial changes in terrestrial vegetation across the globe (Stocker et al. 2013) and there is substantial evidence that shifts in vegetation productivity and distributions are already occurring (Mitchard & Flintrop 2013; Niang et al. 2014; Stevens et al. 2016). As a result, there is a growing recognition that simulating the structural and functional changes in vegetation over the next 25 to 50 years is crucial in understanding the impacts of climate change on terrestrial ecosystems (Hannah et al. 2002; McMahon et al. 2011; Shafer et al. 2015).

Predictions of vegetation responses to projected future climate change tend to be based on process-based model approaches such as Dynamic Global Vegetation Models (DGVMs). These numerical, mechanistic models simulate the large-scale dynamics of terrestrial ecosystems by allowing the distribution of discrete plant functional types (PFTs) to evolve dynamically in response to climate, atmospheric CO_2, plant water use efficiency, soil type, competition for water, light, and nutrients, and disturbances such as fire (Prentice et al. 2007; Pavlick et al. 2013). DGVMs have been proven useful for making predictions regarding long-term changes in vegetation dynamics in response to changing climate and increasing atmospheric CO_2 concentrations (Cramer et al. 2001; Sitch et al. 2003; Sitch et al. 2008; Scheiter & Higgins 2009; Quillet et al. 2010; Pavlick et al. 2013; Moncrieff et al. 2015). To date, modelling studies have demonstrated that elevated atmospheric CO_2 concentrations have a 'fertilization' effect on vegetation, particularly C_3 plants, by increasing photosynthesis and water use efficiency (Bond & Midgley 2000; Ainsworth & Long 2005; Higgins & Scheiter 2012). These impacts are however expected to vary considerably across regions with different seasonal characteristics, plant species and local environmental conditions (Maignan et al. 2011). Furthermore, a number of ecological and dynamic processes are not yet fully understood and this results in limitations in the representation of vegetation dynamics and the simulation results of models (Quillet et al. 2010; Fisher et al. 2010; Rezende et al. 2016). There is a need to assess the credibility of the DGVM outputs, especially as some of them are already being used for prominent policy and planning applications, impact studies

from local to national scale, inputs into conservation management plans (e.g. Driver et al. 2012) to global simulations of carbon balance (e.g. Le Quéré et al. 2016).

The rationale for this chapter is that the confidence in model projections depends on the ability of DGVMs to simulate present-day vegetation dynamics (Zhu et al. 2013). Improving the representation of vegetation dynamics in DGVMs under present climatic conditions is essential for projecting future climate change impacts such as biome boundary shifts (Sitch et al. 2008; Baudena et al. 2015). Validation of DGVMs particularly at large spatial scales is challenging due to the long time scale of vegetation dynamics assessed and the lack of observational data (Kelley et al. 2013). Satellite observations provide a useful source of data to compare the simulated historical vegetation dynamics from a DGVM and to determine where improvements can be made. Several studies have evaluated DGVMs using satellite-derived observations of leaf area index (LAI) (e.g. Buermann et al. 2001; Maignan et al. 2011; Zhu et al. 2013; Pavlick et al. 2013; Anav et al. 2013). LAI represents the total surface area of leaves above a unit area of ground and is expressed as m^2(plant)/m^2(ground) (Murray-Tortarolo et al. 2013). It is considered an essential biophysical variable in all DGVMs and its correct representation, both temporarily and spatially, is key to predicting correct carbon fluxes and implications for vegetation change (Sabater et al. 2008; Murray-Tortarolo et al. 2013). Furthermore, LAI is often used to classify vegetation into different biomes, which are then compared to observed vegetation (Hickler et al. 2006)

6.1.2. Objectives and rationale

Building on the understanding of dynamics of vegetation over SSA over the last 34-years (Chapter 3-5), the purpose of this study is to evaluate historical outputs of LAI from the adaptive Dynamic Global Vegetation Model (aDGVM) by comparing satellite-based observation to model simulated values of LAI over Sub-Saharan Africa. The third generation AVHRR LAI3g product provides a unique opportunity to assess LAI estimates from the aDGVM. While a perfect correlation between the two is not expected, the assessment presented here should assist in the improvement the model and lead to an increase in the overall performance across a range of different vegetation types.

The aDGVM used here was developed and tested for African tropical tree–grass systems. Whilst it has been shown to successfully simulate the current distribution of African biomes (Scheiter & Higgins 2009) as well as the vegetation biomass in a long-term fire exclusion experiment in the Kruger National Park, South Africa (Higgins et al. 2007) it is constrained by a lack of knowledge of the historical vegetation state (Moncrieff et al. 2014). This study presented here is the first to (i) run the aDGVM with daily climate data at a large scale with historic and two RCP scenarios, and (ii) to assess the aDGVMs ability to reproduce the inter and intra-annual patterns of variability of LAI across Africa. To date, daily data have only been used as measurements in single study site applications.

6.2. Methodology

6.2.1. The Adaptive Dynamic Global Vegetation Model (aDGVM): version 1

The adaptive Dynamic Global Vegetation Model (aDGVM) is an individual based dynamic vegetation model that was explicitly developed and tested for grass-tree systems in savannas (Scheiter & Higgins 2009). A full description of the model is provided in Scheiter and Higgins (2009) with updated versions described in Scheiter et al. (2012). The aDGVM combines plant physiology with adaptive dynamic carbon allocation and leaf phenology, and an improved representation of fire impacts. The model is individual-based in that it simulates growth, reproduction and mortality of each individual plant. Light and water competition between plants is also simulated in the model. The aDGVM records variables including biomass, height, leaf area index and leaf phenology for individual plants. The model includes four basic plant functional types (PFTs): savanna tree, forest tree, C_4 grass and C_3 grass. Version 1 of the aDGVM does not include a shrub plant functional type. It has been noted by Moncrieff et al. (2015) that conceptual work is needed to properly incorporate the shrub functional type into the DGVM framework, and that several shrub sub-types may be required to reflect differences in shrub flammability and drought resistance. This shortcoming is most likely to constrain the performance of the aDGVM in shrub-dominated ecosystems, namely fire-prone Mediterranean shrublands and drought-prone semi-arid and arid shrublands.

In the model, savannah trees are fire tolerant and shade intolerant while forest trees are fire sensitive and shade tolerant. The model does not simulate different species as it assumes that vegetation dynamics are adequately described by a ‘typical’ tree and grass type. The inputs required by the model include site-specific soil and climate conditions. This model only considers the influence of climate on vegetation and does not account for the feedbacks between climate and vegetation.

6.2.2. Historical climate data (1982-2011)

The conformal-cubic atmospheric model (CCAM) (McGregor 2005) was used to provide historical regional climate simulations over Africa. Historical climate data from CCAM was used in this study, as opposed to CRU TS 4.00 for example, since these downscaled models will be used in upcoming studies to understand future changes in vegetation of Africa using the aDGVM.

Six Coupled General Circulation Models (CGCMs) (Table 6.1) of the Coupled Model Intercomparison Project Phase 5 (CMIP5) and and Assessment Report Five (AR5) of the Intergovernmental Panel on Climate Change (IPCC), were dynamically downscaled to 50x50km resolution. The downscaling of the CGCMs involved using the sea-ice concentrations and bias-corrected sea surface temperatures of the CGCMs, to force CCAM simulations (Katzfey et al. 2009; Engelbrecht et al. 2011). In these simulations, CCAM was

coupled to the CSIRO Atmospheric Biosphere Land Exchange (CABLE) model. CABLE is a dynamic land-surface model with the capability to interactively simulate the carbon flux between the land-surface and atmosphere (Law et al. 2006; Kowalczyk et al. 2006). The selection of CGCMs was based on the ability of the model to simulate present-day El Niño attributes, which is a key driver of climate variability across southern Africa as well as practical considerations such as data storage and computational capacity (Engelbrecht et al. 2015). The simulations were performed on the computer clusters of the Centre for High Performance Computing (CHPC) of the Meraka Institute of the CSIR in Cape Town, South Africa.

CCAM simulated climate outputs for 1982 to 2011 were used in this study to match the AVHRR LAI3g dataset. Observed greenhouse gas concentrations were used in simulations of historical climate. The models ability to simulate present-day climate over Africa has been extensively demonstrated (Engelbrecht et al. 2009; 2013; Malherbe et al. 2013; Engelbrecht et al. 2015). The ensemble average simulated temperature and rainfall for the period 1982 to 2011 is shown in Figure 6.1.

Table 6.1: List of the 6 Coupled General Circulation Models (CGCMs) from the Coupled Model Inter-comparison Project Phase 5 (CMIP5) (IPCC AR5)

Originating group(s)	Country	I.D.
The Centre for Australian Weather and Climate Research (CSIRO/Australian Bureau of Meteorology)	Australia	ACCESS1-0
US Dept. of Commerce / NOAA / Geophysical Fluid Dynamics Laboratory	USA	GFDL-CM3
Météo-France / Centre National de Recherches Météorologiques	France	CNRM-CM5
Max Planck Institute for Meteorology	Germany	MPI-ESM-LR
Bjerknes Centre for Climate Research (coordinator)	Norway	NorESM1-M
University Corporation for Atmospheric Research (UCAR)	International consortium	CCSM4

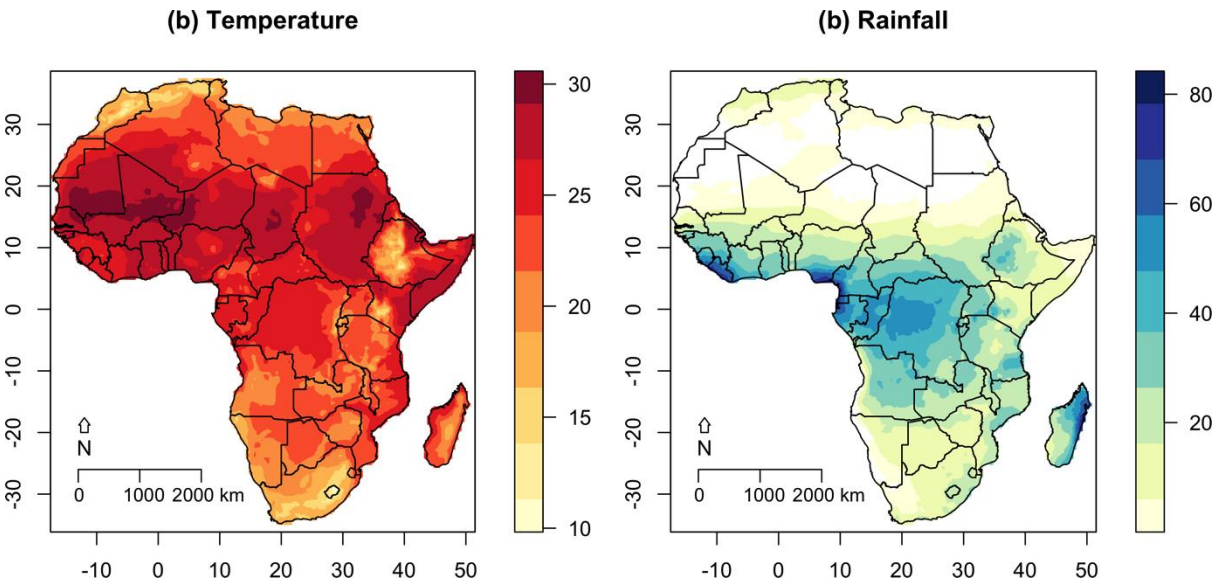

Figure 6.1: Ensemble average of the 6 regional CCAM simulations for (A) mean temperature (°C) and (B) rainfall totals (mm per year) over Africa for the period 1982-2011

6.2.3. Satellite data

AVHRR LAI3g dataset (1982-2011)

For the evaluation of model simulations, the AVHRR LAI3g (third generation) product was used. Leaf Area Index (LAI) datasets were generated from the GIMMS AVHRR NDVI3g time-series using an Artificial Neural Network (ANN) (Zhu et al. 2013). The neural network for generating was trained with overlapping AVHRR NDVI3g and MODIS LAI data. The dataset have the same temporal and spatial characteristics as the AVHRR NDVI3g dataset (refer to Chapter 3); two values per month with a spatial resolution of 1/12 degrees (8km). It provides one of the longest LAI time-series currently available and covers the period July 1981 to December 2011. The dataset has been used to study vegetation dynamics globally (e.g. Mao et al. 2013; Cook & Pau 2013; Zhu et al. 2016) and over parts of Africa (Musau et al. 2016).

Validation of the AVHRR LAI3g product was carried out directly by using field data predominantly from the northern latitude cropland, grassland and boreal forest biomes and indirectly through (i) inter-comparisons with similar satellite derived products, (ii) comparisons with climatic variables, and (iii) comparison with simulations from 18 Earth System Models (Zhu et al. 2013). Over East Africa, the patterns of and variability of AVHRR LAI3g matches field-based LAI records but the saturation effect, similar to NDVI3g, is observed in forest biomes (Pfeifer et al. 2014).

6.2.4. LAI simulations

Simulations of LAI using the aDGVM (version 1) were conducted for the entire continent at a resolution of 50km to match the downscaled climate models. A 210-year model spin up was conducted using climate data for the period 1971-1980. This spin-up is necessary to run the

model into a steady state. Previous simulations using the aDGVM have shown that a 200-year spin-up is sufficient to reach steady state (Scheiter & Higgins 2009). Simulations of vegetation were then forced with historical climate data from 6 CCAM downscaled models (refer to section 6.3.2 for details). All simulations were run with observed historical atmospheric CO_2 concentrations and with fire included in the model runs. The model was initialized with low grass biomass and 100 small trees. The vegetation simulated by the aDGVM is translated into a biome type using the classification scheme described in Scheiter et al. (2012), Higgins & Scheiter (2012), and Moncrieff et al. (2014) and provided in Appendix E Figure E.1. Leaf Area Index was output from the aDGVM and analysed for the period 1982 to 2011 to match the satellite-based observations.

6.2.5. Evaluation of historical simulations of LAI

The observed AVHRR LAI3g was compared to model simulated values of LAI for the period 1982 to 2011 by evaluating (i) spatial patterns of LAI over sub-Saharan Africa, (ii) month of maximum LAI, (iii) annual vegetation cycles summarised according to biome (Sayre et al. 2013: refer to Figure 1.1 in Chapter 1), (iv) spatial correlation between simulated and observed LAI, and (v) long-terms linear trends in LAI (Figure 6.2). The analysis focuses on the historical period 1982 to 2011 to match the AVHRR LAI3g observations. LAI less than 0.1 were masked from the analysis.

Since both LAI and LAI variability are important in identifying impacts of climate change on vegetation both the long-term average and inter-annual variability (IAV) of LAI was assessed and compared to remotely sensed observations. The magnitude of the IAV was calculated as the standard deviation of annual mean LAI between 1982 and 2011.

In order to further evaluate the model's ability to capture the spatial variability of LAI over sub-Saharan Africa, a spatial correlation (Pearson's correlation coefficient) was conducted. Correlation maps based on both the monthly time series and anomaly time-series were analysed. The former are indicative of the models ability to reproduce the seasonal cycle whereas the latter are representative of the model performance for reproducing inter-annual variability. Since, the spatial resolution of the two datasets is not the same, the AVHRR NDVI3g data (0.08° resolution) were resampled to 0.5° to match the aDGVM outputs using bilinear interpolation.

Trends in LAI were assessed using the Theil-Sen technique (Theil 1950; Sen 1968). To present the results, zonal average plots of trends across Africa were created for the observed and simulated LAI time-series.

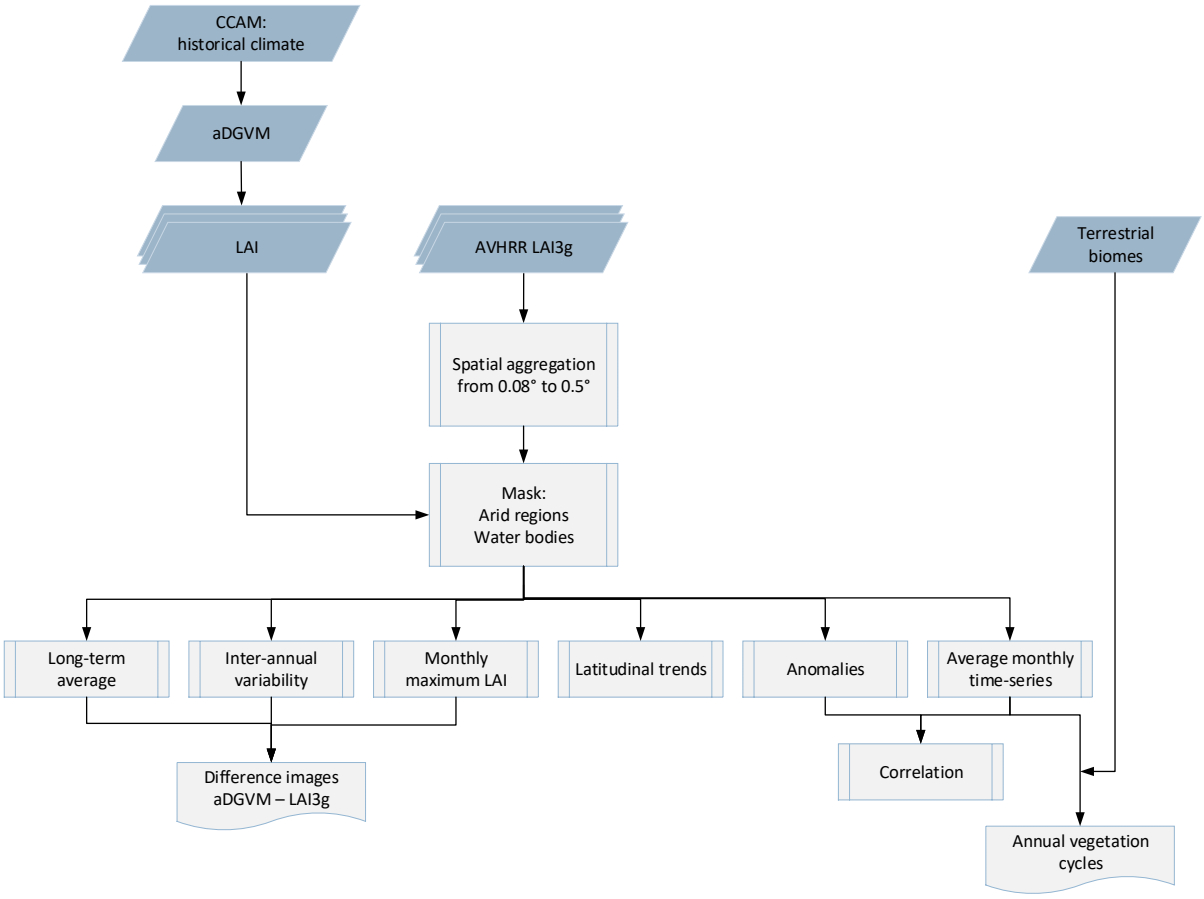

Figure 6.2: Flow diagram of the approach taken to evaluate the ability of the aDGVM to simulate leaf area index (LAI) in the current climate (1982-2011)

6.3. Results

6.3.1. Spatial patterns of LAI

The broad-scale spatial patterns of the simulated vegetation from the aDGVM are generally similar to the observed patterns of LAI over sub-Saharan Africa (Figure 6.3 and 6.4). Areas of disagreement between the observed and simulated LAI are however evident. The simulated mean LAI values over the tropical humid region of central Africa and Madagascar are generally lower relative to the observations (Figure 6.5) whereas over parts of semi-arid regions of East Africa, the northern extent of the Sahel, and parts of southern Africa dominated by grassland the simulated LAI values were higher than the observed values (Figure 6.5). The semi-arid areas tend to be used for agricultural purposes (Thornton et al. 2006) and the overestimation could be due to land-use impacts not accounted for in the simulation. It is important to note, however, that the satellite-derived LAI have biases. As outlined in Chapter 3 for NDVI3g, LAI3g also tends to underestimate LAI in densely vegetated areas or over areas that experience high percentage of cloudy days per year and to overestimate LAI in arid regions.

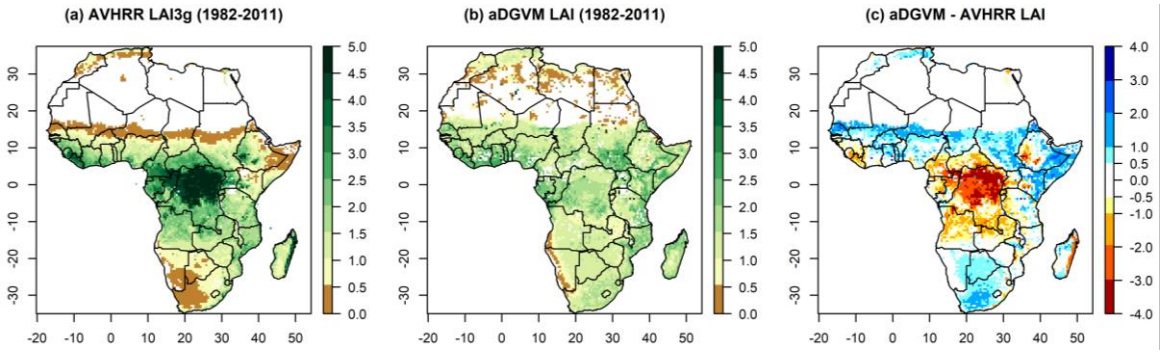

Figure 6.3: Mean Annual LAI for years 1982-2011 from (a) AVHRR LAI3g data set, (b) simulated by aDGVM, and (c) the model bias (aDGVM-LAI3g)

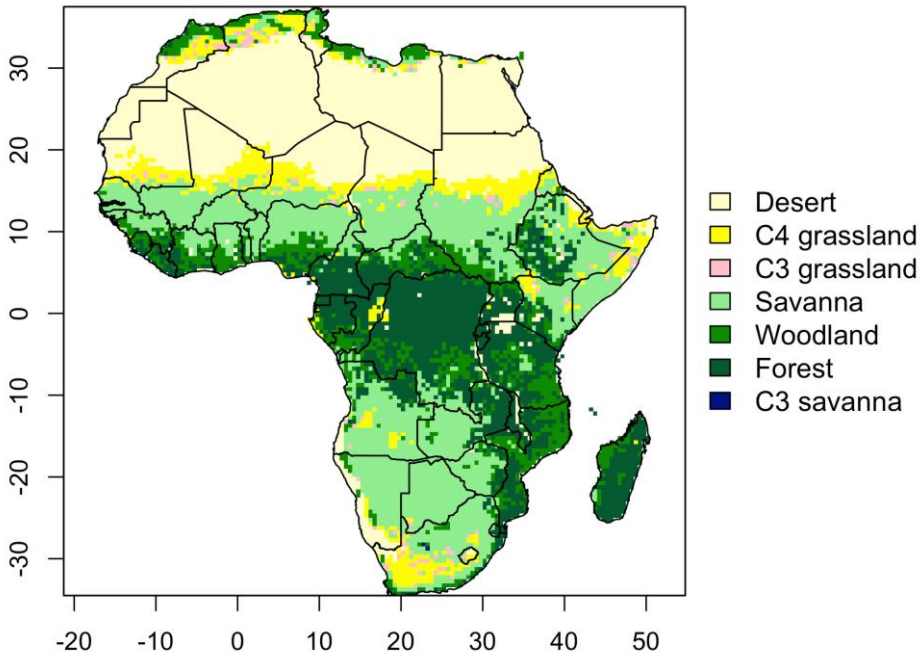

Figure 6.4: Simulated historical vegetation by aDGVM according to plant functional type (PFT) based on the median of the ensemble. The classification scheme of simulated vegetation types into different biome types is provided in Appendix E Figure E.1.

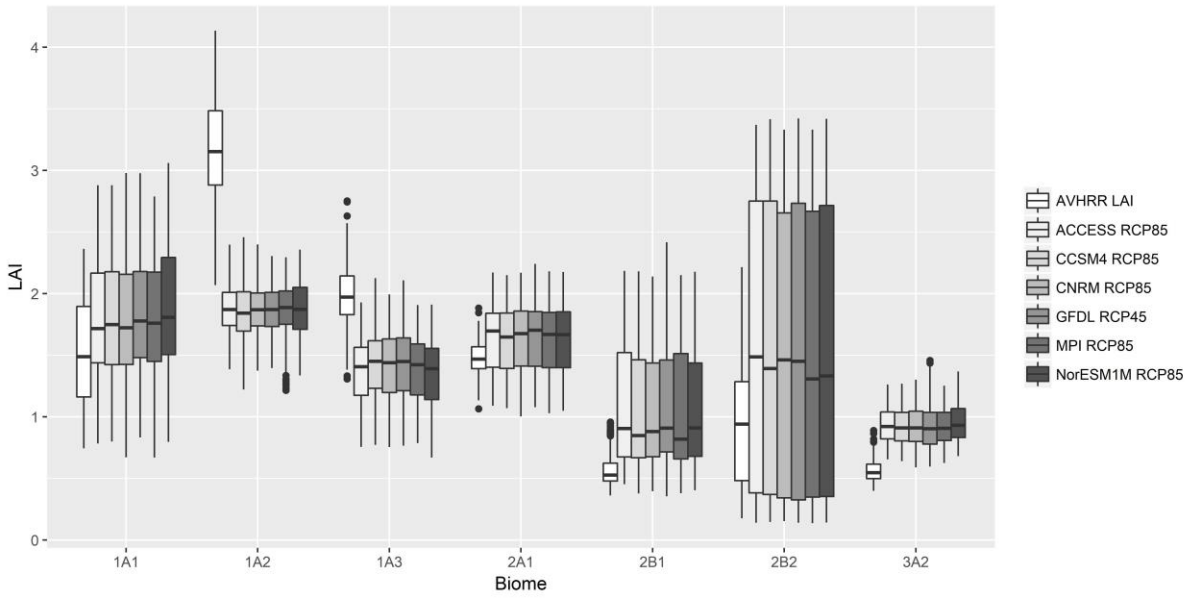

Figure 6.5: Goodness of fit between the AVHRR LAI and the simulated LAI values from aDGVM using 6 downscaled climate models for 7 major biome categories; tropical seasonally dry forest (1A1), tropical lowland humid forest (1A2), tropical montane humid forest (1A3), tropical lowland grassland, savanna and shrublands (2A1), Mediterranean scrub and grassland (2B1), temperate grassland (2B2), and warm desert and semi-desert scrub and grassland (3A2) (Sayre et al. 2013).

6.3.2. Seasonal cycles of LAI

The simulated timing of the month of maximum LAI over savanna and grassland regions matches the observations fairly well with only a 2 to 3 month lag in simulated maximum LAI (Figure 6.6 and 7.8). The correlation map (Figure 6.7) further demonstrates this fit with high association between that the observed and simulated LAI values over southern African savannas ($r > 0.8$). Over the tropical montane humid forests of the southern hemisphere the model also performs well with the simulated annual cycle follow a similar pattern to that of the observed LAI (Figure 6.8).

In general, the month of maximum simulated LAI demonstrated a clear pattern that replicates the difference in the timing of the northern and southern hemisphere summers. This fails to capture a number of the more detailed seasonal patterns over parts of sub-Saharan Africa. Firstly, over winter-rainfall region of South Africa the aDGVM simulated maximum occurs in February six months before the observations. This mismatch is evident in the comparisons of the annual cycle of LAI3g and the ensemble mean LAI from the aDGVM for this biome (Figure 6.8). This demonstrates the current limits of the aDGVM to simulate the phenology of the Mediterranean vegetation of the south-west Cape of South Africa.

Over parts of Kenya and Somalia the peak vegetation observed in March is not replicated by the aDGVM, which demonstrates considerable variability in the month of maximum LAI. This region experiences two rainfall seasons; one from April to May and another from October to December (Nicholson 1996). The first rainfall season is longer than the second; often

referred to as the “long” and “short” rains. The times-series of LAI from aDGVM over this region demonstrates that the model is able to simulate this bimodality with the first peak in March and the second in November (Appendix E Figure E.2). The magnitude of the second peak in November is higher than the first and this could account for the difference between the observed and simulated LAI time-series.

Lastly, over northern extent of tropical forests the peak vegetation occurs in October/ November up to eight months after the observations. Over the forested areas of northern Angola the observed LAI3g demonstrates an earlier peak than the neighbouring forest area. These differences could be result of this region experiencing vegetation growth throughout the entire year and has no distinct pattern of seasonality.

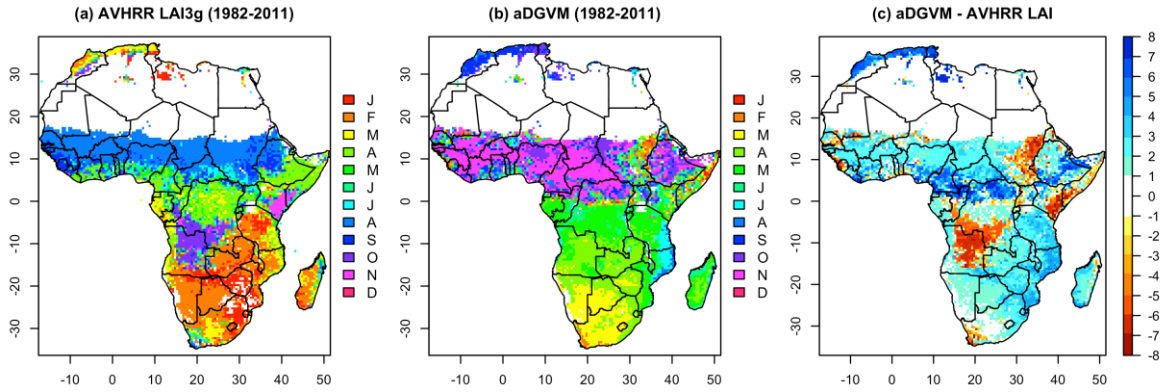

Figure 6.6: Mean month of maximum leaf area index for years 1982– 2011 from (a) AVHRR LAI3g data set, (b) simulated by aDGVM, and (c) the lag in months between the occurrence of maximum AVHRR NDVI3g observations and the aDGVM model output (aDGVM-LAI3g).

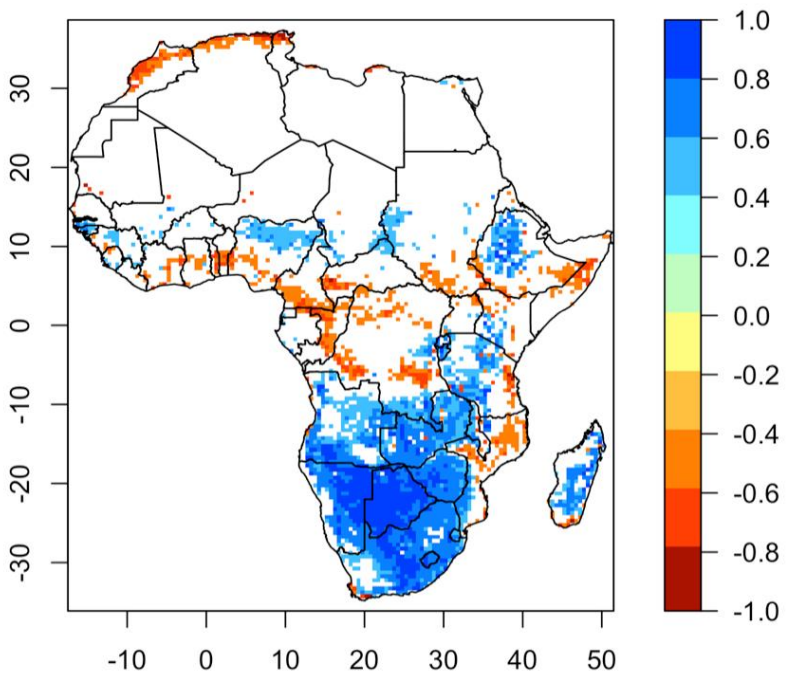

Figure 6.7: Pearson correlation coefficients (r-values) of simulated LAI with observed LAI3g over Africa for the 1982-2013 period based on monthly time-series. Only statistically significant pixels ($p < 0.05$) are shown. White indicates masked areas with NDVI values < 0.1. The blue (red) colours indicate a positive (negative) correlation.

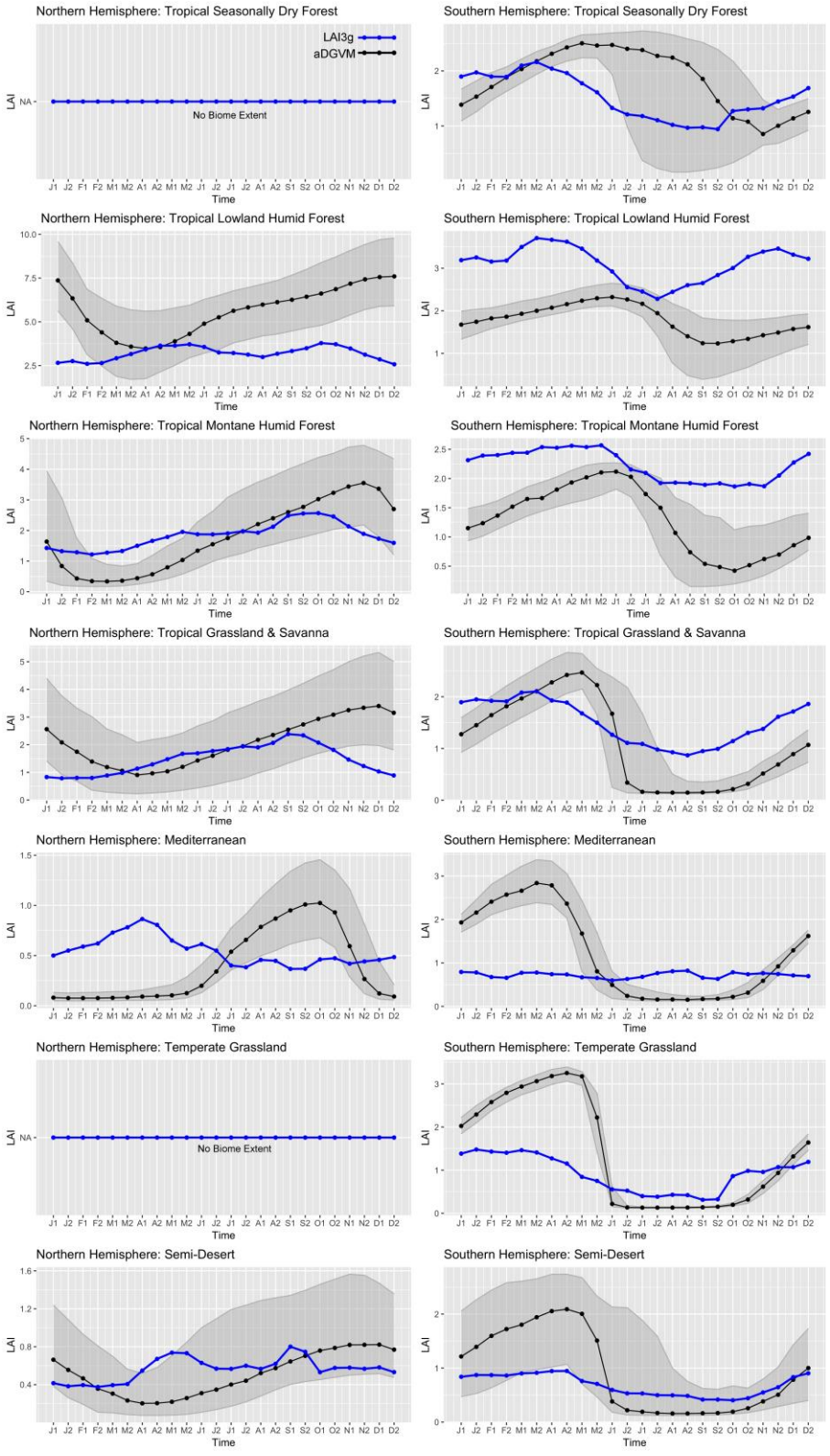

Figure 6.8: Comparison of the 1982 to 2011 average seasonal cycle between simulated LAI (black line) and LAI3g (blue line) per biome category. The graphs are split between the (A) northern and (B) southern hemisphere to account for different LAI peaks in calendar year. The shaded are shows the upper 75th and lower 25th percentile of the 6 different CCAM downloaded model forcing. The bi-weekly (15 day) periods are named by the first letter of the month (J,F,…D) followed by the number (1–2). NA indicates the cases where the biome type is not found in the northern hemisphere.

6.3.3. Temporal trends

Figure 6.9 illustrates the 1982-2011 latitudinal LAI trends from the observed AVHRR LAI3g dataset and the aDGVM. Satellite observations of LAI3g reveal a greening trend, particularly in over the latitudinal band between 0 and 10° north (Figure 6.9a). Over the southern Africa (10-20° south) there is a clear pattern of decreasing LAI3g. These observed patterns have been discussed in detail in Chapter 5 of this thesis. The spatial pattern of trends presented in Chapter 4 provide evidence for latitudinal changes in productivity with significant increases in the northern hemisphere tropics and sub-tropics of both the southern hemisphere and significant decreases over the southern hemisphere tropics.

The trends in LAI outputs from the DGVM (Figure 6.9b) do not match the trend in the observed time-series exactly and the correlation between annual anomaly time-series of observed and simulated LAI is very weak ($r < 0.3$; $p < 0.05$). For the simulated LAI times-series, increases are observed over most of sub-Saharan Africa particularly over the 10-20° north range in northern latitude. This pattern matches the expected impacts of the CO_2 fertilisation effect and could suggest an expansion of the savanna and grasslands into semi-desert regions. A slight negative trend is observed in the southern hemisphere between 28 and 30° South but there is less agreement between the models on this trend (as indicated by the larger grey confidence interval band).

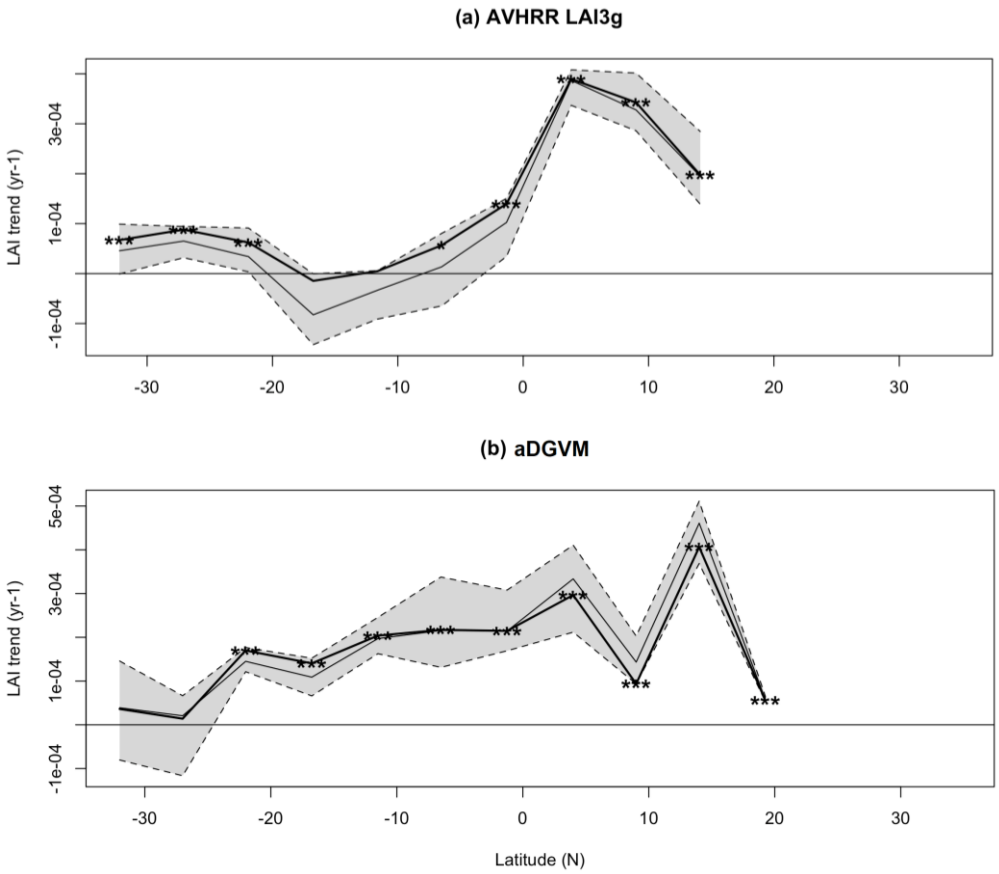

Figure 6.9: Latitudinal gradient of the Theil-Sen trend for (a) observed AVHR LAI3g and (b) aDGVM outputs for each of the 6 downscaled regional climate models for the period 1982-2011. The bold line with significance flags (*) is the estimated trend slope. The grey-coloured area and the thin line are the 95% confidence interval and the median represented by the light grey line. NDVI values below 0.1 and urban areas were masked from the analysis.

6.4. Discussion

Overall, the aDGVM was able to capture the observed global phenological patterns over savanna and grassland regions as well as the tropical forests of southern Africa to some extent. This performance shows promise for extending the model to consider the dynamics of other vegetation types of SSA. This study has demonstrated that simulations of LAI by the aDGVM could be improved in a number of key spatial and temporal aspects including average productivity, annual seasonal fluctuations and inter-annual variability over Africa.

Firstly, overestimation of simulated LAI over East African savannas and parts of Sahel and the underestimations in the trees in the humid tropical forests are likely a result of model biases in the calculation of LAI. In the aDGVM LAI is not calculated directly but based on leaf biomass, specific leaf area (SLA), and the cover of grasses and trees. A study by Pavlick (2013) using the JeDi-DGVM RCM found a reversed pattern where LAI tends to be overestimated over central Africa and over the Sahel region. Another by Ardo (2015) however found that estimates of gross primary productivity derived from satellite

observations were higher than corresponding estimates derived from the LPJ-GUESS dynamic vegetation model. These model biases tend to be dependent on the dynamic vegetation model used as well as the source of the satellite observation used; AVHRR versus MODIS for example. The exclusion of shrub component from the aDGVM1 may also have resulted in the difference observed in vegetation biomass between the observed and simulated values. The latest version of the aDGVM now includes a shrub PFT (Scheiter et al. 2013) so it would be beneficial for a future study to compare the outputs from aDGVM2 with remotely sensed vegetation indices.

Secondly, over the savanna and grassland regions, the peak LAI in the simulated time-series lags behind the observed by 2 to 3 months. There are two possible explanations for this lag. Firstly, the trigger function used to initiate leaf flush may not appropriate. Currently, the model assumes that leaf flush has to be greater than zero for 10 subsequent days before a tree moves from the dormant to the metabolic state and initiates leaf flush. This period might be too long. Secondly, the aDGVM allocates more carbon to leaves when leaf biomass is low (i.e. early in the growing season). A more realistic approach might be to allocate more or less the total carbon gain to leaves in the first 2 or 3 weeks after leaf flush, which would accelerate greening and remove the lag observed in this study.

The mismatching in the peak timing over south-western Cape of South Africa and tropical forests in the northern hemisphere highlights the need to improve the aDGVM performance in these regions by making adjustments to the model. This is required if impact studies are to successfully use aDGVM simulations over these regions. Furthermore, there may be important differences in other characteristics of the seasonal cycle such as the length of growing season, which our approach does not consider.

Lastly, the poor association between the inter-annual variability of LAI between simulated and observed times-series could indicate limitations in the aDGVM in replicating patterns of inter-annual availability and hence the drivers of variability over Africa such as the role of ENSO. Moreover, the linear trends in simulated LAI demonstrate an increase over southern Africa not replicated by the LAI3g observations. The positive trends particularly over central southern Africa can be attributed to the lack of human land-use processes and drivers being included in the aDGVM. The inclusion of land-use within DGVMs is fairly complex due to the lack of information on the spatial distribution of land-use/land-cover and uncertainties as to how these processes change over time as a result of population growth and demand for agriculture, for example (Müller et al. 2007). To date, the majority of work on the inclusion of land-use within modelling processes has been for the purposes of assessing the impact of land-use/land-cover change on the global carbon cycle using specially developed DGVMs or Earth System Models (ESMs) (e.g. Strassmann et al. 2008; Hurtt et al. 2011; Arneth et al. 2017).

It is important to note here, that satellite time-series of LAI do not represent true observations of ground-based productivity and there may still be some residual biases and noise in the AVHRR LAI3g data after validation and smoothing. As with the NDVI time-series, LAI saturates in densely vegetated areas such as the tropical forests of Africa (Mutanga & Skidmore 2004; Zhu et al. 2013). Furthermore, over arid and semi-arid regions where the vegetation cover is not continuous the reflectance of bare soil results in a certain proportion of LAI values representing the background soil brightness (Pinzon & Tucker 2014b). Furthermore, the disagreement between simulated and observed vegetation presented in this study may also reflects the limitations of the coarse resolution (50 km grid) model outputs to represent smaller scale vegetation variations captured by the satellite observations (8 km grids).

6.5. Conclusion

This study has provided the first assessment of LAI outputs from the aDGVM using satellite-based observed (LAI3g) over sub-Saharan Africa for the period 1982-2011. While vegetation models including the aDGVM have developed a great deal after the last 10 years, there is still a need for improvement. The model performs well over grassland and savanna regions of southern Africa but tends to underestimate grass productivity in East Africa and over the Sahel and overestimate tree cover in tropical humid forests of central and West Africa. The model is currently not setup to capture the unique seasonal pattern of the Mediterranean-type vegetation of south-west cape of South Africa and to some extent the northern hemisphere tropical forests. These model biases combined with the poor representation of temporal variability of LAI highlights the need to improve the calculation of LAI in the model. The correct representation of LAI, both spatially and temporally, in DGVMs is key to predicting future vegetation biomass over Africa as a result of climate change.

The findings presented here will facilitate model improvements particularly in terms of mean annual productivity, season fluctuations, and temporal variability of LAI. This study has also provided valuable insight into the illustrated the utility of remotely sensed vegetation indices to assist in the comparison, refinement and overall improvement of simulation of vegetation by DGVMs. Future research should explore additional variables to test against model simulations such as growing season variables (start, end and length).

Chapter 7:

7. Conclusion

7.1 Introduction

The detection and identification of the impacts of climate change and increasing atmospheric CO_2 on terrestrial ecosystems has emerged as a critical issue in ecological research worldwide, for several reasons. Terrestrial ecosystems currently sequester roughly 25% of anthropogenic CO_2 emissions (Le Quéré et al. 2016), ensuring that the anthropogenic CO_2 increase is significantly less than would be the case without this ecosystem service. Without a clear understanding of the location, and current and anticipated strength of carbon sinks, projection of the global carbon budget remains uncertain, with important climate policy implications. The response of vegetation, via Net Primary Productivity (NPP), indicated by changes in Leaf Area Index (LAI), also underpins ecosystem resilience to climate change, and supports biodiversity. Credible projections of this response are needed for medium- and long-term conservation and ecosystem management efforts. The timing and amplitude of the annual vegetation growth cycle (indicated by LAI changes) is also a critical indicator of ecosystem resilience and adaptive response under climate change. If this could be more fully understood and projected with greater confidence, early detection of imminent risks and opportunities for effective conservation and management options would be significantly improved.

There remain substantial uncertainties in the projections of future changes in terrestrial ecosystems, particularly for sub-Saharan Africa (Midgley & Bond 2015). The lack of empirical evidence and information on the impact of climate change and rising atmospheric concentrations of CO_2 on vegetation dynamics is currently limiting the ability to resolve divergences in projections (Friedlingstein et al. 2014). The monitoring of terrestrial environments using remotely sensed vegetation indices over long periods of time, combined with improved models of vegetation function, provide critical information about the sensitivity and potential vulnerability of the global carbon cycle to climate and atmospheric CO_2 change. Most important among these models is a class of mechanistic model named Dynamic Global Vegetation Models or DGVM (Prentice et al. 2007). Such models currently provide a potentially important approach to improving understanding of the processes involved in observed changes, and from this to contribute to refining the ability to project further changes with greater credibility and confidence.

Using the 34-year Global Inventory Modeling and Mapping Studies (GIMMS) Normalized Difference Vegetation Index (NDVI) product, this study aimed to evaluate and assess the response of vegetation dynamics over Sub-Saharan Africa to climate variability and change

over the last four decades – a period of substantial climatic and atmospheric CO_2 change (Steffen et al. 2007), and compare this with the projections of a DGVM. The third generation NDVI product currently provides the longest temporal record of terrestrial vegetation dynamics, and thus an unprecedented opportunity to assess the response of vegetation to recent changes in climate and increasing CO_2. Climate analyses indicate the temperature has changed (Engelbrecht et al. 2015) and global CO_2 atmospheric concentrations has risen to 399.4 ± 0.1 ppm by 2015 (Le Quéré et al. 2016). On top of accumulated anthropogenic CO_2 increases prior to 1980, CO_2 increases appear to be leading to vegetation shifts in savannas (Wigley et al. 2009; Buitenwerf et al. 2012; Stevens et al. 2016) and arid ecosystems (Donohue et al. 2013) in particular.

In this thesis, ecosystem indicators including vegetation productivity and phenology metrics were analysed to assess critical changes and shifts in the productivity behaviour of terrestrial ecosystems in the context of climate and atmospheric CO_2 change. Phenological behaviour was classified spatially in order to define vegetation types or “biomes”. The findings are compared with the patterns found in other studies to determine if they differ and explore why this may be the case. Finally, seasonal cycles and trends of vegetation change were compared with reconstructions and projections made by a dynamic global vegetation model (DGVM), and discrepancies highlighted in order to identify where credible projections may be made, and where improvements are needed to achieve credible projections. This study is unique in that it incorporates a range of methodological approaches and techniques to detect and attribute changes in vegetation dynamics across SSA at both the seasonal and inter-annual scale, and in that it provides a critical test for the use of remotely sensed observations to assess the outputs from DGVMs.

7.2 Summary of contributions

The results presented in thesis contribute to the larger body of existing knowledge on the response of vegetation to climate variability and change by providing a comprehensive and holistic assessment over SSA in terms of (i) drivers of variability, (ii) recent changes in climate, (iii) trends and abrupt shifts in vegetation, and (iv) the role of climate in driving the observed changes in vegetation. Moreover, new insights are gained from the comparison between observed remotely sensed vegetation indices and historical simulated values from the adaptive DGVM. The main findings of this thesis are discussed in the following section and are each linked to the 3 main research questions set out in Chapter 1:

1. Is there evidence for abrupt local or regional shifts in vegetation productivity and phenology?

2. How has vegetation productivity and phenology responded to climate and atmospheric CO_2 change, and how does this compare with the current understanding of the drivers of ecosystem change?
3. Can improvements be made to the simulations of vegetation by Dynamic Global Vegetation Models (DGVMs) in order to increase the confidence in projections of future regional vegetation change?

The first key finding is concerned with the spatial differences in vegetation change observed over SSA and addresses the first research question of this thesis. Results presented in Chapter 5 provide evidence for a number of important spatial and temporal patterns of change in vegetation productivity and phenology over SSA, which are generally consistent with independently reported long-term trends (e.g. de Jong et al. 2012; Mao et al. 2013; Vrieling et al. 2013; de Jong et al. 2013; Ivits et al. 2014; Hoscilo et al. 2015; Liu et al. 2015; e.g. Zhu et al. 2016). Significant added value was provided to previous studies through the application of a range of methodological approaches on productivity and phenology metrics, which facilitated an assessment of vegetation dynamics at both the seasonal and inter-annual scale.

A clear latitudinal pattern of change was found where significant increases both productivity and the length of the growing season were observed over the northern hemisphere tropics (0-10°N) and sub-tropics of southern hemisphere (20-35°S) and significant decreases observed over the southern hemisphere tropics (0-20°S). The results from piecewise linear trends technique (BFAST) demonstrated that greening over 0-10°N latitudinal band, East Africa, central Botswana, and parts of South Africa accounts for nearly 50% of the observed changes in vegetation productivity over SSA. Previous research has provided evidence to suggest that terrestrial ecosystems at the global scale have been greening over the last few decades (e.g. Field et al. 2014; Zhu et al. 2016).

Another important finding from this Chapter was that the majority of southern Africa (0-20°S) has experienced a recent setback in vegetation productivity with browning trends prevailing post 2010. This suggests that changes in vegetation is this region are fairly recent and that changes in NDVI times-series are often more complex than simple linear trends over time.

The second key finding from this thesis is concerned with the role of climate in driving both short-term variability and long-term trends in vegetation across SAA and address the second research question of this thesis. By modelling the response of AVHRR NDVI3g to various climatic factors the results presented in Chapter 4 demonstrate that short-term variations in climate affect vegetation growth and seasonality across SSA at different time lags. Evidence is provided to indicate that the inter-annual variability in NDVI over SSA is primarily driven by rainfall and associated large-scale climate fluctuations and oscillations in SST and atmospheric pressure. Stronger associations are evident over the semi-arid regions of SSA,

which include southern Africa, the Sahel, and East Africa regions confirming that vegetation productivity in these regions is strongly limited by rainfall. Vegetation tends to show a stronger positive response to rainfall in the 3 months preceding vegetation growth suggesting that time-lag effects are of significant value when assessing climate variations in vegetation growth.

The results further demonstrate that the most dominant mode of climate variability over eastern and southern Africa is the El Niño-Southern Oscillation (ENSO). NDVI anomalies as well as vegetation productivity and phenology over both these regions correspond with identified ENSO-precipitation teleconnection patterns (Ropelewski & Halpert 1987; Anyamba & Eastman 1996; Anyamba et al. 2002; Schreck & Semazzi 2004c; Nicholson 2015) where negative (positive) anomalies in NDVI are associated with warm phase of ENSO over southern (East) Africa. Furthermore, during the warm phase of ENSO the length of the growing season are restricted over southern Africa but enhanced over East Africa, particularly in the second season. Over southern Africa, NDVI correlates with ENSO three months after the peak event (i.e. in March) whereas over East Africa the strongest correlations are observed at peak event in December. This finding is supported by a number of other studies in the region, which have shown that the above normal rainfall during El Niño results in an extended growing season (e.g. Anyamba et al. 2001; Anyamba et al. 2002).

Results from Chapter 5 provide evidence to suggest that recent changes in temperature, solar irradiance, and rainfall are associated with regions across SSA experiencing long-term changes in length of the season as well as vegetation productivity within that primary growing season. This finding could provide an indication of the impacts of climate change over the region. Continued monitoring of vegetation seasonality across these regions is required in order to determine in shifts in seasonality persist with future increases in temperature and changes in rainfall patterns. The use of climate change scenarios and DGVMs with detailed phenology characteristics, such as green-up date, will be particularly useful to further interrogate the link between changes in vegetation seasonality and climate.

Some results important to the interpretation of and attribution of changes in vegetation were:

- The consistent greening trend over the Sahel provides evidence for the recovery of vegetation from drought conditions that affected the region in the early to mid-1980s.
- While acknowledging that NDVI tends to saturate in densely vegetated areas, patterns of increasing productivity and length of season were observed over the parts of West and central Africa suggesting that forests are expanding into the surrounding savanna regions. This expansion is interpreted as a response to increases in rainfall combined potentially with increases in atmospheric CO_2 concentration as well as reforestation efforts in some countries.

- Patterns of gradually increasing productivity were detected over the south western Cape, eastern coastline, and north-east extent of South Africa which are consistent with the observed patterns of bush encroachment and expansion of alien invasive species in these regions.
- The declines in vegetation productivity observed over southern Africa are most likely due to land-use changes and reduction in woody vegetation as a result of non-climatic factors including the clearing for agriculture and population expansions. This is as firstly, no substantial changes in climate parameters were observed over this region and secondly the simulations of vegetation productivity derived from aDGVM indicate that vegetation greenness should have been increasing across this region over the last 30 years. This provides an indication that land-use is limiting the increase in vegetation driven by the CO_2 fertilisation effect.
- Differing patterns of greening and browning were observed over East Africa suggesting the role of local-scale factors driving vegetation change. Future studies at a finer spatial resolution combined with alternative indicators such as EVI will be required to assess if shifts in vegetation productivity and phenology occurred over this region.

A number of previous studies over Africa have documented increases shifts the distribution of biomes as a result of increases in woody vegetation biomass and increased concentrations of atmospheric CO_2 (e.g. Bond & Midgley 2000; Buitenwerf et al. 2012; Mitchard & Flintrop 2013; Devine et al. 2017). The role of CO_2 in driving changes in NDVI could not be fully established in this study as both similar patterns of change in both time-series and do not necessarily provide evidence of major driving forces of vegetation variability. The influence of rising CO_2 on vegetation growth has been primarily studied using Dynamic Global Vegetation Models and simulations using different climate and CO2 scenarios will need to be run using the aDGVM and CCAM climate inputs in required.

The third key finding is concerned with the use of the aDGVM in simulating historical vegetation over SSA and provides the necessary foundation to address the thrid research question. In Chapter 6 the historical outputs of leaf area index (LAI) from the adaptive Dynamic Global Vegetation Model (aDGVM) were evaluated by comparing satellite-based observation to model simulated values of LAI over SSA. This is first assessment to date using remotely sensed information to access aDGVM outputs. The motivation behind the inclusion of this chapter in this thesis is that the confidence in model projections of future vegetation states depends to a large degree on how well these models can simulate present-day vegetation dynamics. The results provided valuable insight into the utility of remotely sensed vegetation indices to assist in the validation, refinement and overall improvement of simulation of vegetation by DGVMs.

The results demonstrate that the simulations of LAI by the aDGVM need be improved in a number of key spatial and temporal aspects including average productivity, annual seasonal fluctuations and inter-annual variability over Africa. While the model performs well over grassland and savanna regions of southern Africa it tends to underestimate grass productivity in East Africa and over the Sahel and overestimate tree cover in tropical humid forests of central and West Africa. Version 1 of the aDGVM was specifically designed for tree-grass systems and does not include a shrub plant functional type. This exclusion of shrub component is likely to have resulted in the difference observed in vegetation biomass between the observed and simulated values. The latest version of the aDGVM now includes a shrub PFT so it would be beneficial for a future study to compare the outputs from aDGVM2 with remotely sensed vegetation indices.

Secondly, the aDGVM1 is currently not setup to capture the unique seasonal pattern of the Mediterranean-type vegetation of south-west cape of South Africa and to some extent the northern hemisphere tropical forests. Lastly, simulated values of LAI do not follow the same inter-annual pattern as the observed time-series indicating a key limitation in the aDGVM in replicating patterns of inter-annual availability and hence the drivers of variability over Africa such as the role of ENSO.

These biases and limits of the model are likely to have implications for the performance of model in projecting future vegetation cover over these regions. The findings will facilitate model improvements particularly in the spatial and temporal representation of LAI over SSA. This is of paramount importance when considering to develop a system to monitor and project future vegetation change over SSA as a result of climate change. Future research should explore additional variables to test against model simulations such as growing season variables (start, end and length) as well as the potential to integrate the inputs of LAI from remotely sensed vegetation indices in the aDGVM.

7.3 Future research

Overall, this thesis furthers the understanding of landscape-scale vegetation change across sub-Saharan Africa in the context of climate change. This information is increasingly becoming relevant to land use management and conservation in the region including the development of strategic adaptation initiatives. Importantly, the results hold significant value for the testing the performance of dynamic global vegetation models and the prediction of climate driven variations in vegetation in the future.

Continued monitoring using remotely sensed vegetation indices combined with increased climate observational network across the continent will assist in the detection and attribution of climate driven changes in vegetation. Specifically, further research is required to assess the recent browning patterns across southern Africa in order to determine if the decline in

productivity continues to persist. The use of higher spatial resolution products such as MODIS EVI may be more suitable to access specific locations experiencing substantial declines including across regions of northern Mozambique and Tanzania.

The results from Chapter 6 point to the need for the evaluation of growing season metrics using historical simulations as well as future simulations of vegetation dynamics over SSA using aDGVM2. Future research using the aDGVM should focus on refining and re-parameterising the models to consider a wider range of biome types and seasonal vegetation patterns. This will enable improvement simulations of future vegetation dynamics over SSA that can inform strategic adaptation response measures and conservation and resource management decisions.

8. Appendices

Appendix A

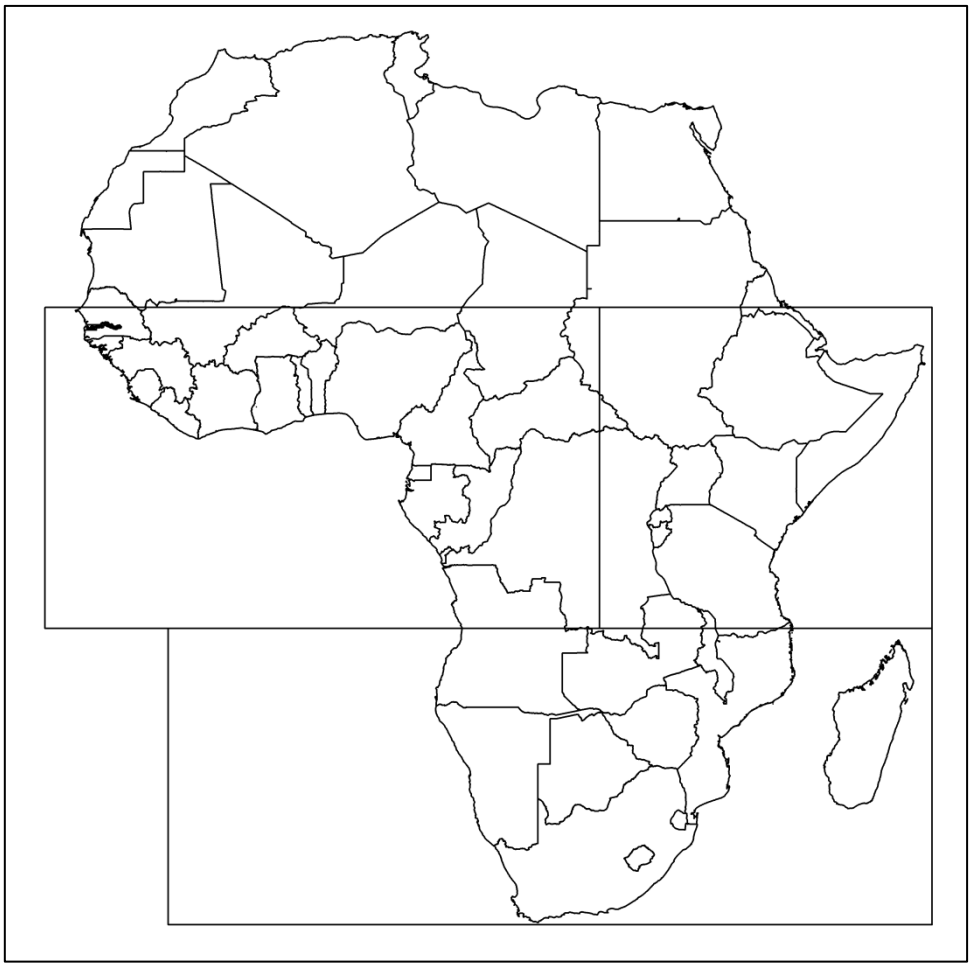

Figure A.1: Extent of West Africa (11.4°S to 15°N; 20°W to 25°E), East Africa (11.3°S to 15°N; 25°E to 52°E), and southern Africa (35°S to 11.4°N; 10°W to 52°E) used in this study. These extents are taken from the IPCC AR5 WG1 (Stocker et al. 2013).

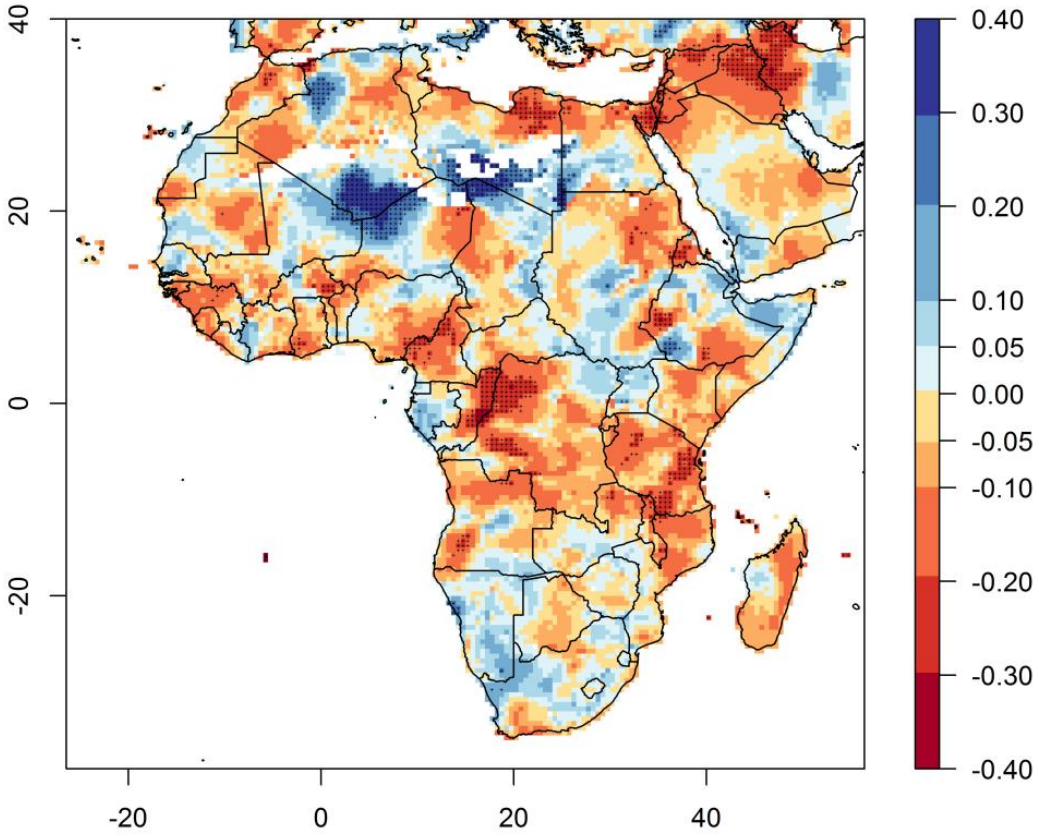

Figure A.2: Observed trends in annual rainfall totals over Africa for the period 1961-2014 based on CRU TS 3.23 data. Crosses indicate grid boxes where the trend is statistically significant. White areas indicate no data.

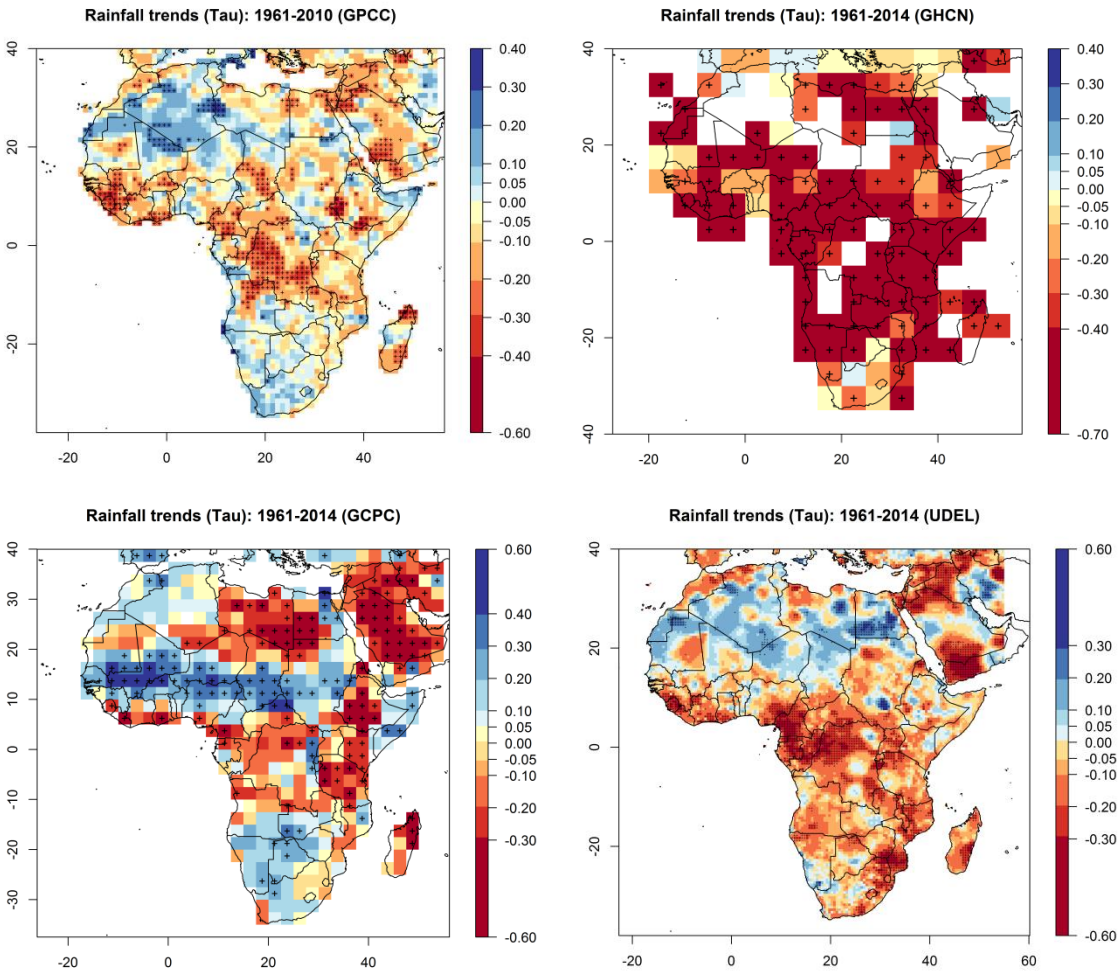

Figure A.3: Observed trends in annual rainfall totals (mm change per decade) over Africa for the period 1961-2014 based on (a) GPCC (Schneider et al. 2014), (b) GHCN 2011), (c) GPCP v2.2 (Adler et al. 2003), and (d) UDEL datasets (Willmott et al. 2001). Crosses indicate grid boxes where the trend is statistically significant. White areas indicate incomplete or missing data.

Appendix B

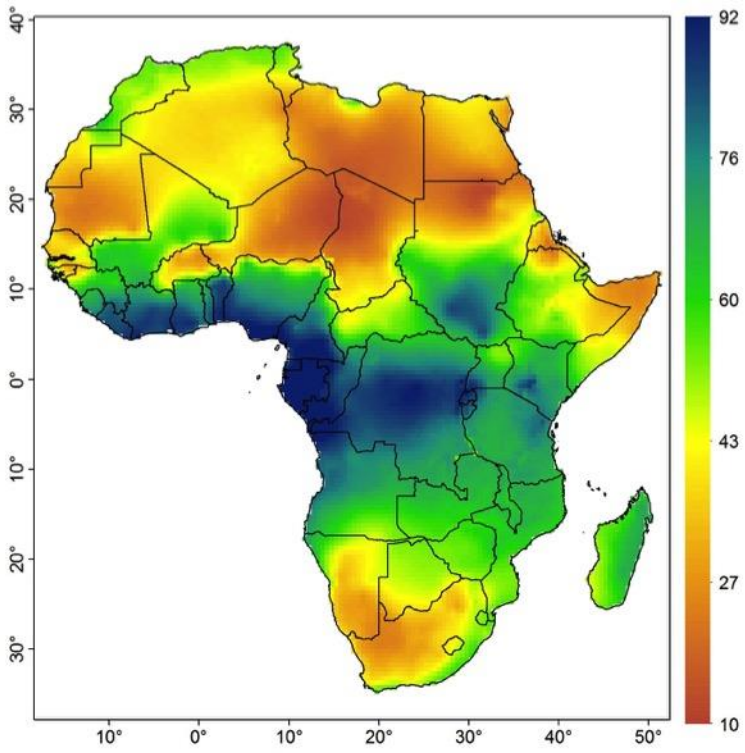

Figure B.1: Multi-year mean annual cloud cover (1982-2015) expressed as a percentage based on CRU TS 4.00 cloud cover product (Harris et al. 2014b).

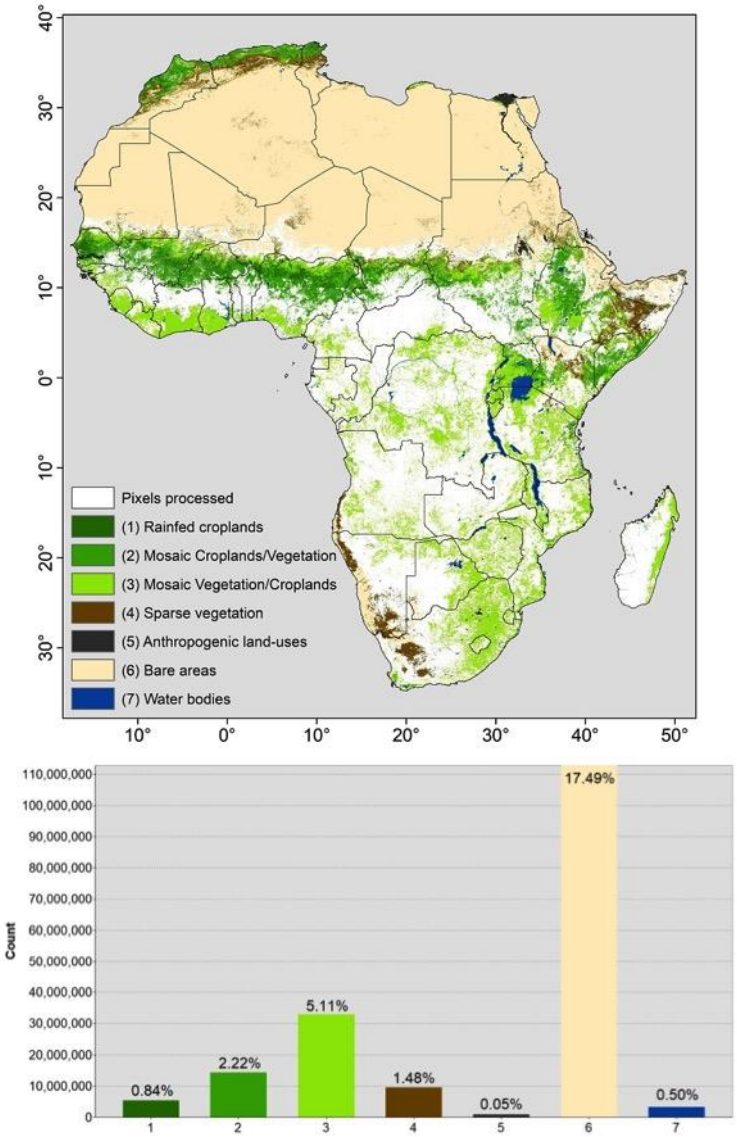

Figure B.2: Areas masked from the analysis include bare ground (NDVI < 0.1), water bodies, and anthropogenic altered areas as defined by the GlobCover version 2.3 2009 (Bontemps et al. 2011). The graph given below the map demonstrates the number of grid cells in each of the classes masked from the analysis.

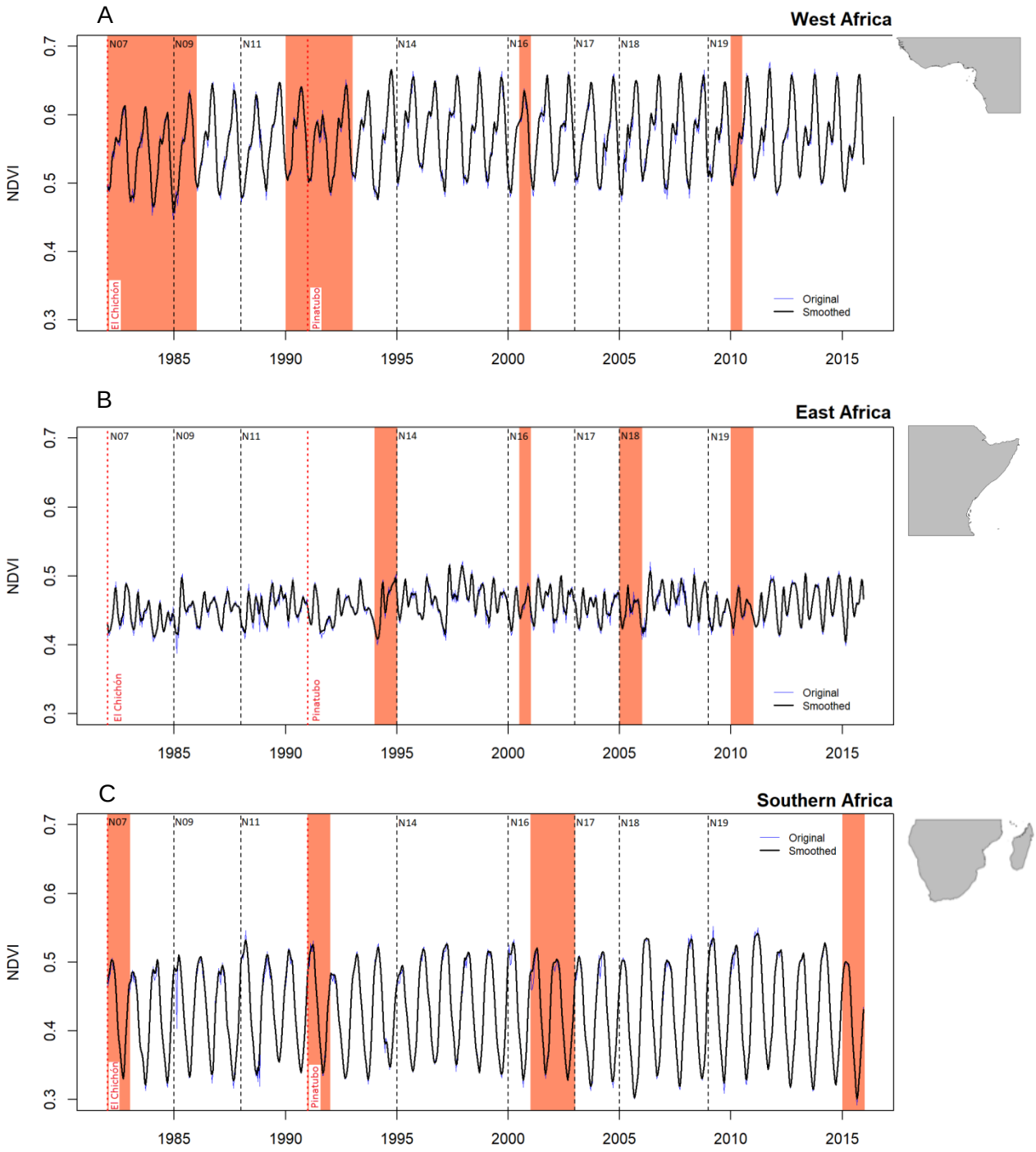

Figure B.3: Time-series of AVHRR NDVI3g (1982-2015) averaged over (A) West Africa, (B) East Africa, and (C) southern Africa smoothed by the adaptive Savitzky-Golay filter. The original NDVI3g time-series (n=24 per year) is shown in blue. The red shaded areas indicate the periods of intense droughts over each of the regions. The black dashed lines label the sensor changing time of AVHRR satellite series. Two volcanic eruptions (El Chichón and Pinatubo eruptions) are indicated with the red dashed lines.

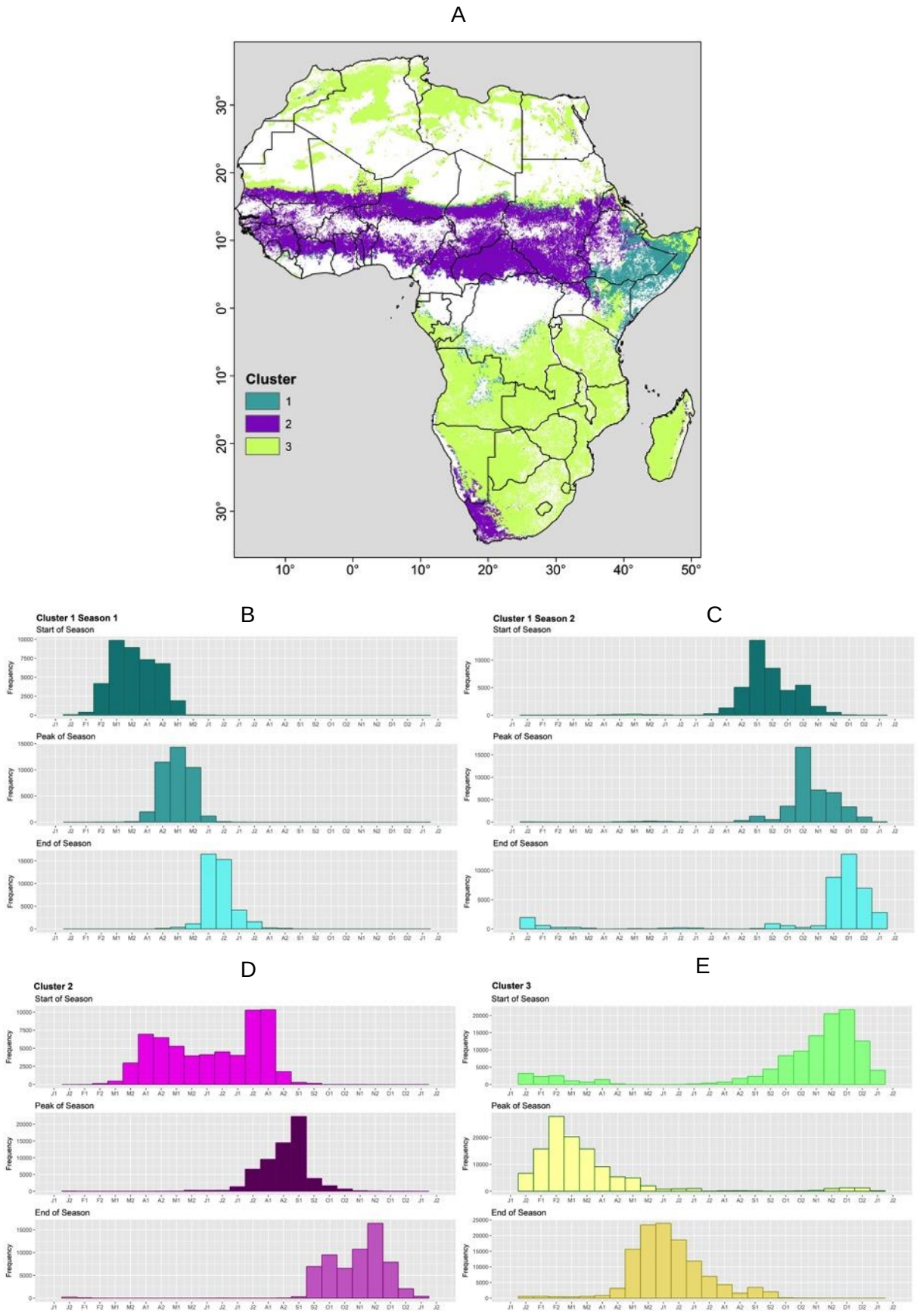

Figure B.4: (A) Spatial representation of the 3 main clusters based on k-mean cluster analysis of start and end date of the vegetation season extracted from sample time-series of average AVHRR NDVI3g from 1982 to 2015. Frequency histogram of the mean start, peak and end date of the growing season for (B) Cluster 1 season 1, (C) Cluster 1 season 2, (D) Cluster 2, and (E) Cluster 3. The bi-weekly (15 day) periods are named by the first letter of the month (J,F,…D) followed by the number (1–2).

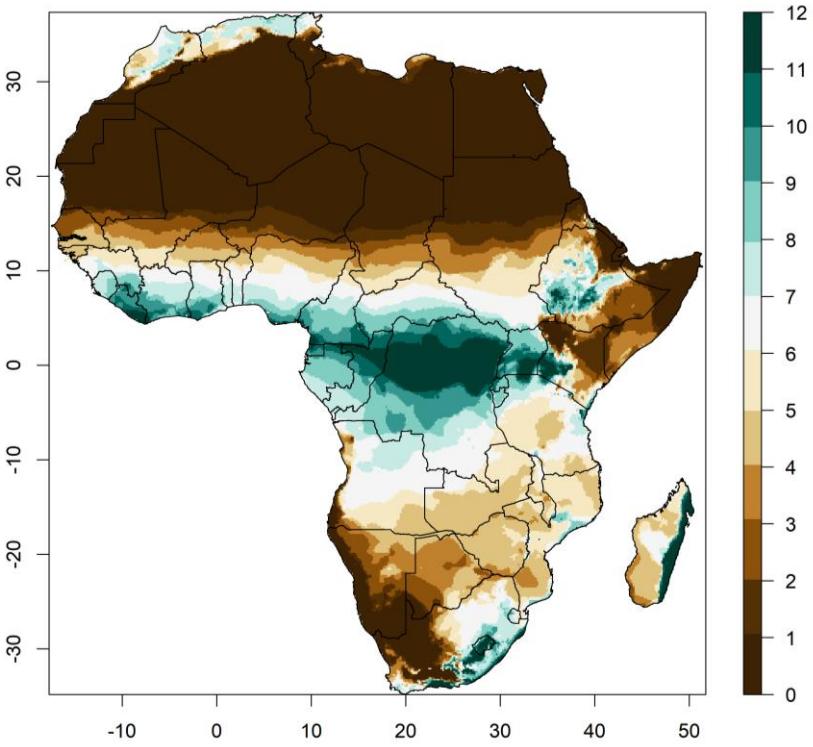

Figure B.5: Length of the wet season (in months) over Africa (Source: FAO/Agrhymet Network and ESRI).

Appendix C

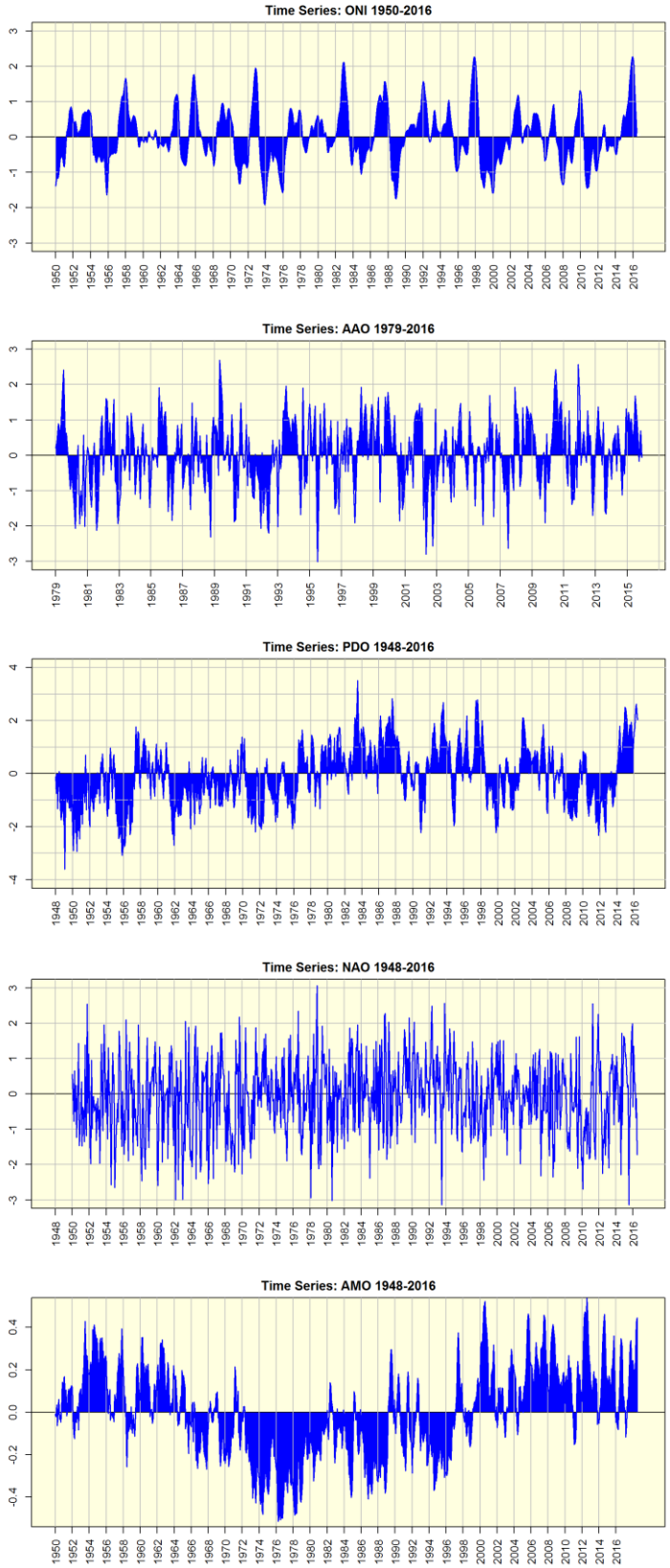

Figure C.1: Time-series of 5 oscillations investigated (based on data from http://www.esrl.noaa.gov/psd/data/climateindices/list/); ENSO, Antarctic Oscillation (AAO), Pacific Decadal Oscillation (PDO), North Atlantic Oscillation (NAO), and Atlantic Multidecadal Oscillation (AMO).

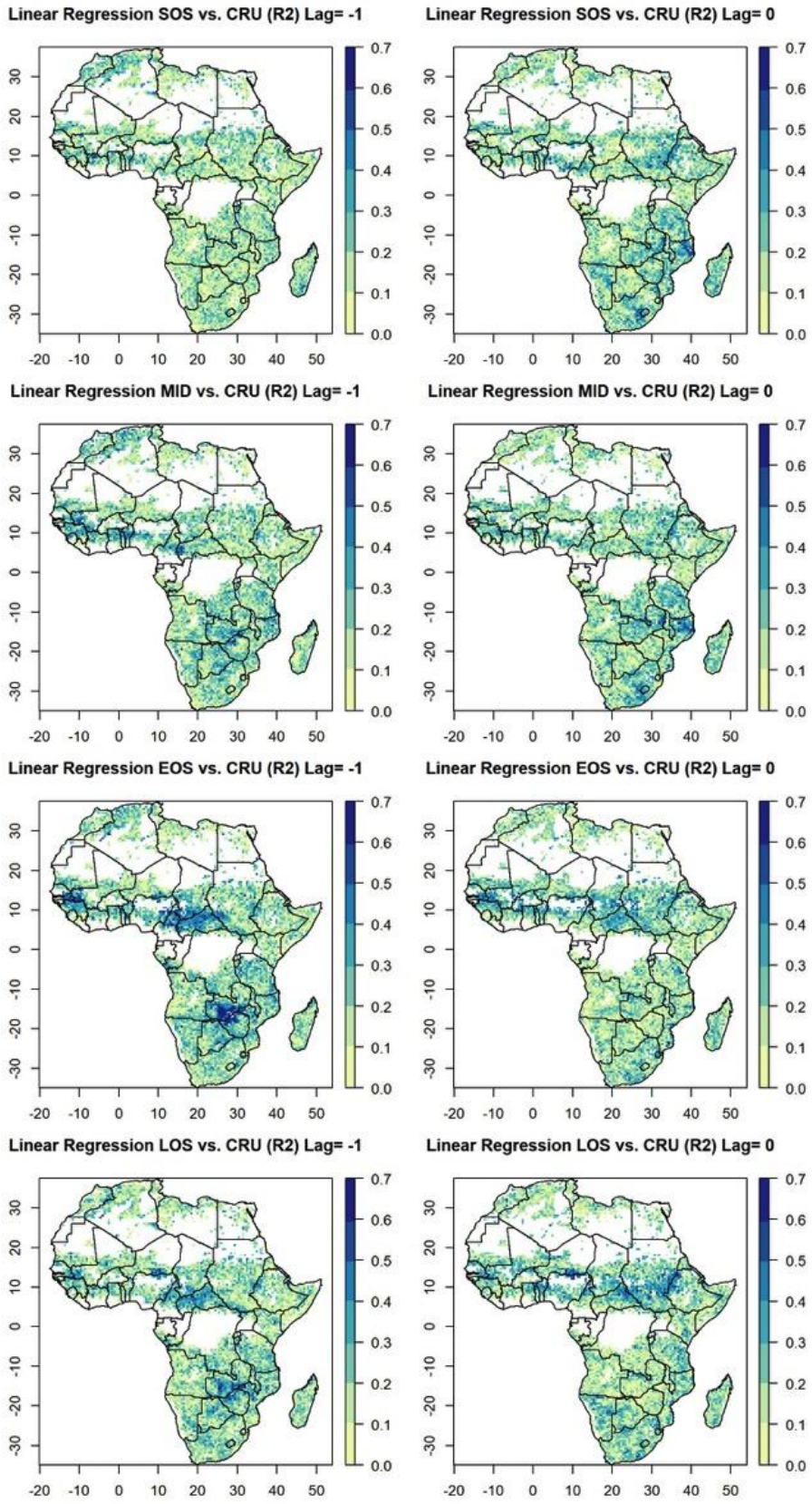

Figure C.2: Spatial distribution of the determination coefficient (R2) of the multiple linear regression between phenology metrics (SOS, MID, EOS, and LOS) for the first growing season and climatic factors for the period 1982–2015 with considering time-lag effects. White regions indicate areas masked from the analysis.

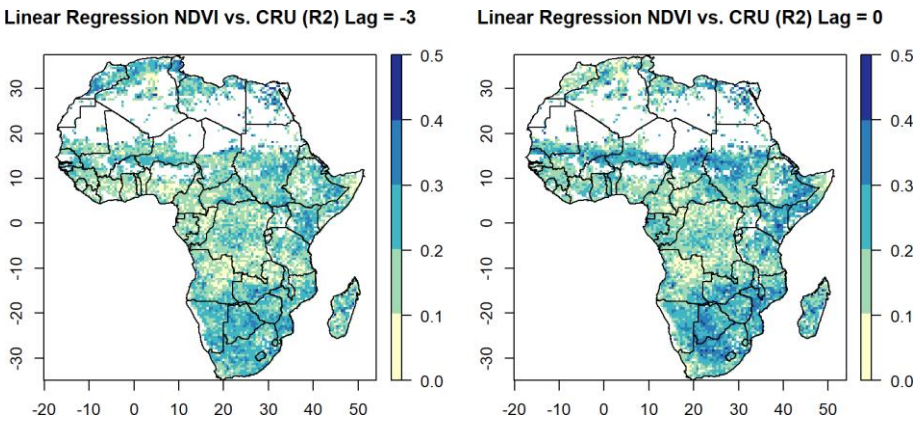

Figure C.3: Spatial distribution of the determination coefficient (R2) of the multiple linear regression between NDVI3g anomalies and climatic factors for the period 1982–2015 with considering time-lag effects. White regions indicate areas masked from the analysis.

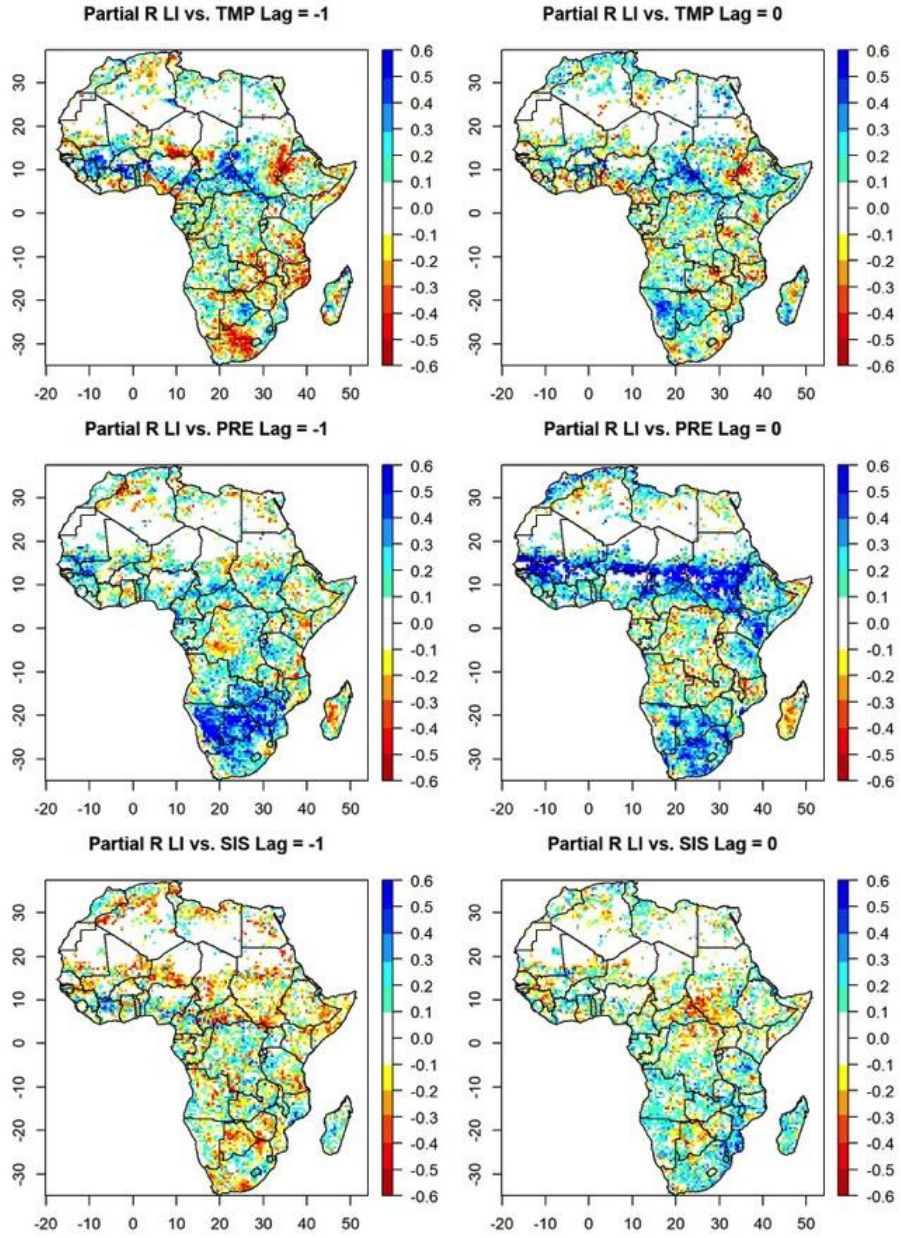

Figure C.4: The responses of LI for the first growing season to CRU temperature (TMP), precipitation (PRE), and solar radiation (SIS) considering time-lag effects. (A) Spatial distribution of the partial correlation coefficient between LI and temperature (TMP) after controlling for precipitation (PRE) and solar radiation (SIS), (B) spatial distribution of the partial correlation coefficient between LI and precipitation (PRE) after controlling for temperature (TMP) and solar radiation (SIS), (C) spatial distribution of the partial correlation coefficient between LI and solar radiation (SIS) after controlling for temperature (TMP) and precipitation (PRE).

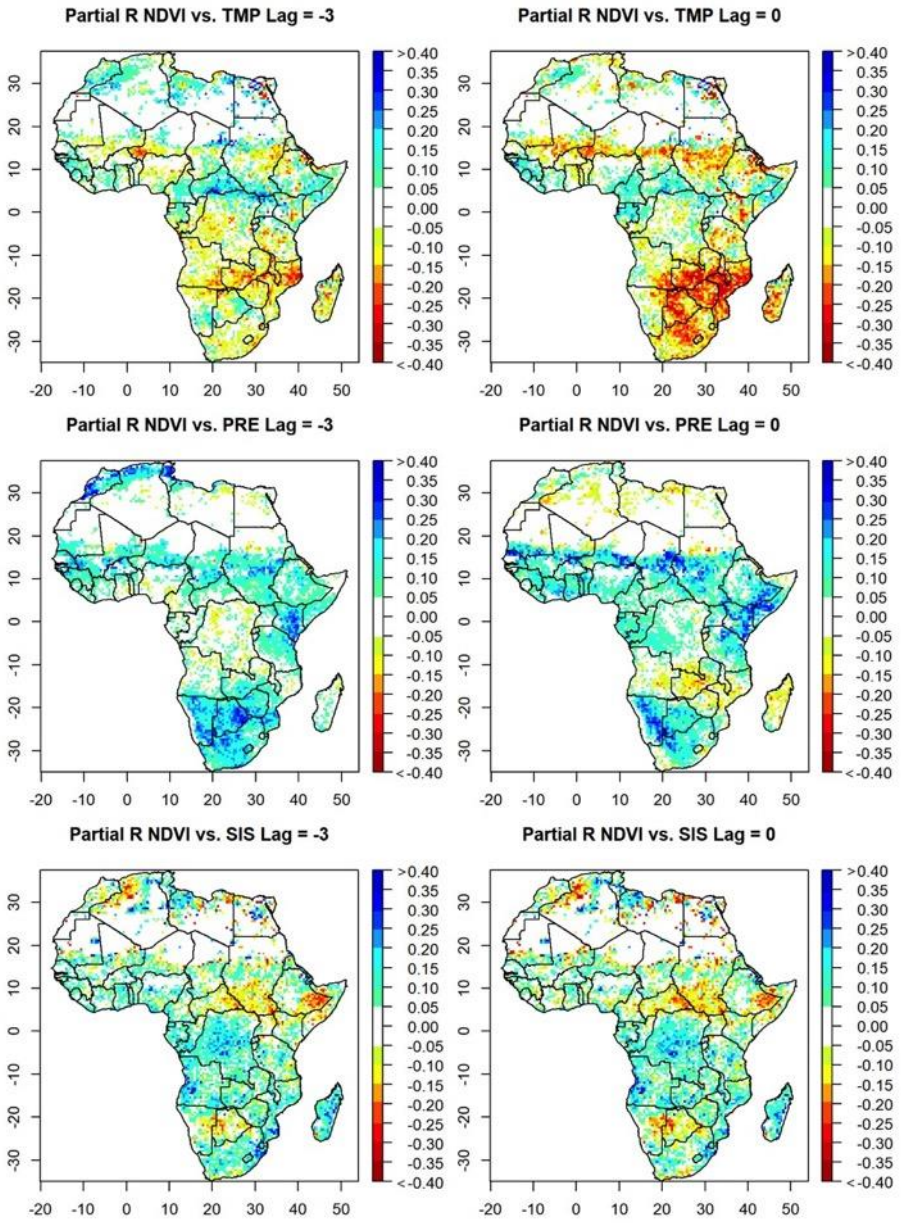

Figure C.5: Same as Fig. C.4 but for AVHRR NDVI3g anomalies

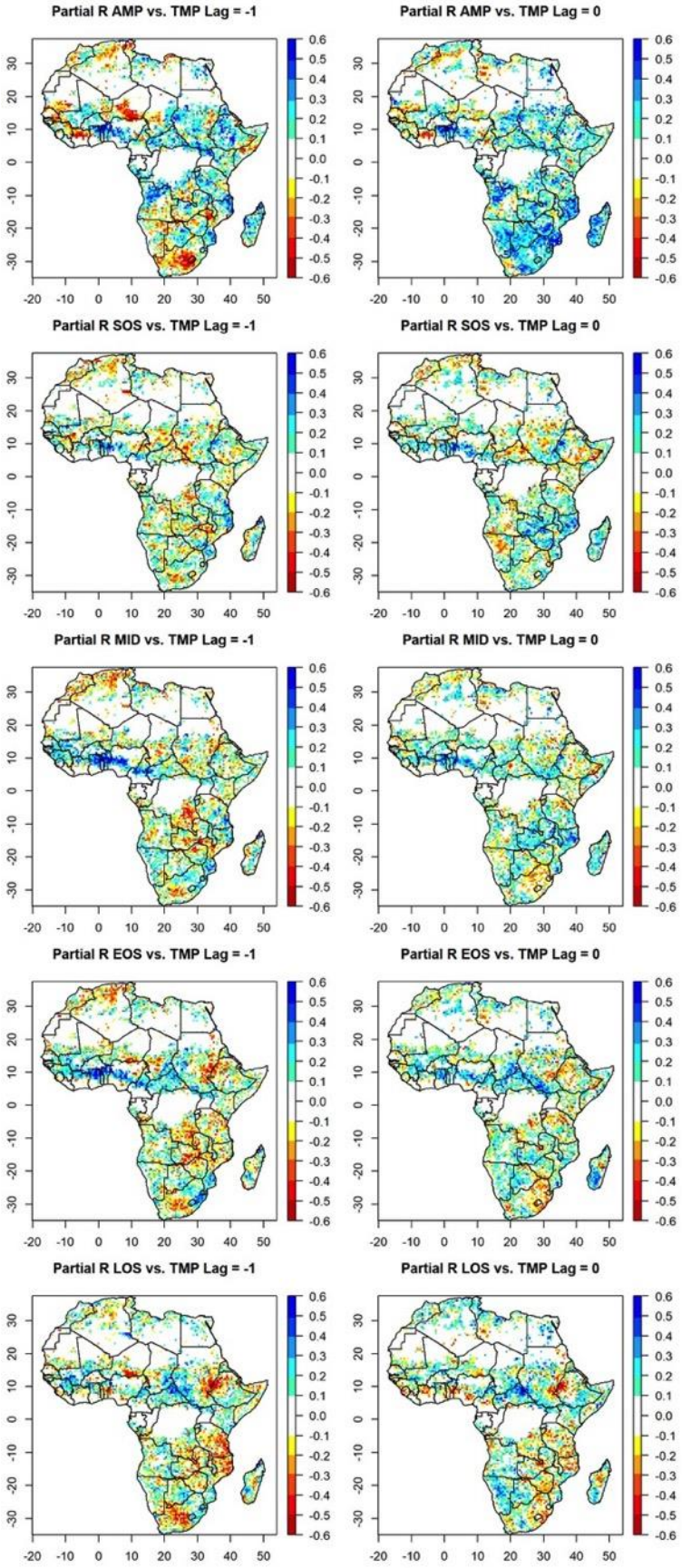

Figure C.6: Spatial distribution of the partial correlation coefficients between phenology metrics (AMP, SOS, MID, EOS, and LOS) for the first growing season and temperature (TMP) after controlling for precipitation (PRE) and solar radiation (SIS).

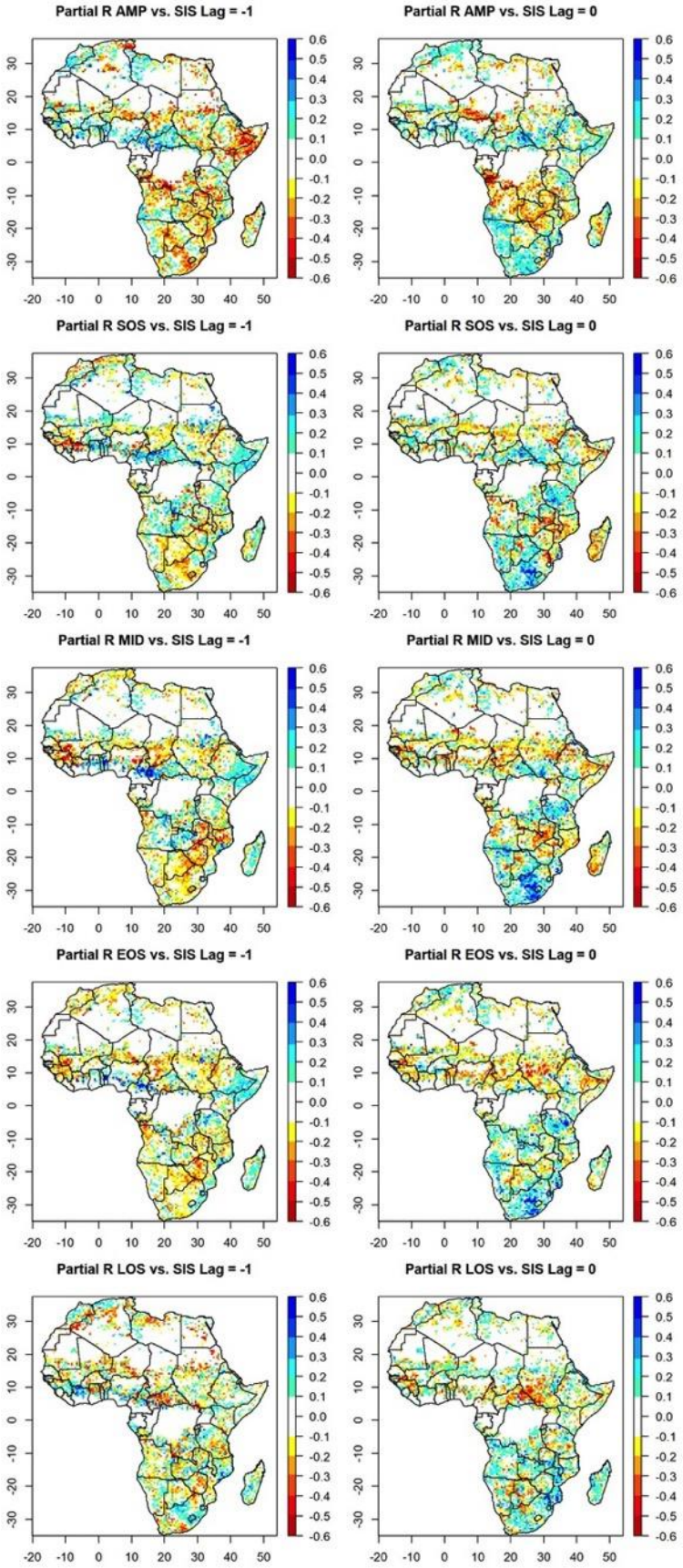

Figure C.7: Same as Fig. C.6 but for solar radiation (SIS)

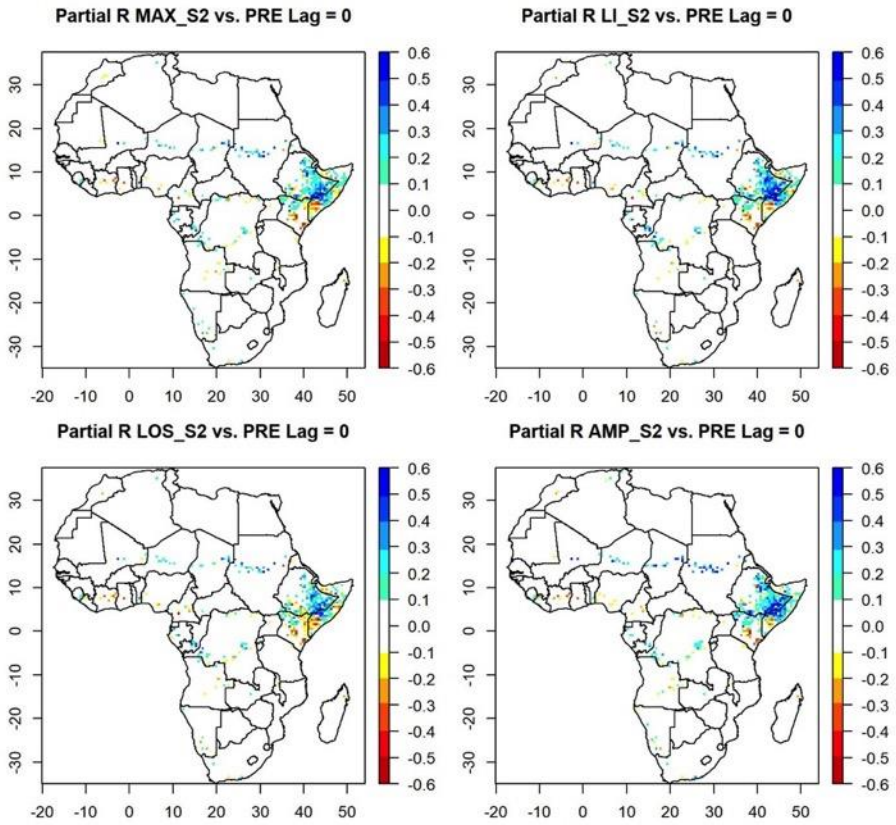

Figure C.8: Spatial distribution of the partial correlation coefficients between MAX, LI, LOS and AMP for the second growing season and precipitation (PRE) after controlling for temperature (TMP) and solar radiation (SIS).

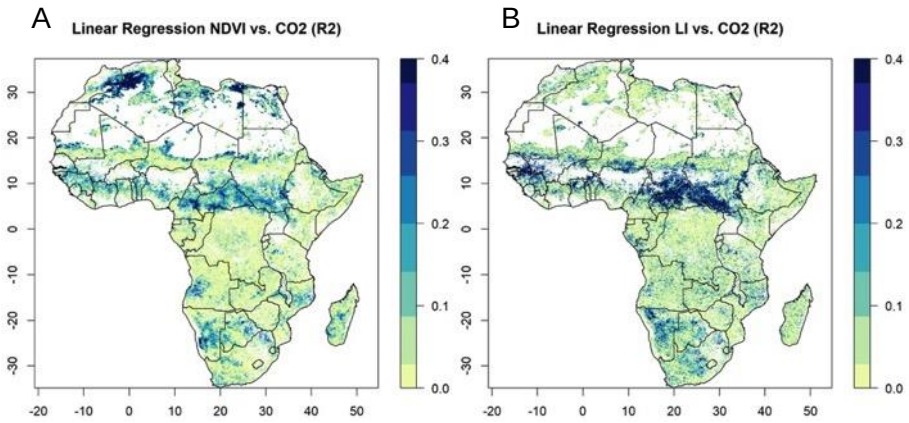

Figure C.9: Spatial distribution of the determination coefficient (R2) of the linear regression model between global monthly mean CO_2 values (ppm) and (A) NDVI3g anomalies and (B) LI for the first growing season over Africa for the 1982-2015 period. White indicates masked areas with NDVI values < 0.1. The blue (red) colours indicate a positive (negative) correlation. (B) Time-series of monthly mean CO_2 values (ppm) from 1982-2013 with the red line indicating the linear trend.

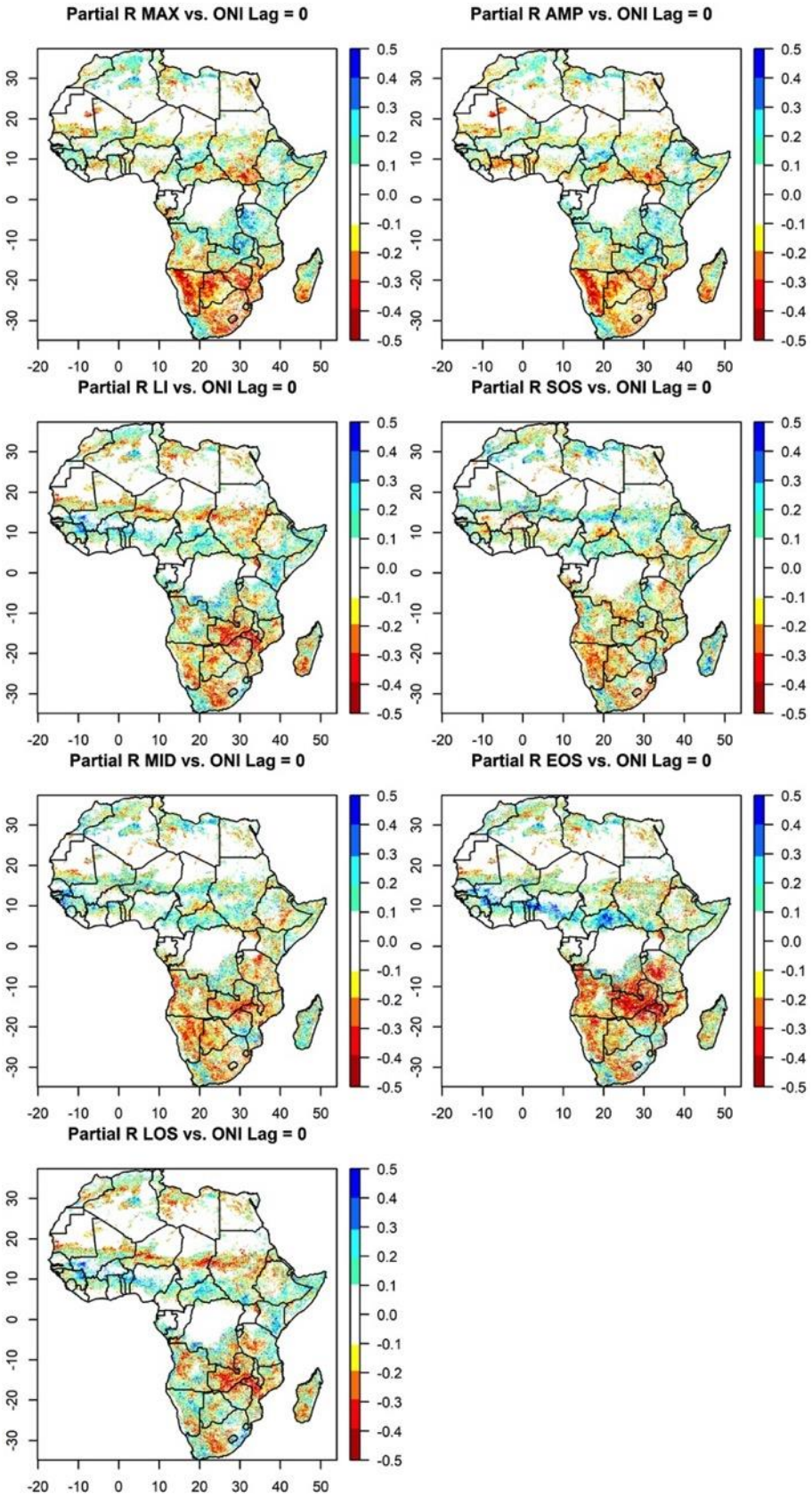

Figure C.10: Partial correlation coefficients (r-value) between MAX, AMP, LI, SOS, MID, EOS, and LOS for the first growing season and ONI sea surface temperature oscillations based on monthly anomalies for the period 1982-2015.

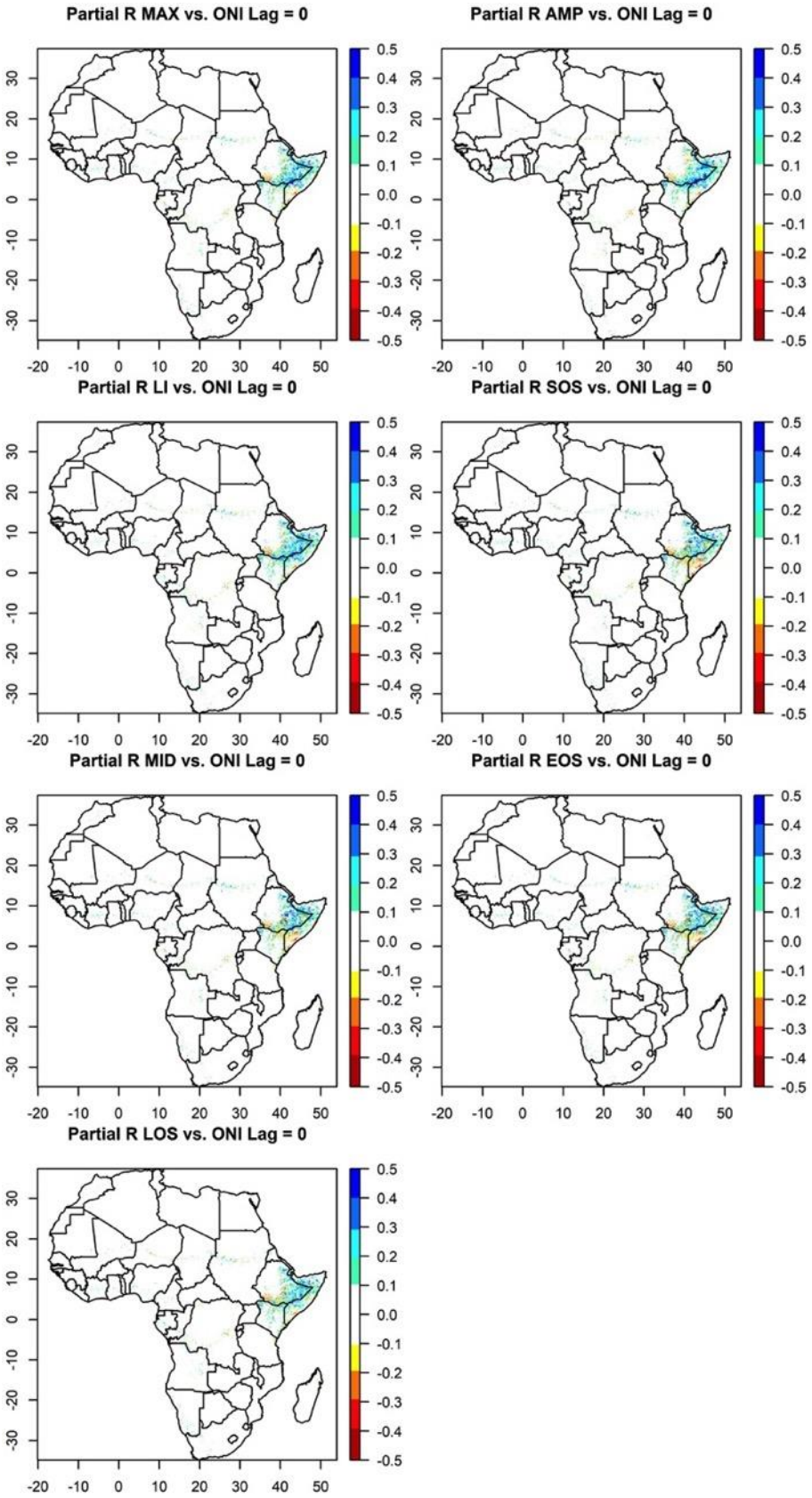

Figure C.11: Same as Fig. C.10 but for second growing season.

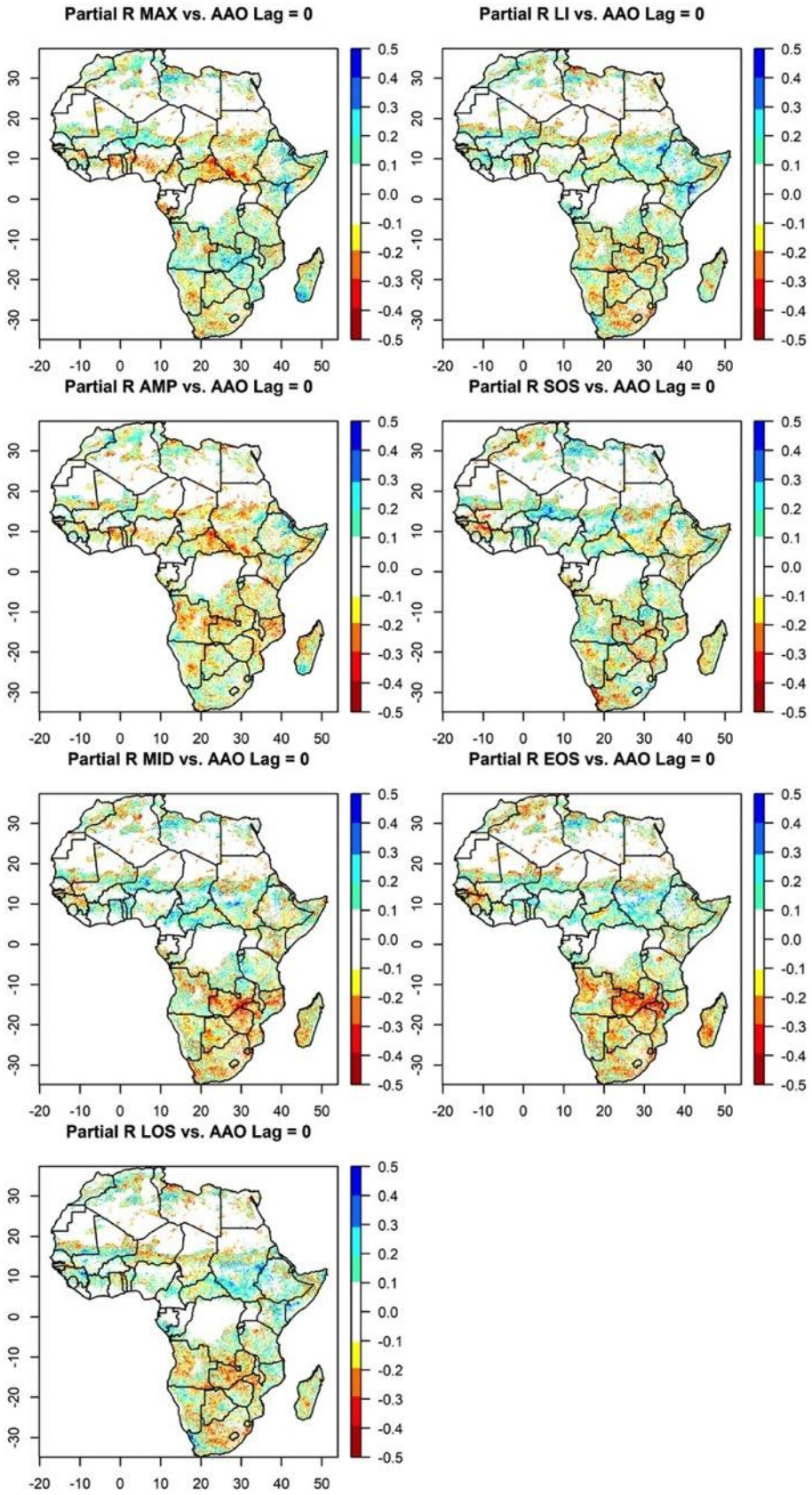

Figure C.12: Same as Fig. C.10 but for AAO atmospheric pressure oscillation.

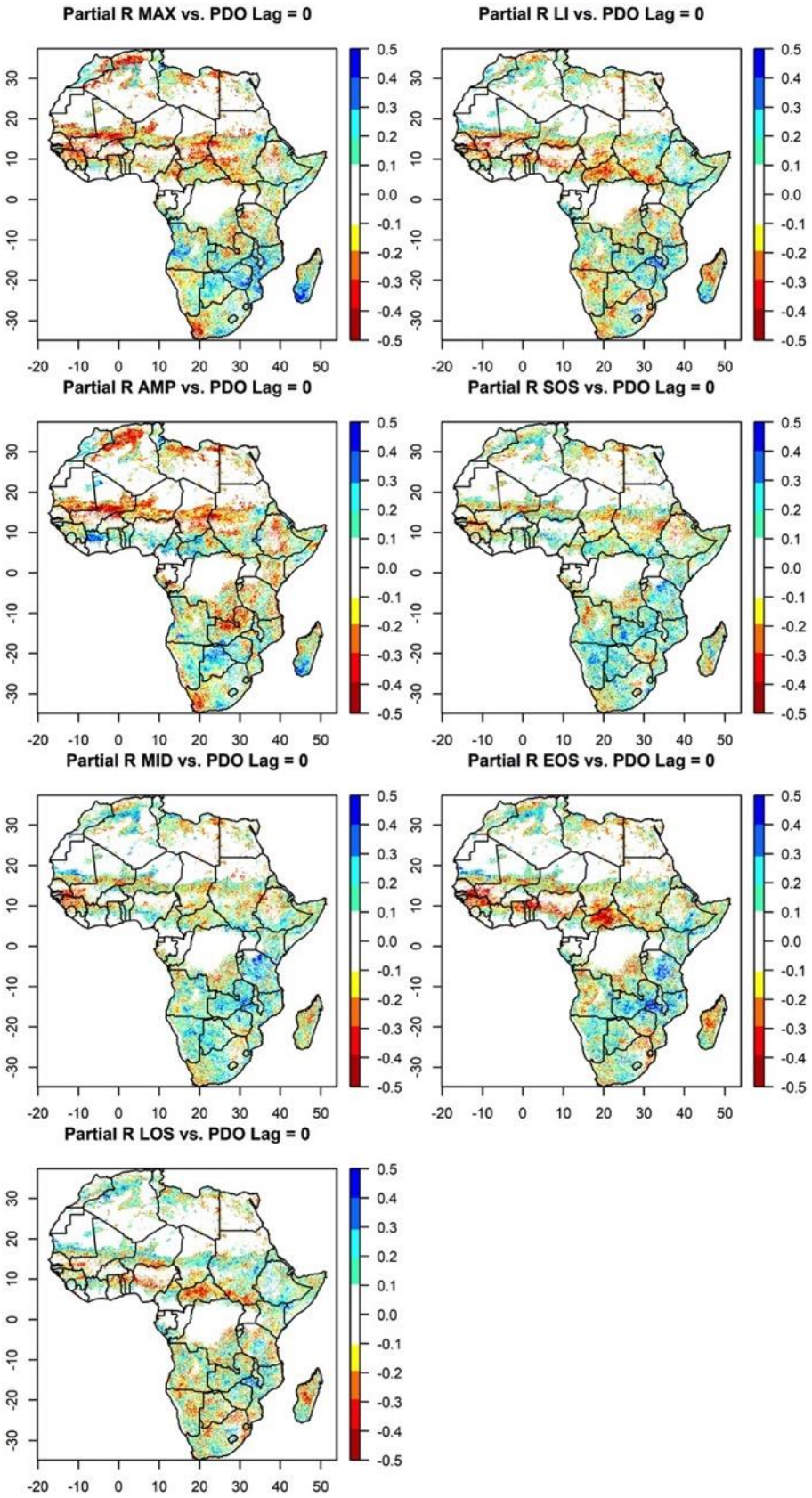

Figure C.13: Same as Fig. C.10 but for PDO sea surface temperature oscillation.

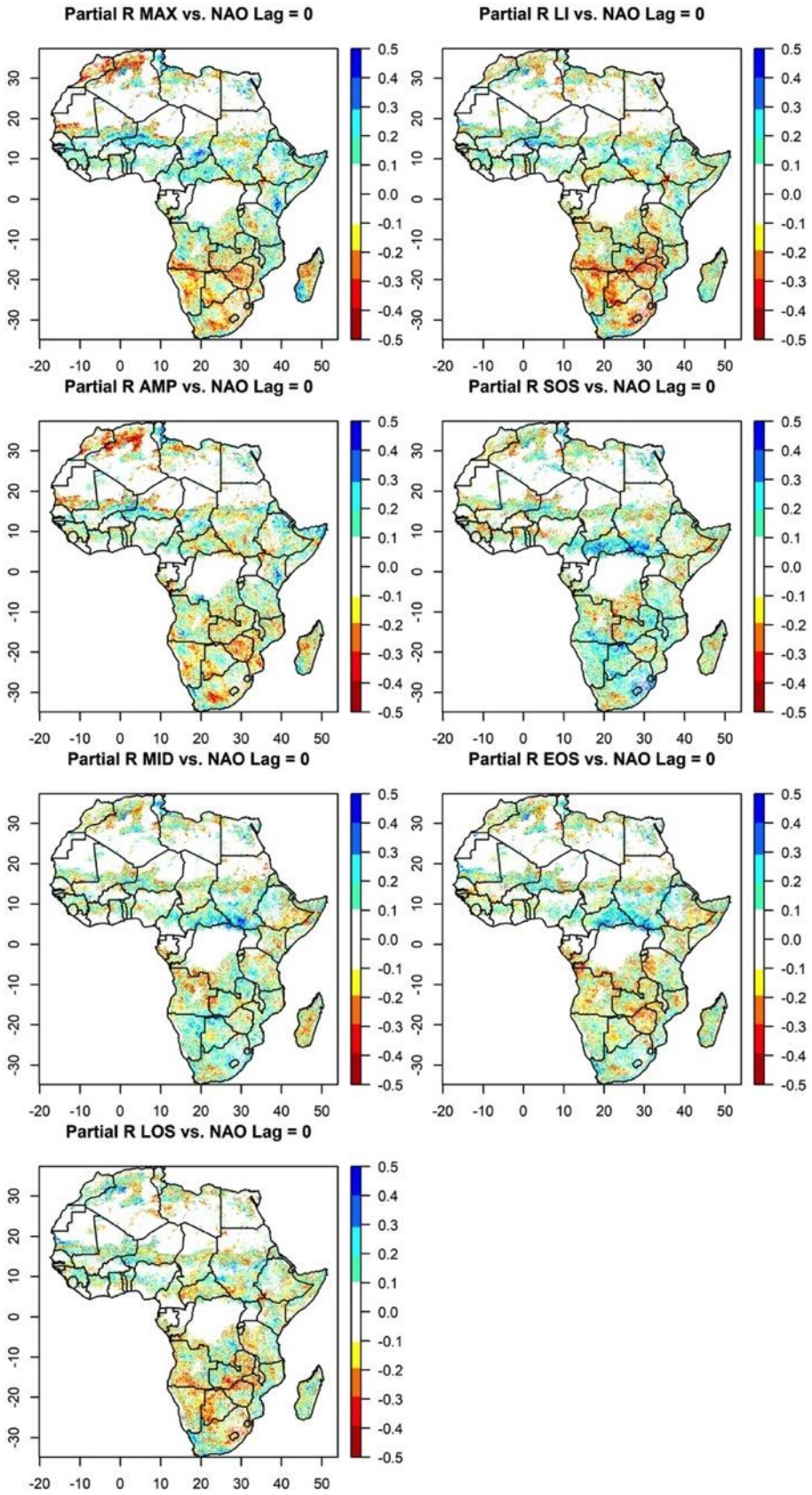

Figure C.14: Same as Fig. C.10 but for NAO atmospheric pressure oscillation

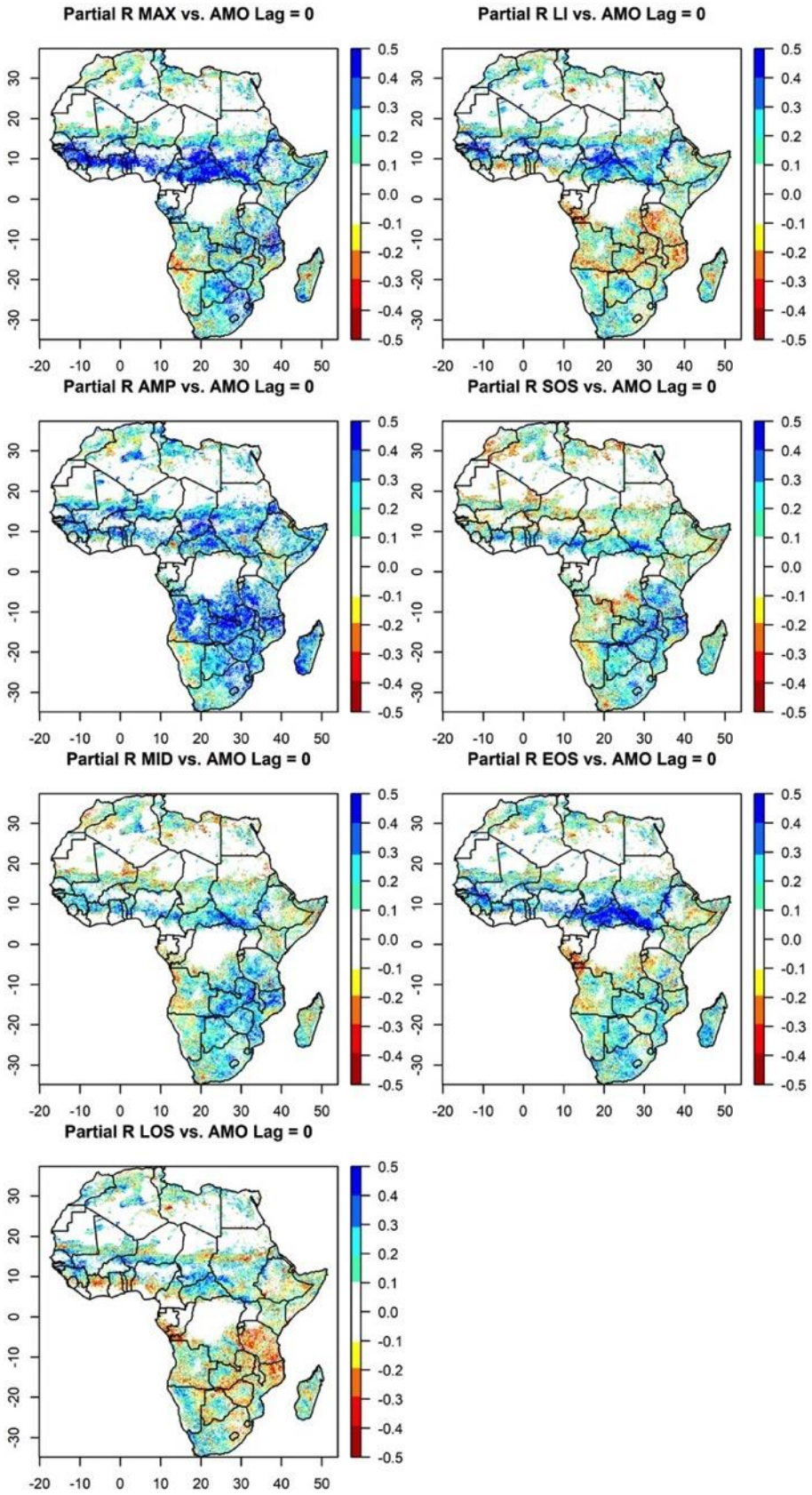

Figure C.15: Same as Fig. C.10 but for AMO sea surface temperature oscillation.

Appendix D

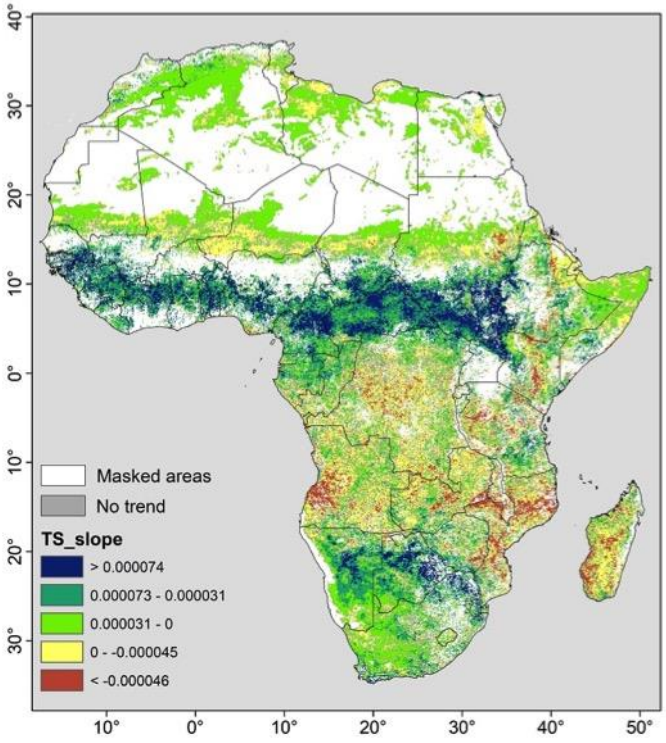

Figure D.1: Theil-Sen trend in AVHRR NDVI3g anomalies for the period 1982-2015. Trends are displayed for statistically significant pixels ($p < 0.05$). Statistically significant ($p < 0.05$) trends are displayed. White indicates pixels that were masked from the analysis and grey represent pixels were no trend was detected.

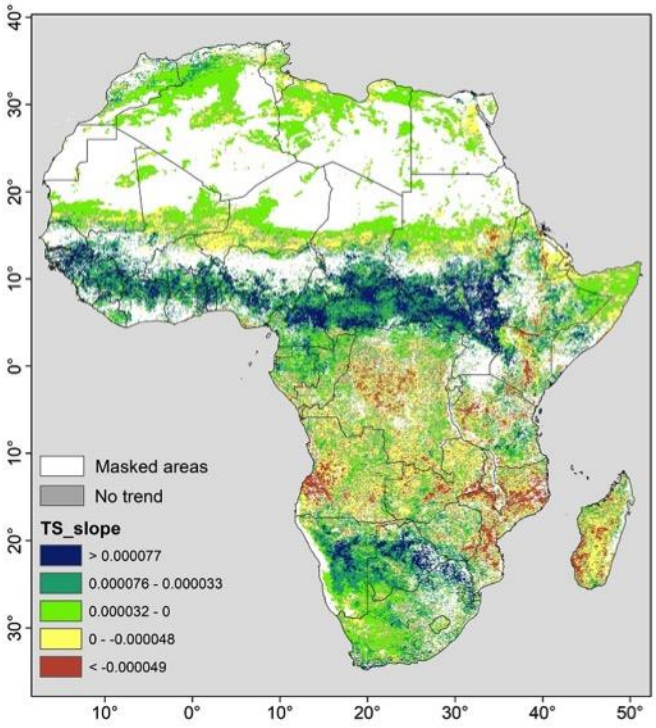

Figure D.2: Same as Fig. D.1 but for seasonally-adjusted AVHRR NDVI3g time-series

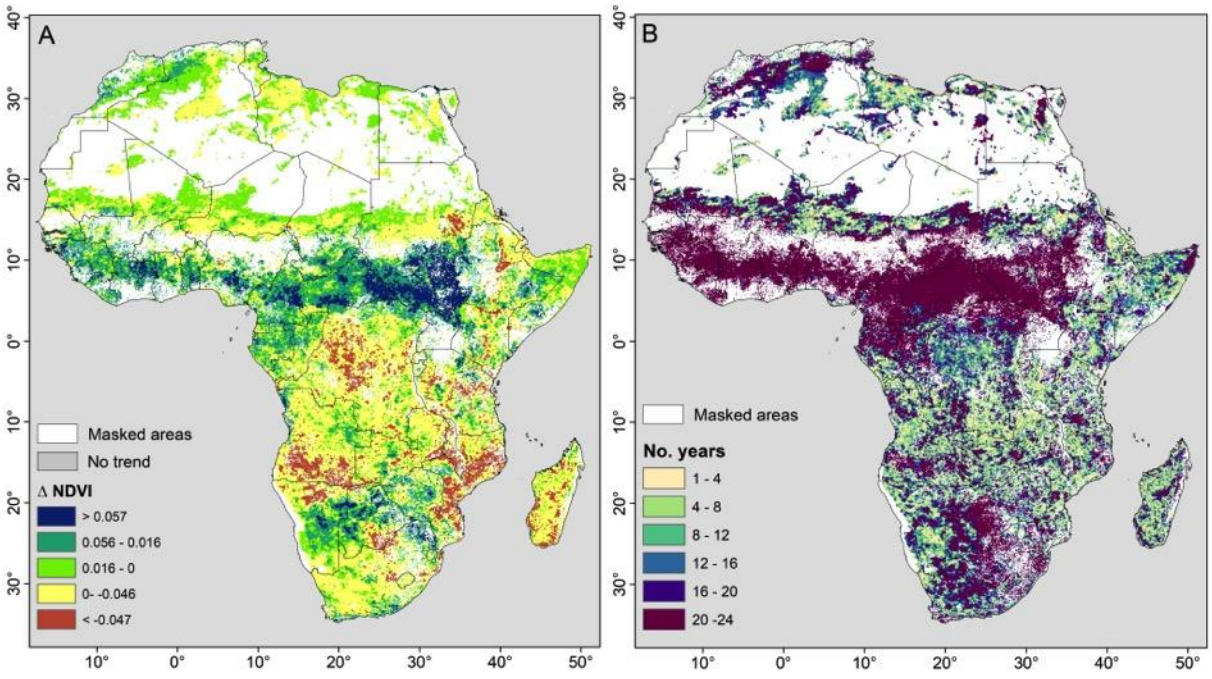

Figure D.3: Trend persistence map for the period 1982-2015. The decade 1982-1991 was used as the reference period. (A) Persistence is expressed as changes Δ in the magnitude of NDVI and (B) number of years that trend persisted. Individual persistence maps are provided in the Supplementary information in Figure S.5. White areas indicate areas that were masked from the analysis.

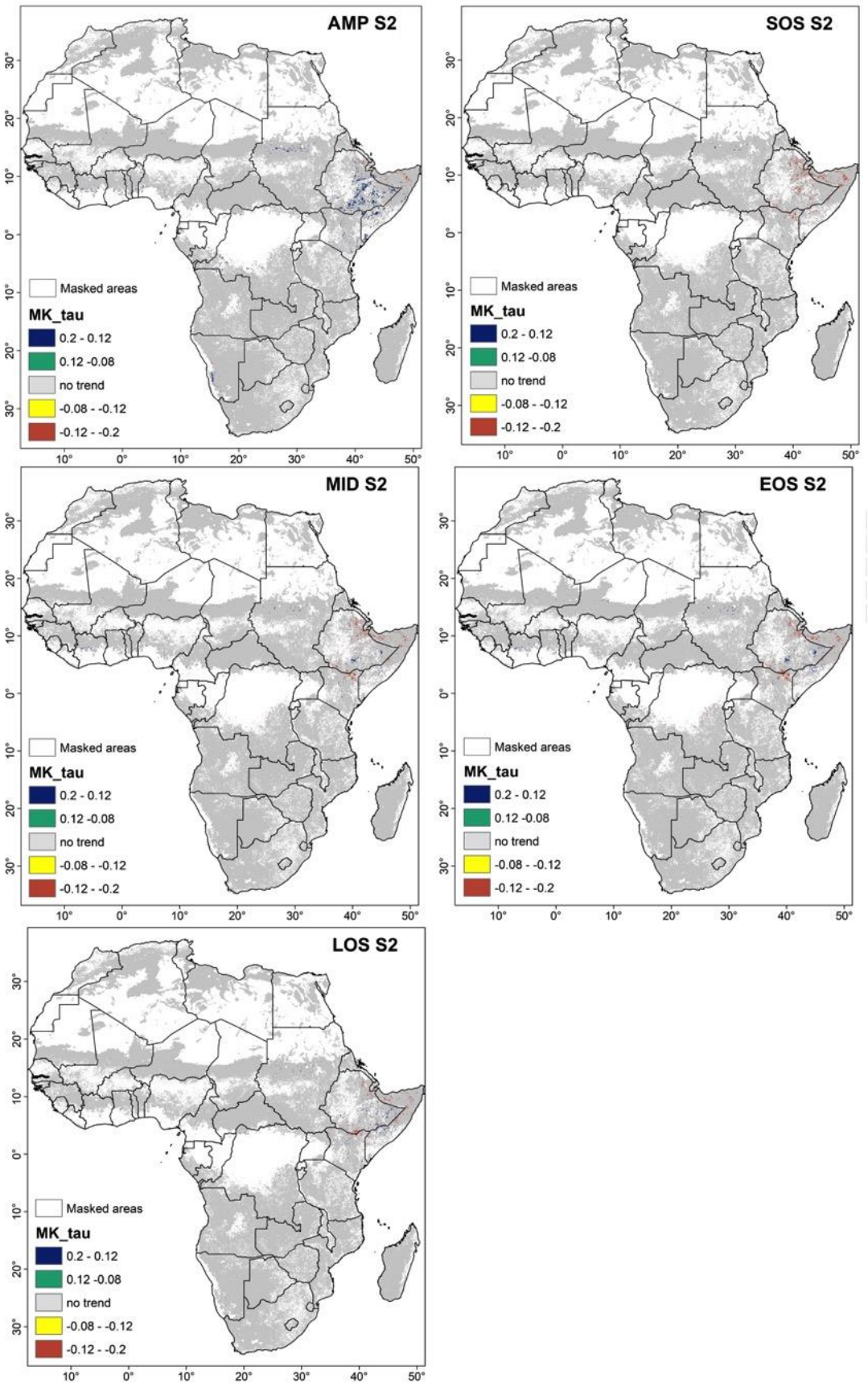

Figure D.4: Trends in start date (SOS) of the second growing season, its peak (MID), its end date (EOS) and the length (LOS) from the AVHRR NDVI3g time series for 1982 to 2015 over Africa using the Mann Kendall trend test. White indicates pixels that were masked from the analysis and grey represent pixels were no trend (p < 0.05) was detected.

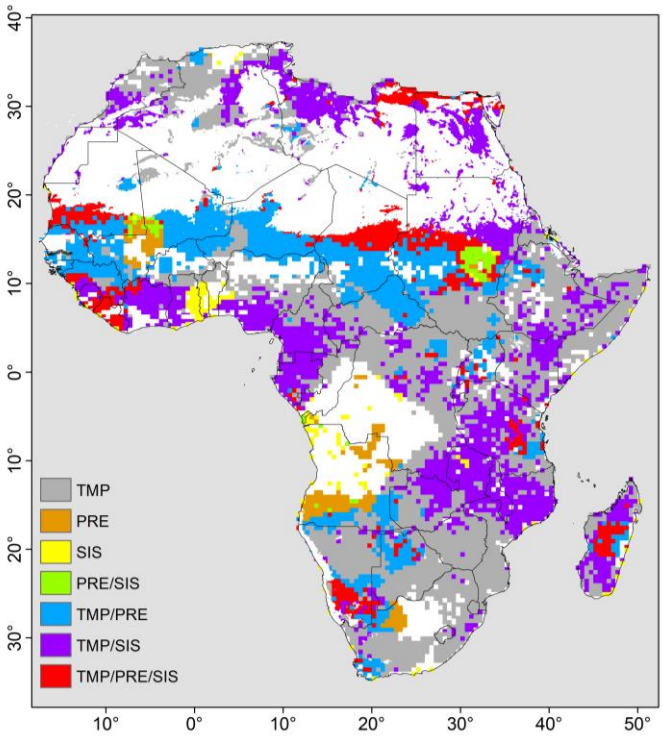

Figure D.5: Comparison between trends in climatic factors and maximum NDVI3g (MAX) considering all pixels over Africa for the period 1982-2015. TMP refers to temperature, PRE to rainfall, and SIS to incoming solar radiation.

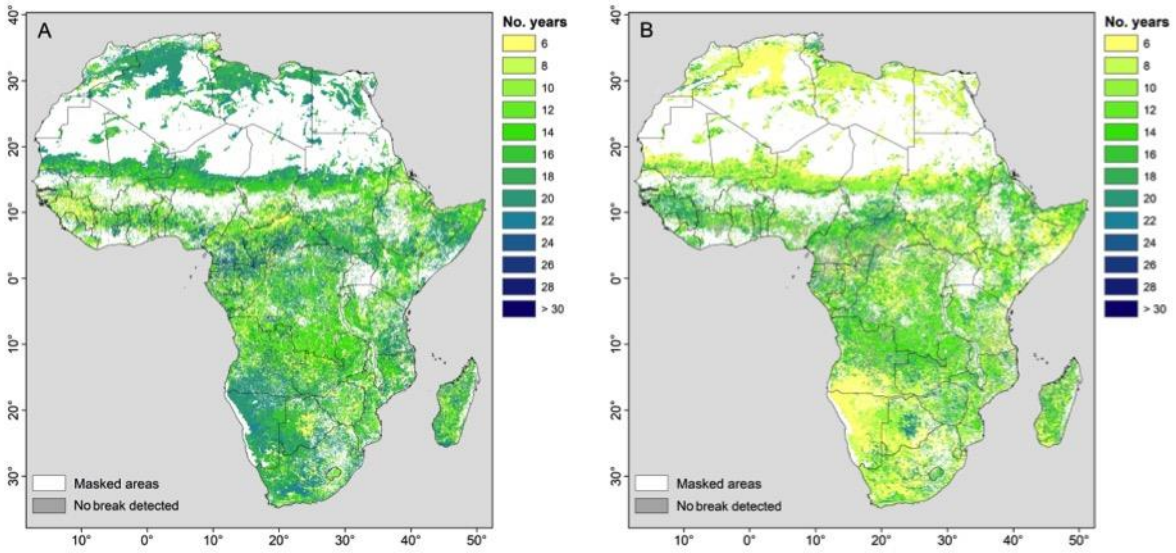

Figure D.6: Length of (A) first and (B) second segment expressed as the number of years. White areas indicate areas that were masked from the analysis and grey areas represent pixels were no break ($p < 0.05$) was detected in the NDVI3g time-series.

Appendix E

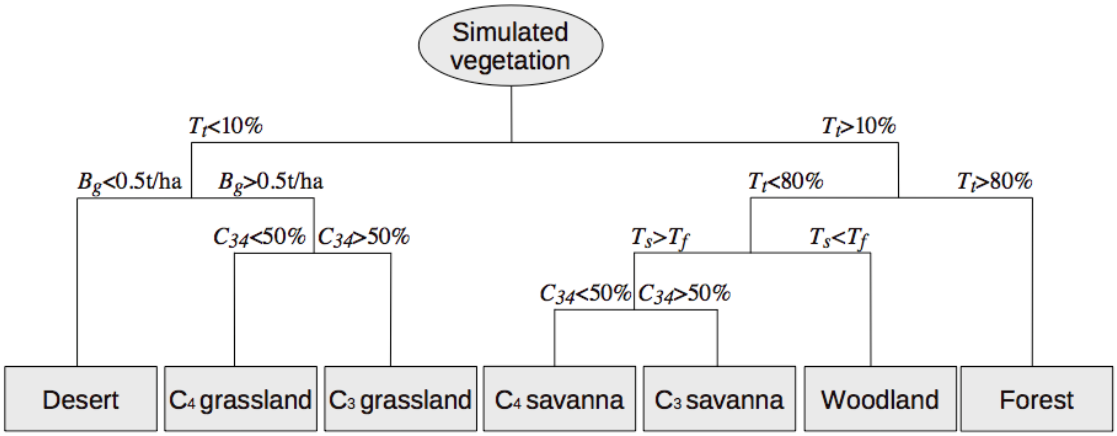

Figure E.1: Scheme for classification of simulated vegetation into different biome types. T_t: totoal tree cover; T_s: savanna tree cover; T_f: forest tree cover; B_g: grass biomass; C_{34}: C_3 to C_4 grass ratio. Savanna trees are, in the model, fire tolerant and shade intolerant while forest trees are fire sensitive and shade tolerant (Higgins & Scheiter 2012; Scheiter et al. 2012).

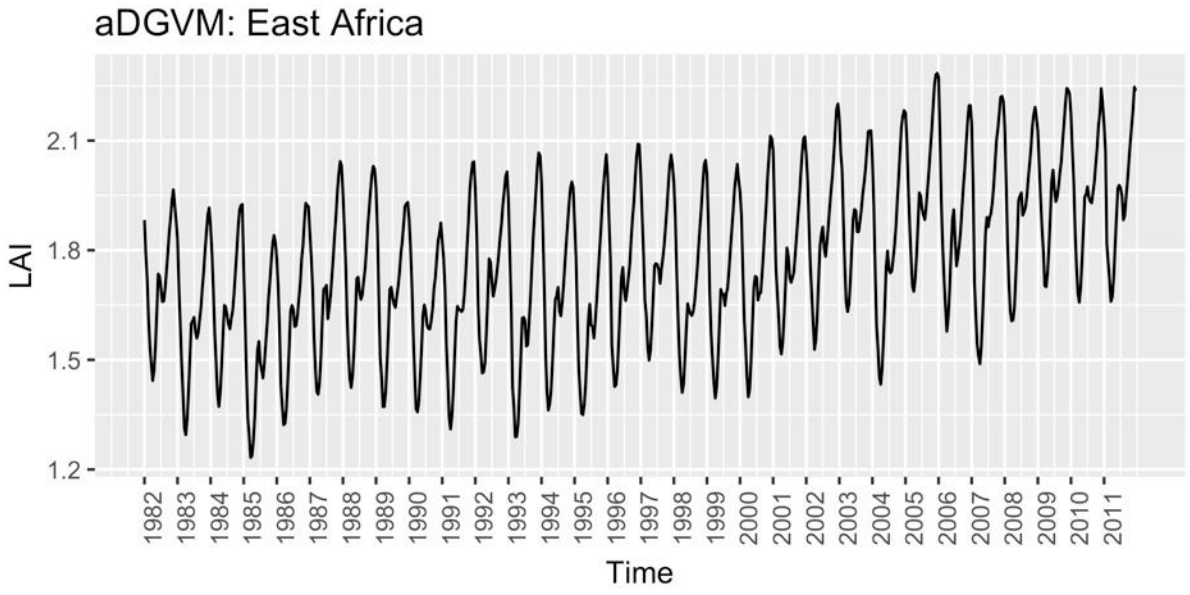

Figure E.2: Time-series of simulated LAI from aDGVM for East Africa (11.3°S to 15°N; 25°E to 52°E) for the period 1982 to 2011.

9. References

Adler, R.F., Huffman, G.J., Chang, A., Ferraro, R., Xie, P., Janowiak, J., Rudolf, B., Schneider, U., Curtis, S. & Bolvin, D. 2003, "The version-2 global precipitation climatology project (GPCP) monthly precipitation analysis (1979-present)", *Journal of Hydrometeorology,* vol. 4, no. 6, pp. 1147-1167.

Ainsworth, E.A. & Long, S.P. 2005, "What have we learned from 15 years of free- air CO2 enrichment (FACE)? A meta- analytic review of the responses of photosynthesis, canopy properties and plant production to rising CO2", *New Phytologist,* vol. 165, no. 2, pp. 351-372.

Aleman, J.C., Blarquez, O., Gourlet-Fleury, S., Bremond, L. & Favier, C. 2017, "Tree cover in Central Africa: determinants and sensitivity under contrasted scenarios of global change", *Scientific Reports,* vol. 7, pp. 41393.

Ambrosino, C., Chandler, R.E. & Todd, M.C. 2011, "Southern African monthly rainfall variability: An analysis based on generalized linear models", *Journal of Climate,* vol. 24, no. 17, pp. 4600-4617.

Anav, A., Murray-Tortarolo, G., Friedlingstein, P., Sitch, S., Piao, S. & Zhu, Z. 2013, "Evaluation of land surface models in reproducing satellite Derived leaf area index over the high-latitude northern hemisphere. Part II: Earth system models", *Remote Sensing,* vol. 5, no. 8, pp. 3637-3661.

Anyamba, A. & Eastman, J. 1996, "Interannual variability of NDVI over Africa and its relation to El Niño/Southern Oscillation", *Remote Sensing,* vol. 17, no. 13, pp. 2533-2548.

Anyamba, A. & Tucker, C. 2005, "Analysis of Sahelian vegetation dynamics using NOAA-AVHRR NDVI data from 1981–2003", *Journal of Arid Environments,* vol. 63, no. 3, pp. 596-614.

Anyamba, A., Tucker, C. & Eastman, J. 2001, "NDVI anomaly patterns over Africa during the 1997/98 ENSO warm event", *International Journal of Remote Sensing,* vol. 22, no. 10, pp. 1847-1860.

Anyamba, A. & Tucker, C.J. 2012, "Historical perspective of AVHRR NDVI and vegetation drought monitoring" in *Remote Sensing of Drought: Innovative Monitoring Approaches*, ed. Wardlow, B.D, Anderson, M.C, Verdin, J.P, CRC Press, Florida, pp. 23.

Anyamba, A., Tucker, C.J. & Mahoney, R. 2002, "From El Niño to La Niña: Vegetation response patterns over east and southern Africa during the 1997–2000 period", *Journal of Climate,* vol. 15, no. 21, pp. 3096-3103.

Arneth, A., Sitch, S., Pongratz, J., Stocker, B., Ciais, P., Poulter, B., Bayer, A., Bondeau, A., Calle, L. & Chini, L. 2017, "Historical carbon dioxide emissions caused by land-use changes are possibly larger than assumed", *Nature Geoscience,* vol. 10, no. 2, pp. 79-84.

Azzali, S. & Menenti, M. 2000, "Mapping vegetation-soil-climate complexes in southern Africa using temporal Fourier analysis of NOAA-AVHRR NDVI data", *International Journal of Remote Sensing,* vol. 21, no. 5, pp. 973-996.

Baudena, M., Dekker, S.C., van Bodegom, P.M., Cuesta, B., Higgins, S.I., Lehsten, V., Reick, C.H., Rietkerk, M., Scheiter, S. & Yin, Z. 2015, "Forests, savannas, and grasslands: bridging the knowledge gap between ecology and Dynamic Global Vegetation Models", *Biogeosciences,* vol. 12, no. 6, pp. 1833-1848.

Bellone, T., Boccardo, P. & Perez, F. 2009, "Investigation of Vegetation Dynamics using Long-Term NormalizedDifference Vegetation Index Time-Series", *American Journal of Environmental Sciences,* vol. 5, pp. 461-467.

Berrahmouni, N., Tapsoba, F. & Berte, C.J. 2014, *The Great Green Wall for the Sahara and the Sahel Initiative: building resilient landscapes in African drylands*, Food and Agriculture Organization of the United Nations, Rome.

Bodart, C., Brink, A.B., Donnay, F., Lupi, A., Mayaux, P. & Achard, F. 2013, "Continental estimates of forest cover and forest cover changes in the dry ecosystems of Africa between 1990 and 2000", *Journal of Biogeography,* vol. 40, no. 6, pp. 1036-1047.

Bond, W.J. & Midgley, G.F. 2000, "A proposed CO2- controlled mechanism of woody plant invasion in grasslands and savannas", *Global Change Biology,* vol. 6, no. 8, pp. 865-869.

Bontemps, S., Defourny, P., Bogaert, E.V., Arino, O., Kalogirou, V. & Perez, J.R. 2011, *GLOBCOVER 2009 Products description and validation report*, Université catholique de Louvain (UCL) & European Space Agency (esa), Vers. 2.2, 53 pp, http://due.esrin.esa.int/files/GLOBCOVER2009_Validation_Report_2.2.pdf [accessed 9 October 2017].

Brandt, M., Mbow, C., Diouf, A.A., Verger, A., Samimi, C. & Fensholt, R. 2015, "Ground- and satellite- based evidence of the biophysical mechanisms behind the greening Sahel", *Global Change Biology,* vol. 21, no. 4, pp. 1610-1620.

Brown, M.E., de Beurs, K. & Vrieling, A. 2010, "The response of African land surface phenology to large scale climate oscillations", *Remote Sensing of Environment,* vol. 114, no. 10, pp. 2286-2296.

Buermann, W., Dong, J., Zeng, X., Myneni, R.B. & Dickinson, R.E. 2001, "Evaluation of the utility of satellite-based vegetation leaf area index data for climate simulations", *Journal of Climate,* vol. 14, no. 17, pp. 3536-3550.

Buitenwerf, R., Bond, W., Stevens, N. & Trollope, W. 2012, "Increased tree densities in South African savannas:> 50 years of data suggests CO2 as a driver", *Global Change Biology,* vol. 18, no. 2, pp. 675-684.

Buitenwerf, R., Rose, L. & Higgins, S.I. 2015, "Three decades of multi-dimensional change in global leaf phenology", *Nature Climate Change,* vol. 5, pp. 364-368.

Buontempo, C., Booth, B. & Moufouma-Okia, W. 2010, *Sahelian climate: past, current, projections*, Met Office Hadley Centre, Devon, UK.

Cai, W., Borlace, S., Lengaigne, M., Van Rensch, P., Collins, M., Vecchi, G., Timmermann, A., Santoso, A., McPhaden, M.J. & Wu, L. 2014, "Increasing frequency of extreme El Niño events due to greenhouse warming", *Nature climate change,* vol. 4, no. 2, pp. 111-116.

Camberlin, P., Janicot, S. & Poccard, I. 2001, "Seasonality and atmospheric dynamics of the teleconnection between African rainfall and tropical sea- surface temperature: Atlantic vs. ENSO", *International Journal of Climatology,* vol. 21, no. 8, pp. 973-1005.

Chamaille- Jammes, S., Fritz, H. & Murindagomo, F. 2006, "Spatial patterns of the NDVI–rainfall relationship at the seasonal and interannual time scales in an African savanna", *International Journal of Remote Sensing,* vol. 27, no. 23, pp. 5185-5200.

Chen, J., Jönsson, P., Tamura, M., Gu, Z., Matsushita, B. & Eklundh, L. 2004, "A simple method for reconstructing a high-quality NDVI time-series data set based on the Savitzky–Golay filter", *Remote Sensing of Environment,* vol. 91, no. 3, pp. 332-344.

Cho, M.A., Ramoelo, A. & Dziba, L. 2017, "Response of Land Surface Phenology to Variation in Tree Cover during Green-Up and Senescence Periods in the Semi-Arid Savanna of Southern Africa", *Remote Sensing,* vol. 9, no. 7, pp. 689.

Christensen, J.H., Hewitson, B., Busuioc, A., Chen, A., Gao, X., Held, R., Jones, R., Kolli, R.K., Kwon, W. & Laprise, R. 2007, "Regional climate projections" in *Climate Change, 2007: The Physical Science Basis.Contribution of Working group I to the Fourth Assessment Report of the Intergovernmental Panel on Climate Change*, ed. S. Solomon, University Press, Cambridge, pp. 847-940.

Churkina, G. & Running, S.W. 1998, "Contrasting climatic controls on the estimated productivity of global terrestrial biomes", *Ecosystems,* vol. 1, no. 2, pp. 206-215.

Clements, N., Sarkar, S.K., Zhao, Z. & Kim, D. 2014, "Applying multiple testing procedures to detect change in East African vegetation", *The Annals of Applied Statistics,* vol. 8, no. 1, pp. 286-308.

Cook, B.I. & Pau, S. 2013, "A global assessment of long-term greening and browning trends in pasture lands using the GIMMS LAI3g dataset", *Remote Sensing,* vol. 5, no. 5, pp. 2492-2512.

Cramer, W., Bondeau, A., Woodward, F.I., Prentice, I.C., Betts, R.A., Brovkin, V., Cox, P.M., Fisher, V., Foley, J.A. & Friend, A.D. 2001, "Global response of terrestrial ecosystem structure and function to CO2 and climate change: results from six dynamic global vegetation models", *Global Change Biology,* vol. 7, no. 4, pp. 357-373.

Creese, A. & Pokam, W. 2016, *Africa's Climate Helping Decision-Makers Make Sense Of Climate Information*, Future Climate for Africa, Cape Town, South Africa.

Dardel, C., Kergoat, L., Hiernaux, P., Mougin, E., Grippa, M. & Tucker, C. 2014a, "Re-greening Sahel: 30years of remote sensing data and field observations (Mali, Niger)", *Remote Sensing of Environment,* vol. 140, pp. 350-364.

Dardel, C., Kergoat, L., Hiernaux, P., Mougin, E., Grippa, M. & Tucker, C. 2014b, "Re-greening Sahel: 30years of remote sensing data and field observations (Mali, Niger)", *Remote Sensing of Environment,* vol. 140, pp. 350-364.

Davenport, M.L. & Nicholson, S.E. 1993, "On the relation between rainfall and the Normalized Difference Vegetation Index for diverse vegetation types in East Africa", *International Journal of Remote Sensing,* vol. 14, no. 12, pp. 2369-2389.

Davis, C.L., Hoffman, M.T. & Roberts, W. 2017, "Long-term trends in vegetation phenology and productivity over Namaqualand using the GIMMS AVHRR NDVI3g data from 1982 to 2011", *South African Journal of Botany,* vol. 111, pp. 76-85.

De Beurs, K. & Henebry, G. 2005, "A statistical framework for the analysis of long image time series", *International Journal of Remote Sensing,* vol. 26, no. 8, pp. 1551-1573.

de Jong, R., de Bruin, S., Schaepman, M. & Dent, D. 2011a, "Quantitative mapping of global land degradation using Earth observations", *International Journal of Remote Sensing,* vol. 32, no. 21, pp. 6823-6853.

de Jong, R., de Bruin, S., de Wit, A., Schaepman, M.E. & Dent, D.L. 2011b, "Analysis of monotonic greening and browning trends from global NDVI time-series", *Remote Sensing of Environment,* vol. 115, no. 2, pp. 692-702.

de Jong, R., Verbesselt, J., Schaepman, M.E. & Bruin, S. 2012, "Trend changes in global greening and browning: contribution of short- term trends to longer- term change", *Global Change Biology,* vol. 18, no. 2, pp. 642-655.

De Jong, R., Verbesselt, J., Schaepman, M.E. & De Bruin, S. 2011, "Detection of Breakpoints in Global NDVI time series", *34th International Symposium on Remote Sensing of Environment (ISRSE)*, pp. 10.

de Jong, R., Verbesselt, J., Zeileis, A. & Schaepman, M.E. 2013, "Shifts in global vegetation activity trends", *Remote Sensing,* vol. 5, no. 3, pp. 1117-1133.

Degefu, M.A., Rowell, D.P. & Bewket, W. 2017, "Teleconnections between Ethiopian rainfall variability and global SSTs: observations and methods for model evaluation", *Meteorology and Atmospheric Physics,* vol. 129, no. 2, pp. 173-186.

Delègue, M., Fuhr, M., Schwartz, D., Mariotti, A. & Nasi, R. 2001, "Recent origin of a large part of the forest cover in the Gabon coastal area based on stable carbon isotope data", *Oecologia,* vol. 129, no. 1, pp. 106-113.

Devine, A.P., McDonald, R.A., Quaife, T. & Maclean, I.M. 2017, "Determinants of woody encroachment and cover in African savannas", *Oecologia,* vol. 183, no. 4, pp. 939-951.

DeVries, B., Verbesselt, J., Kooistra, L. & Herold, M. 2015, "Robust monitoring of small-scale forest disturbances in a tropical montane forest using Landsat time series", *Remote Sensing of Environment,* vol. 161, pp. 107-121.

Diallo, D.D., Goalbaye, T., Mahamat-Saleh, M., Sarr, P.S., Masse, D., Wood, S.A., Diop, L., Dick, R.P., Diop, A. & Guisse, A. 2017, "Effects of major woody species of the Senegalese Great Green Wall on N mineralization and microbial biomass in soils", *Bois et Forets des Tropiques,* vol. 333, no. 3, pp. 43-54.

Diatta, S. & Fink, A.H. 2014, "Statistical relationship between remote climate indices and West African monsoon variability", *International Journal of Climatology,* vol. 34, no. 12, pp. 3348-3367.

Donohue, R.J., Roderick, M.L., McVicar, T.R. & Farquhar, G.D. 2013, "Impact of CO2 fertilization on maximum foliage cover across the globe's warm, arid environments", *Geophysical Research Letters,* vol. 40, no. 12, pp. 3031-3035.

Driver, A., Sink, K., Nel, J., Holness, S., Van Niekerk, L., Daniels, F., Jonas, Z., Majiedt, P., Harris, L. & Maze, K. 2012, *National Biodiversity Assessment 2011: An assessment of South Africa's biodiversity and ecosystems,* Synthesis Report..South African National Biodiversity Institute and Department of Environmental Affairs, Pretoria.

Eastman, J.R. 2009, *IDRISI Taiga guide to GIS and image processing,* Clark Labs.Clark University, Worcester (MA), USA.

Eastman, J.R., Sangermano, F., Ghimire, B., Zhu, H., Chen, H., Neeti, N., Cai, Y., Machado, E.A. & Crema, S.C. 2009, "Seasonal trend analysis of image time series", *International Journal of Remote Sensing,* vol. 30, no. 10, pp. 2721-2726.

Egeru, A., Wasonga, O., Kyagulanyi, J., Majaliwa, G.M., MacOpiyo, L. & Mburu, J. 2014, "Spatio-temporal dynamics of forage and land cover changes in Karamoja sub-region, Uganda", *Pastoralism,* vol. 4, no. 1, pp. 6.

Eklundh, L., Ardö, J., Jönsson, P. & Sjöström, M. 2012, "High resolution mapping of vegetation dynamics from Sentinel-2", *European Space Agency, Sentinel-2 Preparatory Symposium,*Rome, April 23-27, pp. 7.

Eklundh, L. & Jönsson, P. 2012, *Timesat 3.1 Software Manual,* Lund University, Sweden, Malmö and Lund.

Eklundh, L. & Olsson, L. 2003, "Vegetation index trends for the African Sahel 1982–1999", *Geophysical Research Letters,* vol. 30, no. 8, pp. 1430.

Enfield, D.B., Mestas- Nuñez, A.M. & Trimble, P.J. 2001, "The Atlantic multidecadal oscillation and its relation to rainfall and river flows in the continental US", *Geophysical Research Letters,* vol. 28, no. 10, pp. 2077-2080.

Engelbrecht, F.A., Landman, W.A., Engelbrecht, C., Landman, S., Bopape, M., Roux, B., McGregor, J. & Thatcher, M. 2011, "Multi-scale climate modelling over Southern Africa using a variable-resolution global model", *Water SA,* vol. 37, no. 5, pp. 647-658.

Engelbrecht, C., Engelbrecht, F. & Dyson, L. 2013, "High- resolution model- projected changes in mid- tropospheric closed- lows and extreme rainfall events over southern Africa", *International Journal of Climatology,* vol. 33, no. 1, pp. 173-187.

Engelbrecht, F.A., Thambiran, T. & Davis, C.L. 2017 in press, *Chapter 3: Climate Change over South Africa: From trends and projected changes to vulnerability assessments and the status quo of national adaptation strategies*, Department of Environmental Affairs, South Africa's 3rd National Communication to UNFCCC.

Engelbrecht, F., McGregor, J. & Engelbrecht, C. 2009, "Dynamics of the Conformal- Cubic Atmospheric Model projected climate- change signal over southern Africa", *International Journal of Climatology,* vol. 29, no. 7, pp. 1013-1033.

Engelbrecht, F., Adegoke, J., Bopape, M., Naidoo, M., Garland, R., Thatcher, M., McGregor, J., Katzfey, J., Werner, M. & Ichoku, C. 2015, "Projections of rapidly rising surface temperatures over Africa under low mitigation", *Environmental Research Letters,* vol. 10, no. 8, pp. 085004.

FAO 2015, *Global Forest Resources Assessment 2015*, http://www.fao.org/3/a-i4808e.pdf, Rome.

Fauchereau, N., Trzaska, S., Rouault, M. & Richard, Y. 2003, "Rainfall variability and changes in southern Africa during the 20th century in the global warming context", *Natural Hazards,* vol. 29, no. 2, pp. 139-154.

Fensholt, R., Langanke, T., Rasmussen, K., Reenberg, A., Prince, S.D., Tucker, C., Scholes, R.J., Le, Q.B., Bondeau, A. & Eastman, R. 2012, "Greenness in semi-arid areas across the globe 1981–2007—an Earth Observing Satellite based analysis of trends and drivers", *Remote Sensing of Environment,* vol. 121, pp. 144-158.

Fensholt, R., Sandholt, I. & Rasmussen, M.S. 2004, "Evaluation of MODIS LAI, fAPAR and the relation between fAPAR and NDVI in a semi-arid environment using in situ measurements", *Remote Sensing of Environment,* vol. 91, no. 3, pp. 490-507.

Fensholt, R., Nielsen, T.T. & Stisen, S. 2006, "Evaluation of AVHRR PAL and GIMMS 10-day composite NDVI time series products using SPOT- 4 vegetation data for the African continent", *International Journal of Remote Sensing,* vol. 27, no. 13, pp. 2719-2733.

Fensholt, R. & Rasmussen, K. 2011, "Analysis of trends in the Sahelian 'rain-use efficiency'using GIMMS NDVI, RFE and GPCP rainfall data", *Remote Sensing of Environment,* vol. 115, no. 2, pp. 438-451.

Fensholt, R., Rasmussen, K., Kaspersen, P., Huber, S., Horion, S. & Swinnen, E. 2013, "Assessing Land Degradation/Recovery in the African Sahel from Long-Term Earth Observation Based Primary Productivity and Precipitation Relationships", *Remote Sensing,* vol. 5, no. 2, pp. 664-686.

Field, C.B., Barros, V.R., Mach, K. & Mastrandrea, M. 2014, *Climate change 2014: impacts, adaptation, and vulnerability. Working Group II Contribution to the IPCC 5th Assessment Report-Technical Summary*, Cambridge University Press, UK.

Fisher, R., McDowell, N., Purves, D., Moorcroft, P., Sitch, S., Cox, P., Huntingford, C., Meir, P. & Ian Woodward, F. 2010, "Assessing uncertainties in a second- generation dynamic vegetation model caused by ecological scale limitations", *New Phytologist,* vol. 187, no. 3, pp. 666-681.

Fitchett, J.M., Grab, S.W. & Thompson, D.I. 2015, "Plant phenology and climate change: Progress in methodological approaches and application", *Progress in Physical Geography,* vol. 39, no. 4, pp. 460-482.

Forkel, M., Carvalhais, N., Verbesselt, J., Mahecha, M.D., Neigh, C.S. & Reichstein, M. 2013, "Trend change detection in NDVI time series: Effects of inter-annual variability and methodology", *Remote Sensing,* vol. 5, no. 5, pp. 2113-2144.

Friedlingstein, P., Meinshausen, M., Arora, V.K., Jones, C.D., Anav, A., Liddicoat, S.K. & Knutti, R. 2014, "Uncertainties in CMIP5 climate projections due to carbon cycle feedbacks", *Journal of Climate,* vol. 27, no. 2, pp. 511-526.

Gao, Q., Zhu, W., Schwartz, M.W., Ganjurjav, H., Wan, Y., Qin, X., Ma, X., Williamson, M.A. & Li, Y. 2016, "Climatic change controls productivity variation in global grasslands", *Scientific reports,* vol. 6, pp. 26958.

Giglio, L., Randerson, J., Van der Werf, G., Kasibhatla, P., Collatz, G., Morton, D. & DeFries, R. 2010, "Assessing variability and long-term trends in burned area by merging multiple satellite fire products", *Biogeosciences,* vol. 7, no. 3.

Gillett, N., Kell, T. & Jones, P. 2006, "Regional climate impacts of the Southern Annular Mode", *Geophysical Research Letters,* vol. 33, no. 23.

Gong, D. & Wang, S. 1999, "Definition of Antarctic oscillation index", *Geophysical Research Letters,* vol. 26, no. 4, pp. 459-462.

Gonzalez, P., Tucker, C.J. & Sy, H. 2012, "Tree density and species decline in the African Sahel attributable to climate", *Journal of Arid Environments,* vol. 78, pp. 55-64.

Hannah, L., Midgley, G., Lovejoy, T., Bond, W., Bush, M., Lovett, J., Scott, D. & Woodward, F. 2002, "Conservation of biodiversity in a changing climate", *Conservation Biology,* vol. 16, no. 1, pp. 264-268.

Harris, A., Carr, A. & Dash, J. 2014a, "Remote sensing of vegetation cover dynamics and resilience across southern Africa", *International Journal of Applied Earth Observation and Geoinformation,* vol. 28, pp. 131-139.

Harris, I., Jones, P., Osborn, T. & Lister, D. 2013, "Updated high- resolution grids of monthly climatic observations–the CRU TS3. 10 Dataset", *International Journal of Climatology,* vol. 34, pp. 623–642.

Harris, I., Jones, P., Osborn, T. & Lister, D. 2014b, "Updated high- resolution grids of monthly climatic observations–the CRU TS3. 10 Dataset", *International Journal of Climatology,* vol. 34, no. 3, pp. 623-642.

Harrison, L., Funk, C.C., Verdin, J.P., Pedreros, D.H., Shukla, S. & Husak, G.J. 2015, "Contrasting rainfall declines in northern and southern Tanzania: Potential differential impacts of west Pacific warming and east Pacific cooling", *American Geophysical Union, Fall Meeting 2015*AGU, 12/2015.

Hartig, F., Dyke, J., Hickler, T., Higgins, S.I., O'Hara, R.B., Scheiter, S. & Huth, A. 2012a, "Connecting dynamic vegetation models to data–an inverse perspective", *Journal of Biogeography,* vol. 39, no. 12, pp. 2240-2252.

Hartig, F., Dyke, J., Hickler, T., Higgins, S.I., O'Hara, R.B., Scheiter, S. & Huth, A. 2012b, "Connecting dynamic vegetation models to data–an inverse perspective", *Journal of Biogeography,* vol. 39, no. 12, pp. 2240-2252.

Hayward, D.F. & Oguntoyinbo, J.S. 1987, *Climatology of West Africa,* Rowman & Littlefield.

Herrmann, S.M., Anyamba, A. & Tucker, C.J. 2005, "Recent trends in vegetation dynamics in the African Sahel and their relationship to climate", *Global Environmental Change,* vol. 15, no. 4, pp. 394-404.

Herrmann, S.M. & Mohr, K.I. 2011, "A continental-scale classification of rainfall seasonality regimes in Africa based on gridded precipitation and land surface temperature products", *Journal of Applied Meteorology and Climatology,* vol. 50, no. 12, pp. 2504-2513.

Herrmann, S.M. & Tappan, G.G. 2013, "Vegetation impoverishment despite greening: A case study from central Senegal", *Journal of Arid Environments,* vol. 90, pp. 55-66.

Heumann, B.W., Seaquist, J., Eklundh, L. & Jönsson, P. 2007, "AVHRR derived phenological change in the Sahel and Soudan, Africa, 1982–2005", *Remote Sensing of Environment,* vol. 108, no. 4, pp. 385-392.

Hewitson, B. & Crane, R. 2006, "Consensus between GCM climate change projections with empirical downscaling: precipitation downscaling over South Africa", *International Journal of Climatology,* vol. 26, no. 10, pp. 1315-1337.

Hickler, T., Prentice, I.C., Smith, B., Sykes, M.T. & Zaehle, S. 2006, "Implementing plant hydraulic architecture within the LPJ Dynamic Global Vegetation Model", *Global Ecology and Biogeography,* vol. 15, no. 6, pp. 567-577.

Higgins, S.I., Bond, W.J., February, E.C., Bronn, A., Euston-Brown, D.I., Enslin, B., Govender, N., Rademan, L., O'Regan, S. & Potgieter, A.L. 2007, "Effects of four decades of fire manipulation on woody vegetation structure in savanna", *Ecology,* vol. 88, no. 5, pp. 1119-1125.

Higgins, S.I. & Scheiter, S. 2012, "Atmospheric CO2 forces abrupt vegetation shifts locally, but not globally", *Nature,* vol. 488, no. 7410, pp. 209-212.

Hijmans, R.J., Cameron, S.E., Parra, J.L., Jones, P.G. & Jarvis, A. 2005, "Very high resolution interpolated climate surfaces for global land areas", *International Journal of Climatology,* vol. 25, no. 15, pp. 1965-1978.

Hill, M., Hanan, N., Hoffmann, W., Scholes, R., Prince, S., Ferwerda, J., Lucas, R., Baker, I., Arneth, A. & Higgins, S. 2011, "Remote sensing and modeling of savannas: The state of the dis-union", *Proceedings of the 34th International Symposium on Remote Sensing of the Environment (ISRSE)*ISRSE, Sydney, Australia, 10–15 April 2011.

Hirsch, R.M., Helsel, D., Cohn, T. & Gilroy, E. 1993, "Statistical analysis of hydrologic data.", *Handbook of hydrology,* vol. 17, pp. 11-55.

Hobbs, J.E., Lindesay, J.A. & Bridgman, H.A. 1998, *Climates of the southern continents: present, past and future,* 1st edn, Wiley, New York.

Hobbs, R.J. 1990, "Remote sensing of spatial and temporal dynamics of vegetation" in *Remote Sensing of Biosphere Functioning*, eds. R.J. Hobbs & H.A. Mooney, Springer, New York, pp. 203-219.

Hollander, M. & Wolfe, D. 1973, *Nonparametric statistical procedures,* Willey, New York.

Hoscilo, A., Balzter, H., Bartholomé, E., Boschetti, M., Brivio, P., Brink, A., Clerici, M. & Pekel, J. 2015, "A conceptual model for assessing rainfall and vegetation trends in sub-Saharan Africa from satellite data", *International Journal of Climatology,* vol. 35, no. 12, pp. 3582-3592.

Huber, S. & Fensholt, R. 2011, "Analysis of teleconnections between AVHRR-based sea surface temperature and vegetation productivity in the semi-arid Sahel", *Remote Sensing of Environment,* vol. 115, no. 12, pp. 3276-3285.

Huete, A., Didan, K., Miura, T., Rodriguez, E.P., Gao, X. & Ferreira, L.G. 2002, "Overview of the radiometric and biophysical performance of the MODIS vegetation indices", *Remote Sensing of Environment,* vol. 83, no. 1, pp. 195-213.

Huete, A.R., Liu, H. & van Leeuwen, W.J. 1997, "The use of vegetation indices in forested regions: issues of linearity and saturation", *Geoscience and Remote Sensing, 1997. IGARSS'97. Remote Sensing-A Scientific Vision for Sustainable Development., 1997 IEEE International*IEEE, Singapore, Aug 3 1997, pp. 1966.

Huete, A. & Tucker, C. 1991, "Investigation of soil influences in AVHRR red and near-infrared vegetation index imagery", *International Journal of Remote Sensing,* vol. 12, no. 6, pp. 1223-1242.

Hulme, M., Doherty, R., Ngara, T., New, M. & Lister, D. 2001, "African climate change: 1900-2100", *Climate Research,* vol. 17, no. 2, pp. 145-168.

Hurrell, J.W. 2002, "Decadal trends in the North Atlantic oscillation", *Climate Change: Evaluating recent and future climate change,* vol. 4, pp. 201.

Hurtt, G.C., Chini, L.P., Frolking, S., Betts, R., Feddema, J., Fischer, G., Fisk, J., Hibbard, K., Houghton, R. & Janetos, A. 2011, "Harmonization of land-use scenarios for the period 1500–2100: 600 years of global gridded annual land-use transitions, wood harvest, and resulting secondary lands", *Climatic Change,* vol. 109, no. 1-2, pp. 117.

Indeje, M., Semazzi, F.H. & Ogallo, L.J. 2000, "ENSO signals in East African rainfall seasons", *International Journal of Climatology,* vol. 20, no. 1, pp. 19-46.

Ivits, E., Horion, S., Fensholt, R. & Cherlet, M. 2014, "Global ecosystem response types derived from the standardized precipitation evapotranspiration index and FPAR3g series", *Remote Sensing,* vol. 6, no. 5, pp. 4266-4288.

Jalloh, A., Nelson, G.C., Thomas, T.S., Zougmoré, R.B. & Roy-Macauley, H. 2013, *West African agriculture and climate change: a comprehensive analysis. IFPRI Research Monograph,* 1st edn, International Food Policy Research Institute, Washington, D.C.

James, R. & Washington, R. 2013, "Changes in African temperature and precipitation associated with degrees of global warming", *Climatic Change,* vol. 117, no. 4, pp. 859-872.

Joly, M. & Voldoire, A. 2009, "Influence of ENSO on the West African monsoon: temporal aspects and atmospheric processes", *Journal of Climate,* vol. 22, no. 12, pp. 3193-3210.

Jones, P., Jonsson, T. & Wheeler, D. 1997, "Extension to the North Atlantic Oscillation using early instrumental pressure observations from Gibraltar and South-West Iceland", *International Journal of Climatology,* vol. 17, no. 13, pp. 1433-1450.

Jones, P., Lister, D., Osborn, T., Harpham, C., Salmon, M. & Morice, C. 2012, "Hemispheric and large- scale land- surface air temperature variations: An extensive revision and an update to 2010", *Journal of Geophysical Research: Atmospheres,* vol. 117, no. D5.

Jong, R., Schaepman, M.E., Furrer, R., Bruin, S. & Verburg, P.H. 2013, "Spatial relationship between climatologies and changes in global vegetation activity", *Global Change Biology,* vol. 19, no. 6, pp. 1953-1964.

Jönsson, P. & Eklundh, L. 2004, "TIMESAT—a program for analyzing time-series of satellite sensor data", *Computers & Geosciences,* vol. 30, no. 8, pp. 833-845.

Justice, C.O., Townshend, J., Holben, B. & Tucker, e.C. 1985, "Analysis of the phenology of global vegetation using meteorological satellite data", *International Journal of Remote Sensing,* vol. 6, no. 8, pp. 1271-1318.

Katzfey, J., McGregor, J., Nguyen, K. & Thatcher, M. 2009, "Dynamical downscaling techniques: impacts on regional climate change signals", *18th World IMACS congress and MODSIM09 international congress on modelling and simulation*, pp. 2377.

Kelley, D., Prentice, I.C., Harrison, S., Wang, H., Simard, M., Fisher, J. & Willis, K. 2013, "A comprehensive benchmarking system for evaluating global vegetation models", *Biogeosciences,* vol. 10, pp. 3313-3340.

Kendall, M.G. 1938, "A new measure of rank correlation", *Biometrika,* vol. 30, no. 1/2, pp. 81-93.

Kim, D., Thomas, V., Olson, J., Williams, M. & Clements, N. 2013, "Statistical trend and change-point analysis of land-cover-change patterns in East Africa", *International Journal of Remote Sensing,* vol. 34, no. 19, pp. 6636-6650.

Klopper, E., Vogel, C.H. & Landman, W.A. 2006, "Seasonal climate forecasts–potential agricultural-risk management tools?", *Climatic Change,* vol. 76, no. 1-2, pp. 73-90.

Kowalczyk, E.A., Wang, Y., Law, R., Davies, H., McGregor, J. & Abramowitz, G. 2006, *The CSIRO Atmosphere Biosphere Land Exchange (CABLE) model for use in climate models and as an offline model,* CSIRO Marine and Atmospheric Research.

Lamb, P. 1980, "Sahelian drought", *New Zealand Journal of Geography,* vol. 68, no. 1, pp. 12-16.

Landmann, T. & Dubovyk, O. 2014, "Spatial analysis of human-induced vegetation productivity decline over eastern Africa using a decade (2001–2011) of medium resolution MODIS time-series data", *International Journal of Applied Earth Observation and Geoinformation,* vol. 33, pp. 76-82.

Lanfredi, M., Simoniello, T. & Macchiato, M. 2004, "Temporal persistence in vegetation cover changes observed from satellite: Development of an estimation procedure in the test site of the Mediterranean Italy", *Remote Sensing of Environment,* vol. 93, no. 4, pp. 565-576.

Law, R.M., Kowalczyk, E.A. & WANGs, Y. 2006, "Using atmospheric CO2 data to assess a simplified carbon- climate simulation for the 20th century", *Tellus B,* vol. 58, no. 5, pp. 427-437.

Le Maitre, D.C., Forsyth, G.G., Dzikiti, S. & Gush, M.B. 2016, "Estimates of the impacts of invasive alien plants on water flows in South Africa", *Water SA,* vol. 42, no. 4, pp. 659-672.

Le Quéré, C., Andrew, R.M., Canadell, J.G., Sitch, S., Korsbakken, J.I., Peters, G.P., Manning, A.C., Boden, T.A., Tans, P.P. & Houghton, R.A. 2016, "Global carbon budget 2016", *Earth System Science Data,* vol. 8, no. 2, pp. 605.

Lebel, T. & Ali, A. 2009, "Recent trends in the Central and Western Sahel rainfall regime (1990–2007)", *Journal of Hydrology,* vol. 375, no. 1, pp. 52-64.

Lewis, S.L., Lopez-Gonzalez, G., Sonké, B., Affum-Baffoe, K., Baker, T.R., Ojo, L.O., Phillips, O.L., Reitsma, J.M., White, L. & Comiskey, J.A. 2009, "Increasing carbon storage in intact African tropical forests", *Nature,* vol. 457, no. 7232, pp. 1003-1006.

Liebmann, B., Hoerling, M.P., Funk, C., Bladé, I., Dole, R.M., Allured, D., Quan, X., Pegion, P. & Eischeid, J.K. 2014, "Understanding recent Eastern Horn of Africa rainfall variability and change", *Journal of Climate,* vol. 27, no. 23, pp. 8630-8645.

Linderholm, H.W., Ou, T., Jeong, J., Folland, C.K., Gong, D., Liu, H., Liu, Y. & Chen, D. 2011, "Interannual teleconnections between the summer North Atlantic Oscillation and

the East Asian summer monsoon", *Journal of Geophysical Research: Atmospheres,* vol. 116, no. D13.

Lindesay, J. 1988, "South African rainfall, the Southern Oscillation and a Southern Hemisphere semi- annual cycle", *Journal of Climatology,* vol. 8, no. 1, pp. 17-30.

Lindesay, J. & Vogel, C. 1990, "Historical evidence for Southern Oscillation- southern African rainfall relationships", *International Journal of Climatology,* vol. 10, no. 7, pp. 679-689.

Liu, Y., Li, Y., Li, S. & Motesharrei, S. 2015, "Spatial and temporal patterns of global NDVI trends: Correlations with climate and human factors", *Remote Sensing,* vol. 7, no. 10, pp. 13233-13250.

Lyon, B. & DeWitt, D.G. 2012, "A recent and abrupt decline in the East African long rains", *Geophysical Research Letters,* vol. 39, no. 2.

MacKellar, N., Hewitson, B. & Tadross, M. 2007, "Namaqualand's climate: Recent historical changes and future scenarios", *Journal of Arid Environments,* vol. 70, no. 4, pp. 604-614.

MacKellar, N., New, M. & Jack, C. 2014, "Observed and modelled trends in rainfall and temperature for South Africa: 1960-2010", *South African Journal of Science,* vol. 110, no. 7 & 8, pp. 51-63.

Maignan, F., Bréon, F., Chevallier, F., Viovy, N., Ciais, P., Garrec, C., Trules, J. & Mancip, M. 2011, "Evaluation of a global vegetation model using time series of satellite vegetation indices", *Geoscientific Model Development,* vol. 4, no. 4, pp. 1103-1114.

Malherbe, J., Engelbrecht, F.A. & Landman, W.A. 2013, "Projected changes in tropical cyclone climatology and landfall in the Southwest Indian Ocean region under enhanced anthropogenic forcing", *Climate Dynamics,* vol. 40, no. 11-12, pp. 2867-2886.

Mantua, N.J., Hare, S.R., Zhang, Y., Wallace, J.M. & Francis, R.C. 1997, "A Pacific interdecadal climate oscillation with impacts on salmon production", *Bulletin of the American Meteorological Society,* vol. 78, no. 6, pp. 1069-1079.

Mao, J., Shi, X., Thornton, P.E., Hoffman, F.M., Zhu, Z. & Myneni, R.B. 2013, "Global latitudinal-asymmetric vegetation growth trends and their driving mechanisms: 1982–2009", *Remote Sensing,* vol. 5, no. 3, pp. 1484-1497.

Martiny, N., Camberlin, P., Richard, Y. & Philippon, N. 2006, "Compared regimes of NDVI and rainfall in semi- arid regions of Africa", *International Journal of Remote Sensing,* vol. 27, no. 23, pp. 5201-5223.

Martiny, N., Richard, Y. & Camberlin, P. 2005, "Interannual persistence effects in vegetation dynamics of semi-arid Africa", *Geophysical Research Letters,* vol. 32, no. 24, pp. L24403.

Masih, I., Maskey, S., Mussá, F. & Trambauer, P. 2014, "A review of droughts on the African continent: a geospatial and long-term perspective", *Hydrology and Earth System Sciences,* vol. 18, no. 9, pp. 3635-3649.

McGregor, J.L. 2005, *C-CAM: Geometric aspects and dynamical formulation,* CSIRO Atmospheric Research.

McHugh, M.J. & Rogers, J.C. 2001, "North Atlantic oscillation influence on precipitation variability around the southeast African convergence zone", *Journal of Climate,* vol. 14, no. 17, pp. 3631-3642.

McMahon, S.M., Harrison, S.P., Armbruster, W.S., Bartlein, P.J., Beale, C.M., Edwards, M.E., Kattge, J., Midgley, G., Morin, X. & Prentice, I.C. 2011, "Improving assessment and modelling of climate change impacts on global terrestrial biodiversity", *Trends in Ecology & Evolution,* vol. 26, no. 5, pp. 249-259.

McSweeney, C., Lizcano, G., New, M. & Lu, X. 2010, "The UNDP Climate Change Country Profiles: Improving the accessibility of observed and projected climate information for studies of climate change in developing countries", *Bulletin of the American Meteorological Society,* vol. 91, no. 2, pp. 157-166.

Midgley, G., Hannah, L., Millar, D., Thuiller, W. & Booth, A. 2003, "Developing regional and species-level assessments of climate change impacts on biodiversity in the Cape Floristic Region", *Biological Conservation,* vol. 112, no. 1, pp. 87-97.

Midgley, G.F. & Bond, W.J. 2015, "Future of African terrestrial biodiversity and ecosystems under anthropogenic climate change", *Nature Climate Change,* vol. 5, no. 9, pp. 823-829.

Midgley, G.F., Aranibar, J.N., Mantlana, K.B. & Macko, S. 2004, "Photosynthetic and gas exchange characteristics of dominant woody plants on a moisture gradient in an African savanna", *Global Change Biology,* vol. 10, no. 3, pp. 309-317.

Mitchard, E.T., Saatchi, S.S., Gerard, F., Lewis, S. & Meir, P. 2009, "Measuring woody encroachment along a forest-savanna boundary in Central Africa", *Earth Interactions,* vol. 13, no. 8, pp. 1-29.

Mitchard, E.T. & Flintrop, C.M. 2013, "Woody encroachment and forest degradation in sub-Saharan Africa's woodlands and savannas 1982-2006", *Philosophical transactions of the Royal Society of London.Series B, Biological sciences,* vol. 368, no. 1625, pp. 20120406.

Mitchell, T.D. & Jones, P.D. 2005, "An improved method of constructing a database of monthly climate observations and associated high- resolution grids", *International Journal of Climatology,* vol. 25, no. 6, pp. 693-712.

Mohamed, M., Babiker, I.S., Chen, Z., Ikeda, K., Ohta, K. & Kato, K. 2004, "The role of climate variability in the inter-annual variation of terrestrial net primary production (NPP)", *Science of the Total Environment,* vol. 332, no. 1, pp. 123-137.

Mohino, E., Janicot, S. & Bader, J. 2011, "Sahel rainfall and decadal to multi-decadal sea surface temperature variability", *Climate Dynamics,* vol. 37, no. 3-4, pp. 419-440.

Moncrieff, G.R., Scheiter, S., Bond, W.J. & Higgins, S.I. 2014, "Increasing atmospheric CO2 overrides the historical legacy of multiple stable biome states in Africa", *New Phytologist,* vol. 201, no. 3, pp. 908-915.

Moncrieff, G., Scheiter, S., Slingsby, J. & Higgins, S. 2015, "Understanding global change impacts on South African biomes using Dynamic Vegetation Models", *South African Journal of Botany,* vol. 101, pp. 16-23.

Moulin, C. & Chiapello, I. 2004, "Evidence of the control of summer atmospheric transport of African dust over the Atlantic by Sahel sources from TOMS satellites (1979–2000)", *Geophysical Research Letters,* vol. 31, no. 2.

Moulin, C., Lambert, C.E., Dulac, F. & Dayan, U. 1997, "Control of atmospheric export of dust from North Africa by the North Atlantic Oscillation", *Nature,* vol. 387, no. 6634, pp. 691.

Müller, C., Eickhout, B., Zaehle, S., Bondeau, A., Cramer, W. & Lucht, W. 2007, "Effects of changes in CO2, climate, and land use on the carbon balance of the land biosphere during the 21st century", *Journal of Geophysical Research: Biogeosciences,* vol. 112, no. G2.

Müller, R., Pfeifroth, U., Träger-Chatterjee, C., Cremer, R., Trentmann, J. & Hollmann, R. 2015, *Surface Solar Radiation Data Set-Heliosat (SARAH)-*, EUMETSAT Satellite Application Facility on Climate Monitoring: Offenbach, Germany, http://www.cmsaf.eu/EN/Home/Archiv.html.

Murray-Tortarolo, G., Anav, A., Friedlingstein, P., Sitch, S., Piao, S., Zhu, Z., Poulter, B., Zaehle, S., Ahlström, A. & Lomas, M. 2013, "Evaluation of land surface models in reproducing satellite-derived LAI over the high-latitude northern hemisphere. Part I: Uncoupled DGVMs", *Remote Sensing,* vol. 5, no. 10, pp. 4819-4838.

Musau, J., Patil, S., Sheffield, J. & Marshall, M. 2016, "Spatio-temporal vegetation dynamics and relationship with climate over East Africa", *Hydrology and Earth System Sciences,* vol. http://dx.doi. org/10.5194/hess-2016-502, pp. 2016.

Mutanga, O. & Skidmore, A.K. 2004, "Narrow band vegetation indices overcome the saturation problem in biomass estimation", *International Journal of Remote Sensing,* vol. 25, no. 19, pp. 3999-4014.

Mwavu, E. & Witkowski, E. 2008, "Land- use and cover changes (1988–2002) around Budongo forest reserve, NW Uganda: Implications for forest and woodland sustainability", *Land Degradation & Development,* vol. 19, no. 6, pp. 606-622.

Myneni, R.B., Keeling, C., Tucker, C., Asrar, G. & Nemani, R. 1997, "Increased plant growth in the northern high latitudes from 1981 to 1991", *Nature,* vol. 386, no. 6626, pp. 698-702.

Nagendra, H., Lucas, R., Honrado, J.P., Jongman, R.H., Tarantino, C., Adamo, M. & Mairota, P. 2013, "Remote sensing for conservation monitoring: Assessing protected areas, habitat extent, habitat condition, species diversity, and threats", *Ecological Indicators,* vol. 33, pp. 45-59.

N'Datchoh, E., Konaré, A., Diedhiou, A., Diawara, A., Quansah, E. & Assamoi, P. 2015, "Effects of climate variability on savannah fire regimes in West Africa", *Earth System Dynamics,* vol. 6, no. 1, pp. 161.

Nemani, R.R., Keeling, C.D., Hashimoto, H., Jolly, W.M., Piper, S.C., Tucker, C.J., Myneni, R.B. & Running, S.W. 2003, "Climate-driven increases in global terrestrial net primary production from 1982 to 1999", *Science (New York, N.Y.),* vol. 300, no. 5625, pp. 1560-1563.

New, M., Lister, D., Hulme, M. & Makin, I. 2002, "A high-resolution data set of surface climate over global land areas", *Climate research,* vol. 21, no. 1, pp. 1-25.

New, M., Hewitson, B., Stephenson, D.B., Tsiga, A., Kruger, A., Manhique, A., Gomez, B., Coelho, C.A., Masisi, D.N. & Kululanga, E. 2006, "Evidence of trends in daily climate extremes over southern and west Africa", *Journal of Geophysical Research,* vol. 111, no. 7, pp. D14102.

Niang, I., Ruppel, O.C., Abdrabo, M.A., Essel, C., Lennard, C., Padgham, J., Urquhart, P. & Descheemaeker, K. 2014, "Africa" in *Climate Change 2014: Impacts, Adaptation, and Vulnerability. Part B: Regional Aspects. Contribution of Working Group II to the Fifth Assessment*, eds. V.R. Barros, C.B. Field, D.J. Dokken, et al, Cambridge University Press, UK, pp. 1199-1265.

Nicholson, S.E. 2015, "Long- term variability of the East African 'short rains' and its links to large- scale factors", *International Journal of Climatology,* vol. 35, no. 13, pp. 3979-3990.

Nicholson, S.E. 2000, "The nature of rainfall variability over Africa on time scales of decades to millenia", *Global and Planetary Change,* vol. 26, no. 1, pp. 137-158.

Nicholson, S.E. 1996, "A review of climate dynamics and climate variability in Eastern Africa" in *The Limnology, Climatology and Paleoclimatology of the East African Lakes*, ed. O.E. Johnson TC, 1st edn, Gordon and Breach, Amsterdam, pp. 25-56.

Oba, G., Post, E. & Stenseth, N.C. 2001, "Sub- saharan desertification and productivity are linked to hemispheric climate variability", *Global Change Biology,* vol. 7, no. 3, pp. 241-246.

O'Connor, T.G., Puttick, J.R. & Hoffman, M.T. 2014, "Bush encroachment in southern Africa: changes and causes", *African Journal of Range & Forage Science,* vol. 31, no. 2, pp. 67-88.

Olsson, L., Eklundh, L. & Ardö, J. 2005, "A recent greening of the Sahel—trends, patterns and potential causes", *Journal of Arid Environments,* vol. 63, no. 3, pp. 556-566.

Osborn, T. & Jones, P. 2014, "The CRUTEM4 land-surface air temperature data set: construction, previous versions and dissemination via Google Earth", *Earth System Science Data,* vol. 6, no. 1, pp. 61-68.

Pavlick, R., Drewry, D.T., Bohn, K., Reu, B. & Kleidon, A. 2013, "The Jena Diversity-Dynamic Global Vegetation Model (JeDi-DGVM): a diverse approach to representing terrestrial biogeography and biogeochemistry based on plant functional trade-offs", *Biogeosciences,* vol. 10, pp. 4137-4177.

Pettorelli, N., Vik, J.O., Mysterud, A., Gaillard, J., Tucker, C.J. & Stenseth, N.C. 2005, "Using the satellite-derived NDVI to assess ecological responses to environmental change", *Trends in ecology & evolution,* vol. 20, no. 9, pp. 503-510.

Pfeifer, M., Lefebvre, V., Gonsamo, A., Pellikka, P.K., Marchant, R., Denu, D. & Platts, P.J. 2014, "Validating and linking the GIMMS leaf area index (LAI3g) with environmental controls in tropical Africa", *Remote Sensing,* vol. 6, no. 3, pp. 1973-1990.

Philippon, N., Rouault, M., Richard, Y. & Favre, A. 2011, "The influence of ENSO on winter rainfall in South Africa", *International Journal of Climatology,* vol. 32, no. 15, pp. 2333-2347.

Pinzon, J. & Tucker, C. 2013, "Revisiting error, precision and uncertainty in NDVI AVHRR data: Development of a consistent NDVI3g time series", *Remote Sensing,* vol. in preparation.

Pinzon, J.E. & Tucker, C.J. 2014a, "A non-stationary 1981–2012 AVHRR NDVI3g time series", *Remote Sensing,* vol. 6, no. 8, pp. 6929-6960.

Pinzon, J.E. & Tucker, C.J. 2014b, "A non-stationary 1981–2012 AVHRR NDVI3g time series", *Remote Sensing,* vol. 6, no. 8, pp. 6929-6960.

Pohl, B., Fauchereau, N., Reason, C. & Rouault, M. 2010, "Relationships between the Antarctic Oscillation, the Madden-Julian Oscillation, and ENSO, and consequences for rainfall analysis", *Journal of Climate,* vol. 23, no. 2, pp. 238-254.

Prentice, I.C., Bondeau, A., Cramer, W., Harrison, S.P., Hickler, T., Lucht, W., Sitch, S., Smith, B. & Sykes, M.T. 2007, "Dynamic global vegetation modeling: quantifying terrestrial ecosystem responses to large-scale environmental change" in *Terrestrial ecosystems in a changing world*, eds. J.G. Canadell, D.E. Pataki & L.F. Pitelka, Springer, Berlin, pp. 175-192.

Pricope, N.G., Husak, G., Lopez-Carr, D., Funk, C. & Michaelsen, J. 2013, "The climate-population nexus in the East African Horn: Emerging degradation trends in rangeland and pastoral livelihood zones", *Global Environmental Change,* vol. 23, no. 6, pp. 1525-1541.

Prince, S. 1991, "A model of regional primary production for use with coarse resolution satellite data", *International Journal of Remote Sensing,* vol. 12, no. 6, pp. 1313-1330.

Qin, D., Manning, M., Chen, Z., Marquis, M., Averyt, K., Tignor, M. & Miller, H. 2007, "Climate change 2007: the physical science basis" in *Fourth Assessment Report of the Intergovernmental Panel on Climate Change*, ed. S. Solomon, University Press Cambridge, Cambridge, UK.

Quillet, A., Peng, C. & Garneau, M. 2010, "Toward dynamic global vegetation models for simulating vegetation–climate interactions and feedbacks: recent developments, limitations, and future challenges", *Environmental Reviews,* vol. 18, no. NA, pp. 333-353.

Reason, C., Allan, R., Lindesay, J. & Ansell, T. 2000, "ENSO and climatic signals across the Indian Ocean basin in the global context: Part I, Interannual composite patterns", *International Journal of Climatology,* vol. 20, no. 11, pp. 1285-1327.

Reason, C. & Rouault, M. 2005, "Links between the Antarctic Oscillation and winter rainfall over western South Africa", *Geophysical Research Letters,* vol. 32, no. 7.

Reason, C. & Rouault, M. 2002, "ENSO- like decadal variability and South African rainfall", *Geophysical Research Letters,* vol. 29, no. 13.

Reed, B.C. 2006, "Trend analysis of time-series phenology of North America derived from satellite data", *GIScience & Remote Sensing,* vol. 43, no. 1, pp. 24-38.

Rezende, L., Arenque, B., Aidar, S.d.T., Moura, M., Von Randow, C., Tourigny, E., Menezes, R. & Ometto, J. 2016, "Evolution and challenges of dynamic global vegetation models for some aspects of plant physiology and elevated atmospheric CO2", *International journal of biometeorology,* vol. 60, no. 7, pp. 945-955.

Richard, Y. & Poccard, I. 1998, "A statistical study of NDVI sensitivity to seasonal and interannual rainfall variations in Southern Africa", *International Journal of Remote Sensing,* vol. 19, no. 15, pp. 2907-2920.

Richardson, A.D., Keenan, T.F., Migliavacca, M., Ryu, Y., Sonnentag, O. & Toomey, M. 2013, "Climate change, phenology, and phenological control of vegetation feedbacks to the climate system", *Agricultural and Forest Meteorology,* vol. 169, pp. 156-173.

Richardson, D.M. & Van Wilgen, B.W. 2004, "Invasive alien plants in South Africa: how well do we understand the ecological impacts?: working for water", *South African Journal of Science,* vol. 100, no. 1 & 2, pp. p. 45-52.

Rishmawi, K., Prince, S.D. & Xue, Y. 2016, "Vegetation responses to climate variability in the northern arid to sub-humid zones of Sub-Saharan Africa", *Remote Sensing,* vol. 8, no. 11, pp. 910.

Rodríguez- Fonseca, B., Janicot, S., Mohino, E., Losada, T., Bader, J., Caminade, C., Chauvin, F., Fontaine, B., García- Serrano, J. & Gervois, S. 2011, "Interannual and decadal SST- forced responses of the West African monsoon", *Atmospheric Science Letters,* vol. 12, no. 1, pp. 67-74.

Rodríguez-Fonseca, B., Mohino, E., Mechoso, C.R., Caminade, C., Biasutti, M., Gaetani, M., Garcia-Serrano, J., Vizy, E.K., Cook, K. & Xue, Y. 2015, "Variability and predictability of west African droughts: a review on the role of sea surface temperature anomalies", *Journal of Climate,* vol. 28, no. 10, pp. 4034-4060.

Rojas, O., Li, Y. & Cumani, R. 2014, *Understanding the Drought Impact of El Niño on the Global Agricultural Areas: An Assessment Using FAO's Agricultural Stress Index (ASI)*, Food and Agriculture Organization of the United Nations, Rome.

Ropelewski, C.F. & Halpert, M.S. 1987, "Global and regional scale precipitation patterns associated with the El Niño/Southern Oscillation", *Monthly Weather Review,* vol. 115, no. 8, pp. 1606-1626.

Rouault, M. & Richard, Y. 2005, "Intensity and spatial extent of droughts in southern Africa", *Geophysical Research Letters,* vol. 32, no. 15.

Rouget, M., Richardson, D.M., Cowling, R.M., Lloyd, J.W. & Lombard, A.T. 2003, "Current patterns of habitat transformation and future threats to biodiversity in terrestrial ecosystems of the Cape Floristic Region, South Africa", *Biological Conservation,* vol. 112, no. 1, pp. 63-85.

Rowell, D.P., Booth, B.B., Nicholson, S.E. & Good, P. 2015, "Reconciling past and future rainfall trends over east Africa", *Journal of Climate,* vol. 28, no. 24, pp. 9768-9788.

Sabater, J.M., Rüdiger, C., Calvet, J., Fritz, N., Jarlan, L. & Kerr, Y. 2008, "Joint assimilation of surface soil moisture and LAI observations into a land surface model", *Agricultural and Forest Meteorology,* vol. 148, no. 8, pp. 1362-1373.

Savitzky, A. & Golay, M.J. 1964, "Smoothing and differentiation of data by simplified least squares procedures.", *Analytical Chemistry,* vol. 36, no. 8, pp. 1627-1639.

Sayre, R.G., Comer, P., Hak, J., Josse, C., Bow, J., Warner, H., Larwanou, M., Kelbessa, E., Bekele, T. & Kehl, H. 2013, *A new map of standardized terrestrial ecosystems of Africa -*

An Ecophysiographic Stratification Approach, Association of American Geographers, Washington, D.C.

Scheiter, S. & Higgins, S.I. 2009, "Impacts of climate change on the vegetation of Africa: an adaptive dynamic vegetation modelling approach", *Global Change Biology,* vol. 15, no. 9, pp. 2224-2246.

Scheiter, S., Langan, L. & Higgins, S.I. 2013, "Next- generation dynamic global vegetation models: learning from community ecology", *New Phytologist,* vol. 198, no. 3, pp. 957-969.

Scheiter, S., Higgins, S.I., Osborne, C.P., Bradshaw, C., Lunt, D., Ripley, B.S., Taylor, L.L. & Beerling, D.J. 2012, "Fire and fire- adapted vegetation promoted C4 expansion in the late Miocene", *New Phytologist,* vol. 195, no. 3, pp. 653-666.

Schneider, U., Becker, A., Finger, P., Meyer-Christoffer, A., Ziese, M. & Rudolf, B. 2014, "GPCC's new land surface precipitation climatology based on quality-controlled in situ data and its role in quantifying the global water cycle", *Theoretical and Applied Climatology,* vol. 115, no. 1-2, pp. 15-40.

Scholes, R.J., Biggs, R., Assessment, M.E. & Assessment, Southern African Millennium Ecosystem 2004, *Ecosystem services in southern Africa: a regional assessment,* Millennium Ecosystem Assessment.

Schreck, C.J. & Semazzi, F.H. 2004, "Variability of the recent climate of eastern Africa", *International Journal of Climatology,* vol. 24, no. 6, pp. 681-701.

Schulze, G. 2007, "Atmospheric observations and numerical weather prediction", *South African Journal of Science,* vol. 103, no. 7-8, pp. 318-323.

Sellers, P.J. 1985, "Canopy reflectance, photosynthesis and transpiration", *International Journal of Remote Sensing,* vol. 6, no. 8, pp. 1335-1372.

Sen, P.K. 1968, "Estimates of the regression coefficient based on Kendall's tau", *Journal of the American Statistical Association,* vol. 63, no. 324, pp. 1379-1389.

Seneviratne, S., Nicholls, N., Easterling, D., Goodess, C., Kanae, S., Kossin, J., Luo, Y., Marengo, J., McInnes, K. & Rahimi, M. 2012, "Changes in climate extremes and their impacts on the natural physical environment: An overview of the IPCC SREX report", *EGU General Assembly Conference Abstracts*, pp. 12566.

Shafer, S.L., Bartlein, P.J., Gray, E.M. & Pelltier, R.T. 2015, "Projected future vegetation changes for the Northwest United States and Southwest Canada at a fine spatial resolution using a dynamic global vegetation model", *PloS one,* vol. 10, no. 10, pp. e0138759.

Shongwe, M., Van Oldenborgh, G., Van Den Hurk, B., De Boer, B., Coelho, C. & Van Aalst, M. 2009, "Projected changes in mean and extreme precipitation in Africa under global warming. Part I: Southern Africa", *Journal of Climate,* vol. 22, no. 13, pp. 3819-3837.

Siam, M.S., Wang, G., Demory, M. & Eltahir, E.A. 2014, "Role of the Indian Ocean sea surface temperature in shaping the natural variability in the flow of Nile River", *Climate Dynamics,* vol. 43, no. 3-4, pp. 1011-1023.

Singh, J. & Kruger, A. 2017, "Is the summer season losing potential for solar energy applications in South Africa?", *Journal of Energy in Southern Africa,* vol. 28, no. 2, pp. 52-60.

Sitch, S., Huntingford, C., Gedney, N., Levy, P., Lomas, M., Piao, S., Betts, R., Ciais, P., Cox, P. & Friedlingstein, P. 2008, "Evaluation of the terrestrial carbon cycle, future plant geography and climate- carbon cycle feedbacks using five Dynamic Global Vegetation Models (DGVMs)", *Global Change Biology,* vol. 14, no. 9, pp. 2015-2039.

Sitch, S., Smith, B., Prentice, I.C., Arneth, A., Bondeau, A., Cramer, W., Kaplan, J., Levis, S., Lucht, W. & Sykes, M.T. 2003, "Evaluation of ecosystem dynamics, plant geography and terrestrial carbon cycling in the LPJ dynamic global vegetation model", *Global Change Biology,* vol. 9, no. 2, pp. 161-185.

Southworth, J., Ryan, S.J., Bunting, E., Herrero, H.V., Nagendra, H., Gibbes, C. & Agarwal, S. 2017, "Protected Areas, Climate Change, and Ecosystem Sustainability", *Reference Module in Earth Systems and Environmental Sciences,* vol. doi: 10.1016/B978-0-12-409548-9, pp. 10432-10434.

Steffen, W., Crutzen, P.J. & McNeill, J.R. 2007, "The Anthropocene: are humans now overwhelming the great forces of nature", *AMBIO: A Journal of the Human Environment,* vol. 36, no. 8, pp. 614-621.

Stevens, N., Bond, W., Hoffman, M.T. & Midgley, G. 2015, *Change is in the air: ecological trends and their drivers in South Africa,* 1st edn, South African Environmental Observation Network, Pretoria.

Stevens, N., Erasmus, B.F., Archibald, S. & Bond, W.J. 2016, "Woody encroachment over 70 years in South African savannahs: overgrazing, global change or extinction aftershock?", *Philosophical transactions of the Royal Society of London.Series B, Biological sciences,* vol. 371, no. 1703, pp. 10.1098/rstb.2015.0437.

Stocker, T., Qin, D. & Platner, G. 2013, *Climate Change 2013: The Physical Science Basis. Working Group I Contribution to the Fifth Assessment Report of the Intergovernmental Panel on Climate Change. Summary for Policymakers,* Cambridge University Press, Cambridge, UK.

Strassmann, K., Joos, F. & Fischer, G. 2008, "Simulating effects of land use changes on carbon fluxes: past contributions to atmospheric CO2 increases and future commitments due to losses of terrestrial sink capacity", *Tellus B,* vol. 60, no. 4, pp. 583-603.

Tadross, M., Suarez, P., Lotsch, A., Hachigonta, S., Mdoka, M., Unganai, L., Lucio, F., Kamdonyo, D. & Muchinda, M. 2009, "Growing-season rainfall and scenarios of future change in southeast Africa: implications for cultivating maize", *Climate Research,* vol. 40, no. 2-3, pp. 147-161.

Tan, B., Morisette, J.T., Wolfe, R.E., Gao, F., Ederer, G.A., Nightingale, J. & Pedelty, J.A. 2011, "An enhanced TIMESAT algorithm for estimating vegetation phenology metrics from MODIS data", *Selected Topics in Applied Earth Observations and Remote Sensing, IEEE Journal of,* vol. 4, no. 2, pp. 361-371.

Theil, H. 1950, "A rank-invariant method of linear and polynomial regression analysis", *Proceedings of the Royal Netherlands Academy of Sciences,* vol. 53, pp. 386-392.

Thonicke, K., Venevsky, S., Sitch, S. & Cramer, W. 2001, "The role of fire disturbance for global vegetation dynamics: coupling fire into a Dynamic Global Vegetation Model", *Global Ecology and Biogeography,* vol. 10, no. 6, pp. 661-677.

Thornton, P.K., Jones, P.G., Owiyo, T., Kruska, R., Herrero, M., Kristjanson, P., Notenbaert, A., Bekele, N., Orindi, V. & Otiende, B. 2006, *Mapping climate vulnerability and poverty in Africa: Report to the Department for International development,* Ilri.

Tierney, J.E., Smerdon, J.E., Anchukaitis, K.J. & Seager, R. 2013, "Multidecadal variability in East African hydroclimate controlled by the Indian Ocean", *Nature,* vol. 493, no. 7432, pp. 389-392.

Townshend, J.R. & Justice, C. 1986, "Analysis of the dynamics of African vegetation using the normalized difference vegetation index", *International Journal of Remote Sensing,* vol. 7, no. 11, pp. 1435-1445.

Tucker, C.J., Pinzon, J.E., Brown, M.E., Slayback, D.A., Pak, E.W., Mahoney, R., Vermote, E.F. & El Saleous, N. 2005, "An extended AVHRR 8- km NDVI dataset compatible with MODIS and SPOT vegetation NDVI data", *International Journal of Remote Sensing,* vol. 26, no. 20, pp. 4485-4498.

Tucker, C.J., Dregne, H.E. & Newcomb, W.W. 1991, "Expansion and contraction of the Sahara Desert from 1980 to 1990", *Science,* vol. 253, no. 5017, pp. 299-301.

Ugbaje, S.U., Odeh, I.O., Bishop, T.F. & Li, J. 2017, "Assessing the spatio-temporal variability of vegetation productivity in Africa: quantifying the relative roles of climate variability and human activities", *International Journal of Digital Earth,* vol. 10, no. 9, pp. 879-900.

Van Den Bergh, F., Wessels, K.J., Miteff, S., Van Zyl, T.L., Gazendam, A.D. & Bachoo, A.K. 2012, "HiTempo: a platform for time-series analysis of remote-sensing satellite data in a high-performance computing environment", *International Journal of Remote Sensing,* vol. 33, no. 15, pp. 4720-4740.

van Wilgen, B.W. 2009, "The evolution of fire and invasive alien plant management practices in fynbos", *South African Journal of Science,* vol. 105, no. 9-10, pp. 335-342.

van Wilgen, B.W., Forsyth, G.G. & Le Maitre, D.C. 2008, *The prioritization of species and primary catchments for the purposes of guiding invasive alien plant control operations in the terrestrial biomes of South Africa*, CSIR Natural Resources and the Environment, Stellenbosch.

Verbesselt, J., Hyndman, R., Newnham, G. & Culvenor, D. 2010a, "Detecting trend and seasonal changes in satellite image time series", *Remote Sensing of Environment,* vol. 114, no. 1, pp. 106-115.

Verbesselt, J., Hyndman, R., Zeileis, A. & Culvenor, D. 2010b, "Phenological change detection while accounting for abrupt and gradual trends in satellite image time series", *Remote Sensing of Environment,* vol. 114, no. 12, pp. 2970-2980.

Verger, A., Filella, I., Baret, F. & Peñuelas, J. 2016, "Vegetation baseline phenology from kilometric global LAI satellite products", *Remote Sensing of Environment,* vol. 178, pp. 1-14.

Vincke, C., Diedhiou, I. & Grouzis, M. 2010, "Long term dynamics and structure of woody vegetation in the Ferlo (Senegal)", *Journal of Arid Environments,* vol. 74, no. 2, pp. 268-276.

Vrieling, A., de Beurs, K.M. & Brown, M.E. 2011, "Variability of African farming systems from phenological analysis of NDVI time series", *Climatic Change,* vol. 109, no. 3-4, pp. 455-477.

Vrieling, A., de Leeuw, J. & Said, M.Y. 2013, "Length of Growing Period over Africa: Variability and Trends from 30 Years of NDVI Time Series", *Remote Sensing,* vol. 5, no. 2, pp. 982-1000.

Wang, G. 2003, "Reassessing the impact of North Atlantic Oscillation on the sub- Saharan vegetation productivity", *Global Change Biology,* vol. 9, no. 4, pp. 493-499.

Wang, J., Rich, P. & Price, K. 2003, "Temporal responses of NDVI to precipitation and temperature in the central Great Plains, USA", *International Journal of Remote Sensing,* vol. 24, no. 11, pp. 2345-2364.

Wang, J., Dong, J., Liu, J., Huang, M., Li, G., Running, S.W., Smith, W.K., Harris, W., Saigusa, N. & Kondo, H. 2014a, "Comparison of gross primary productivity derived from GIMMS NDVI3g, GIMMS, and MODIS in Southeast Asia", *Remote Sensing,* vol. 6, no. 3, pp. 2108-2133.

Wang, S., Huang, J., He, Y. & Guan, Y. 2014b, "Combined effects of the Pacific decadal oscillation and El Niño-southern oscillation on global land dry–wet changes", *Scientific reports,* vol. 4, pp. 6651.

Wang, W., Evan, A.T., Flamant, C. & Lavaysse, C. 2015, "On the decadal scale correlation between African dust and Sahel rainfall: The role of Saharan heat low–forced winds", *Science advances,* vol. 1, no. 9, pp. e1500646.

Ward, D., Hoffman, M.T. & Collocott, S.J. 2012, "Magersfontein O Magersfontein: The influence of local and global drivers on a century of woody plant encroachment in the dry Kimberley savanna", *Arid Zone Ecology Forum 2012,*South Africa, 17-19 October 2012.

Wessels, K., Steenkamp, K., Von Maltitz, G. & Archibald, S. 2010, "Remotely sensed vegetation phenology for describing and predicting the biomes of South Africa", *Applied Vegetation Science,* vol. 14, no. 1, pp. 49-66.

Wessels, K.J., Prince, S.D., Carroll, M. & Malherbe, J. 2007a, "Relevance of rangeland degradation in semiarid northeastern South Africa to the nonequilibrium theory", *Ecological Applications,* vol. 17, no. 3, pp. 815-827.

Wessels, K., Prince, S., Malherbe, J., Small, J., Frost, P. & VanZyl, D. 2007b, "Can human-induced land degradation be distinguished from the effects of rainfall variability? A case study in South Africa", *Journal of Arid Environments,* vol. 68, no. 2, pp. 271-297.

Wessels, K., Van den Bergh, F. & Scholes, R. 2012, "Limits to detectability of land degradation by trend analysis of vegetation index data", *Remote Sensing of Environment,* vol. 125, pp. 10-22.

Wessels, K.J., Steenkamp, K., Von Maltitz, G. & Archibald, S. 2011, "Detecting inter-annual variability in the phenological characteristics of southern Africa's vegetation using satellite imagery" in *Observations on Environmental Change in South Africa*, ed. L. Zietsman, SUN MeDIA, Stellenbosch, pp. 88.

WFP 2016, *El Niño: Undermining Resilience - Implications of El Niño in Southern Africa from a Food and Nutrition Security Perspective*, World Food Programme, Rome.

Wigley, B.J., Bond, W.J. & Hoffman, M.T. 2009, "Thicket expansion in a South African savanna under divergent land use: local vs. global drivers?", *Global Change Biology,* vol. 16, no. 3, pp. 964-976.

Willmott, C.J., Matsuura, K. & Legates, D. 2001, "Terrestrial air temperature and precipitation: Monthly and annual time series (1950-1999)", *Center for climate research version,* vol. 1.

Woodward, F.I., Lomas, M.R. & Quaife, T. 2008, "Global responses of terrestrial productivity to contemporary climatic oscillations", *Philosophical transactions of the Royal Society of London.Series B, Biological sciences,* vol. 363, no. 1504, pp. 2779-2785.

Wu, D., Zhao, X., Liang, S., Zhou, T., Huang, K., Tang, B. & Zhao, W. 2015, "Time- lag effects of global vegetation responses to climate change", *Global Change Biology,* vol. 21, no. 9, pp. 3520-3531.

Yue, S., Pilon, P., Phinney, B. & Cavadias, G. 2002, "The influence of autocorrelation on the ability to detect trend in hydrological series", Hydrological Processes, vol. 16, no. 9, pp. 1807-1829.

Zeng, N. & Neelin, J.D. 2000, "The role of vegetation–climate interaction and interannual variability in shaping the African savanna", *Journal of Climate,* vol. 13, no. 15, pp. 2665-2670.

Zhang, X., Friedl, M.A., Schaaf, C.B., Strahler, A.H., Hodges, J.C.F., Gao, F., Reed, B.C. & Huete, A. 2003, "Monitoring vegetation phenology using MODIS", *Remote Sensing of Environment,* vol. 84, no. 3, pp. 471-475.

Zhang, X., Wu, S., Yan, X. & Chen, Z. 2017a, "A global classification of vegetation based on NDVI, rainfall and temperature", *International Journal of Climatology,* vol. 37, no. 5, pp. 2318-2324.

Zhang, X., Friedl, M.A., Schaaf, C.B., Strahler, A.H. & Liu, Z. 2005, "Monitoring the response of vegetation phenology to precipitation in Africa by coupling MODIS and TRMM instruments", *Journal of Geophysical Research,* vol. 110, no. D12, pp. D12103.

Zhang, X., Hodges, J.C., Schaaf, C.B., Friedl, M.A., Strahler, A.H. & Gao, F. 2001, "Global vegetation phenology from AVHRR and MODIS data", *Geoscience and Remote Sensing Symposium, 2001. IGARSS'01. IEEE 2001 International*IEEE, , pp. 2262.

Zhang, X., Liu, L. & Yan, D. 2017b, "Comparisons of Global Land Surface Seasonality and Phenology Derived from AVHRR, MODIS and VIIRS Data", *Journal of Geophysical Research: Biogeosciences,* vol. 122, no. 6, pp. 1506-1525.

Zhang, Y., Wallace, J.M. & Battisti, D.S. 1997, "ENSO-like interdecadal variability: 1900-93", *Journal of Climate,* vol. 10, no. 5, pp. 1004-1020.

Zhang, Y., Gao, J., Liu, L., Wang, Z., Ding, M. & Yang, X. 2013, "NDVI-based vegetation changes and their responses to climate change from 1982 to 2011: A case study in the Koshi River Basin in the middle Himalayans", *Global and Planetary Change,* vol. 108, pp. 139-148.

Zhao, T. & Dai, A. 2016, "Uncertainties in historical changes and future projections of drought. Part II: model-simulated historical and future drought changes", *Climatic Change,* vol. 144, no. 3, pp. 535-548.

Zhao, X., Zhou, D. & Fang, J. 2012, "Satellite- based Studies on Large- Scale Vegetation Changes in China", *Journal of Integrative Plant Biology,* vol. 54, no. 10, pp. 713-728.

Zhou, Y., Huang, A., Zhao, Y., Yang, Q., Jiang, J. & La, M. 2015, "Influence of the sea surface temperature anomaly over the Indian Ocean in March on the summer rainfall in Xinjiang", *Theoretical and Applied Climatology,* vol. 119, no. 3-4, pp. 781-789.

Zhu, Z., Bi, J., Pan, Y., Ganguly, S., Anav, A., Xu, L., Samanta, A., Piao, S., Nemani, R.R. & Myneni, R.B. 2013, "Global data sets of vegetation leaf area index (LAI) 3g and Fraction of Photosynthetically Active Radiation (FPAR) 3g derived from Global Inventory Modeling and Mapping Studies (GIMMS) Normalized Difference Vegetation Index (NDVI3g) for the period 1981 to 2011", *Remote Sensing,* vol. 5, no. 2, pp. 927-948.

Zhu, Z., Piao, S., Myneni, R.B., Huang, M., Zeng, Z., Canadell, J.G., Ciais, P., Sitch, S., Friedlingstein, P. & Arneth, A. 2016, "Greening of the Earth and its drivers", *Nature Climate Change,* vol. 6, pp. 791-795.